

GEOLOGIC INVESTIGATION OF RECURRENCE INTERVALS  
AND REGENCY OF FAULTING ALONG THE  
SAN GREGORIO FAULT ZONE, SAN MATEO COUNTY, CALIFORNIA

Gerald E. Weber and William R. Cotton

William Cotton and Associates  
314 Tait Avenue  
Los Gatos, California 95030

USGS CONTRACT NO. 14-08-0001-16822  
Supported by the EARTHQUAKE HAZARDS REDUCTION PROGRAM

OPEN-FILE NO.81-263

U.S. Geological Survey  
OPEN FILE REPORT

This report was prepared under contract to the U.S. Geological Survey and has not been reviewed for conformity with USGS editorial standards and stratigraphic nomenclature. Opinions and conclusions expressed herein do not necessarily represent those of the USGS. Any use of trade names is for descriptive purposes only and does not imply endorsement by the USGS.

GEOLOGIC INVESTIGATION OF RECURRENCE INTERVALS  
AND REGENCY OF FAULTING ALONG THE  
SAN GREGORIO FAULT ZONE, SAN MATEO COUNTY, CALIFORNIA

by

GERALD E. WEBER, PRINCIPAL INVESTIGATOR  
WILLIAM R. COTTON, PRINCIPAL INVESTIGATOR

WILLIAM COTTON AND ASSOCIATES  
314 Tait Avenue  
Los Gatos, California 95030

for

Gordon Greene, Technical Officer  
U. S. Geological Survey  
345 Middlefield Road  
Menlo Park, California 94025

Final Technical Report  
Contract No. 14-08-0001-16822  
\$52,000

August 1, 1980

The views and conclusions contained in this document are those of the authors and should not be interpreted as necessarily representing the official policies, either expressed or implied, of the U. S. Government.

William Cotton and Associates

## CONTENTS

	Page
INTRODUCTION	1
ACKNOWLEDGEMENTS	2
REGIONAL GEOLOGY	4
SANTA CRUZ TERRACE	4
Age of Terrace	4
Marine Terrace Deposits	4
Sub-Terrace (Bedrock) Geology	10
Pigeon Point Structural Block	10
Pomponio Structural Block	10
Santa Cruz Mountains Structural Block	11
SAN GREGORIO FAULT ZONE	12
WIDTH OF THE FAULT ZONE AND DISTRIBUTION OF FAULTS	12
STRAIN AND DISPLACEMENT RATES ALONG THE SAN GREGORIO FAULT ZONE	15
STRAIN ACCUMULATION OR CREEP	17
SEISMOLOGY	17
PALEOSEISMOLOGY AND EARTHQUAKE RECURRENCE INTERVALS	18
FAULT SCARPS ALONG THRUST FAULTS: SOME CONSIDERATIONS	20
INITIAL CHARACTERISTICS	20
DIP OF FAULT PLANE	20
MAGNITUDE OF SURFACE DISPLACEMENT	20
CONSOLIDATION AND ROCK STRENGTH	21
THRUST FAULTING IN MARINE TERRACE TERRANE	22
PATTERNS OF FAULTING - BEDROCK VS. TERRACE DEPOSITS	22
NEAR-SURFACE EFFECTS AND SCARP FORMATION	22
FAULT SCARP MODIFICATION	29
Erosional Processes and Age of Fault Scarps	30
MODEL FOR RECOGNITION OF MULTIPLE FAULTING EVENTS ALONG REVERSE FAULTS	30
AÑO NUEVO THRUST FAULT	38
FIELD RELATIONSHIPS AND DESCRIPTIVE GEOLOGY	38
SURFACE MAPPING OF THE AÑO NUEVO THRUST FAULT	38
Magnetometer Surveys	38
Seismic Refraction Surveys	40
Hand Auger Core Holes	41
NORTHWESTERN EXTENT OF THE AÑO NUEVO THRUST FAULT	42
SUMMARY	43
PALINSPASTIC RECONSTRUCTION OF LATE PLEISTOCENE FAULT MOVEMENT - AÑO NUEVO THRUST FAULT	44
Geologic Constraints and Assumptions Used in Reconstruction	44
Analysis of Sea-Cliff Exposure - Año Nuevo Thrust Fault	48
Analysis of the Exploratory Trench Exposures	54
Correlation of Faulting Events - Sea-cliff and trench sections	57
Discussion and Summary	58

	Page
FRIJOLES FAULT	63
INTRODUCTION	63
PATTERN OF FAULTING AND FAULT OFFSETS	67
LATE PLEISTOCENE SLIP RATES	72
RELATION OF MOVEMENT ON THE CASCADE QUARRY REVERSE FAULT TO MOVEMENT ON THE FRIJOLES FAULT AND THE SAN GREGORIO FAULT ZONE	75
Structural Attitude of Faults Exposed in the Cascade Quarry Area	75
Fault Striations and Slickensides - Direction of Movement	77
MAXIMUM PROBABLE VERTICAL AND HORIZONTAL SURFACE DISPLACEMENTS ALONG THE CASCADE QUARRY REVERSE FAULT. FAULT DIMENSIONS AND RELATIONSHIP TO EARTHQUAKE MAGNITUDE	79
RATIO OF HORIZONTAL SLIP ON THE CASCADE QUARRY REVERSE FAULT TO HORIZONTAL SLIP ACROSS THE SAN GREGORIO FAULT ZONE AT POINT AÑO NUEVO	84
RECURRENCE INTERVALS FOR FAULTING EVENTS ALONG THE FRIJOLES FAULT AND THE CASCADE QUARRY REVERSE FAULT	85
Introduction	85
Holocene Sag Pond Deposits at Point Año Nuevo	85
Late Pleistocene Slip Rates and Recurrence Intervals	86
Analysis of Recurrent Movement Along the Cascade Quarry Reverse Fault	87
Summary	91
CONCLUSIONS	92
GEOLOGIC REFERENCES	95
APPENDIX A - Año Nuevo Thrust Fault, Point Año Nuevo: Seismic Refraction Surveys, Magnetometer Surveys, Logs of Hand Auger Core Holes, Logs of Test Pits	
APPENDIX B - Frijoles Fault, Cascade Ranch: Seismic Refraction Surveys, Magnetometer Surveys, and Logs of Hand Auger Core Holes	

## ILLUSTRATIONS

Figure	Page
1. Major structural elements of the San Gregorio fault zone.	5
2. Index map showing detailed study areas and survey locations.	6
3. Diagram of major elements of a marine terrace.	7
4. Age determination of the first emergent marine terrace.	8
5. Quaternary deposits and late Pleistocene faults at Point Año Nuevo.	9
6. Regional faults.	13
7. Generalized sea-cliff geology, south side Punta del Año Nuevo.	14
8a-d. Palinspastic reconstruction of Late Pleistocene fault movement - Año Nuevo thrust fault at sea-cliff exposure.	23-26
9. Año Nuevo thrust fault - generalized geology.	27
10. Model for recognition of multiple faulting events along reverse faults.	31
11a-b. Palinspastic reconstruction of Late Pleistocene fault movements - Año Nuevo thrust fault at Trench AN-1.	35-36
12. Sea-cliff exposure of the Año Nuevo thrust fault.	39
13. Año Nuevo thrust fault.	45
14. Time-vs.-vertical displacement plot of possible faulting events (fault line scarp model).	59
15. Time-vs.-vertical displacement plot of possible faulting events (compromise model).	60
16. Time-vs.-vertical displacement plot of possible faulting events (maximum event model).	62
17. Generalized sea-cliff geology across the Frijoles fault on the south shore of Point Año Nuevo.	64
18. Deformed Holocene sediments along the Frijoles fault.	65
19. Generalized cross section showing sea-cliff geology across the mouth of Pescadero Creek.	66
20a-d. Four alternate interpretations of the faulting pattern - southern portion of San Gregorio fault zone.	68

Figure	Page
21. Comparison of fault patterns between major wrench faults experiencing convergent and divergent wrenching.	69
22. Deformation of shoreline angles.	73
23a-d. Four alternate interpretations of the fault pattern and offset shoreline angles.	74
24. Planimetric map of Cascade Ranch Quarry showing structural attitudes of Cascade Quarry reverse fault.	78
 Plate (In pockets)	
I. San Gregorio fault zone, Año Nuevo thrust fault - Planimetric Map, 1:1200.	
II. San Gregorio fault zone, Año Nuevo thrust fault - Plan Map, 1:600.	
III. San Gregorio fault zone, Frijoles fault-map of Cascade Ranch Quarry.	
IV. San Gregorio fault zone, Año Nuevo thrust fault - Detailed log of sea-cliff exposure along south shore of Point Año Nuevo.	
V. San Gregorio fault zone, Año Nuevo thrust fault - Trench AN-1.	
VI. San Gregorio fault zone, Año Nuevo thrust fault - Detail of Fault Trench AN-1.	
VII. Año Nuevo Stratigraphic Section 2.	
VIII. Año Nuevo Stratigraphic Section 3.	
IX. Año Nuevo Stratigraphic Section 4 - Marine terrace deposits.	
X. Año Nuevo Stratigraphic Section 5 - Marine terrace deposits SW of thrust fault (down dropped block).	
XI. Año Nuevo Stratigraphic Column 1 - Marine terrace deposits exposed in sea cliff 1000 feet east of Año Nuevo thrust fault at Cave Beach.	
XII. San Gregorio fault zone - Cascade Trench #1.	
XIII. San Gregorio fault zone, Frijoles fault - Cascade Ranch Quarry wall and Trench #1.	
XIV. San Gregorio fault zone, Frijoles fault - Detailed log of Quarry wall, Cascade Ranch.	

Plate

- XV. Cascade Ranch Stratigraphic column - Marine terrace stratigraphy on upthrown block.
- XVI. San Gregorio fault zone, Frijoles fault - Cascade Ranch spillway.
- XVII. San Gregorio fault zone - Cascade Trench #2.
- XVIII. San Gregorio fault zone - Cascade Trench #3.

GEOLOGIC INVESTIGATION OF RECURRENCE INTERVALS  
AND REGENCY OF FAULTING ALONG THE  
SAN GREGORIO FAULT ZONE, SAN MATEO COUNTY, CALIFORNIA

INTRODUCTION

This report presents the results of our work during the past two years along the San Gregorio fault zone near Point Año Nuevo in southern San Mateo County, California. This work, done for the U. S. Geological Survey under the Earthquake Hazards Reduction Program (Contract No. 14-08-0001-16822) is an extension of a pre-existing and presently-continuing study of the San Gregorio fault zone initiated by one of the investigators (Weber) in 1973. This report is not viewed as the final product but as a progress report describing our present understanding of a portion of the fault zone near Point Año Nuevo. Although this study has provided a large amount of data regarding fault activity and recurrence intervals, it has not answered all of our questions about this large complex fault zone. Indeed, as with most studies, it has raised almost as many new questions as it has attempted to answer.

The initial goals of our study and the goals of our continuing studies of the San Gregorio fault zone are as follows:

1. Prepare detailed maps and logs of thrust faults and stratigraphy in the San Gregorio fault zone.
2. Distinguish evidence of individual faulting events. Determine the number of faulting events and the maximum displacement associated with each event. Reconstruct the sequence of events for each fault studied.
3. Determine the recency of movement along each fault. Estimate long-term slip rates and recurrence intervals for individual faults and for the San Gregorio fault zone.
4. Examine the relationships between fault activity and maximum surface displacements for primary and secondary faults within the fault zone. Use this data to develop a technique for evaluating the degree of hazard posed by secondary faults compared to that posed by primary faults within the fault zone.
5. Use long-term slip rates and recurrence intervals to estimate the magnitude of the maximum credible earthquake along the San Gregorio fault zone.

Although many questions remain unanswered, during this study we believe that we have achieved all of these goals at least partially. In particular, we have developed the ability to recognize individual faulting events along reverse (thrust) faults through examination of stratigraphic relationships, cross-cutting relationships and fault geometries. This has allowed us to reconstruct sequences of events and to estimate recurrence intervals for earthquakes that produce surface rupture.

Our study has focused primarily on two reverse faults within the San Gregorio fault zone - the Año Nuevo thrust fault and an unnamed reverse fault, referred to in this report as the Cascade Quarry reverse fault, that is part of the Frijoles fault complex. These two faults were chosen for study because they are reverse faults, they have excellent exposures, and they offset the first emergent marine terrace, the Santa Cruz terrace (Bradley and Griggs, 1976).

Reverse faults and reverse-oblique faults appear to be particularly amenable to studies of sequential fault movement because the continuing movement of the hanging-wall block out over the footwall block protects and preserves the depositional record on the footwall block. Hence, over a period of years the fault scarp associated with each faulting event is eroded, and the sediment is washed off of the hanging-wall block onto the footwall block. This sedimentary record of the previous faulting event is preserved by the next faulting event which pushes the hanging-wall block out over the sedimentary sequence on the footwall block.

The geologic and geographic setting at Point Año Nuevo is almost ideal for a study of late Pleistocene sequential movement along reverse faults. First, exposures of the late Pleistocene marine terrace deposits and the faults both in sea cliffs and in man-made cuts are excellent. Second, both the Año Nuevo thrust fault and the Cascade Quarry reverse fault offset the wave-cut platform and the deposits of the first marine terrace. The presence of the marine terrace is of utmost importance to the study because both the age of the formation of the marine terrace and the original orientation of the wave-cut platform, dipping approximately  $\frac{1}{2}$ -1 degree seaward, are well known. The terrace therefore provides a well-defined datum plane from which to measure structural deformation. It also provides an ideal starting point in time for the reconstruction of the faulting events; the wave-cut platform was created in the surf zone of a transgressing sea that reached a highstand of sea level 105,000 years B.P. Third, the erosion and deposition rates in both the shallow marine and the subaerial environments that existed on the marine terraces were low to moderate. These low rates allowed the evidence of sequential fault movement in the terrace sediments to be preserved.

#### ACKNOWLEDGEMENTS

It would be impossible to acknowledge all of the numerous persons who have assisted us during the field investigations, the data analysis, and the written preparation of this study. Nevertheless, the following deserve particular recognition for their efforts. Without the help of Lloyd K. Oshiro in field work, compilation, data interpretation, and drafting of the final figures and plates, this report never would have been completed. Damon Brown, Dave Cochrane, Vince Ramirez, Jim Lettire, and many others assisted in the field investigations and in data compilation. Kevin Coppersmith and Sharyl Fernandez assisted in the initial cleaning and logging of the sea cliff section along the Año Nuevo thrust fault in the spring of 1976.

In particular we would like to thank Ken Lajoie for his continuing help over the years in field work and in dating samples and for numerous fruitful discussions regarding a myriad of geologic problems associated with marine terraces and faulting. Amino acid dates on fossil mullusks were provided courteously by Ken Lajoie of the U. S. Geological Survey and John Wehmiller

of the University of Delaware. Elizabeth Mathieson, John Coyle and Hans Nielsen helped to edit the manuscript and finalize the graphics.

Special thanks go to Rudi Rossi of Cascade Ranch for his help and understanding and for allowing us to conduct our investigations, including the excavation of exploratory trenches through his artichoke fields, at Cascade Ranch.

Finally, we would like to thank the rangers and personnel of the State Parks and Beaches for their continuing help during this study. Roger Werts, Mike Bradeen, Walter and Candy Ward, George Gray, and Nina Gordon are only a few of the many who have been particularly helpful over the years.

## REGIONAL GEOLOGY

The study areas lie within the San Gregorio fault zone and upon the first emergent marine terrace (Santa Cruz terrace) near Point Año Nuevo (Figures 1, 2 and 5). Point Año Nuevo is a broad, cusped headland jutting out about 1½ - 2 miles from the normal trend of the Santa Cruz County coastline. The entire approximate 2-mile-wide projection of the point and island is completely within the Santa Cruz marine terrace, and except for minor irregularities the topographic surface slopes gently from elevations of about 120-140 ft. on the northeast edge of the terrace to elevations of 5-15 ft. on the west and southwest at the sea cliff. The sea cliffs along the south shore of Point Año Nuevo rise gently from near sea level at the point to approximately 70 ft. to the east near the surface trace of the Frijoles fault. These cliffs provide excellent exposures of the marine terrace deposits and of the numerous faults within the San Gregorio fault zone.

### SANTA CRUZ TERRACE -

Age of Terrace - The Santa Cruz terrace (Bradley and Griggs, 1976) is the dominant topographic feature in the area. It was formed by wave erosion in a sea slowly rising to a highstand about 105,000 years B.P. The age of the wave-cut platform was determined through the use of amino-acid racemization techniques applied to fossil mollusks (*Saxidomus giganteus* and *Protothaca staminea*) collected from the fossil shell debris found on the old wave-cut platform (see Figure 3 for a diagram showing terrace terminology). The amino-acid racemization technique used by Lajoie and Wehmiller provides only D/L ratios for the amino acid Leucine. Therefore, the interpretation of the age of the mollusk must be done using other factors including a latitudinal plot of samples combined with a consideration of the temperature aspect of the entire marine fauna (i.e. cool-water or warm-water fauna). The age of 105,000 ± years B.P. for the fauna found on the wave-cut platform of the Santa Cruz terrace at Año Nuevo is based on the interpretations of Drs. K. R. Lajoie and George Kennedy of the U. S. Geological Survey. Because the fauna has a cool-water aspect and the D/L ratio value lies close to the 100,000-year age for this latitude, the fauna is interpreted to have lived in the sea that reached a highstand of sea level about 105,000 years B.P. during oxygen isotope stage 5c (Bloom and others, 1974). Refer to Figure 4 for an indication of the age determinations of the first emergent marine terrace at Santa Cruz and Point Año Nuevo. For additional information regarding the dating of mollusks using amino-acid stereochemistry, refer to Wehmiller and others, 1977.

Marine Terrace Deposits - As indicated in Figure 3, the old wave-cut platform is overlain by a regressive sequence of shallow marine deposits that in turn are overlain by subaerial fluvial deposits, soils, and wind-blown sand. The terrace deposits are thickest along the back or inner edge of the terrace and thin progressively toward the seaward or "distal edge." Shallow marine deposits in many of the distal areas have been removed completely from the wave-cut platform by subaerial erosion, and fluvial deposits directly overlies the wave-cut platform.

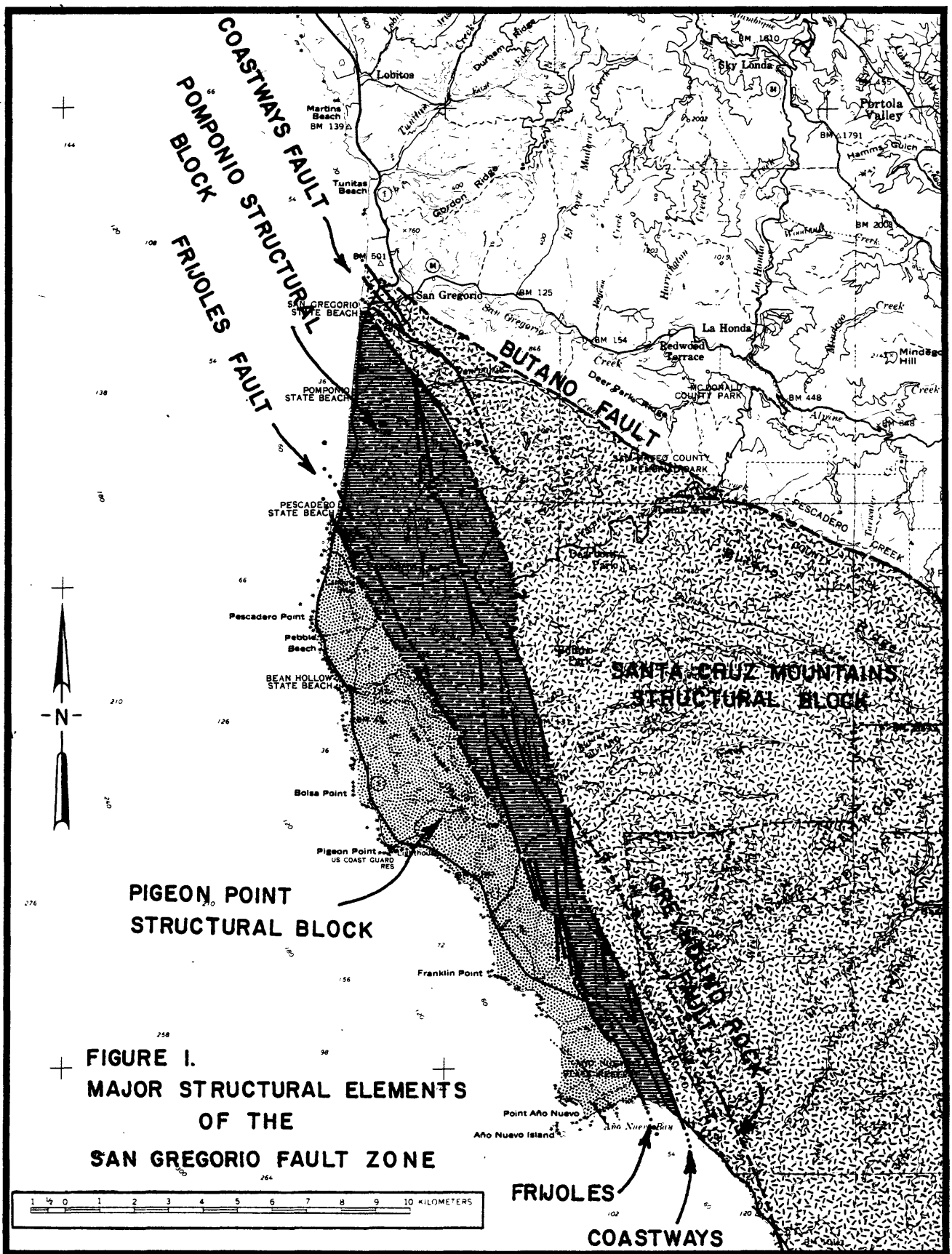
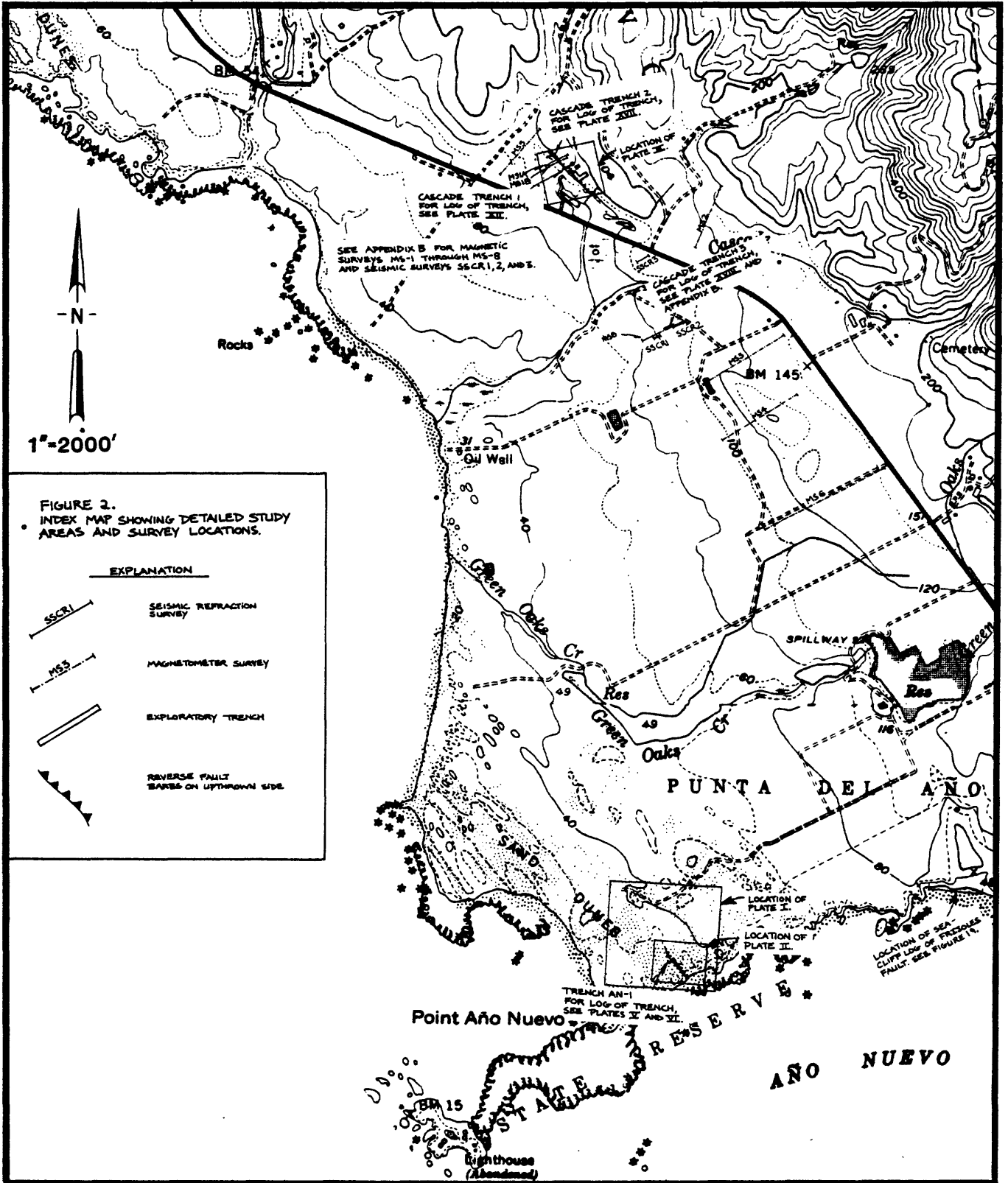


FIGURE I.  
 MAJOR STRUCTURAL ELEMENTS  
 OF THE  
 SAN GREGORIO FAULT ZONE

Base: San Francisco Bay Region Topographic Map,  
 Sheet 3 of 3, U. S. Geological Survey, 1970, 1:125,000



Base map from U. S. Geological Survey 7.5 minute Año Nuevo and Franklin Point Quadrangles

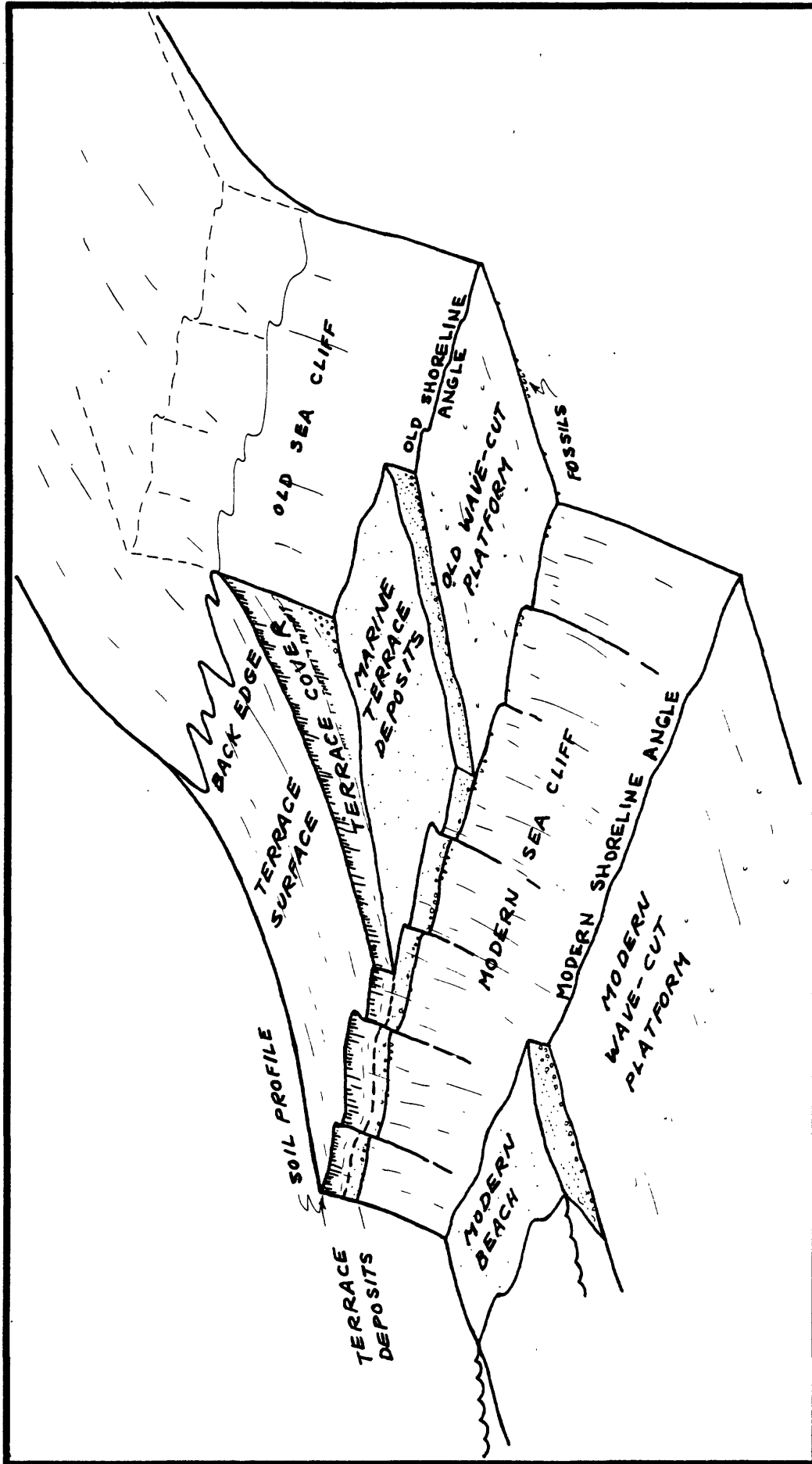
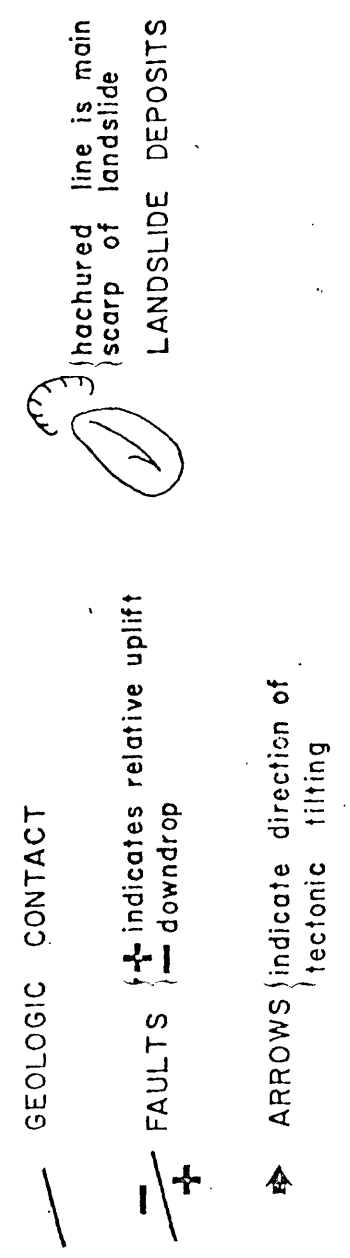
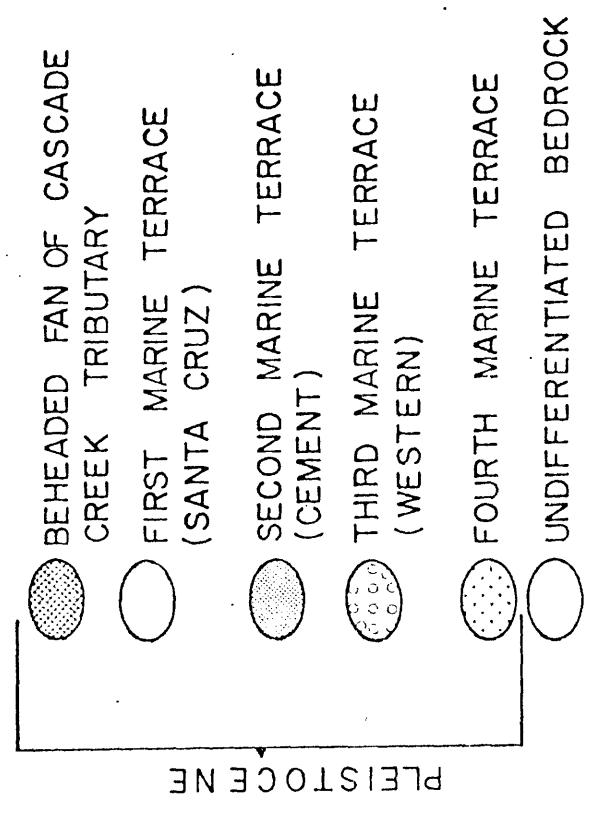
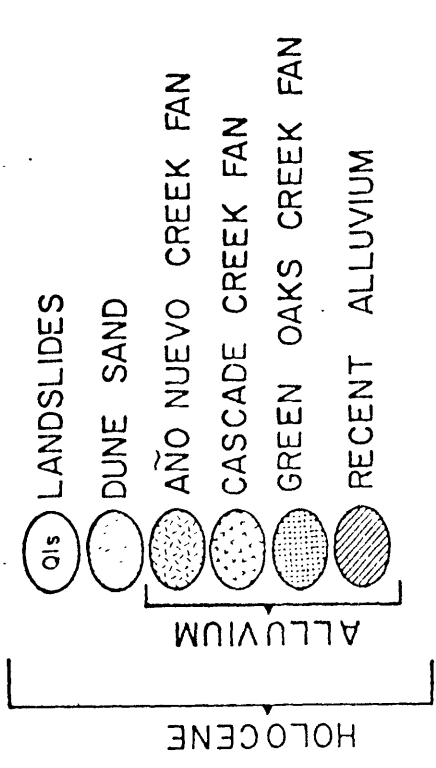
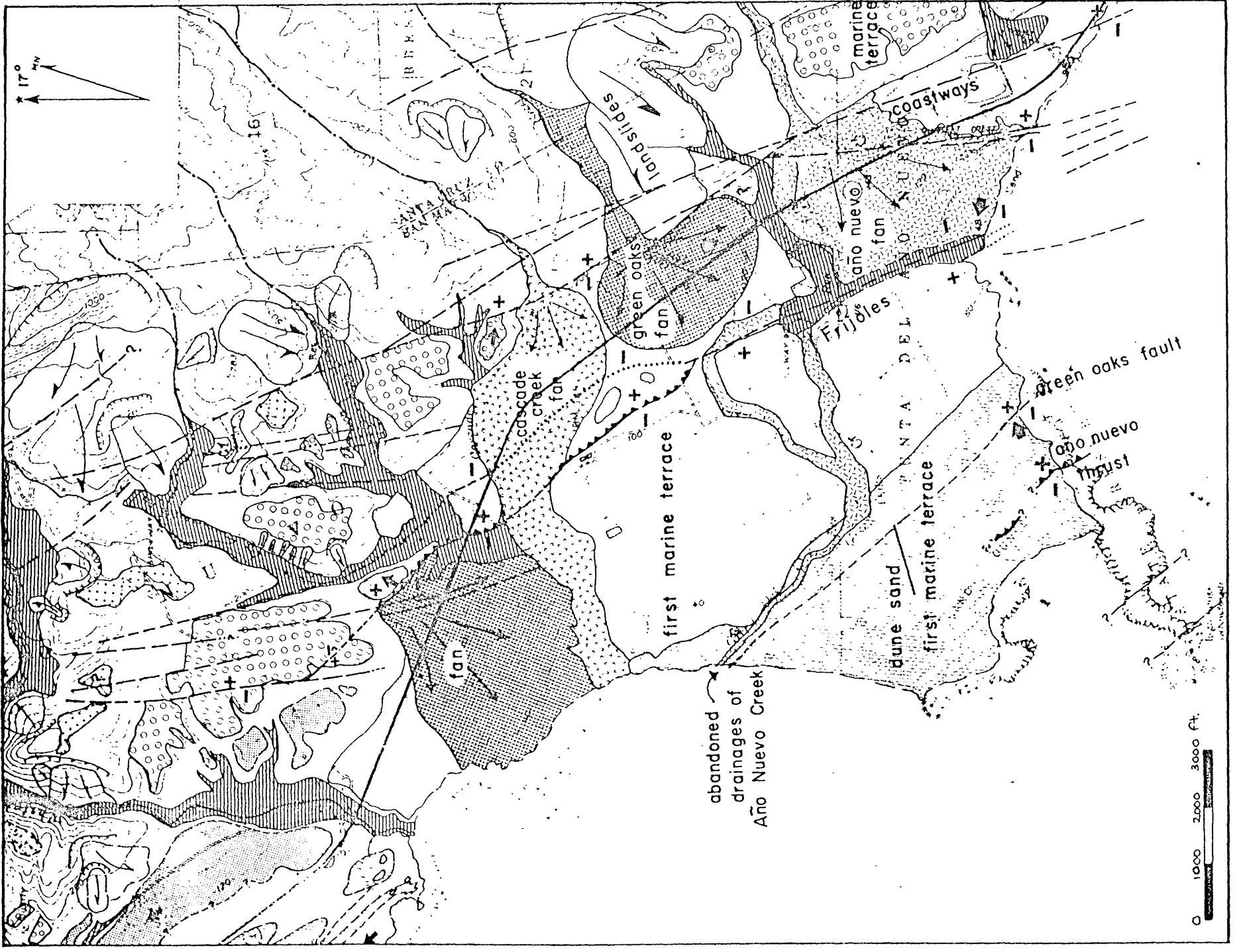


FIGURE 3 Diagram of the major elements of a marine terrace. Indicates relationship of wave-cut platform to the overlying terrace deposits and the shoreline angle.



QUATERNARY DEPOSITS & LATE PLEISTOCENE  
 FAULTS at POINT AÑO NUEVO, SAN MATEO CO.,  
 CALIFORNIA. by: Gerald E. Weber

FIGURE 5

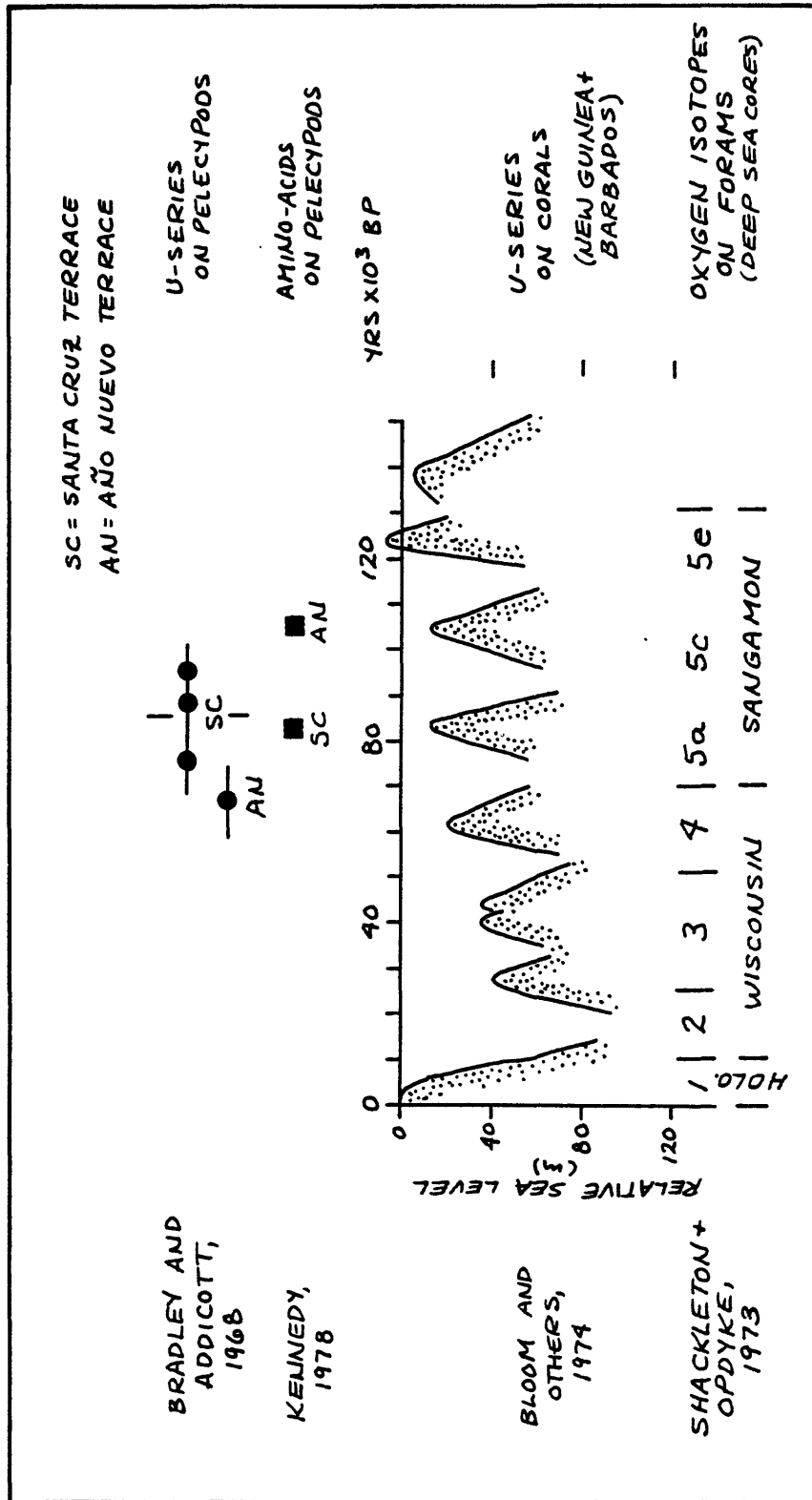


FIGURE 4 Age determination of the first emergent marine terrace at Point Santa Cruz and Point Año Nuevo.

Near Point Año Nuevo, fluvial deposits can be recognized easily by the abundance of Santa Cruz mudstone clasts in the deposits. The Santa Cruz mudstone, a siliceous mudstone of late Miocene age, crops out only northeast of the San Gregorio fault zone. Because of their relatively low resistance to erosion, mudstone clasts do not persist in beach or nearshore environments. Therefore, the mudstone clasts are only a minor constituent of nearshore sands, gravels and conglomerates. In contrast, they constitute the bulk of the pebble and cobble-sized clasts in the fluvial deposits that have been washed out of the Santa Cruz Mountains across and to the southwest of the fault zone.

The wave-cut platform generally is free of fossils although most of it has abundant burrows and borings from marine invertebrate organisms, primarily pholads. In the central coast area, there are no fossil localities from older (higher) terraces, and only three fossil localities have been found on the youngest (lowest) terrace (Santa Cruz terrace). Two of these localities, fortuitously, are at Point Año Nuevo and provide the needed age control for this study.

Sub-Terrace (Bedrock) Geology - At Point Año Nuevo, the Santa Cruz terrace is cut into a variety of middle to upper Tertiary sedimentary rocks. The sedimentary rock unit into which the terrace is cut at any one place varies with the position of the terrace with respect to the San Gregorio fault zone. As indicated in Figure 1, the San Gregorio fault zone has been interpreted as having two primary fault strands (zones of movement) separating three distinct structural provinces or blocks. Of the two study areas, the Año Nuevo thrust fault area lies entirely within the Pigeon Point structural block, and the Frijoles fault study area lies partially within the Pigeon Point block and partially within the Pomponio structural block.

Pigeon Point Structural Block - The Pigeon Point structural block bounds the San Gregorio fault zone on the west and includes areas underlain by three different bedrock formations. Immediately southwest of the Frijoles fault near Point Año Nuevo, the wave-cut platform has been eroded principally into the basal argillic mudstone and the fine-grained sandstone of the Purisima formation. From 2000 ft. east of Point Año Nuevo to the point, the sub-terrace bedrock consists of siliceous mudstone of the Monterey formation and sandstone, siltstone and mudstone of the Vaqueros(?) formation (Clark and Brabb, 1978). North of Point Año Nuevo, the sub-terrace bedrock is the upper Cretaceous Pigeon Point formation, a heterogeneous sequence of interbedded sandstone, mudstone and conglomerate that is thought to have been deposited by turbidity currents upon the continental slope or continental rise.

Pomponio Structural Block - The Pomponio structural block is bounded by the primary strands of the San Gregorio fault zone, the Frijoles and Coastways faults. The sub-terrace bedrock unit in this block consists entirely of sandstone, siltstone and argillic mudstone of the Purisima formation.

Santa Cruz Mountains Structural Block - Northeast of the San Gregorio fault zone, from just north of Point Año Nuevo (Whitehouse Creek) south into Santa Cruz County, all of the marine terraces, regardless of age and present elevation, are cut into the upper Miocene Santa Cruz mudstone. The Santa Cruz mudstone consists of a sequence of siliceous mudstone that is exposed extensively in the Santa Cruz Mountains. The sequence thickens to the west and appears to be thickest where it abuts against the San Gregorio fault zone. The Texas Company's Poletii #1 well was drilled through 8,850 ft. of mudstone at a location along the coast about halfway between Point Año Nuevo and Davenport, within the Santa Cruz Mountains block (Clark & Brabb, 1978, p. 5). Farther to the east and northeast and higher in the Santa Cruz Mountains, the bedrock outcrops expose thick sequences of middle and lower Tertiary sandstone and siltstone and the underlying basement rock, a hornblende-biotite quartz diorite.

In summary, the distribution of bedrock (pre-Quaternary) units is different for each of the structural blocks, and this difference in rock type allows the distinction of the source area for many of the late Quaternary fluvial deposits that are part of the marine terrace sequence. Similarly, the nature of the basal shallow marine deposits on the wave-cut platform varies with the variation in rock types available to surf zone processes. Consequently, it often is possible to distinguish the origin of a stratigraphic unit in the marine terrace deposits as shallow marine or fluvial simply on the basis of the dominant rock type in the coarse-grained cobble or pebble conglomerates. Refer to Clark and Brabb, 1978; Clark, 1966, 1970; Touring, 1959; and Brabb, 1970, for more detailed information on the pre-Quaternary geology of the area.

## SAN GREGORIO FAULT ZONE

The San Gregorio fault zone is a major fault branching from the San Andreas fault zone near Bolinas Lagoon north of the Golden Gate. It trends S 15-20 degrees E, roughly parallel to the coastline, and extends at least 190 km to the Monterey area (Figure 6). The San Gregorio fault zone probably connects to the Sur fault zone and in turn to the San Simeon fault zone and the Hosgri fault. Therefore, the San Gregorio fault zone actually may extend for more than 420 km to the vicinity of Point Arguello, forming a large, complex coastal boundary fault. The San Gregorio-Hosgri fault zone appears to be the longest and to have the greatest total offset of the subsidiary faults within the San Andreas system. The San Gregorio fault zone appears to have the same relationship to the San Andreas as the Hayward and Calaveras faults do with regard to the overall tectonic stress pattern in central California. The Hayward-Calaveras and the San Gregorio faults, in addition to the San Andreas fault itself, probably have been the major zones of late Tertiary slippage within the San Andreas system.

Most of the San Gregorio fault zone lies offshore, but a 4-km segment of the Seal Cove fault at the north end of Half Moon Bay and a 26-km segment of the San Gregorio fault between San Gregorio and Point Año Nuevo lie onshore. Individual fault strands within the San Gregorio fault zone are numerous, and the pattern of faulting is complex. In general, the fault strands are poorly exposed except on the south shore of Point Año Nuevo where at least five individual fault strands are exposed in the sea cliff (Figures 5 and 7).

WIDTH OF THE FAULT ZONE AND DISTRIBUTION OF FAULTS - The San Gregorio fault zone is an extremely wide, complex zone of faulting. In the northwestern portion of its onshore exposure, the fault zone appears to be approximately three miles wide and to consist of two widely-separated primary fault strands that bound a relatively-undeformed structural block, the Pomponio block (Figure 1). The two primary faults, the Coastways fault and the Frijoles fault, bound the Pomponio structural block. The block is 15,000 ft. wide at the northwest end of its onshore exposure and narrows progressively to the southeast at Point Año Nuevo where it is approximately 3,000 ft. wide.

Although the two primary fault strands appear to be the loci of most of the fault movement, there are numerous secondary faults within the San Gregorio fault zone. As is evident on Figures 1, 5, and 7, those secondary faults are most prevalent near the southeastern end of the onshore fault segment, and all of the faults shown have offset the wave-cut platform and the deposits of the Santa Cruz terrace. Hence, all of these secondary faults have experienced late Pleistocene movement, and some of them can be demonstrated to have experienced recurrent late Pleistocene movement.

At Point Año Nuevo, if all of the secondary faults that have experienced late Pleistocene movement are included in the San Gregorio fault zone, the zone is about 3 km wide. Five of these faults are clearly visible in the seacliff, and a sixth fault and possibly a seventh lie between the Point and Año Nuevo Island (Figure 7). The elevation of the marine terrace platform on the island is about 15 ft. higher than on the point. That difference could have been produced only by tectonic deformation, either folding or, more probably, faulting.

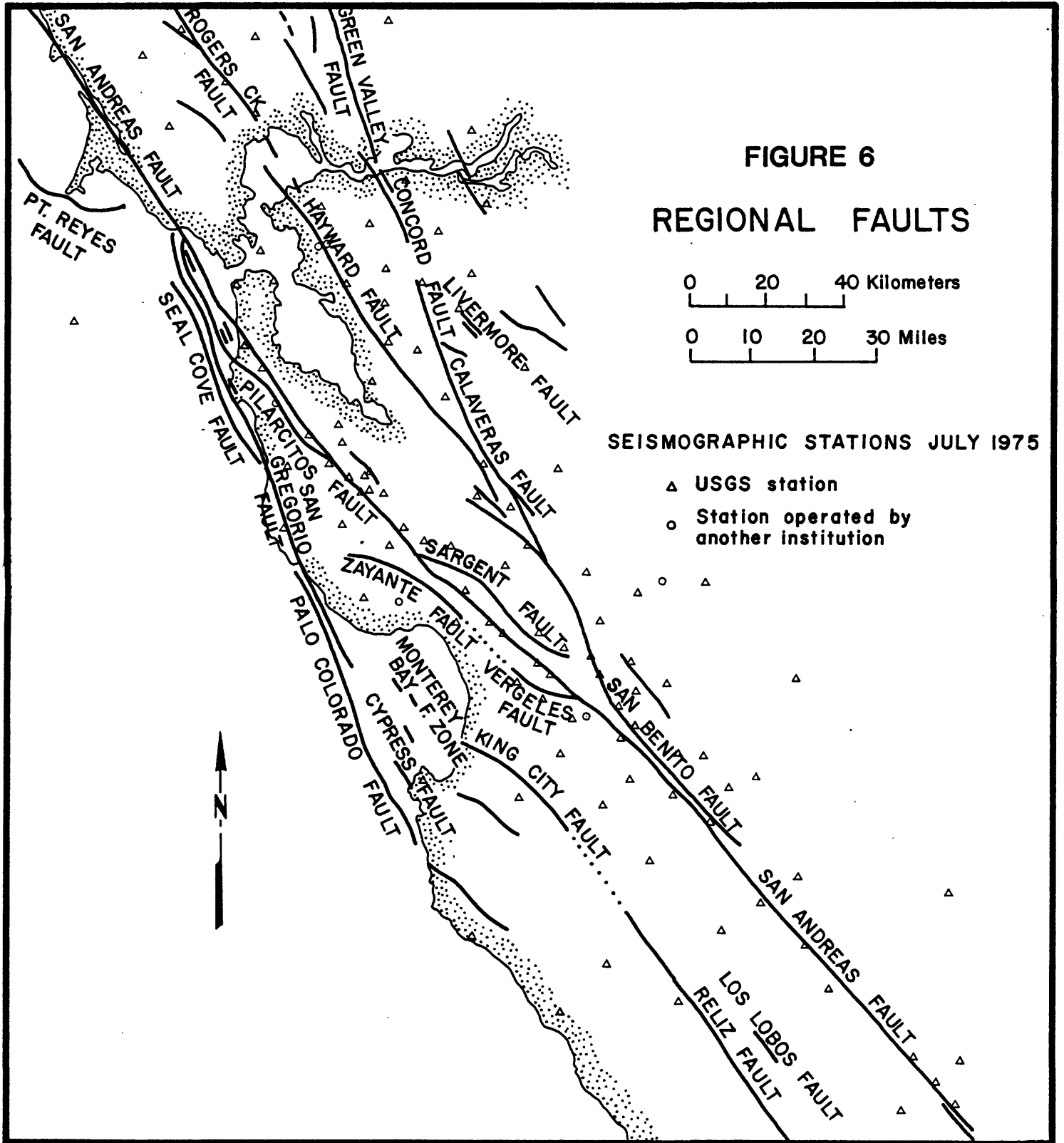
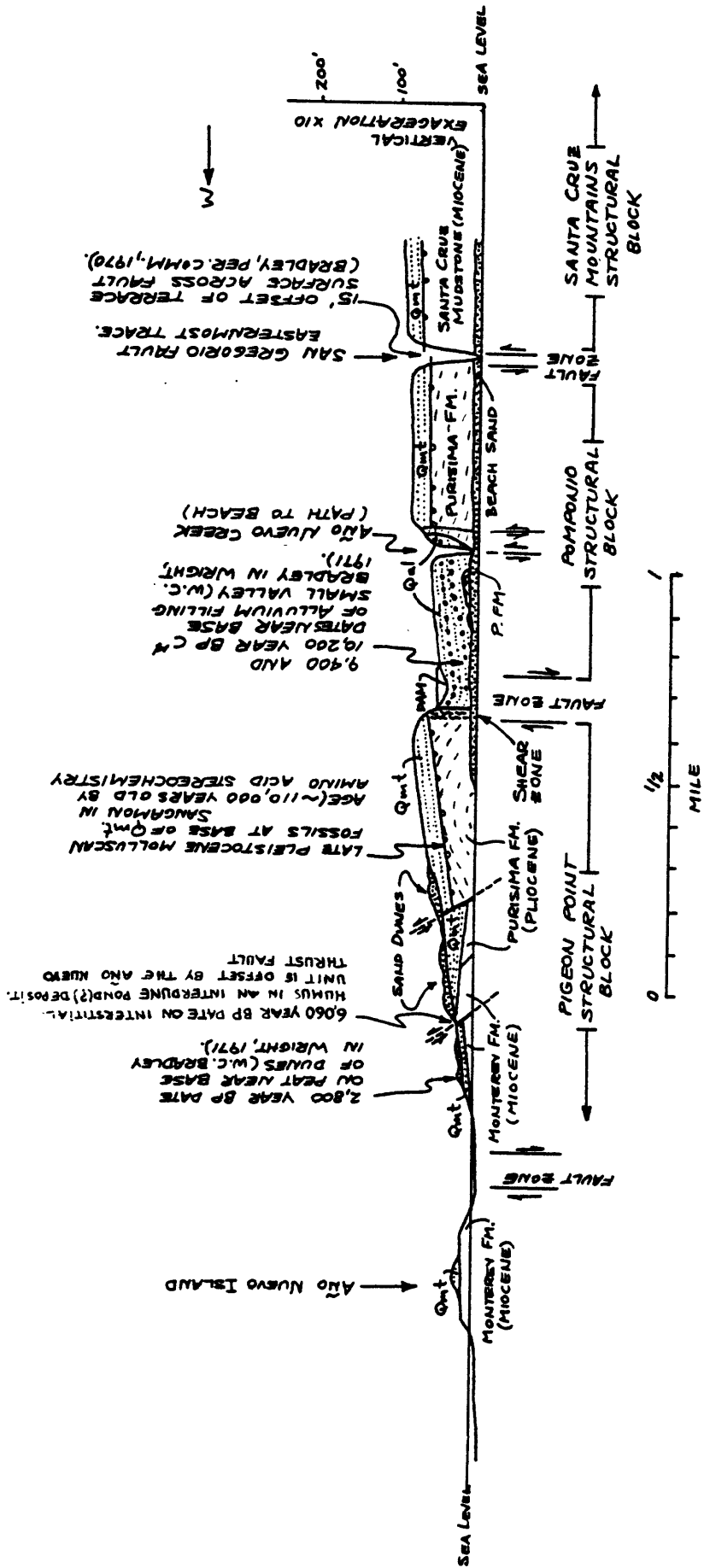


FIGURE 7 GENERALIZED SEACLIFF GEOLOGY  
 SOUTH SIDE OF PUNTA DEL AÑO NUEVO  
 SAN MATEO COUNTY



Two closely-spaced fault strands that offset the Santa Cruz terrace near Greyhound Rock lie northeast of the Coastways fault and apparently are part of the San Gregorio fault zone. Although their surface trace through the mountainous areas is difficult to delineate, these faults may represent another major fault strand of the San Gregorio fault zone. These faults, however, apparently do not represent a principal displacement shear.

The fault zone, therefore, appears to consist of at least seven and possibly eight individual fault strands that have experienced movement during the late Pleistocene. These strands are distributed over a zone approximately 5 km (3 miles) wide. Because of the excellent sea-cliff exposures along the south shore of Point Año Nuevo and the presence of the wave-cut platform of the Santa Cruz terrace which serves as a continuous late Pleistocene "time line," the San Gregorio fault zone appears to be anomalously wide. Were it not for the excellent exposure and the terrace, it is doubtful that most of these secondary faults could have been identified as having any Pleistocene movement, much less late Pleistocene movement.

The presence of these numerous late Pleistocene secondary fault strands and the pattern of faulting create serious problems with delineation of the size, shape, and lateral limits of the fault zone. Throughout most of its onshore portion, the Frijoles fault, with its complex of anastomosing and en echelon faults, appears to be the southwest boundary of the San Gregorio fault zone. At Año Nuevo, however, faults that obviously are genetically related to the San Gregorio fault zone, that have experienced late Pleistocene movement, and that probably are all "active" lie greater than 2 km southwest of the Frijoles fault. These secondary faults cannot be shown to branch off of or connect with the primary faults, and the locations of the surface traces of these secondary faults to the northwest and southeast of Point Año Nuevo are not known, yet they obviously are part of the fault zone.

STRAIN AND DISPLACEMENT RATES ALONG THE SAN GREGORIO FAULT ZONE - The San Gregorio fault zone has long been recognized as juxtaposing strikingly different lithologic units along its 26-km onshore segment. The fault zone separates a thick section of middle and upper Tertiary rocks overlying granitic basement on the east from a relatively thin upper Tertiary section overlying Cretaceous sedimentary rocks on the west. Numerous workers (Branner and others, 1909; Brabb, 1970; Clark and Brabb, 1978; and Graham and Dickinson, 1978) have noted these discontinuities across the fault and have attempted to use them to determine the nature, timing, and amount of movement on the San Gregorio fault zone.

Based on its pattern of faulting (multiple vertical or near-vertical, near-linear fault strands in a wide zone), its branching from the San Andreas fault zone at Bolinas Lagoon, and the large stratigraphic discontinuities across the fault, most recent workers have considered the San Gregorio fault zone to be a predominantly right-lateral strike-slip fault that is part of the greater San Andreas fault system. Hill and Dibblee (1953) were the first workers to suggest that the San Gregorio might be a major right-lateral strike-slip fault. They based their suggestion on the similar characteristics and the relative orientations of the San Gregorio and San Andreas fault zones.

Recent studies of the offset of onshore geologic features by Graham and Dickinson (1978) indicate that approximately 115 km of right-lateral

strike-slip movement has occurred on the San Gregorio-Hosgri trend, probably within the past 13 million years because strike-slip movement on this fault began in late Miocene or post-middle Miocene. This suggests that the long-term strain rate along the San Gregorio fault zone has been approximately 9 mm/yr since the middle Miocene.

Direct evidence for late Pleistocene right-lateral strike-slip movement within the San Gregorio fault zone includes the apparent offset of small stream courses on the Santa Cruz terrace, geomorphic features, the pattern of faulting (left-stepping en echelon faults), and the apparent offset of shoreline angles of late Pleistocene marine terraces. Weber and Lajoie (1977 and 1979), and Weber and others (1977) have shown that two primary fault strands, the Coastways and Frijoles faults, offset the shoreline angles of the marine terraces in a right-lateral sense, and the higher (older) terraces have experienced progressively greater offset. A third primary (?) fault strand (Greyhound Rock fault) also may have experienced large amounts of late Pleistocene right-lateral strike-slip offset, but the evidence for such is not convincing.

Although only two marine terraces can be correlated through the fault zone, analysis of the shoreline angle offsets indicates that the average rate of right-lateral offset in late Pleistocene time (0-125,000 years B.P.) ranged from 1.0 to 2.0 cm/yr. and averaged 1.6 cm/yr. Average offset rates for the three primary traces are: Frijoles fault - 0.2 cm/yr., Coastways fault - 1.0 cm/yr., and Greyhound Rock fault - 0.4 cm/yr. Because of uncertainties associated with the offset on the Greyhound Rock fault, problems associated with age determinations for the Western terrace, and lower slip rates based on stream offsets, we would assign a Late Pleistocene right-lateral strike-slip displacement rate of 7-11 mm/yr to the San Gregorio fault zone. This is compatible with the late Tertiary slip rate of approximately 9 mm/yr. determined by Graham and Dickinson (1978).

In addition to the apparent large horizontal displacement along the fault zone, vertical displacement has occurred on all of the individual fault strands. Scarps in late Pleistocene alluvium and the steep linear front of the Santa Cruz Mountains along the Coastways fault are strong geomorphic evidence of considerable vertical offset on the Coastways fault during the Pleistocene and Pliocene. Similarly, the 0.8-km-wide southern portion of the Pomponio structural block, between the Coastways and Frijoles fault strands, has been downdropped as much as 40 m to form a graben that presently is being filled with alluvial sediments. Where exposed in the sea cliff near the mouth of Año Nuevo Creek, these deposits, dated at about 9,000-10,000 years by  $^{14}\text{C}$ , have been tilted slightly to the west and are tightly folded into a vertical orientation against the fault plane of the Frijoles fault strand. Several cyclical peat layers within these deformed Holocene alluvial deposits adjacent to the fault plane may represent episodic deepening of a sag pond caused by discrete tectonic movements on the fault. Well-preserved northeast-facing scarps across late Pleistocene alluvial fans can be traced to the northwest along the Frijoles fault where it crosses the Santa Cruz terrace at Point Año Nuevo. These scarps delineate the trace of the Frijoles fault and the southwestern edge of the graben.

In summary, the pattern of movement along the San Gregorio fault is characterized by right-lateral strike-slip movement with the two main loci of movement being the primary fault strands, the Coastways fault and the

Frijoles fault. The pattern of apparent vertical movements suggests that the Santa Cruz Mountains structural block (Figure 1) has been rising slowly during the late Tertiary and Pleistocene relative to the Pomponio and Pigeon Point blocks. Similarly, the Pigeon Point block has been elevated with respect to the Pomponio block during the Pliocene and Pleistocene, a fact emphasized by the absence of Purisima formation rocks in the Pigeon Point block. The Pigeon Point block appears to have been a site of non-deposition during the late Tertiary except at Point Año Nuevo, where the pattern of faulting is far more complex and the tectonics poorly understood. The Pomponio block appears to have been a downdropped block forming a graben between the Frijoles and Coastways faults during most of the Pliocene as it was the site of continuing deposition of Purisima formation sands and silts. During the late Pleistocene, the northern end of this block appears to have been uplifted while the southernmost portion at Point Año Nuevo has been continually downdropped, creating a small graben now filled with late Pleistocene fluvial sediments.

STRAIN ACCUMULATION OR CREEP - As indicated by Coppersmith and Griggs (1978, p. 35), there is no indication of strain accumulation or fault slip in the triangulation-survey data of the U. S. Coast and Geodetic Survey for the San Gregorio fault zone. Most of the resurveyed triangulation lines show no statistically-significant slip over the 16-year period between surveys.

Similarly, fault creep has not been observed or measured along individual faults of the San Gregorio fault zone. In our field mapping, we have taken particular care to look for evidence of creep such as cracked or offset cultural features, but to date no detailed or systematic studies have been made.

SEISMOLOGY - The historic record of seismicity for the San Gregorio fault zone is inadequate for assessing future seismicity in this area of the central California coast. Indeed, several large historic earthquakes occurred in the Monterey Bay area before the development of more accurate methods of locating earthquake epicenters (Griggs, 1973), but there are insufficient data to allow this information to be used in a meaningful way.

Only in the past 15-20 years has an array of seismographs been established to provide accurate monitoring of seismic activity along the Santa Cruz-San Mateo County coast. During this time, most of the earthquakes have occurred in the offshore areas southeast of Point Año Nuevo and have ranged in Richter magnitude from 2 to 4. Approximately 20 of the earthquakes occurred near the middle of Monterey Bay. The largest ( $M = 4.6$ ) occurred in 1971 (Coppersmith and Griggs, 1978). Fault plane solutions were calculated for several earthquakes that occurred between 1971 and 1977 (Coppersmith and Griggs, 1978). The highest-quality solutions indicated regional right-lateral shear with a component of compressional stress. Most solutions with non-vertical nodal planes are compatible with reverse faulting along planes dipping eastward at about 65 degrees.

The greatest historic earthquakes along the San Gregorio trend occurred on October 22, 1926, in Monterey Bay. The two shocks, both  $M = 6.1$ , occurred within one hour of each other. Mitchell (1928), in a detailed study of the intensities, found that both Santa Cruz and Monterey experienced intensities greater than VII on the eight-point Sieberg scale (Sieberg, 1923). The two largest earthquakes of the 1926 sequence were

located within 5 km of the mapped trace of the San Gregorio fault zone and about 15 km northwest of Monterey. Two significant aftershocks were centered about 20 km northwest of Santa Cruz, also within 5 km of the San Gregorio fault (Gawthrop, 1978). As Gawthrop points out, if these events were part of the main sequence, a 40-km rupture along the San Gregorio fault is inferred to be the cause of the earthquake sequence.

Based on these data it is clear that the San Gregorio fault zone is seismically active and that moderate to large historic earthquakes have occurred along it. Greene and others (1973) estimated that a half-length rupture of the fault could vary from 65-100 km. That rupture length is compatible with Gawthrop's suggestion that the 1926 events resulted from an approximately 40-km-long rupture along the San Gregorio fault zone. Using these rupture lengths, it is conceivable that an earthquake of Richter magnitude 7.2-7.9 could be generated along the fault zone (Greene and others, 1973). If the San Gregorio fault zone is connected to the Hosgri, the combined fault length is approximately 400 km, and a larger earthquake should be expected along the San Gregorio fault zone. A written communication from Wesson to Hall, Sarna-Wojcicki, and Dupre (1974) suggests that an earthquake of magnitude 8.5 might occur along the San Gregorio if the fault displacement has a significant vertical component. It therefore is entirely reasonable to expect future earthquakes of magnitude 7.0-7.5, and there is a distinct likelihood that a magnitude 8.0 to possibly 8.5 could occur along the San Gregorio fault zone.

PALEOSEISMOLOGY AND EARTHQUAKE RECURRENCE INTERVALS - Because there is essentially no historic record of seismicity along the onshore segment of the San Gregorio fault zone from Point Año Nuevo to Moss Beach, the evaluation of earthquake hazards, the determination of maximum earthquake magnitude, and the level of activity of the fault zone must all be inferred from paleoseismology, the study of prehistoric earthquakes.

Wallace (1970, 1980), Sieh (1978), and other researchers have used geologic techniques to approximate the size and number of earthquakes and their recurrence intervals along the San Andreas and other active faults. The techniques include analysis of such features as (adapted from Wallace, 1980):

- a) Microstratigraphic relationships along faults observed in natural or man-made exposures.
- b) Fault scarps and their profiles and erosional modifications.
- c) Offsets of geomorphic features and changes in profiles of stream channels crossing the fault.
- d) Regional geologic relationships that reveal long-term rates of displacement.
- e) Seismically-produced sedimentary structures (load and deformational structures and evidence of liquefaction events).
- f) Evidence of progressively greater offset through time of marine, lacustrine, and river terraces.

To examine and analyze the paleoseismic history of a fault effectively, one must find a study site that provides numerous distinct stratigraphic units, datable materials, and a particular geologic feature or set of relationships that records the occurrence of each faulting event.

The type of geologic feature or relationship that can be used to indicate unequivocally the occurrence of a paleoearthquake and associated faulting can vary from one site to another. In studies at Pallett Creek in Southern California, Sieh (1978) used sandblow deposits, clastic dikes composed of fine-coarse grained sand injected into sag pond deposits, as indicators of liquefaction events that must have been initiated by the intense seismic shaking associated with major earthquakes along the San Andreas fault. Slope angles and the number of facets on fault scarps, along with the sharpness of scarp crests, have been used by Wallace (1977, 1978) and Bucknam and Anderson (1979) to determine the number and approximate dates of faulting events in the Great Basin. On the Garlock fault, Burke (1979) used microstratigraphy and the presence of numerous unconformities to infer between nine and seventeen events in the past 15,000 years. Sims (1975) developed techniques to determine recurrence intervals by analyzing deformational structures in lacustrine sediments that are thought to have been produced by seismic loading in unconsolidated units weakened by liquefaction.

In our studies, we have used several different types of geologic evidence to develop models to explain the features exposed in man-made exposures and in sea cliffs because we found that no single technique was diagnostic.

## FAULT SCARPS ALONG THRUST FAULTS: SOME CONSIDERATIONS

INITIAL CHARACTERISTICS - A considerable volume of literature has been produced over the past three to four years regarding formation and modification of fault scarps. The primary work on this subject by Wallace (1977) presents a detailed analysis of the shape of fault scarps formed by normal faulting in the Great Basin, an analysis of processes of scarp modification, and an excellent discussion regarding the descriptive terms for fault scarp shapes and components. In this paper, we will use the same terminology for scarps and slope processes used by Wallace (1977, p. 1267-68).

During this study we found it necessary to develop new techniques of reconstructing sequences of events along thrust faults. Our attempts to apply Wallace's methods to our own study were complicated by our lack of knowledge of the initial characteristics and shape of the rupture zone and the scarp formed by movement along a thrust fault.

Although Wallace's scarp model for normal faults is not directly applicable to the original shape of thrust fault scarps, we have used a similar technique to analyze the modification of the scarps formed both by high-angle reverse faults and by low-angle thrust faults. Our preliminary analysis indicates that the initial shape of the fault scarp appears to be primarily controlled by 1) the magnitude of the surface displacement, 2) the strength and/or consolidation of the rocks, and 3) the angle of dip of the fault plane. Other factors will control the shape of the scarp, but these three factors are by far the most important and probably are of greater importance in determining the scarp shape of a reverse fault than that of a normal fault because reverse faults tend to form "overhanging" scarps which are inherently unstable.

DIP OF FAULT PLANE - The steeper the dip of the fault plane, the greater is the possibility that the scarp will closely resemble the scarps described by Wallace (1977). Along high-angle reverse faults the scarp may form with a well-developed free face along the fault plane and may have a relatively sharp crest. If, however, the dip of the fault plane is low, then it is very unlikely that a free face will form because the overthrust block will collapse. Under these circumstances, which apparently are quite common, the lip of the overthrust plate slides over the ground surface on the footwall block, generally "bulldozing" the rock and soils present on the footwall block. The scarp under these conditions would consist of a rounded mound-like ridge, a hump, or a mole-track scarp. Most of the material in the mole-track scarp would be crushed and broken rock and soil which would be highly susceptible to erosion.

MAGNITUDE OF SURFACE DISPLACEMENT - The initial shape and characteristics of the scarp also depend upon the magnitude of surface displacement. Obviously, the greater the vertical displacement is, the larger is the overhanging face of the scarp, and the greater is the possibility that the overhanging scarp will collapse during or shortly after fault movement. The initial scarps under these circumstances would consist primarily of a debris or talus slope developed almost entirely from gravity fall off the hanging-wall block. If the displacement is very small (less than 1 - 1½ feet), then it is probable that only a small mole-track scarp or hump will be present. It is highly doubtful that a free face would form during such a small

displacement. Consequently, a free face on the scarp may form during thrust faulting, but it is unlikely that one would be formed either during large displacements or during extremely small displacements. Therefore, a free face would be formed most commonly for some intermediate magnitude of vertical displacement.

CONSOLIDATION AND ROCK STRENGTH - The consolidation and strength of a rock also affect the shape of the scarp formed during faulting. The harder and more consolidated a rock is, the better are the chances that a free face will develop along the scarp; it is almost certain that no free faces will be formed on scarps in soft, poorly-consolidated sediment. In poorly consolidated materials, the surface rupture probably would produce a complex debris slope or mole-track scarp composed of bulldozed fault breccia and debris from the hanging-wall block. An excellent example of the effect of lithology on scarp characteristics is the observation of Barrows (1975, p. 103-104) on the surface rupture along the Oak Hill fault during the February 9, 1971, San Fernando earthquake. The scarp was defined sharply only over a graded bedrock surface where it was a prominent, partly overhanging 80-cm- (32 in.) -high scarp. There also was evidence of 32 in. (80 cm) of left-lateral slip. The dip of the fault plane was 62 degrees in bedrock that consisted of interbedded sandstone, siltstone, and conglomerate of the Towsley/Pico formation. The structural attitude of the bedrock was similar but not identical to that of the fault.

In both directions away from the sharply-defined scarp in the bedrock outcrop, the scarp could be traced for hundreds of feet as a mole-track scarp or surface hump in unconsolidated alluvium. Although the ground surface was cracked and warped, there was no evidence of faulting in the walls of a trench excavated across the mole-track portion of the scarp (Barrows, 1975, p. 103). Well-defined shear planes did not form in the soft, unconsolidated sediments; much of the deformation may have occurred as intergranular rotation and shifting of clasts and grains without formation of shear surfaces. Similar features also were observed along other faults, such as the Veterans fault, in the San Fernando area (Barrows 1975, p. 112, 113).

There is a relationship between rock hardness, scarp height, and the dip of the fault plane that controls the scarp shape. There are undoubtedly various combinations of factors that control the formation of an initial free face. Although these factors cannot be defined quantitatively yet, we can approximate quite well the probable shape of the initial fault scarp.

## THRUST FAULTING IN MARINE TERRACE TERRANE

In the two areas near Point Año Nuevo where we have studied reverse faulting we have worked exclusively on fault offsets of the lowest marine terrace (Santa Cruz terrace); consequently, both faults have a similar geologic setting. The wave-cut platform in both study areas is formed in hard, well-consolidated sedimentary rocks. Near Point Año Nuevo, the rocks are siliceous mudstone of the Monterey formation and sandstone of the Vaqueros formation. At the Cascade Ranch Quarry the bedrock consists of sandstone and siltstone of the Purisima formation. The hard bedrock is overlain by a marine terrace sequence that consists of relatively soft, poorly-consolidated to moderately-poorly-consolidated shallow marine sands and gravels overlain by poorly- to moderately-consolidated clay-rich fluvial deposits and slope-wash. The shallow marine sands are the softest and least consolidated of the rock units because of the absence of significant amounts of interstitial clay.

PATTERNS OF FAULTING - BEDROCK VS. TERRACE DEPOSITS - Within the bedrock units, most of the fault movement has taken place along pre-existing faults which are the primary zones of weakness. Movement generally is constrained to one or possibly a few fault planes. This should not be construed to mean that fault movement during earthquakes along reverse faults is constrained to a single fault. The patterns of breakage associated with the 1971 San Fernando earthquake (Oakeshott, 1975, and USGS and NOAA, 1971) are extremely complex; movement was distributed over many faults, most of which were disconnected and separated by thousands of feet at the surface. We suggest that on a small scale, for example along a single zone of surface rupture along one fault viewed in cross section, fault movement is constrained to one or possibly a few fault planes in moderate to well-consolidated bedrock. But in weakly consolidated surficial deposits, reverse faults typically rupture along numerous fault planes which splay off of the main fault creating an extremely wide complex zone of faulting.

A thrust-fault contact between bedrock units is exposed at only one place in the study area, at the sea-cliff exposure of the Año Nuevo thrust fault. Here, the fault is a 4-6-in.-wide gouge zone of slick plastic clay. The shearing is confined to a fairly narrow zone, and there is only one zone of breakage where the wave-cut platform is offset (Refer to Plate IV and Figures 8 and 9).

The zone of faulting in the terrace deposits exposed in the exploratory trenches, quarry, spillway, and sea cliff is far more complex. The most common characteristics observable are that the fault splays into multiple surfaces of breakage that flatten or assume a lower angle of dip in the soft, poorly-consolidated terrace deposits. The splaying of the fault into multiple shear planes probably results from a complex interaction between changing shear resistances in the rock and changes in the local stress field within the zone of movement during a faulting episode. Although there are multiple fault surfaces within the bedrock units on both the footwall and hanging-wall blocks, the intensity of fracturing is greater and the pattern of flattening is more consistent within the terrace deposits.

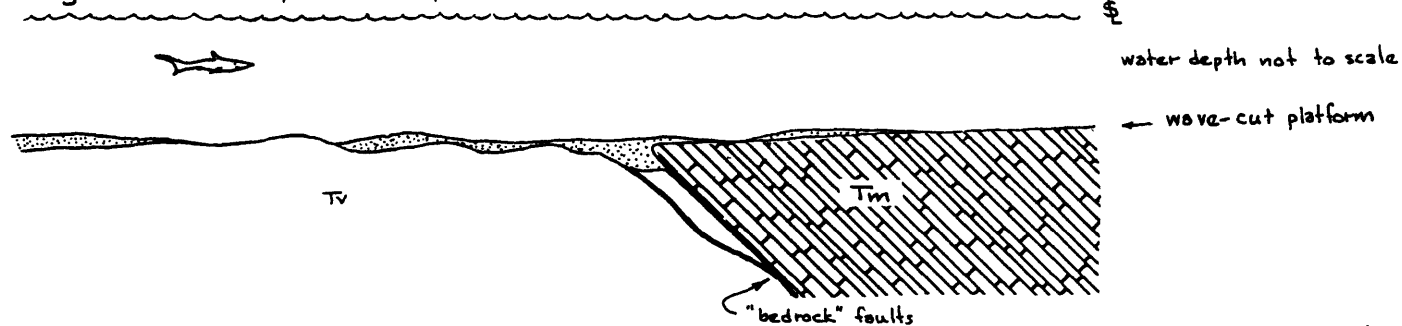
NEAR-SURFACE EFFECTS AND SCARP FORMATION - During this study we have noted distinctive features and patterns associated with thrust faults, and we believe that these features can be used to interpret the history of movement.

WEST

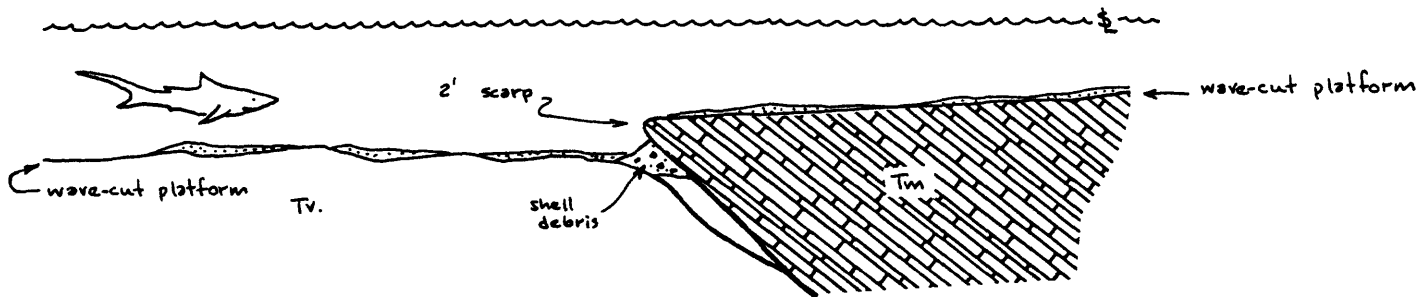
EAST

# FIGURE 8A

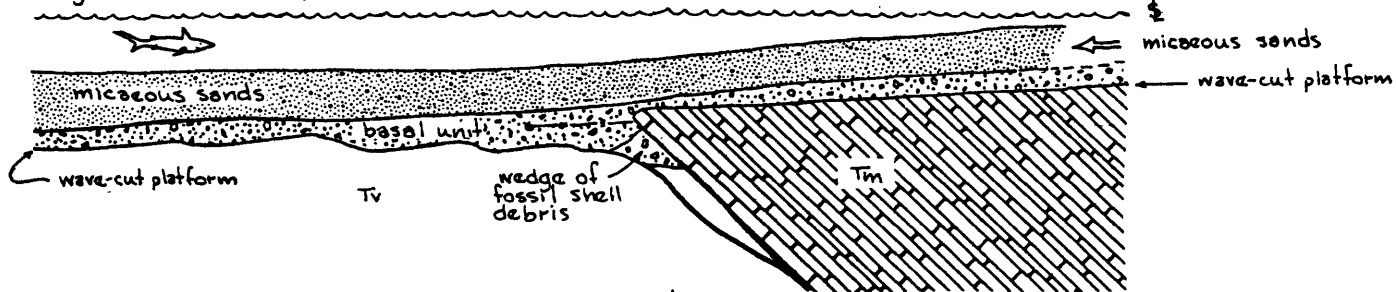
Stage 1 - Initial Shape (wave-cut platform 105,000 yrs. B.P.)



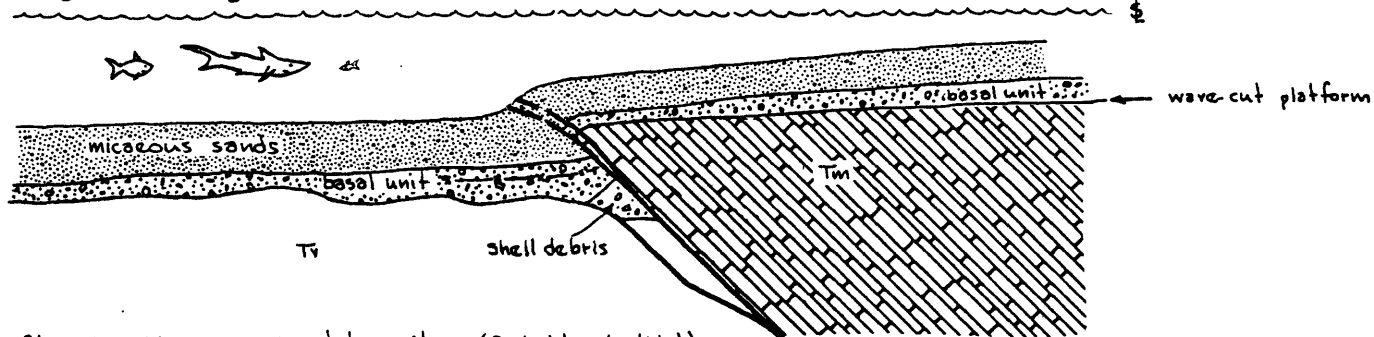
Stage 2 - Faulting Event Event # 1



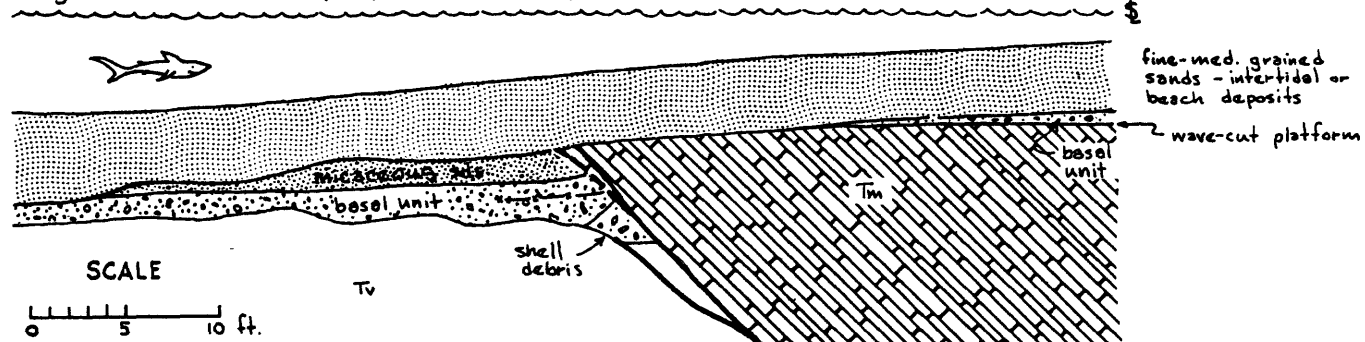
Stage 3 - Marine deposition



Stage 4 - Faulting Event Event # 2



Stage 5 - Marine erosion & deposition (Probably intertidal)



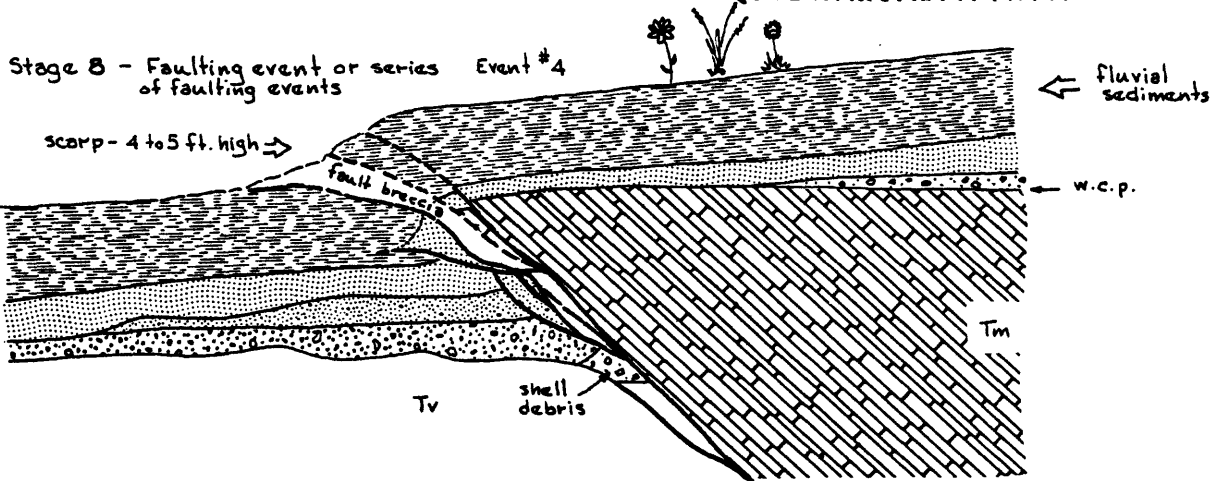
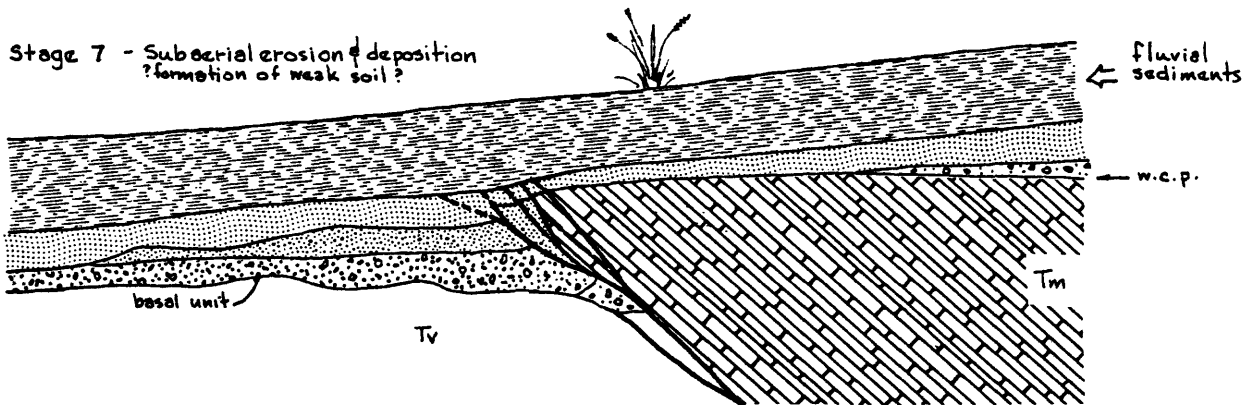
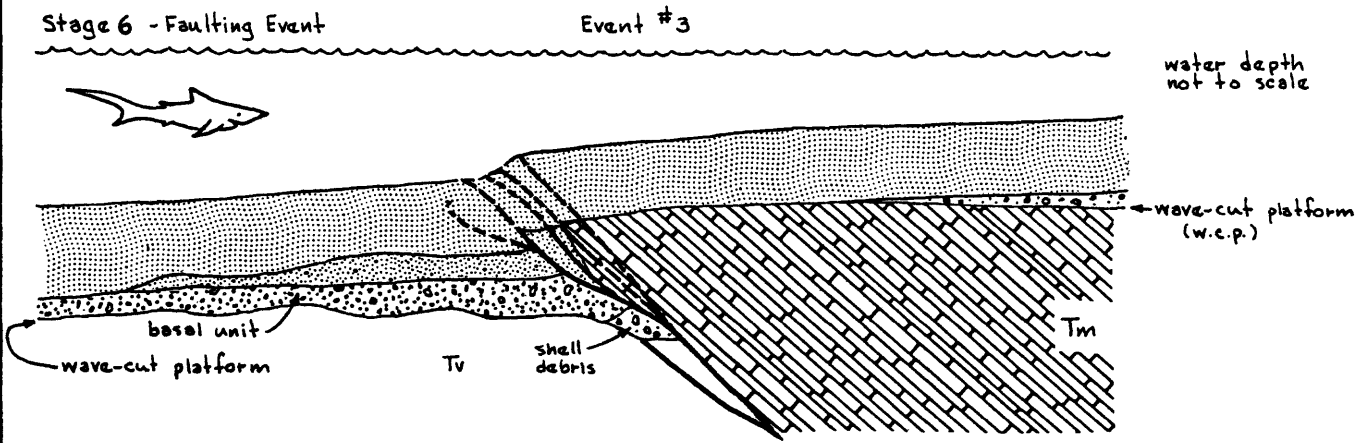
SCALE

0 5 10 ft.

no vertical exaggeration

Palimpsestic reconstruction of Late Pleistocene fault movement - Año Nuevo thrust fault at sea-cliff exposure

FIGURE 8B

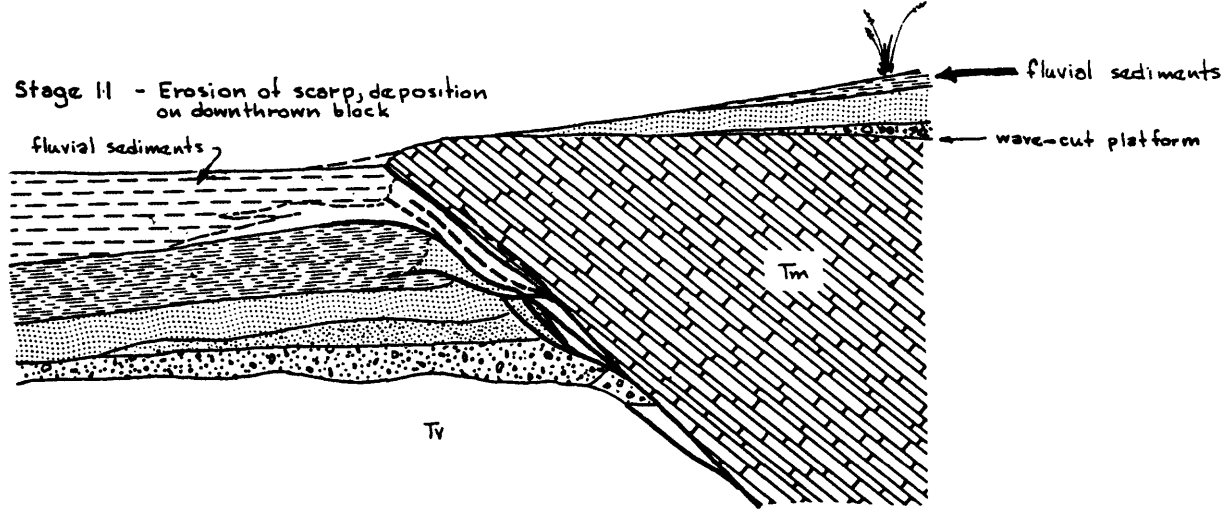
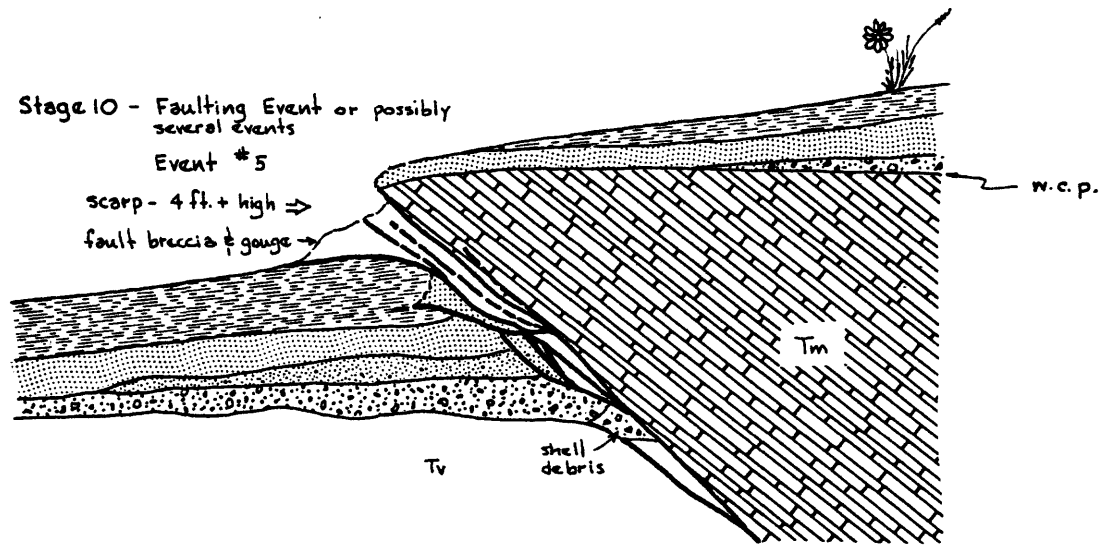
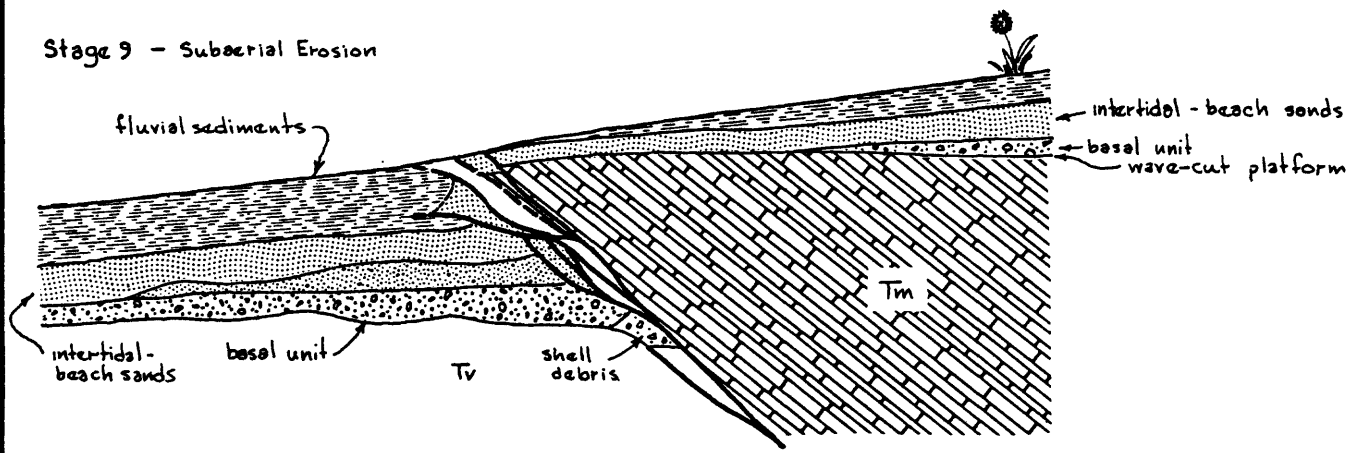


SCALE

0      5      10 ft.

no vertical exaggeration

Palimpsestic reconstruction of Late Pleistocene fault movement -  
Año Nuevo thrust fault at sea-cliff exposure (continued)



SCALE  
0 5 10 ft.  
no vertical exaggeration

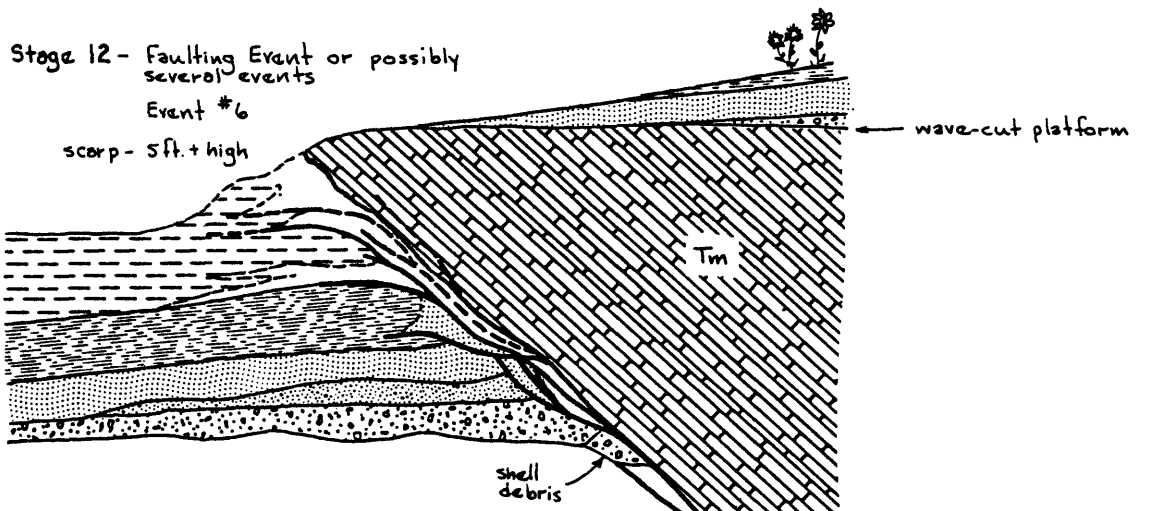
Palinspastic reconstruction of Late Pleistocene fault movement - Año Nuevo thrust fault at sea-cliff exposure (continued)

FIGURE 8D

Stage 12 - Faulting Event or possibly several events

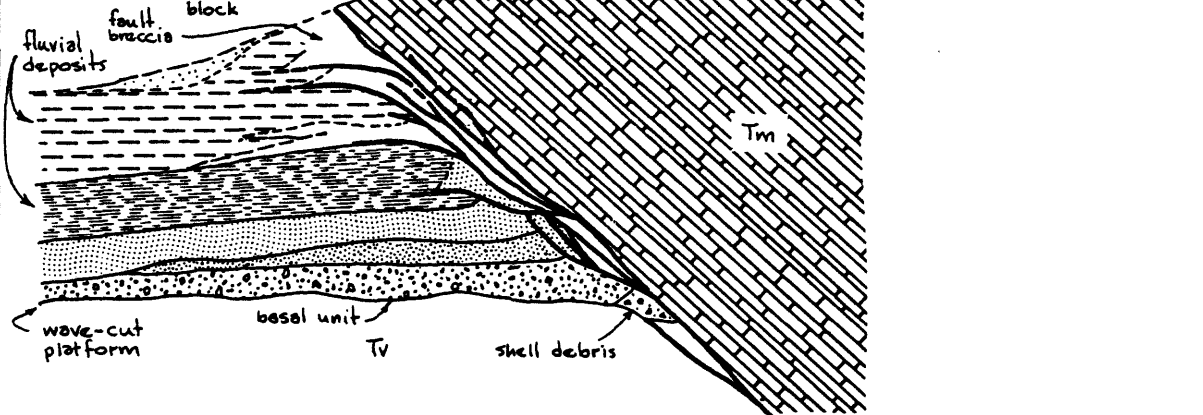
Event #6

scarp - 5 ft. + high



Stage 13 - Partial erosion of scarp.

Deposition on downthrown block



SCALE

0 5 10 ft.

no vertical exaggeration

Palinspastic reconstruction of Late Pleistocene fault movement - Año Nuevo thrust fault at sea-cliff exposure (continued)

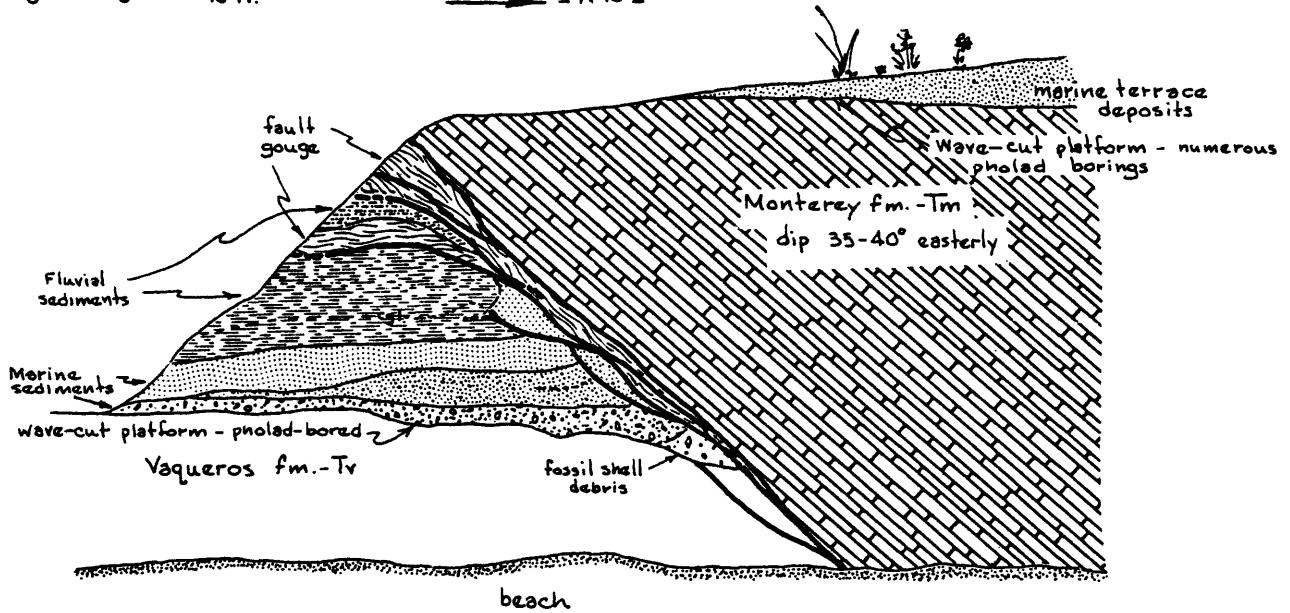
FIGURE 9

AÑO NUEVO THRUST FAULT  
SEA-CLIFF EXPOSURE  
Scale 1" = 10'

Geology generalized - for a more accurate  
and detailed log of the sea cliff exposure  
refer to Plate IV.

0 5 10 ft.

→ N 15 E



Vaqueros fm. - Dusky-yellowish brown phosphatic mudstone and thick bedded arkosic sandstone. Highly sheared in a zone about 50 ft. wide southwest of the Año Nuevo thrust fault. Tectonically-mixed clasts of mudstone and sandstone in matrix of sheared mudstone.

The mode of development of some of the features and their significance with respect to faulting events are discussed below.

Depending on fault plane dip, magnitude of displacement, and rock strength, movement along the fault will produce either an overhanging free face on the hanging-wall block, a mole-track scarp, or a mound of collapsed and/or "bulldozed" rubble and debris.

In our opinion, it is highly unlikely that a scarp with a well-developed overhanging free face would form in marine terrace sediments simply because of the poor consolidation of the sediments. If a free face were to form, it most likely would form in well-developed clay-rich "B" soil horizons or in relatively hard, clay-rich fluvial sediments, probably during the "dry" season when the clays are brittle. If a free face were to form during a faulting event, there probably would be less splaying of the fault into multiple shear planes, and the "bulldozing" action on the foot-wall block would be minor.

The most probable sequence of events during a faulting episode in marine terrace sediments is that the hanging-wall block is thrust up and over the footwall block to form a hump or mole-track scarp. The hanging-wall block slides out on the former ground surface so that soft sediments and soils are "bulldozed" up in front of the lip of the overthrust block. The leading edge of the overthrust block is a relatively thin wedge of soft marine terrace sediments that is pushed across the ground surface. Eventually, the frictional resistance to movement along the base of the overthrust plate exceeds the strength of the rock in the overthrust plate, and the movement is transferred from the original shear surface to a second or possibly more shear surfaces that splay off of the main fault break. During one faulting event, it is probable that several fault breaks will splay out from the same main fault. Many of these faults will flatten near the surface and become parallel to bedding on the footwall block which they are overriding; as the overthrust lip advances, the fault plane slides along the ground surface, which is parallel to the underlying bedding planes.

During fault movement, as the hanging-wall block slides out across the surface of the footwall block, the soft terrace sediments on the footwall block are "bulldozed" out in front of the overthrust plate, but they also are deformed by drag underneath the plate. Some of the sediments on the footwall block that initially are shoved ahead of the "bulldozing" upper plate do not maintain that position because the fault overrides the brecciated rock as the hanging-wall block is pushed farther and farther out over the footwall block. The sediments on the footwall block commonly are folded into broad anticlines and synclines by compression and are deformed by drag folding near the fault contact (Plates XII, XIII). Much of the deformation of the sediments on the footwall block is the result of what might best be described as a "rolling and mixing" action that apparently produces the extensive sub-fault conglomerate masses and breccias indicated in Plates XII, XIV, and XVI. There are few shear planes in these sub-fault conglomerates which appear to have been produced by grain and clast rotation, lateral and vertical transportation, and a rolling or dragging action beneath the fault plane. Because of the high clay content in the matrix, the deformation would have been plastic rather than brittle, particularly if the clayey matrix were wet. Much of the material in these breccias and conglomerates is thought to have originated as fault breccia, fault gouge, and colluvium and slopewash eroded off the fault scarp. These materials,

deposited between fault movements and also created during previous episodes of fault movement, eventually were overridden by subsequent fault movements, and the broken rock masses were incorporated into the "sub-fault" conglomerates.

Some of the fault breccias do not originate as masses of rock crushed, rolled, and dragged along under the overthrust plate. The lip of the overthrust plate itself brecciates and breaks up into masses of mixed rock with a clayey matrix. Consequently, the near-surface portion of the fault zone consists of a wide zone of broken and mixed rock. Near the surface, where subjected to the effects of weathering, most of these breccias and masses of mixed rock do not exhibit well-formed shear planes. Again, much of the deformation apparently occurs as inter-clast rotation and particle movement in a plastic (clayey) matrix. In addition, any thin shear planes must be obscured rapidly by weathering and translocation of clays.

Another feature present in the sub-fault masses of mixed and deformed rock is evidence of local "underthrusting" associated with the "bulldozing." Where jumbled masses of rock material on the footwall block seem to have been pushed ahead of the lip of the thrust, they sometimes are underlain by what appears to be the lip of the overthrust block that has acted in a manner similar to that of a bulldozer blade.

It often is not possible to link any one or two of these features to a particular faulting event or group of events because the faulting is complex, there are many splays off of the main fault, and a single faulting event along a thrust fault often causes movement along several closely-space faults. Although some features are indicative of a faulting episode, it is impossible to determine if two fault features are conclusive evidence of one or two separate faulting events.

In summary, thrust faults are extremely complex and difficult to evaluate because in any one faulting event, they can rupture along more than one surface within the zone of breakage. In soft sediments, thrust faults are characterized by their tendency to splay into multiple breaks with the individual breaks flattening near the surface. Brecciation of the rocks within the zone of movement and on the overthrust plate is intense, and the brecciated materials subsequently are disrupted even further during later fault movements by mixing, rolling and dragging under the overthrust block.

FAULT SCARP MODIFICATION - Our interpretation is that erosional modification of the fault scarps proceeds in a manner similar to that described by Wallace (1977). Any overhanging free face that forms begins to spall as material breaks loose from the face, and a cone of debris accumulates near the base of the scarp. The initial modification of the scarp is by the processes of rock fall, sliding, and slumping. The gravity-controlled slope, the free face, eventually is replaced completely by a debris slope. The larger the overhanging free face is on the scarp, the greater is the possibility that the face will collapse soon after formation and that the dominant slopes will be debris slopes controlled by rock sliding, rolling and other mass movement. The debris slopes form at the angle of repose for the size of material available and range between 27 degrees and 37 degrees. The slope angles of the scarp as a whole and of the debris slope decline primarily as a result of the deposition of a wedge of fine-grained sediment on the downthrown block, at the base of the scarp. This wash-controlled slope eventually overlaps and covers the debris slope.

Because it is doubtful that a free face would form in the terrace sediments, the initial scarp shape is likely to be either a hump or a mole-track scarp. On either of these types of scarps, the initial slopes probably would be debris slopes, and the initial processes of modification would include mass movement (slumps, slides, creep), rill wash, and unconfined overland flow. The predominant earth materials in the scarp would be crushed sediments and soil, materials with a very low resistance to erosion. It is likely that the rate of scarp modification would be very rapid.

Erosional Processes and Age of Fault Scarps - We have been unable to develop any significant data on scarp modification with age as did Wallace (1977) and Bucknam and Anderson (1979) in studies of normal faults in the Great Basin. Complications in our study area include more rapid processes of modification and possibly more frequent fault movement. In addition, there was only a single scarp to study, and it was difficult to determine the original scarp shape.

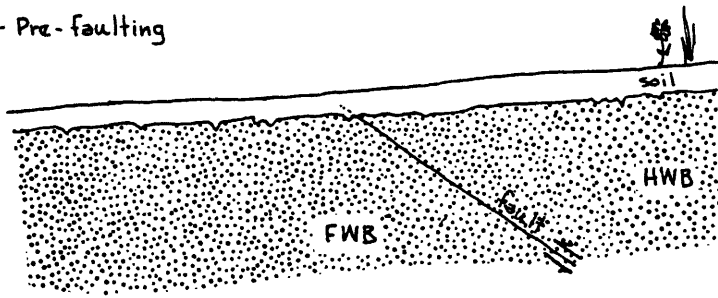
Free faces, if formed along thrust faults, apparently collapse rather rapidly. Wallace (1977) indicates that free faces associated with normal faults in the Great Basin in an arid to semi-arid climate, may last from several hundred to several thousand years depending upon the hardness and the degree of consolidation of the rock in which the scarp is formed. Kahle (1975) points out that the free face of an overhanging fault scarp (39-in. displacement) that formed in sandstone and conglomerate in the San Fernando Valley, California, was almost completely destroyed by weathering and erosion within three months after its formation. Less than half of the overhanging scarp was still present at that time and the original free face had been destroyed. A photo by Kahle (1975, p. 133) taken on May 9, 1971 shows that there had been a complete spalling off and collapse of the overhanging fault plane. Only a small portion of the overhang remained. The process of scarp modification almost exclusively was gravity fall of angular debris.

In the wet temperate climate of coastal central California, it is probable that geomorphic processes operate even more rapidly, and an overhanging free face in moderately-consolidated sediments might be destroyed in a couple of months with the associated overhanging portion of the scarp probably being destroyed within one, perhaps two, rainy seasons.

The origin of the fault scarp seems to preclude the use of principal slope angles to determine the age of the fault scarp. The principal slope angle on the scarp of the Frijoles fault is 14 - 15 degrees and, as expected, the slope is a wash-controlled slope. The scarp is 40-50 ft. high, and there is no evidence of multiple slope angles or scarps that would indicate several episodes of faulting.

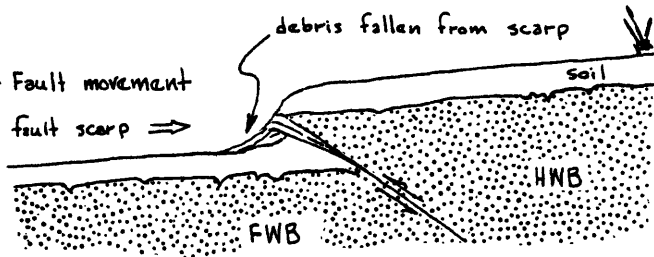
MODEL FOR RECOGNITION OF MULTIPLE FAULTING EVENTS ALONG REVERSE FAULTS - Our basic model consists of movement on a reverse fault accompanied by the formation of a hump or mole-track scarp at the surface (Figure 10). The scarp is gradually reduced by erosion; material is eroded off the hanging-wall block and deposited on the footwall block as a thin wedge of colluvium and slope wash (Figure 10). The dominant processes degrading the upper part of the fault scarp and depositing material on the toe of the slope are rill wash

Stage 1 - Pre-faulting

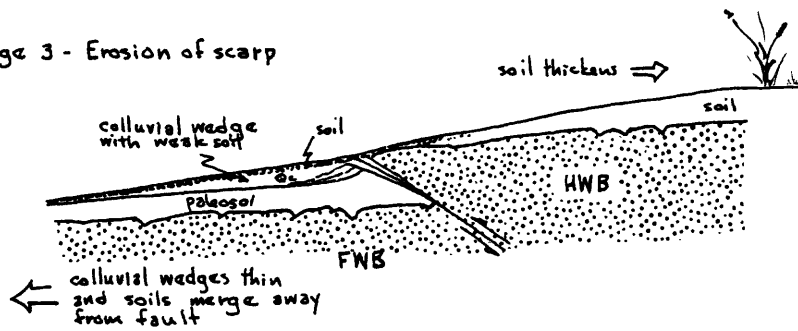


HWB - Hanging Wall Block  
FWB - Foot Wall Block

Stage 2 - Fault movement

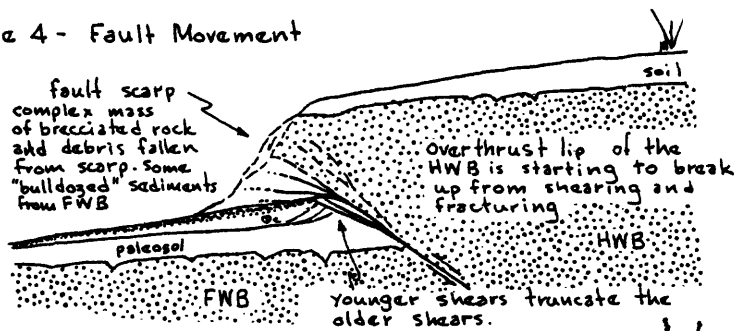


Stage 3 - Erosion of scarp

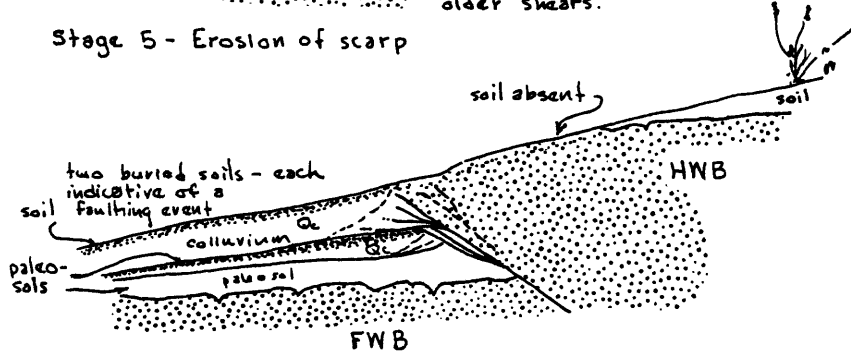


Faulting event recognized from buried soil on FWB

Stage 4 - Fault Movement



Stage 5 - Erosion of scarp



Faulting events recognized by presence of two buried soils and truncation of shears from first event by younger shear planes.

and unconfined overland flow (non-channeled). Mass wasting such as creep, slumps and slides occurs on the scarp, but the effects of these processes are minor compared to those of the wash processes.

A single faulting event followed by erosion of the scarp results in the development of a group of stratigraphic features indicative of faulting:

- 1) The wedge of colluvium thins away from the fault and is composed of materials derived from the upthrown (hanging-wall) block.
- 2) The wedge of colluvium generally has a weakly-developed soil or no soil at all.

If significant amounts of soil material are eroded from the hanging-wall block, these transported soil materials are incorporated into the colluvium that collects on the footwall block. The resulting complex mixture of pre-existing soil and in-situ soil material may resemble a moderately well-developed soil.

- 3) The colluvium buries the pre-faulting event soil; therefore, the buried soil indicates a period of quiescence between faulting events.
- 4) The buried soil unit is offset or truncated by fault planes.
- 5) The soil on the hanging-wall block is thin or absent near the fault and thickens away from the fault.
- 6) If repeated movements occur, each event may be represented by a similar buried stratigraphic unit and/or soil.
- 7) If repeated movements occur, then the shear planes or faults associated with the earlier movements often are truncated by younger shears (Figure 10).

Therefore, under ideal conditions each faulting event is represented in the stratigraphic section on the footwall block by a weakly-developed paleosol and/or a distinct colluvial wedge. The formation of a wedge of colluvium with a weakly-developed soil in response to each faulting event is dependent on 1) the size of the faulting event, 2) the length of time or recurrence interval between faulting events, 3) the climatic conditions and 4) the consolidation and resistance to erosion of the material in the scarp.

If, for example, the individual faulting event is large (surface displacements of 10-15 ft. or greater), the recurrence interval short, and the climate arid, then the scarp may be too large to be completely degraded between faulting events. In a similar fashion, the same scarp might be completely degraded during the same time interval in a wet, temperate climate, or it might be degraded even in an arid climate if the scarp is formed in a poorly-consolidated sediment. Consequently, it is obvious that only under ideal conditions ((1) scarp formed in relatively soft, poorly-consolidated sediments, (2) moderate scarp height, (3) temperate-wet

climate, and (4) relatively long recurrence interval) will a colluvial wedge with a soil be developed as a result of each episode of fault movement.

If the displacement associated with the faulting event is very small, then it is likely that the faulting event will not be represented in the stratigraphic record. A small scarp may degrade rapidly, but the colluvial wedge will be very thin, and most, if not all, of the material transported down the scarp will consist of "A" and "B" soil horizons. Consequently, erosion of material off the scarp will produce a slightly-thickened section of soil on the downthrown block because the transported soil will rapidly blend into the pre-existing soil as it is exposed to weathering processes. It therefore is impossible to recognize evidence of ground rupture occurring during an earthquake using this method if the surface displacement is small because the thickness of soils along the scarp can be quite variable (Plate XVII).

We concluded that we simply were not able to recognize with certainty any faulting events that produced surface displacements of less than 1 - 1½ ft. regardless of the technique used. The faulting events with 1 - 1½ ft. of surface displacement that we believed were recognizable in the footwall block stratigraphy were not clear nor obvious features, and they may well have represented movement along multiple shears during one faulting event rather than two separate events.

Variations on this basic model and other techniques have been used in this study to identify faulting events in the stratigraphic record. In areas of active erosion and deposition, the records of faulting events are not necessarily preserved on the footwall block as buried paleosols. As indicated in the analysis and palinspastic reconstruction of the Año Nuevo thrust fault (Figures 8a, b, c, & d) erosion (either shallow marine or sub-aerial), with one exception, apparently was sufficient to completely degrade the fault scarp, and there were no soils formed. After the erosional removal of the fault scarp, sedimentary units typically were deposited across the fault completely burying it. This relatively uniform layer of sediment was offset by subsequent fault movement, and the scarp was degraded once again by erosion. Typically, the sedimentary units are thinned or completely eroded from the hanging-wall block while the same unit on the footwall block typically is much thicker. Using the absence or thinning of strata on the hanging wall that are present on the footwall, reasonable inferences can be made regarding movement on the fault.

Another of the basic techniques used in the analysis consisted of using cross-cutting relationships such as truncations of strata and faults by younger faults and truncations of faults by unconformities and sedimentary units. This method is simply a combination of microstratigraphy and micro-structural geology. For example, in most of the outcrops it is possible to make reasonable inferences of repeated fault movements by noting such features as:

- 1) Shears of a previous faulting event truncated by another set of shears (Figure 8b, Stage 6 truncated by Stage 8).
- 2) A depositional unit covering (unconformably overlying) a fault and offset by an obviously younger fault or set of faults (Plates XII, XIV). This is considered to be evidence of two faulting events separated by scarp erosion and deposition of a colluvial wedge.

These types of features can be used quite readily, for as a reverse fault continues to move through time, there is an apparent upward migration of the faulting within the sediments on the footwall block (Plates IV, V, VI, XIII and Figures 8, 9). Hence, the record of faulting alternating with deposition and/or erosion is preserved. The trench and sea-cliff logs indicate that the faulting events apparently do migrate upward because as the stratigraphic section on the footwall block thickens, the older previous zones of breakage are not reactivated. This results simply because the zone of maximum displacement is directly beneath the hanging wall and will be rather closely constrained to that position unless it has the opportunity to break toward a "free" or unconfined surface, in the direction of least stress. An obvious example is the non-reattivation of the faults associated with Faulting Event #3, Stage 6, (Figure 8b) or Faulting Event #4 of Stage 8 (Figure 8b). The faults apparently are never reactivated, and the zone of maximum movement (displacement) migrates upward in the section on the down-thrown block.

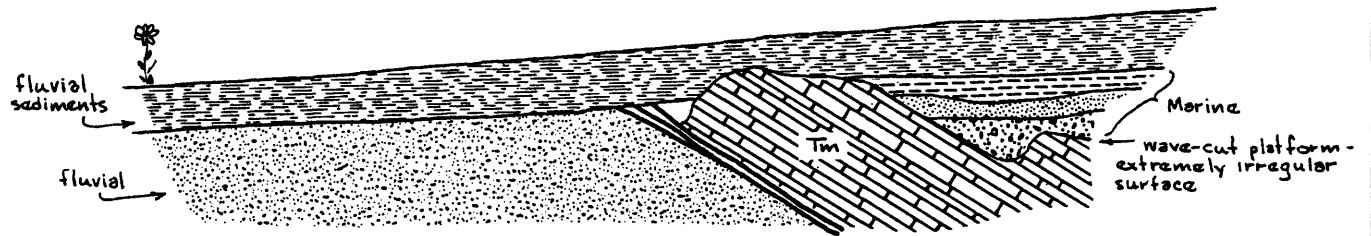
The "bulldozed" zones of rock associated with the fault movements also can be used as indicators of individual faulting events. As indicated in the Año Nuevo thrust fault trench logs (Plates V & VI and Figures 11a and b), wedges of fault breccia apparently were forced into overlying sedimentary layers, mixing a mass of pre-existing breccia with the overlying sediment. Each of these events is discernable because the breccia consists of two depositional units present on the footwall block mixed with brecciated rock derived from the hanging-wall block and fault gouge. In interpreting this feature as evidence of a faulting event, we assume that during fault movement a mass of fault breccia containing broken rock from both the hanging-wall and footwall blocks is pushed into the overlying rock unit on the footwall block. If this is not the case, it is difficult to explain how rock material from the underlying sedimentary unit on the footwall block has become vertically mixed with the next overlying sedimentary unit. Often, the sedimentary units on the footwall block are sufficiently distinct to allow the discrimination of relatively small faulting events, with displacements of approximately 1½ feet. The use of a vertical sequence of these bulldozed and mixed zones on the footwall wall block combined with micro-structural relationships of the shear planes can be used to interpret the history of movement (Figures 11a and b).

The last microstratigraphic method of distinguishing faulting events is the use of "interbedded" sequences of fault breccia and alluvium to indicate different faulting events. If, for example, a fault breccia that has overridden the ground surface of the footwall block or a wedge of fault scarp colluvium is overlain by fluvial sediments and the fluvial sediments in turn are truncated by a fault or overlain by another fault breccia, the sequence preserves the record of two faulting episodes separated by a period of erosion and deposition. Figures 8c and d, Stages 9-12, depict such a sequence. Again, sequences of this type can be used effectively to distinguish relatively small surface displacements.

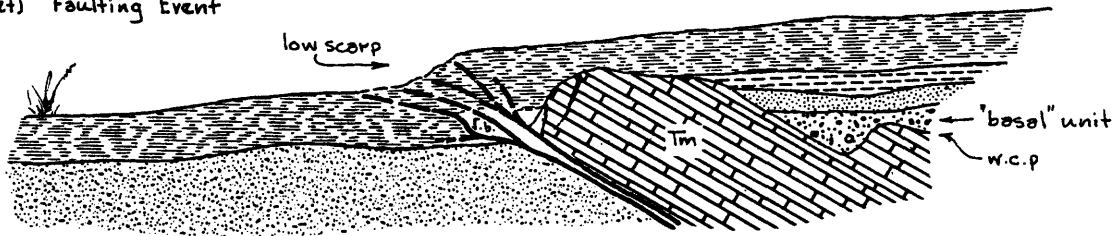
In summary, we have distinguished individual faulting events not by the recognition of any one feature but by careful observation of the micro-stratigraphy and the microstructure of the fault exposures. The model

FIGURE 11A

Stage A(et) - Erosion and deposition

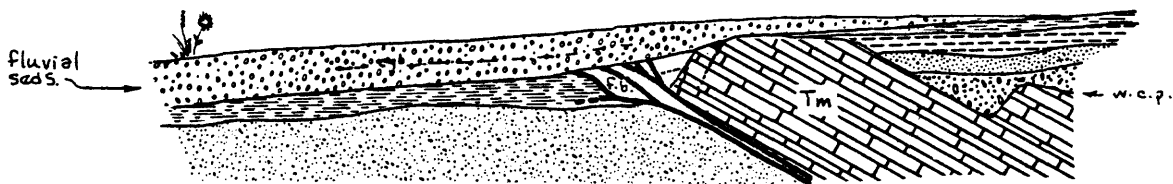


Stage B(et) Faulting Event



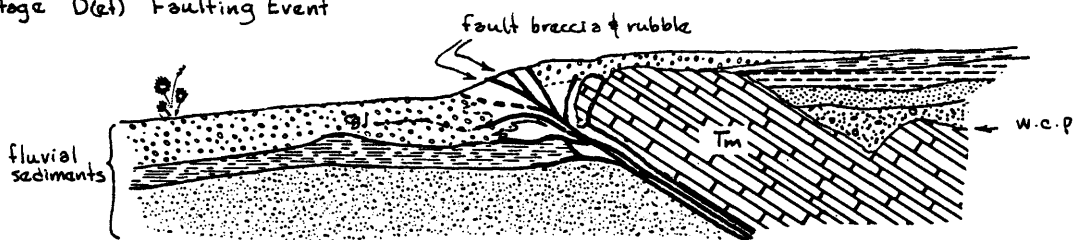
f.b. - fault breccia

Stage C(et) Erosion and deposition



f.b. - fault breccia

Stage D(et) Faulting Event

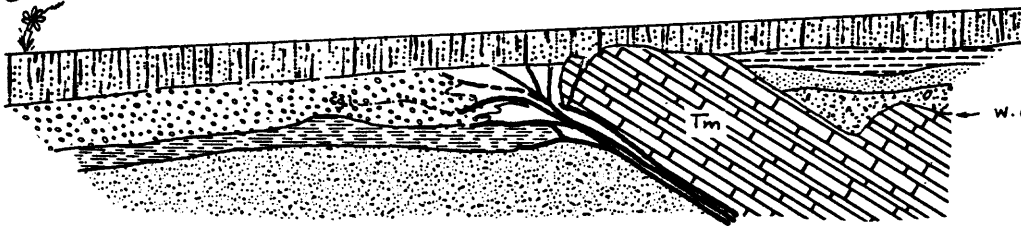


SCALE  
0 5 10 ft.  
no vertical exaggeration

Palinspastic reconstruction of Late Pleistocene fault movement -  
Año Nuevo thrust fault at Trench AN-1

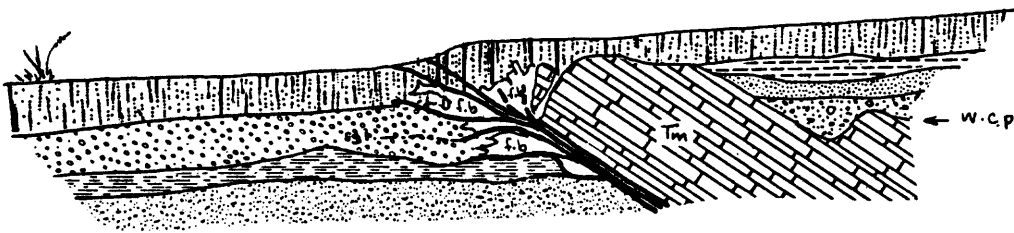
**FIGURE 11B**

Stage E(e1) - Erosion and deposition



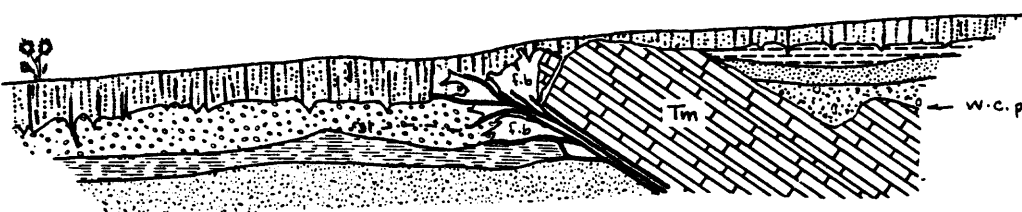
interdune sd deposits  
C-14 age of  
6060 B.P. (Beta-1083)

Stage F(e1) - Faulting event

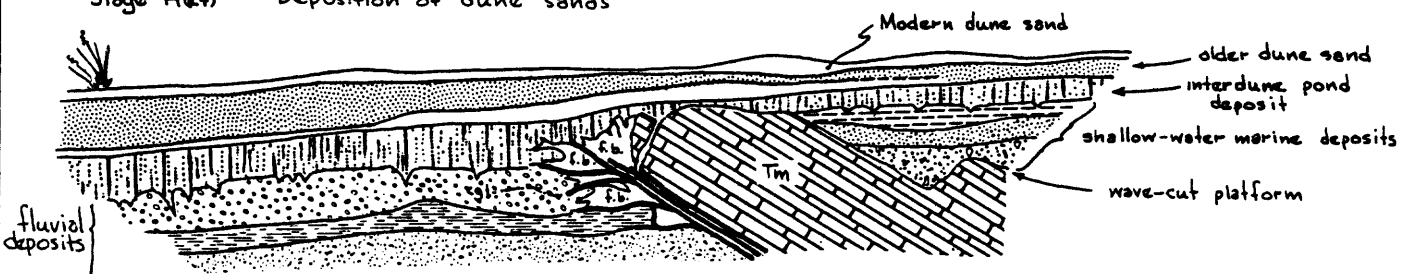


dark black, peaty, clayey sand.

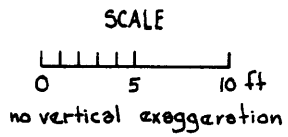
Stage G(e1) - Erosion of scarp - ? minor deposition on foot wall block



Stage H(e1) - Deposition of dune sands



f.b. - fault breccias



Palinspastic reconstruction of Late Pleistocene fault movement - Año Nuevo thrust fault at Trench AN-1 (continued)

used as a basis for interpretation is simple; it is based on the erosion of the fault scarp formed during each faulting event. Because the original model is applicable only in ideal cases, we have used several kinds of stratigraphic and structural relationship (discussed above) to distinguish faulting events. Although some of these relationships are not positive proof of faulting events, they are strong evidence when viewed in the context of the mechanics of thrust faulting and its near-surface effects.

## AÑO NUEVO THRUST FAULT

FIELD RELATIONSHIPS AND DESCRIPTIVE GEOLOGY - The Año Nuevo thrust fault is exposed in the sea cliff along the south shore of Point Año Nuevo about 1400 ft. east of the point (Plate I & II, Figure 5). It is a low-angle reverse fault (thrust) striking N 30 degrees to 50 degrees W, dipping an average of 37 degrees to the northeast, that offsets the wave-cut platform and deposits of the Santa Cruz marine terrace (105,000 B.P.). The fault juxtaposes siliceous mudstones of the Miocene Monterey formation in the hanging-wall block against contorted and sheared arkosic sandstones and mudstones of the Miocene Vaqueros formation (Clark and Brabb, 1978, p. 9) in the footwall block. The Monterey formation is thrust out and over the deposits of the Santa Cruz terrace that lie on the footwall block (Figures 5, 7, and 12).

The total offset of the pre-Quaternary rocks cannot be determined, but it may have been rather extensive because a zone of intense and complex shearing 50-60 ft. wide is present in the sea cliff on the footwall block. The zone of complex fracturing and shearing exposed in the sea cliff could be considered to be even wider, perhaps several hundred feet. The mudstones, sandstones, and andesite breccias exposed in the footwall block in the sea cliff, from the fault west to the vicinity of a small volcanic headland, have been intensely fractured and altered and are cut by numerous siliceous, dolomitic, and pyrite-rich veins. But because this area is near the axis of a gentle anticlinal fold in the Tertiary rocks, much of the fracturing and shearing may be related to extensional faulting and fracturing at the crest of the anticline.

The 105,000-year-B.P. wave-cut platform and deposits of the Santa Cruz terrace have been vertically displaced approximately 17-18 ft. The terrace deposits on the hanging-wall block are very thin and have been completely removed by erosion near the fault. Therefore, only a low, highly-modified fault scarp that follows a narrow linear outcrop of Monterey formation is present at the surface (Plate II, and Figures 2 and 12). Preserved on the footwall block is a 16-ft.-thick sequence of marine terrace deposits that stratigraphically records six to possibly nine faulting events in the past 105,000 years (Figures 8 and 12, Plate IV).

SURFACE MAPPING OF THE AÑO NUEVO THRUST FAULT - The Año Nuevo thrust fault can be traced to the northwest into the dune field simply by following the scattered outcrops of Monterey formation and the low scarp until both are lost in the thin cover of dune sand and vegetation (Plate II) about 290-300 ft. northwest of the sea cliff. We used magnetometer surveys, seismic refraction surveys, and hand-augered core holes in an attempt to locate the "lip" of the thrust fault accurately under the thin layer of "older" dune sand. The data from these studies are in Appendix A, and the locations of these surveys and borings are indicated on Plates I & II and Figure 2.

Magnetometer Surveys - The instrument used was a Geometrics Model G-816 proton precession magnetometer carried on an 8-ft. staff. No corrections for time variations were made because all of the individual surveys at Point Año Nuevo were conducted in less than 5 minutes. The ends of survey lines were marked in the field, and readings were taken at 10-ft. intervals. The data were plotted directly on the base map and on field profiles. The total field reading was used with no

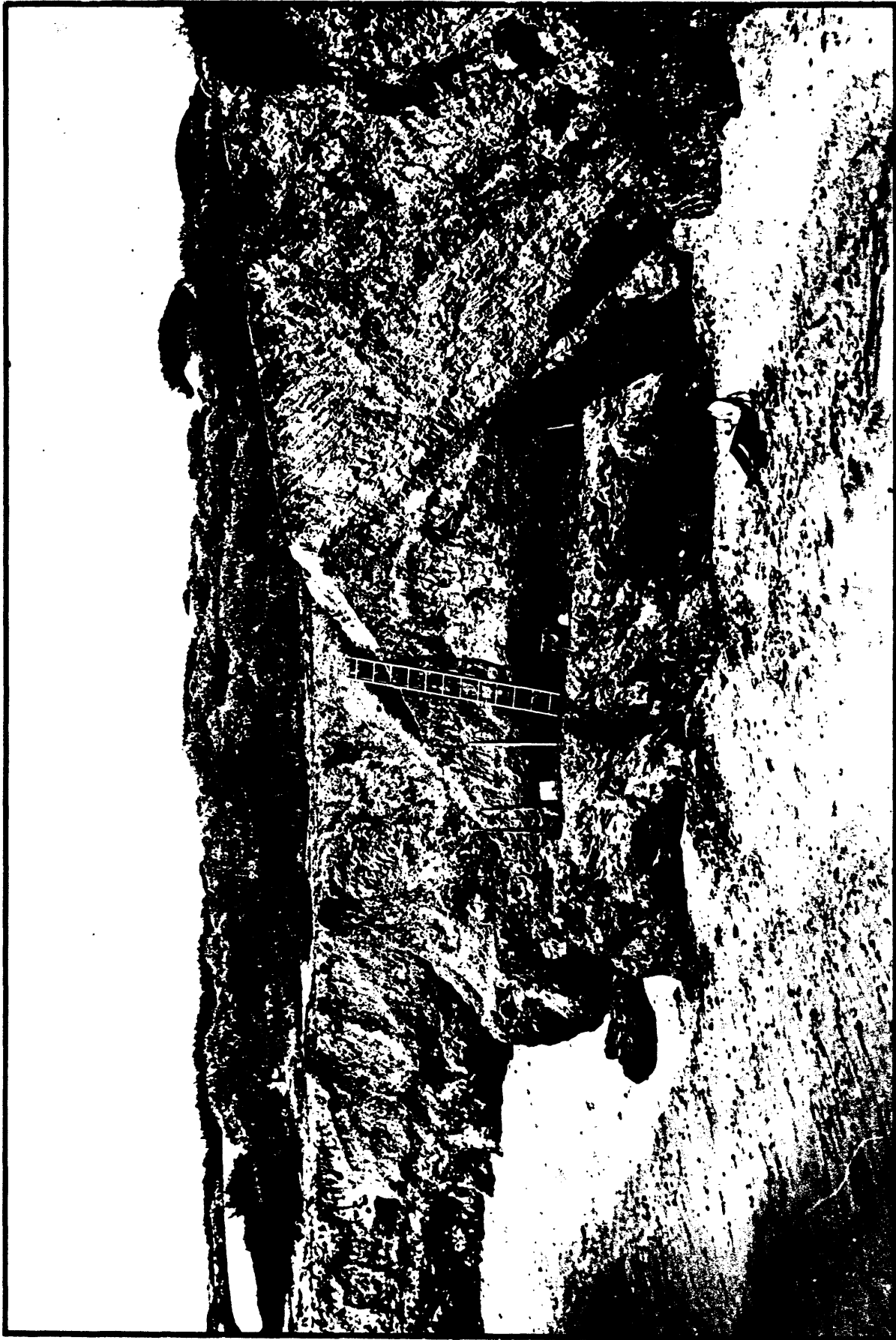


FIGURE 12 Sea-cliff exposure of the Año Nuevo thrust fault. Offset of the wave-cut platform is approximately 17 feet. Ladder standing on the wave-cut platform on the down-thrown block. Platform barely visible on the upthrown block near the right edge of photo.

attempt made to subtract regional gradients. The overall pattern shown on the magnetometer profiles is a linear magnetic high, the crest of which lies about 100 ft. southwest of the surface trace of the fault near the sea cliff. The intensity of the high is approximately 40-70 gammas out of a total field of about 700,000 gammas. The magnetic high can be traced to the northwest 300 ft. where its crest lies only 40 ft. southwest of the surface trace. At the site of Trench AN-1, the crest of the high lies directly beneath the surface trace, and the intensity of the high is only about 30 gammas (Magnetic Surveys L3A and L3B; See Appendix A). Northwest of the trench site (Plates I & II), it is impossible to pick up any consistent pattern in the magnetometer surveys.

The reasons for the presence of a magnetic high in the area of the footwall block are not known, but it may be related either to the presence of shallow marine deposits under the thrust fault or to differences in water content. The shallow marine deposits apparently contain more biotite and magnetite than either the fluvial deposits or the bedrock units, and these would give a slightly higher reading of the total magnetic field. The linear anomaly is larger near the sea cliff because the overlying fluvial deposits and older dune sands are thinnest at that point. The throw on the fault decreases to the northwest, and the thickness of fluvial deposits increases slightly. The thickness of the overlying blanket of dune sand increases greatly to the northwest. That may explain why the linear anomaly decreases and disappears in that direction.

Although the broad linear anomaly can be traced subparallel to the fault through the dune field, the magnetometer surveys were of no real use in pinpointing the surface trace of the fault under the older dune sand. The anomaly is too broad for use in the selection of the site for an exploratory trench. On three of the four profiles, L0, L1A, and L2A, a 50-60 ft.-long exploratory trench centered on the anomaly would not have intersected the fault. On the other hand, centering the exploratory trench on the magnetic anomaly on the fourth profile, L3A-L3B (Plate II), would have placed the trench directly across trace of the fault.

In summary, we found the magnetometer surveys to be of minor use in the selection of the trench sites. In this geologic setting, the magnetometer is not capable of distinguishing the location of the surface trace of the fault with the accuracy needed to allow the placement of an exploratory trench. It seems that thrust faults, with their fault planes dipping at low angles, are not well-suited to mapping by magnetometer; the inclined contact between the different rock types always will produce a gradual change in the total field and hence a broad, ill-defined anomaly.

Seismic Refraction Surveys - Seismic refraction surveys were conducted with a Nimbus-Geometrics Model ES-100 single-channel signal enhancement refraction seismograph. Seismic impulses were produced by a hand-held hammer. Eight seismic refraction surveys were conducted along the Año Nuevo thrust fault near its exposure in the

sea cliffs on the south side of the Point (Plates I & II) (See Appendix A for seismic survey data). Another five seismic surveys were conducted along the access road through the dune field that lies 1000-1200 ft. inland from the south shore.

The seismic surveys were run with the intent of locating the thrust fault and mapping it through the dune field. We believed that if we avoided areas of unconsolidated dune sand by staying in the interdune areas, the fault might be located in two different ways: 1) The depth to the velocity interface (contact) between the marine terrace deposits and the wave-cut platform should vary markedly on opposite sides of the fault. We expected that the depth to the wave-cut platform would be 2-5 ft. on the hanging-wall block and 15-20 ft. on the footwall block. 2) If the seismic refraction survey is run directly over the fault, then an anomalous distance-time plot should occur.

The use of this technique, however, requires the existence of a significant velocity contrast between the bedrock of the wave-cut platform and the overlying marine terrace sediments, and a relatively uniform contact between units. The wave-cut platform usually is assumed to be essentially planar. Unfortunately, the platform is known to have some major irregularities which cause difficulties in interpreting the time-distance plots. A quick scan through the seismic survey time-distance plots (Appendix A) indicates that there is no consistent variation in depth to the velocity interface which would allow one to determine on which side of the fault the survey was conducted. Indeed, some surveys indicate greater depths to velocity interfaces on the hanging-wall block than on the footwall block, and the calculated depths are twice the known depth to bedrock.

The probable reason for the apparent absence of a velocity contrast, particularly on the hanging-wall block, is the intense crushing and shearing of the bedrock and the presence of thick brecciated zones and gouge zones in the fault. The crushed and sheared rocks in the gouge zones and the overthrust lip of the hanging-wall block all have low velocities and cannot be distinguished seismically from the terrace deposits. Therefore, the seismic refraction technique is only marginally useful for mapping the fault in this geologic setting.

Hand Auger Core Holes - Hand augering of core holes through the dune field was the simplest and most efficient technique of delineating the subsurface location of the fault under the thin layer of older dune sand. This was the technique used to site the exploratory trench. Seventeen core holes (Appendix A and Plate II) were advanced to a maximum depth of 9 ft. and the cuttings logged. The hanging-wall block was identified easily by the shallow depths to refusal. The core holes provided useful information on the stratigraphy of the marine terrace deposits and facilitated trench siting in an area underlain by interdune pond deposits.

The only drawbacks to the hand auger technique are that holes tend to collapse readily below the water table in unconsolidated sediments, and augering is very time consuming if the sedimentary cover is thicker than about 5-6 ft.

NORTHWESTERN EXTENT OF THE AÑO NUEVO THRUST FAULT - As indicated in Plates I & II, the Año Nuevo thrust fault cannot be traced more than 200-250 ft. northwest of the exploratory trench. The "lip" of the fault obviously lies between core holes CH-AN-13 and CH-AN-14 at which point its northwest strike becomes more northerly. North of this point, the fault apparently is concealed by a recently-stabilized sand dune.

We attempted to locate the northern extension of the Año Nuevo thrust fault where it intersected the road through the dune field (Plate I). Magnetometer surveys parallel to the road showed no indication of the fault. Field work was hampered by dense vegetation and a 2-4-ft.-thick layer of loose sand at the surface. Seismic refraction surveys that we conducted parallel to the road were interpreted to indicate relatively-thin marine terrace deposits with the wave-cut platform at a depth of 5-10 ft. Time-vs.-distance plots of seismic surveys SS-AN-12 & SS-AN-13 (Appendix A) have enough discontinuities to suggest the possible presence of a fault. Consequently, we were fairly certain that we would find the continuation of the thrust fault at the bend in the road near seismic surveys SS-AN-10 and SS-AN-11 (Plate I).

We also considered the possibility that the Año Nuevo thrust fault might die out under the dune south of the road and that the strain might be transferred to an en echelon fault lying to the northwest. The Año Nuevo thrust fault might be one of a series of left-stepping en echelon faults trending roughly N 55 degrees W through the dune field. This interpretation is supported by the existence of a linear ridge of Monterey formation exposed in the dune field (Plate I). The outcrop lies 6-7 m higher than the anticipated elevation of the wave-cut platform at that point and is therefore an anomalous feature.

To test this hypothesis, we attempted to trench along the access road in the dune field. The task was essentially impossible because the upper 5-6 ft. of all three test pits (AN-TP1 - AN-TP3; Appendix A and Plate I) were in unconsolidated to poorly-consolidated dune sand which continued to cave into the hole. We had to determine the stratigraphy of the pits from the spoil pile materials because it was impossible to keep the pits open for logging. Our cursory examination indicated that nearly identical stratigraphy was exposed in all of the pits; our initial interpretation from the seismic surveys was incorrect. The velocity interface between 5-10 ft. in depth, originally thought to represent the wave-cut platform, is within the marine terrace deposits and probably represents the contact between the older dune sands and the underlying fluvial deposits.

None of the excavations (13-14-ft.-deep pits) was deep enough to expose the wave-cut platform, and there is no indication on any of the seismic survey time-distance plots of a second velocity break that would represent the surface of the bedrock unit. Because the seismic survey lines were 80-100 ft. long, it is probable that the depth to the wave-cut platform is at least 20 ft. and possibly 25-30 ft.

Because there was no indication of faulting in the three test pits nor on the seismic surveys (based on our reinterpretation), we could not locate the Año Nuevo thrust fault in this area nor determine whether the fault continues as far north as the road or dies out. If the fault lies outside of the area that we studied along the road, then the great depth to the wave-cut platform in the vicinity of the test pits and along the road suggests that our area of investigation must lie on the footwall block. If the Año Nuevo thrust fault continues this far to the north, the trend of the fault must be north or slightly east of north, and the fault must lie northeast of seismic survey SS-AN-9.

A fourth test pit, AN-TP-4, was excavated across the bedrock ridge that crops out in the dune field near the end of the road (Plate I) to determine whether or not the ridge is fault bounded. No indication of faulting was found on either side of the outcrop which appeared to be at the crest of a broad rounded ridge or knob. Although the possibility has not been eliminated, it appears that the bedrock ridge is a former sea stack on the 105,000 years B.P. wave-cut platform and that it is not related to faulting.

SUMMARY - Our field studies indicate that the Año Nuevo thrust fault is a relatively small secondary fault, with regard to its late Pleistocene activity, within the San Gregorio fault zone. The total known surface length of the fault is about 600 ft., and its maximum vertical displacement in the late Pleistocene is 18 ft. The fault may die out to the northwest, and its extension offshore to the south and southeast is unknown.

The width of the zone of shearing and fracturing in the mid and late Tertiary rocks suggests that the Año Nuevo thrust fault may have been a relatively active fault during the late Tertiary. Studies of the offshore area by Alpine Geophysical (1971) and of the San Gregorio fault zone by Earth Sciences Associates (1972) give no indication that this fault has ever been recognized on the offshore sparker profiles. The absence of evidence of the fault on the offshore sparker profiles is not evidence of its absence. Because the fault plane apparently is parallel or subparallel to bedding in the Monterey and Vaqueros formation (Brabb and others, 1977), it is doubtful that it would be readily observable on seismic profiles.

Therefore, it is difficult to characterize the Año Nuevo thrust fault because we have been unable to determine its length and total offset, the rates of late Tertiary movement, and its activity in the early-mid Pleistocene. Its exact relationship to other faults within the San Gregorio fault zone also is unknown. We can indicate only that:

- 1) The Año Nuevo thrust fault has an apparent long history of movement, from the late Tertiary to the Holocene.
- 2) It is predominantly a dip-slip fault with reverse movement.
- 3) It is a secondary trace within the San Gregorio fault zone, possibly connected at depth with the Green Oaks fault.
- 4) Its length at the surface can be demonstrated to be approximately 600 ft., but it probably is far greater.
- 5) The rate of vertical displacement for the past 105,000 years is about 0.05 mm/yr.

- 6) There is evidence in the marine terrace stratigraphy of five to nine separate faulting events along this fault during the past 105,000 years.
- 7) The fault offsets pond deposits  $^{14}\text{C}$  dated at 6060 years B.P. Therefore, the most recent episode of movement is Holocene.

PALINSPASTIC RECONSTRUCTION OF LATE PLEISTOCENE FAULT MOVEMENT - AÑO NUEVO THRUST FAULT - The palinspastic reconstructions are based on the detailed logs of the exposure of the fault in the sea cliff along the south shore of Point Año Nuevo and in exploratory Trench AN-1 which was excavated across the fault 350 ft. northwest of the sea cliff exposure (Refer to Figures 2, 8, 9, 11, 12, and 13 and Plates I, II, and IV-XI). A reconstruction of the probable history of faulting was prepared for each of the logged exposures, the exploratory trench, and the sea cliff. Each reconstruction is divided into stages, each of which consists of 1) either a faulting event or series of closely-spaced faulting events or 2) a period of erosion and/or deposition. Once the reconstructions were complete for both areas, the two reconstructions were compared in an attempt to correlate events between them. By combining the two reconstructions, neither of which is complete in itself, we worked out a tentative history of faulting, erosion, and deposition for the Año Nuevo thrust fault.

The reconstructions should be considered neither complete nor unique. It is possible to make other interpretations of much of the data, and we have developed several alternative models to explain the observed relationships. Some of the models contain more faulting events and some fewer events than the proposed model, which we feel is a reasonable compromise. In this or any other reconstruction of geologic history from the geologic record, visible evidence provides us with, at best, only a minimum history. Evidence of many, if not most, of the innumerable complexities associated with fault movement, erosion, and deposition simply was never preserved in the geologic record.

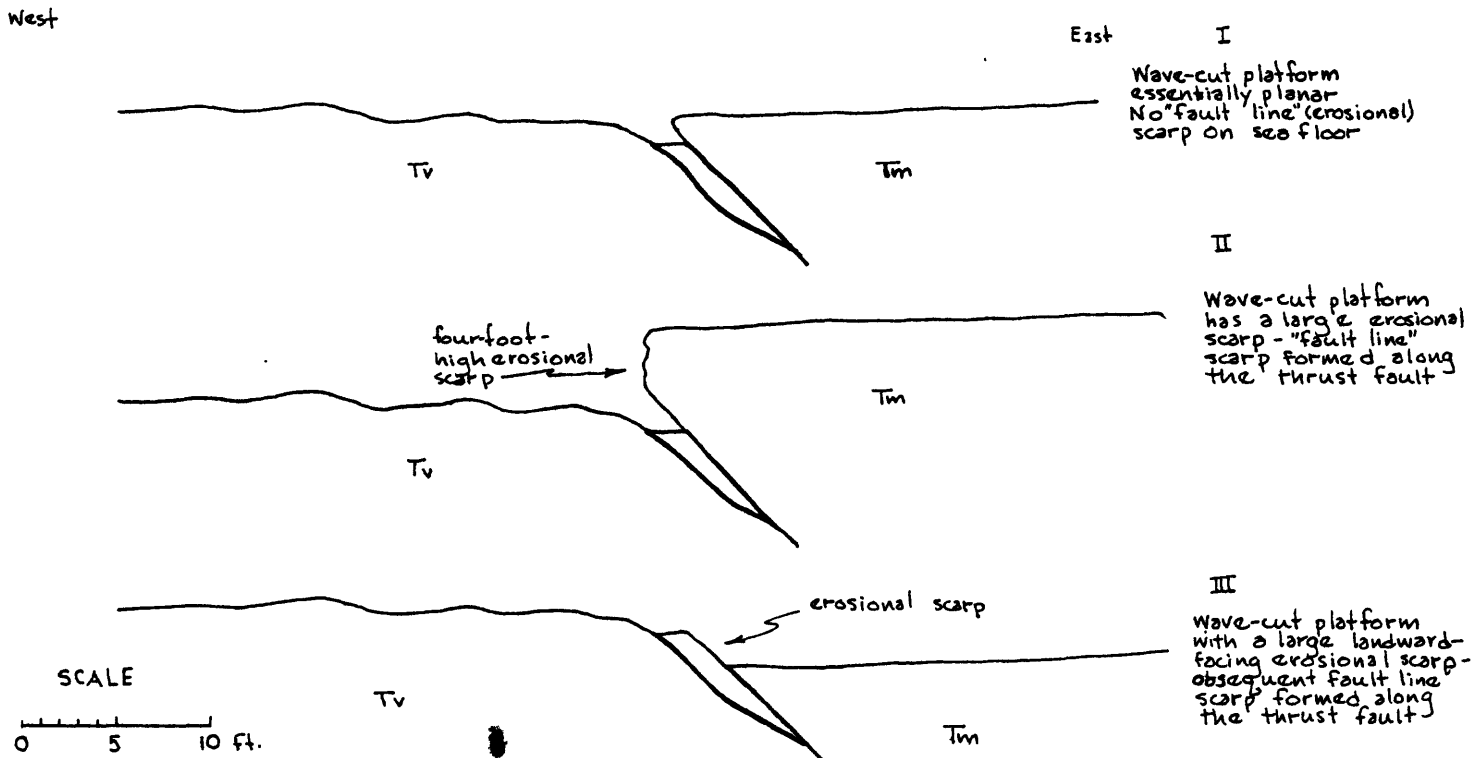
Geologic Constraints and Assumptions Used in Reconstruction - The geologic setting of the Año Nuevo thrust fault is ideal for the reconstruction of fault movement because well-defined geometric and time constraints can be placed upon the sequence of events. The reconstruction begins with the formation of a wave-cut platform approximately 105,000 years B.P. The age of the erosional surface is well known and was determined through amino acid stereochemistry techniques applied to fossil mollusks found on the wave-cut platform. The dates on the fossil material were kindly provided by Dr. K. R. Lajoie of the U. S. Geological Survey and Dr. John Wehmiller of the University of Delaware. The youngest datable stratigraphic unit offset by the fault is an organic-rich interdune pond deposit exposed in the exploratory trench (Plate V). The interstitial organic material (humus), when separated and analyzed, yielded a  $^{14}\text{C}$  age of  $6060 \pm 105$  years B.P. (Beta-1083). The entire sequence of events in the reconstruction must have occurred in the time interval 105,000-5,000 years B.P.

Constraints on the nature and amount of movement that occurred along the thrust fault are provided by the 105,000-year-old wave-cut platform that has been displaced 17-19 ft. vertically,



FIGURE 13 Año Nuevo thrust fault. Wave-cut platform not visible east (right) of fault. Ladder stands on wave-cut platform west (left) of fault. Grids are two feet square. Light colored wedge of sediment in the sub-fault stratigraphy consists of Monterey formation debris washed off the fault scarp. Refer to Plate II.

depending on how the eroded lip of the fault is reconstructed. Therefore, the total late Pleistocene displacement along the fault is constrained to an absolute maximum of 19 ft. and a minimum of 17 ft. The original shape of the wave-cut platform is known to approximate a plane that dips gently (<1 degree) seaward (Bradley & Griggs, 1976). It is not known if the wave cut platform originally was essentially level across the fault. It is possible that a scarp had been formed on the wave-cut platform in the surf zone by differential erosion of the rock on one side of the fault. The three possible original configurations of the wave-cut platform are indicated below:



To simplify the reconstruction, we assumed first that the initial shape of the wave-cut platform was as in I, essentially a near-planar surface across the fault without an erosional scarp on the sea floor. It is possible to test this assumption roughly by looking for differences in the resistance to erosion of the two bedrock units where they presently are subjected to wave erosion in the sea cliff (Plates I & II). Wave erosion along the south shore of Point Año Nuevo has not created a large difference in the position of the cliff face on opposite sides of the fault, nor has an erosional scarp been formed on the sea floor in the intertidal area. The two bedrock materials seem to have similar resistances to wave erosion. If any differences exist, it appears, based on the position of the cliff face on opposite sides of the fault (Plate II), as if the Monterey formation is

less resistant to erosion than the Vaqueros formation in this area. Therefore, if an erosional scarp did form on the ocean floor, it probably resembled configuration III, a landward-facing scarp.

A second assumption is that the maximum surface displacement associated with a single faulting event was 1 m. Although vertical displacements of 12-15 ft. have occurred historically (Bonilla and Buchanan, 1970) these large displacements along reverse faults have all occurred on primary fault traces. The Año Nuevo thrust fault is a relatively small secondary trace of the fault zone, and it seems unlikely that large surface displacements could occur commonly on such a fault. This assumption is supported roughly by what little information is available on secondary traces and by our analysis of the trench and sea-cliff logs. Where the amount of vertical displacement associated with a faulting event can be estimated accurately in this analysis, it appears to be commonly 2-3 ft.

This assumption is also supported by the magnitude vs. maximum displacement plots of Bonilla and Buchanan (1970) which indicate that a maximum surface displacement of 3-5 ft. probably would result from a 6.5-7.0 Richter magnitude earthquake on the fault. We believe that movement along this thrust fault occurs in response to local stress fields which are set up in response to movements along the large primary traces of the fault zone. It therefore seems highly unlikely that major earthquakes large enough (>6.5 magnitude) to create surface displacement greater than 3 ft. would occur along a minor secondary trace that has a total surface length of probably only a few miles.

We also believe that there is little chance that evidence of faulting events with surface displacements of less than 1-1½ ft. can be preserved in the geologic record. Small displacements, in most instances, simply do not leave any distinctive stratigraphic features by which they can be recognized. Surface scarps or mole tracks are very small, and erosion off of such a small scarp probably would produce a sedimentary wedge less than 6 in. thick. In many instances, most of the actual motion or displacement must be absorbed as intergranular rotation.

Using these two assumptions we have developed the following reconstruction of the events that occurred between 105,000 and 5,000 years B.P. In developing these reconstructions and the proposed history of fault movement, erosion, and deposition, we attempted to base each of the faulting events on well-defined geologic evidence in the exposures. Because it was not always possible to find direct evidence, it was necessary to infer several faulting events for which there is no direct stratigraphic record. We used geometric constraints on the shape of the platform and constraints on the amount of maximum surface displacement associated with each faulting event.

## Analysis of Sea-Cliff Exposure - Año Nuevo Thrust Fault -

Stage 1 - Formation of the wave-cut platform - The wave-cut platform of the Santa Cruz marine terrace was formed in the surf zone of a transgressive sea which rose slowly toward a highstand of sea level approximately 105,000 years B.P. (oxygen isotope stage 5c, Bloom and others, 1974). The age of this episode of platform-cutting was determined by amino acid racemization studies performed on fossil mollusks collected from the base of the marine terrace deposits at three different localities along the south shore of Point Año Nuevo: (1) directly under the lip of the thrust fault, (2) approximately 100-150 ft. east, and (3) 1500 ft. east of the fault (Figures 2 and 8, and Plates I, II, and IV).

As indicated in Figure 8a, Stage 1, the shape of the platform is assumed to be essentially planar, with only a few minor erosional irregularities. Where the fault cuts the bedrock units, there are two relatively narrow gouge zones and areas of crushed and brecciated rock. A relatively narrow and shallow erosional channel or grotto probably formed along the fault on the sea floor. At the maximum highstand of sea level associated with this transgression, the coastline lay 3000-6000 ft. east of the thrust fault. Therefore, water depth at the fault was between 40 and 90 ft., well below fair-weather wave base. There is no record of the transgressive stratigraphic sequence that must have been deposited during the rise of sea level. Any deposits related to the transgression must have been destroyed by reworking of the sediments in the nearshore environment during the retreat of the sea from the wave-cut platform. The reworking of sediments on the platform during regression in the outer-nearshore environment may explain the general absence of fossil materials on the wave-cut platform near the fault. Burrows and borings of pholads abound in the wave-cut platform, but none are occupied now by the animals that formed them. It is thought that the shells of these animals were eroded out of their burrows and the burrows filled with sediment.

Stage 2 - Faulting Event #1 (Figure 8a) - Approximately 2 ft. of vertical displacement occurred along the fault, offsetting the wave-cut platform. The offset created a 3 to 4-ft.-deep grotto along the fault trace on the sea floor with the hanging-wall block forming a protective lip. Sub-wave-base deposits of sand and silt, with some lag pebbles and cobbles on the platform and some fossil mollusks, were swept into the grotto and preserved as a wedge of fossil shell debris. In the summer of 1978, we collected three complete articulated specimens of Saxidomus giganteus from the mixture of shell debris and sediment in this wedge below the fault. Because the complete shells were not in their living position, they probably had been transported a short distance. We believe that these specimens were preserved only because the lip of the thrust fault extended 2-3 ft. over the deposits and protected them from erosion.

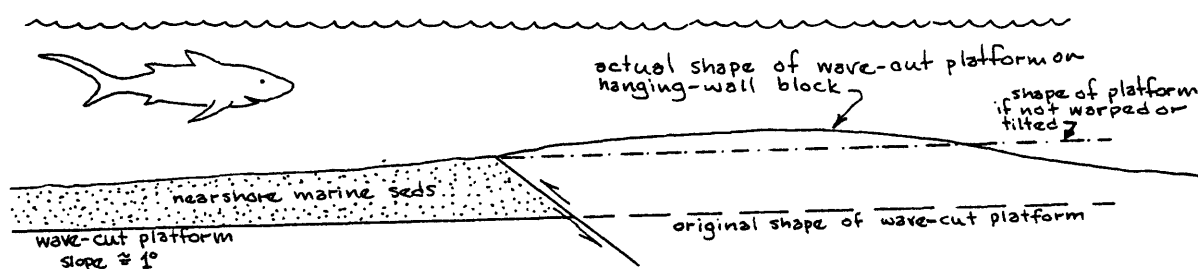
The occurrence of this faulting event is not based on any unique set of shear planes and stratigraphic evidence, but it is inferred from the presence of the wedge of fossil shell debris. The shell debris, the oldest stratigraphic unit preserved on the downdropped block, is almost 2 ft. thick. The preservation of this wedge of sediment in an area where all other shell debris was eroded off the platform must have required the formation of a rather deep, well-protected grotto or notch in the platform. It is most likely that this formed in response to fault movement at some time between the transgression and regression of the sea over this area. If the grotto and lip were solely of erosional origin and formed during the transgression, we would expect some of the original surf zone deposits associated with the transgression to be preserved in this protected area.

Stage 3 - Erosion and deposition in a regressive sea (Figure 8a) - After the faulting event occurred, currents and wave action swept fossil debris, fine-grained sediment, lag deposits, and articulated shells into the grotto under the protective lip. This wedge of shell debris eventually was covered by a "basal unit," which in turn was overlain by fine-grained mica-rich sands interbedded with lenses and beds of pebble and cobble conglomerate. The basal unit, a massive, fine-grained micaceous sand containing scattered pebbles, cobbles, and boulders, is interpreted to be the product of offshore (below fair-weather wave base) deposition of fine sands and silts mixed with numerous lag cobbles, pebbles, and boulders left behind on the wave-cut platform during the transgression of the sea. The fine-grained micaceous sands and interbedded conglomerate beds and lenses overlying the basal unit are interpreted to be deposits of the outer-nearshore environment. Well-developed sets of seaward-dipping cross beds probably indicate that the sediments were deposited near the distal ends of rip-current channels. Both the basal unit and the overlying micaceous sands bury the fault and the fault scarp. The fault scarp must have been completely concealed on the sea floor because these two stratigraphic units are present on both sides of the fault. Nevertheless, the units typically are thinner on the hanging-wall block.

Stage 4 - Faulting Event #2 (Figure 8a) - About 2 ft. of vertical displacement occurred along the fault during this event. It is probable that more than one shear surface developed because the outcrop patterns of faulting suggest that the fault movement usually did not occur along single planes in the terrace sediments. Typically, the faults splay out from the main trace in the bedrock and form multiple shears in the soft terrace sands and silts. It is probable that a 2-ft.-high fault scarp was formed on the sea floor. As with Faulting Event #1, little direct evidence of Faulting Event #2 exists in the depositional sequence. The occurrence of a faulting event is inferred from the shape of the scarp

and lip and from the distribution of the marine sediments. It is possible that the greater-than-4-foot-displacement of the wave-cut platform that existed at this stage in the history of movement could have resulted from a single faulting event, but stratigraphic relationships suggest that that offset is the result of two faulting events.

Stage 5 - Nearshore erosion and deposition in a regressive sea (Figure 8a) - As the sea continued to recede, the water shoaled and the area became a nearshore surf-zone environment. The basal unit and the overlying mica-rich sands were eroded off the hanging-wall block, and the scarp was completely degraded. On the hanging-wall block, the basal unit and the outer-nearshore sands were preserved near the fault only in deep erosional pockets in the bedrock platform. At distances greater than approximately 100 ft. northeast of the surface trace of the fault, both the basal unit and the outer-nearshore sands typically are present although the basal unit is not present everywhere. The distribution of these units suggests that at this stage, the wave-cut platform on the hanging-wall block was being warped into a slight anticline and/or was being tilted back slightly to the northeast as indicated in the following diagram.



After erosion of the fault scarp and part of the deeper-water deposits on both sides of the fault, a thick layer of fine to medium-grained non-micaeous sand, interpreted as a surf-zone deposit, was deposited on the recently-formed erosion surface and completely blanketed the area and covered the fault. We are aware of three models of fault movement and deposition which could explain the stratigraphy and the faulting present in Stage 5 of Figure 8a. The three different models are:

- 1) The interpretation presented above suggests that there were two distinct faulting events resulting in between 4 and 4½ ft. of vertical displacement. The faulting events were interspersed with several well-defined episodes of nearshore erosion and deposition.
- 2) A second interpretation of the stratigraphy and fault geometry shown in Stage 5 of Figure 8a is that the 4-ft. difference in elevation between the wave-cut platform on opposite sides of the fault is due entirely to erosion. The scarp was a fault line scarp in the strictest sense, and all of the stratigraphic differences were the result of nearshore erosional and depositional processes. We

believe that this interpretation does not adequately explain 1) the distribution of the basal unit, 2) the fact that the 4-ft. overhang of Monterey formation was not eroded off and rounded in the surf zone, nor 3) the lack of differences in resistance to erosion between the Vaqueros and Monterey formations.

- 3) The 4-ft. difference in elevation of the wave-cut platform on opposite sides of the fault also could be interpreted as the result of either one episode of faulting with 4 ft. of offset or a smaller single episode of faulting combined with a small erosional scarp across the fault. This would make the 4-ft. vertical displacement of the wave-cut platform in Stage 5 the result of both an initial 1- or 2-ft.-high erosional scarp across the fault and a single faulting event accompanied by 2 to 3 ft. of displacement.

Of the three possible explanations, we find the first preferable and the second least probable. This is based primarily on the absence of an erosional scarp across the fault in the intertidal zone of the modern wave-cut platform.

Stage 6 - Faulting Event #3 (Figure 8b) - Approximately 2 ft. of vertical displacement occurred during this event. There is clear-cut stratigraphic evidence of this event (Figure 8b and Plate IV); the micaceous outer-nearshore sands have been faulted up into juxtaposition with the non-micaceous surf-zone deposits. The faulting within the terrace sediments is complex. Several large, well-defined fault planes and many small, discontinuous breaks are present. Evidence of intergranular rotation is visible; blade- and disc-shaped pebbles have been rotated into orientations parallel to the fault planes. The upthrown block was pushed "bulldozer"-like through the overlying terrace sediments, becoming fractured and brecciated.

Between Stages 6 and 7, the sea receded from the old wave-cut platform, and the thrust fault area was exposed to subaerial processes. Apparently, none of the more recent late Pleistocene highstands of sea level was high enough to allow the sea to transgress over the fault area again.

Stage 7 - Subaerial erosion and deposition (Figure 8b) - Erosion, probably subaerial, removed the scarp and the upper part of the beach deposits left by the regressing sea. This was followed by the deposition of a relatively thick layer of fluvial sands, pebble conglomerates, and clayey sands over the entire area, blanketing the fault. These are the oldest deposits in the area that have high percentages of clay and contain clasts of Santa Cruz mudstone. Because the mudstone clasts weather rapidly and break down primarily into clay, the weathered fluvial sediments are characterized by an extremely high clay content. This sequence of fluvial deposits may have remained undisturbed long enough to allow a weak soil profile to develop. The presence of

poorly-developed structures that resemble soil peds, and the high clay content, may be the result of this rudimentary soil development (Figure 13 and Plate IV). On the other hand, the structures may be "pseudo soil structures" that have formed in response to shrink-swell of the clays present in the deposits. Regardless of the exact origin, the high clay content of the sediments is partly due to the physical translocation of the clay downward in the sediments. This transport of clay has blurred contacts and obscured original sedimentary structures.

Stage 8 - Faulting Event #4 - possibly two events (Figure 8b) -  
This faulting event is poorly understood. It may consist of two or possibly three closely-space episodes of faulting. The evidence for this event(s) is the prominent truncation of the structures produced during Faulting Event #3 and of the fault block of outer-nearshore micaceous sediments by the wedge of non-micaceous surf-zone sand (Figures 8b, 8c, and 13 and Plate IV). This wedge of sand was thrust over the faults of Event #3, "bulldozing" through the sediments lying in front of it. Sediments below and to the west of this fault wedge are strongly disrupted; a zone of mixed rock and sediment is present in the "bulldozed" area. There appears to have been compressional folding of the conglomerate beds within the fluvial deposits. From the geometry of the outcrop, it appears as if the wedge of sand must have moved horizontally about 6 ft. The fault plane at the base of the wedge dips about 10-11 degrees to the east and approaches horizontal. This wedge itself is truncated by a fault, and the surf-zone sand has been dragged and streaked along the fault plane bounding the upper portion of the wedge. These two breaks probably represent two separate episodes of fault movement, but the evidence is only suggestive. If movement occurred as the result of a single faulting event, it took place simultaneously along more than one fault plane in the complex zone of faulting and brecciation that comprises this fault.

By this stage in the development, the fault was a zone of broken rock, brecciated Monterey formation, and clayey fault gouge more than a foot wide in places. We interpret this sequence of breaks to represent one faulting event consisting of 4 ft. of vertical displacement and 6 ft. of horizontal displacement. A 4-ft.-high fault scarp was produced at the surface. There are some geometric and spatial constraints on the faulting of the wedge of surf-zone sand into its position where it truncates the faults of Faulting Event #3. The initial fault movement must have been essentially horizontal with the wedge of sand having originated either as a "fault block" between shears or as part of the hanging-wall block. Despite these constraints on the fault movement, these faults (Figures 8b and 8c and Plate IV) represent at least one complex faulting event or more likely, two separate faulting events.

Stage 9 - Subaerial erosion and deposition - net erosion (Figure 8c) -  
The fault scarp and probably the upper part of the fluvial deposits present on both sides of the fault were removed by erosion. It is possible that a complex sequence of erosion and subaerial deposition occurred in this area during this interval of time, but there is no

positive evidence of deposition. Much of the upper horizon of any previously-formed soil (Stage 7) was removed during this episode of erosion.

Stage 10 - Faulting Event #5 - possibly two events (Figure 8c) - This event produced of 4 ft. of vertical displacement and 6 ft. of horizontal displacement. There is evidence of "bulldozing" along the contact of the fault, and the rupture apparently broke the surface with the fault rubble and breccia being thrust out onto the ground surface on the downthrown block (Figures 8c and 13 and Plate IV). The resulting scarp probably was 4 ft. high. A slight overhang may have been formed by the lip of the upthrown block because Monterey formation was exposed at the surface. This event is recorded as a wide zone of crushed and brecciated Monterey formation overlying the fluvial deposits (Figures 9 and 13).

By this stage, the fault was a 1½-ft.-wide zone of crushed rock with a few well-defined shear planes. In the upper half of the sea-cliff exposure, fault planes or individual shear surfaces are difficult to identify. Because the fault "gouge" or breccia is very coarse and porous, a great deal of the deformation in this zone probably took place as intergranular rotation rather than faulting. In addition, the crushed rocks have been extensively weathered, and a great deal of black humus has been washed down into the breccia. Clay also has been translocated down through these breccias, and many of the spaces between grains have been filled with clay and humus stains, masking evidence of faulting.

Stage 11 - Erosion and deposition (Figure 8c) - When the scarp produced by Faulting Event #5 was eroded, some of the fault breccia was washed slightly downhill. The distal part of this tongue became mixed with clay and silt. Erosion eventually removed the scarp and exposed the Monterey formation at the surface. Because terrace sediments on the upthrown block had been almost completely removed by erosion, a low bedrock scarp existed at the surface along the trace of the fault. During this period, a minimum of 3-4 ft. of net deposition occurred on the downthrown block. Fluvial deposits may have been present on both sides of the fault, and they may have blanketed the area of the fault. It is impossible to determine the total amount of deposition from the outcrop data. Based on stratigraphic sections from the sea cliffs due east and west of the sub-fault exposure, it is probable that most of the sediment was carried into the area either from the north or from the south in a stream channel that paralleled the fault scarp on the downthrown block. It is possible that a very weak soil(?) structure is present in these clayey sands and silts.

Stage 12 - Faulting Event #6 - possibly two events (Figure 8d) - Two closely-spaced shears or faults represent one relatively large faulting event or possibly two separate faulting events (Figures 8d and 9, and Plate IV). The lower fault may represent one faulting event while the upper fault, about 1 ft. higher in the section, may represent a second distinct event. If these faults represent

two distinct events, it is probable that the events occurred close together in time. Both of the faults are characterized by a distinct "bulldozing" of the overthrust block on the underlying colluvium/alluvium. The stratigraphic evidence for the faulting event(s) is the mass of fault breccia and rubble resting on top of the fluvial deposits over which it was thrust. The faults are difficult to trace because shears do not readily form in the granular fault breccia which consists of hard angular fragments of Monterey formation in a weak clay matrix. This rubble seems to deform primarily by grain rotation and by crushing and mixing of the materials. In addition, weathering processes translocate clays, humus and other material down into the fault breccia and crushed rock where the clays tend to coat all of the grains and clasts and to obscure any preexisting shears.

Stage 13 - Erosion (Figure 8d) - The scarp of Faulting Event #6 was reduced by erosion, and small amounts of sediment were deposited on the downthrown block. There was considerable erosion of the terrace sediments on the upthrown block, and a broad linear outcrop of Monterey formation was exposed at the surface. No other stratigraphic record exists in the sea-cliff exposure because a small "v"-shaped gully has been incised into the terrace just west of the thrust fault (Refer to Figure 13 and Plates II and IV).

An argument can be made for at least one more episode of movement along the thrust fault after Stage 13 based on the reconstructed geometry of the wave-cut platform exposed in the sea cliff on the upthrown block. In order to explain the total vertical displacement of the reconstructed wave-cut platform where it has been removed by erosion, it is necessary for the faulting event in Stage 12 to consist of approximately 4 ft. of vertical displacement rather than 2 to 2½ ft. This 2½-ft. discrepancy between the actual displacement of the platform and the cumulative offset of Faulting Event #6 is best explained by a seventh faulting event, evidence of which is not visible in the sea-cliff section because of erosion during the past 5,000-6,000 years.

Analysis of the Exploratory Trench Exposures - The analysis of the exposures in Trench AN-1 was hindered by our lack of knowledge of the position of the wave-cut platform on the footwall block. Hence, in the reconstruction of the sequence of events, it was not possible to begin at the same starting point (105,000 yr B.P. wave-cut platform) as in the analysis of the sea-cliff exposures (For trench logs refer to Plates V & VI). Therefore, it is impossible to examine the trench exposure to see if the same sequence of events is preserved there as in the sea cliff to the south.

It is clear that in the exploratory trench, evidence of only the last few stages of the sea-cliff sequence was exposed. One problem with correlation between the trench and the sea cliff is that the total offset of the wave-cut platform apparently is greater in the vicinity of the sea cliff than at the trench. As best as we can determine from auger holes and seismic refraction surveys, the amount of displacement

on the Año Nuevo thrust fault decreases to the north and northwest, and the fault may die out south of the road through the dune field (Figures 2 and 5 and Plates I and II). Consequently, the maximum surface displacement visible along the thrust fault is in the sea-cliff exposure.

Another characteristic of the portion of the thrust fault exposed in the exploratory trench is that all of the fault movements were characterized by a "bulldozing" process. Zones of crushed rock formed at the leading edges of overthrust plates and were mixed thoroughly with one or more of the sedimentary units. These masses of breccia and crushed rock were pushed or "bulldozed" up into younger sedimentary units. Because of this "bulldozer" effect, there is far more mixing along the contacts within the fault breccia and the complex of faults in the trench exposure than in the sea cliff. This, combined with apparently smaller displacement along faults during each of the faulting events, results in a complex stratigraphic record and fault geometry. Our reconstruction of the geologic events recorded in Trench AN-1 is as follows:

Stage A (exploratory trench) - Erosion of fault scarp and deposition (Figure 11a) - Subaerial erosion lowered and removed the existing fault scarp, and this was followed by the deposition of a sequence of fluvial sediments that covered the fault. The thickness of this depositional unit is unknown. This stage probably can be correlated with Stage 9 in the sea-cliff section but differs from it because it is characterized by net deposition rather than erosion.

Stage B (et) - Faulting event (Figure 11a) - Fault movement produced about 2 to 2½ ft. of vertical displacement. Movement along the fault was complex and was accommodated on a number of shear planes. The only primary evidence for this faulting event is a small amount of light green-gray clayey sand that was transported or "bulldozed" up into the overlying stratigraphic unit (Unit G in Plates V and VI). Fault breccia G was "bulldozed" into the dark to light green sandy clay, forming a vertical, mixed contact. A second probable effect of the faulting event is the intense fracturing of the Monterey formation in the hanging-wall block, particularly in the overthrust lip of bedrock. The presence of broad, open folds in the sediments records the effect of compression in the footwall block. This faulting event can be correlated with Stage 10 of the sea-cliff section although the total offset is less.

Stage C (et) - Erosion and deposition (Figure 11a) - Subaerial erosion of the fault scarp was followed by deposition of a series of fluvial clayey sands. Deposition probably was greater on the footwall block. This stage is correlated with Stage 11 of the sea-cliff section. Deposition in the vicinity of the exploratory trench seems to have been greater than in the vicinity of the sea-cliff section.

Stage D (et) - Faulting event (Figure 11a) - Fault movement with approximately 2 ft. of vertical displacement formed a 2-ft.-high

fault scarp at the surface. Two low-angle shears were formed, and fault breccia was "bulldozed" into the tan-colored clayey sands. It is probable that fault breccia wedge F (Plates V and VI, and Figure 11a) was "bulldozed" into the overlying sediment, but fault movement was transferred from the fault bounding the lower portion of fault breccia wedge F to the fault bounding wedge E when the force resisting the bulldozing breccia mass F became greater than the force resisting movement of breccia wedge E along the fault bounding its lower margin. We visualize the fault movement as having been initiated on the lower break with movement being transferred to the upper fault about halfway through the faulting episode. An alternate hypothesis is that the faults and their associated fault breccias represent two separate faulting events separated by a short time period. One fault break and fault breccia may have formed during a sequence of aftershocks. This event is thought to correlate with Stage 12 of the sea-cliff sequence.

Stage E (et) - Erosion and deposition (Figure 11b) - Subaerial erosion degraded the scarp, the the area was covered by a shallow pond. These deposits consist of fine to medium-grained clayey sand with occasional subangular mudstone clasts. The matrix is black and consists of clay mixed with humus. The deposits are interpreted as having formed in an interdune pond or more probably, in a downwarped area on the terrace surface. The pond was slowly filled with clays, organic materials, aeolian sand, and some mudstone chips washed in from the higher fault scarp area. Analysis of the organic material in the matrix yielded a  $^{14}\text{C}$  age of  $6060 \pm 105$  years B.P. (Beta - 1083). These pond deposits blanketed the fault, and weathering processes produced a weakly-developed soil. This sequence of events apparently can be correlated with Stage 13 of the sea-cliff section although there is no evidence of pond deposits in the vicinity of the sea-cliff section.

Stage F (et) - Faulting event (Figure 11b) - Fault movement with approximately  $1\frac{1}{2}$  ft. of vertical displacement resulted in the formation of a low scarp or mole track at the surface. Evidence for this faulting event is the intimate and thorough mixing of the black interdune pond deposits into fault breccias B and C (Figure 11b and Plates V & VI). Fault breccias A, B, C, and D were thrust upward into the pond deposits with a "bulldozer" effect. These breccias are jumbled masses of mixed rock, and the contacts of the breccias with surrounding units typically are mixed and diffuse. Because the mixing of the rock in the breccias is extensive and the deformation is primarily a result of grain and clast rotation, it is essentially impossible to map shear planes through these units. In addition, the seasonal shrink-swell of the clays has helped to obliterate most of the original shear planes. This faulting event appears to be the most recent episode of movement along the Año Nuevo thrust fault. Because it offset and deformed the interdune pond deposits, we estimate that it occurred within the past 5000-6000 years. The organic material in the deposits probably is decayed plant matter

that collected in the pond over possibly several hundreds to thousands of years both before and after the faulting event. Therefore, the actual age of faulting could be somewhat older than the  $^{14}\text{C}$  age of the deposits.

Stage G (et) - Erosion (Figure 11b) - The low scarp or mole track along the fault was eroded and reduced to a nearly level surface. Portions of the interdune pond deposits probably were eroded off the hanging-wall block and deposited on the footwall block. Continued weathering and soil-forming processes acting on the interdune pond deposits produced a weak soil and caused a slight increase in clay content in the lower half of the depositional unit. Some fingers of clay-rich material extend into the underlying unit and appear to be related either to ped surfaces or to root channels. Weathering processes and shrink-swell of clays have obliterated any shears that may have formed in the pond deposits.

Stage H (et) - Aeolian deposition (Figure 11b) - For unknown reasons, the pond disappeared and the area became the site of aeolian deposition. The Point Año Nuevo dune field is thought to have been initiated as an area of large-scale dune activity between 3000 and 5000 years B.P. The aeolian deposits exposed in the exploratory trench consist of a very weakly-consolidated light gray dune sand that contains minor amounts of clay and humus. This is overlain by unconsolidated modern dune sand which supports present-day vegetation. No discernable soil has formed on the modern dune sand.

Correlation of Faulting Events - Sea-cliff and trench sections - Although the two exposures are separated by only 350 ft., the marine terrace stratigraphic units in the trench and sea cliff cannot be correlated with complete certainty. The factors which apparently control the subaerial erosion and deposition in the area are as follows. Because the total fault displacement and individual fault displacements are greatest at the sea-cliff section, this area of the terrace surface was a topographic high. The area near the exploratory trench appears to have undergone smaller individual fault displacements and to have been a topographic low on the terrace surface. Therefore, some events that appear to be primarily erosional in the sea cliff area probably were recorded as depositional events in the exploratory trench area. The interdune pond deposits (Stage E (et)) prominent in the trench are not present in the sea-cliff exposures at the fault or even 50-60 ft. west of the fault. Similarly, the previous depositional event (Stage C (et)) apparently was not a major depositional event in the sea-cliff section.

In the trench exposure, the marine terrace deposits on the downthrown block are all fluvial. Three distinct fluvial units (Stages pre-A, B, and C) are overlain by the pond deposits (Stage E). Although there are not three distinct depositional units present in the sea-cliff section, there is evidence of three episodes of subaerial erosion and deposition (Stages 7, 9, and 11), and one of subaerial erosion (Stage 13). These stages in the reconstructions match quite well. Tentatively, we would correlate Stage A in the trench exposure reconstruction with Stage 9 in the sea-cliff exposure reconstruction.

Discussion and Summary - Using the stratigraphy and the geometric relationships of the faults exposed in the sea cliff and the exploratory trench, it is possible to analyze the late Pleistocene history of the Año Nuevo thrust fault and to place constraints on the number of faulting events and the recurrence intervals between events. The two reconstructions previously presented are not unique interpretations; nevertheless, they present the basic depositional and erosional events along with the geometric relationships of faulting which must be explained in order to develop a model for fault movement. Using these data and our interpretation, we suggest the following three models as potential reconstructions of fault movement.

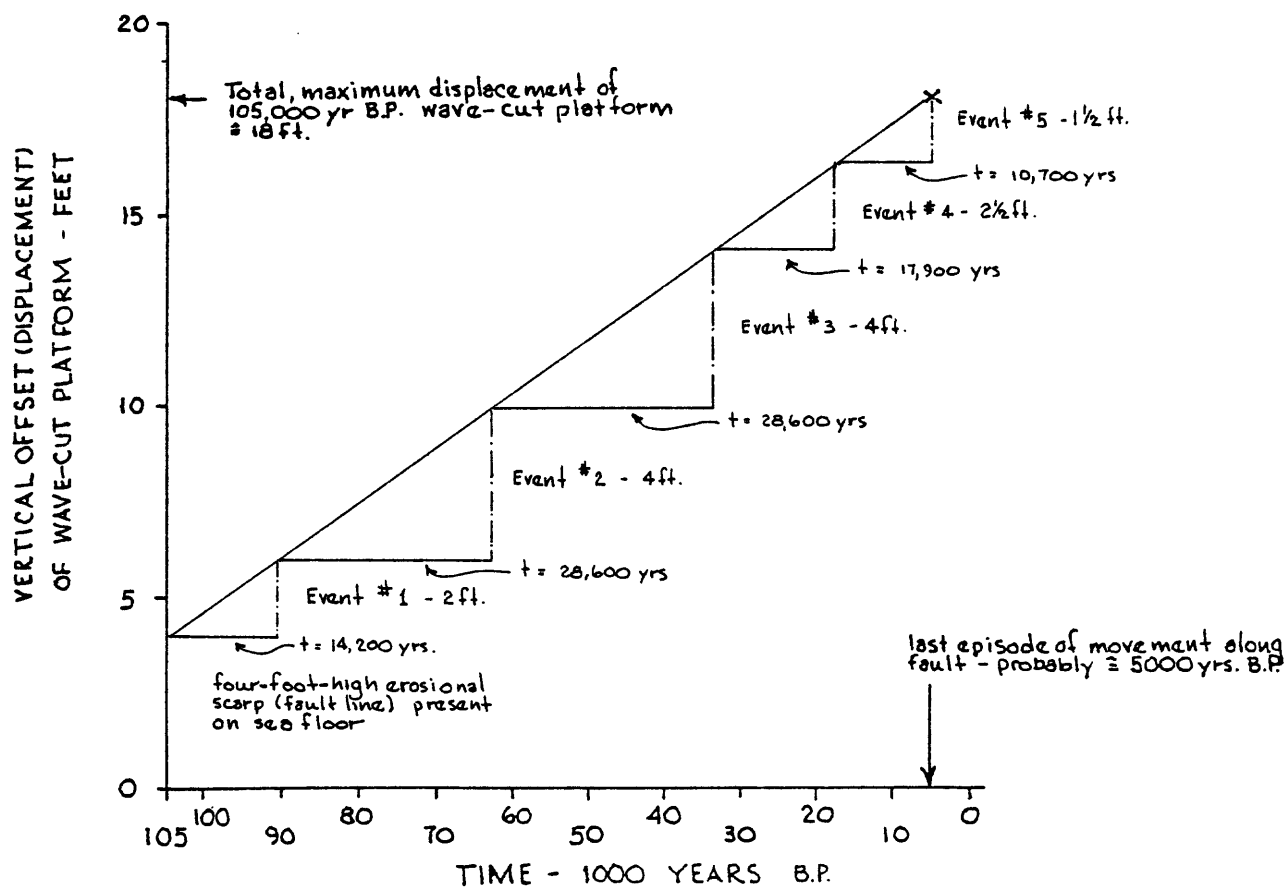
I) Fault Line Scarp Model - The sea-cliff relationships indicate four faulting events with the maximum vertical displacement during each event ranging from 2 to 4 ft. The exploratory trench exposes evidence for a fifth faulting event with approximately 1½ ft. of vertical displacement. This model assumes that the wave-cut platform was formed with a 4-ft.-high fault line scarp on the sea floor and begins the reconstruction of the fault movement at Stage 6; Faulting Event #3 would be considered the first faulting event. A graphic representation of this model is presented in Figure 14. It indicates that five faulting events occurred during a 100,000-year period. Recurrence intervals range from a maximum of 29,000 ± years (a vertical displacement of 4-ft.) to a minimum of 11,000 ± years (a vertical displacement of 1½ ft.). The average recurrence interval for faulting events that resulted in surface rupture is approximately 20,000 years.

II) Compromise Model - The sea-cliff stratigraphy indicates a total of six faulting events. The maximum vertical displacement is 4 feet and the minimum is 2 feet. The stratigraphic and fault relationships in the exploratory trench indicate a seventh faulting event. This is the detailed model presented previously. The seven faulting events occurred over a period of approximately 100,000 years. Figure 15 graphically represents the sequence of events. In this model, the first faulting event occurred between the transgression and regression of the sea which reached a highstand approximately 105,000 years B.P. Because the time interval between transgression and regression at the fault can be approximated as being no more than 5,000-6,000 years, it seems that the first faulting event must have occurred 105,000 years B.P. ± 2,000 years. Using 104,000 years B.P. as the time of the first faulting event, there were six subsequent faulting events in the ensuing 99,000-100,000 years. Recurrence intervals range from a maximum of 25,000 ± years (vertical displacement of 4 ft.) to a minimum of 9,000 ± years (vertical displacement of 1½ ft.). The average recurrence interval is approximately 16,500 years.

III) Maximum Event Model - A third interpretation of the sea-cliff stratigraphy is that Faulting Events 4 and 6 of the compromise model are both actually two faulting events. The

**FIGURE 14**

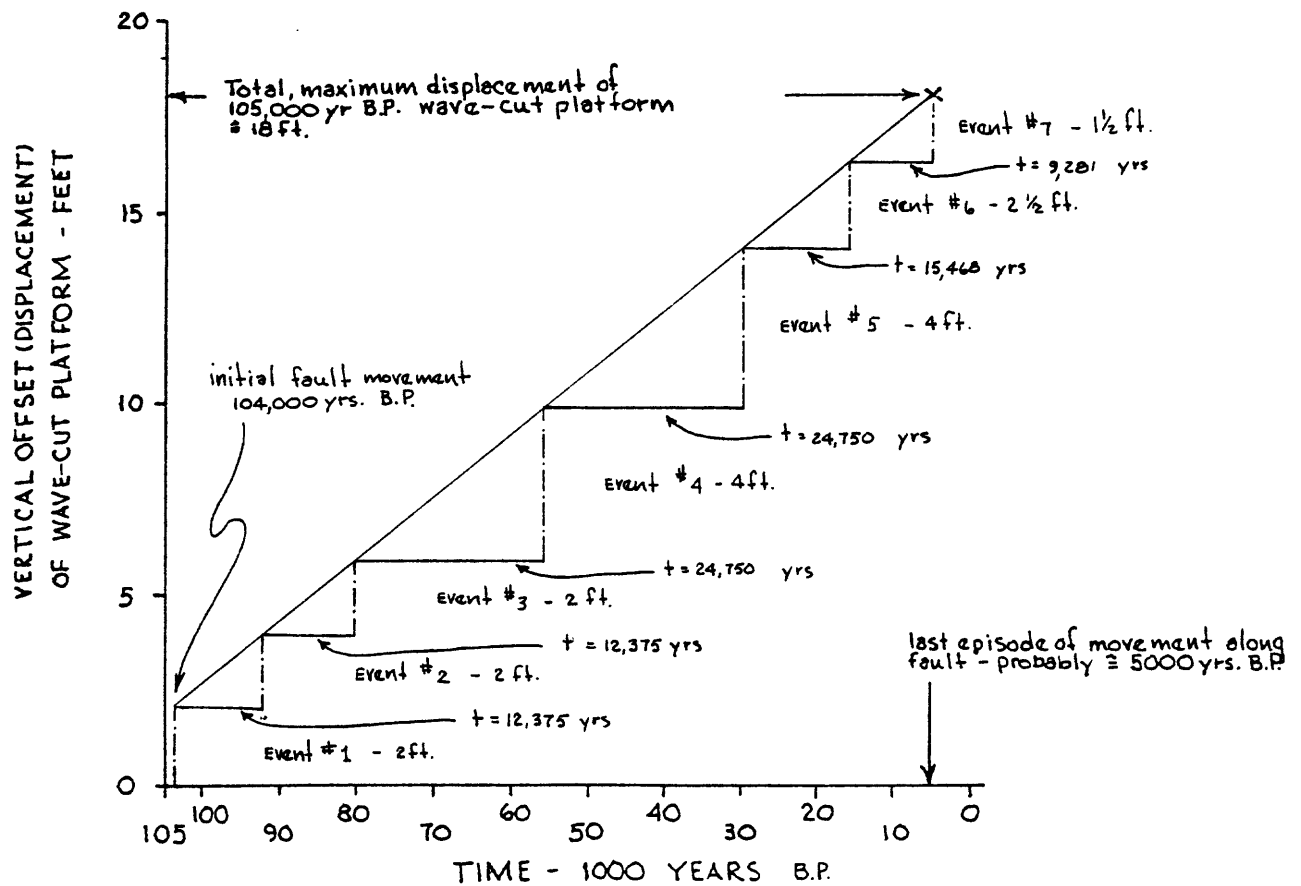
Time-vs.-vertical displacement plot of possible faulting events along the Año Nuevo thrust fault ( fault line scarp model)



Recurrence Interval - range from 10,700 yrs. to 28,600 yrs.  
Average  $\approx$  20,000 yrs.

**FIGURE 15**

Time-vs.-vertical displacement plot of possible faulting events along the Año Nuevo thrust fault (Compromise model)

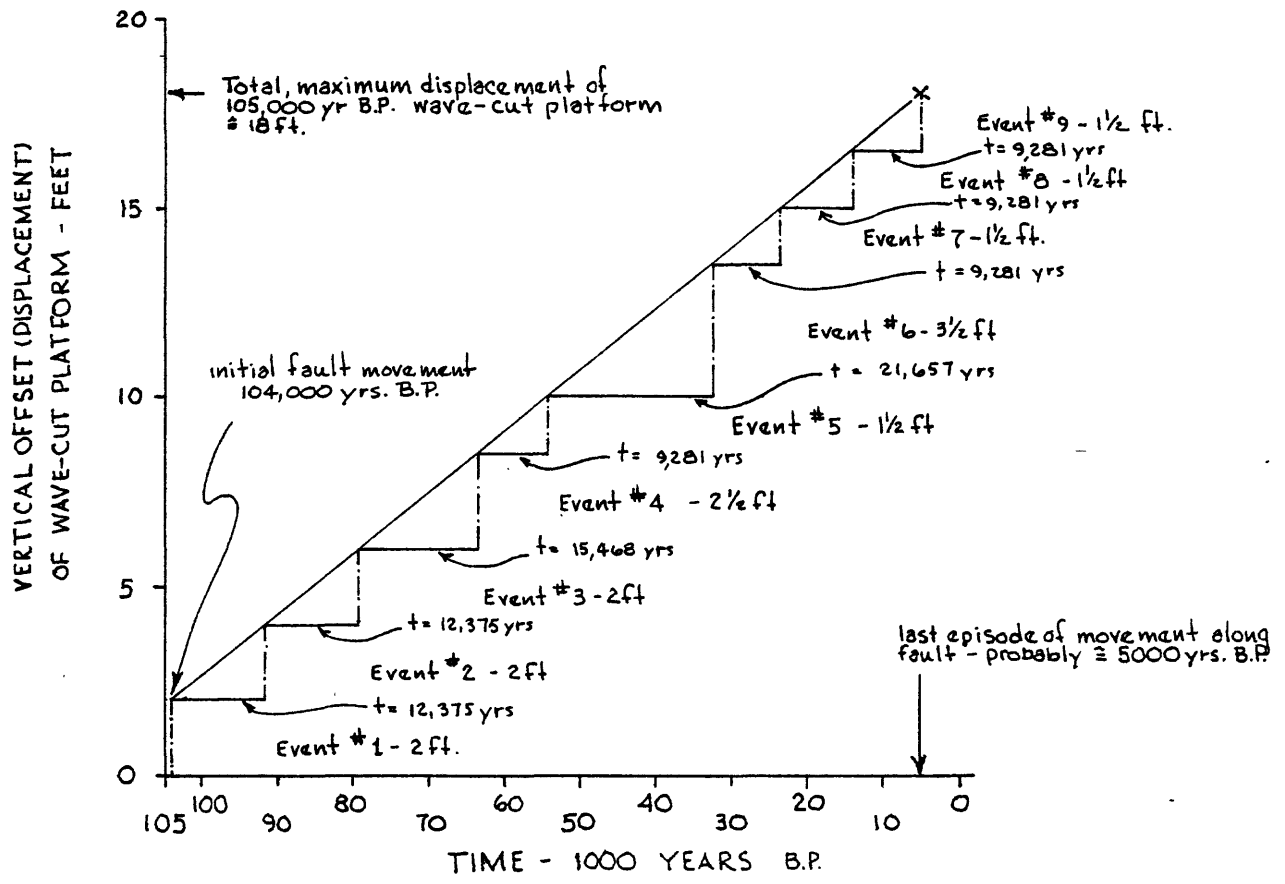


Recurrence interval - range from  $\approx$  9,000 yrs to  $\approx$  25,000 yrs  
Average  $\approx$  16,500 yrs

resulting interpretation is that the sea-cliff section contains evidence of eight faulting events, and the trench section contains evidence of one additional event for a total of nine events. The first faulting event must (as in Model II) have occurred between the transgression and regression of the 105,000 year B.P. highstand sea. If the initial faulting event took place 104,000 years B.P., then the recurrence intervals range from a maximum of  $22,000 \pm$  years (surface displacement of  $3\frac{1}{2}$  ft.) to a minimum of  $9,000 \pm$  years (surface displacement of  $1\frac{1}{2}$  ft.). The average recurrence interval is approximately 12,500 years. Figure 16 graphically represents the sequence of faulting events and intervening periods of quiescence.

**FIGURE 16**

Time-vs.-vertical displacement plot of possible faulting events along the Año Nuevo thrust fault (maximum event model)



Recurrence interval - range from ≈ 9,000 yrs to ≈ 22,000 yrs  
Average ≈ 12,500 yrs

## FRIJOLES FAULT

INTRODUCTION - Both the Frijoles and the Coastways faults appear to be dominant through-going structures (Figure 1), and they form the contacts between the major structural blocks in the San Gregorio fault zone, juxtaposing strikingly different bedrock units. Of these two primary fault strands or apparent zones of principal displacement (Figure 1), the Frijoles fault probably has experienced more of the recent fault movement.

The Frijoles fault itself is difficult to map because it is exposed poorly in the grass- and brush-covered rolling upland areas and marine terrace terrane of coastal San Mateo County. The fault is well exposed in the sea cliff along the south shore of Point Año Nuevo (Figures 17 and 18), but along the rest of its 19-km onshore segment it is partially exposed at only four locations, two of which are man-made excavations.

Despite its poor exposure, the fault can be mapped with reasonable certainty along most of its 19-km length largely on the basis of moderately to well-developed geomorphic features such as scarps, sag ponds, and lineaments. The fault along 5 km of its onshore extent lies within the course of Arroyo de los Frijoles, a major linear stream valley, that has cut a deep gorge through the highland area of marine terrace terrane known as the Mesa. Arroyo de los Frijoles, after which the fault was named, is a striking example of a beheaded and now underfit stream whose headwaters have been diverted by stream capture.

Northwest of Arroyo de los Frijoles, the trace of the Frijoles fault is not as obvious, for the fault apparently lies beneath the alluvial fill at the mouth of Pescadero Creek (Figures 1 and 19). Although there apparently is no exposure of the main fault strand near the mouth of Pescadero Creek, the presence of the fault can be inferred from the striking discordance of Quaternary marine terraces and of "Bedrock" units across the mouth of the creek. Middle Tertiary sandstones unconformable overlying Cretaceous turbidites south of the creek apparently are juxtaposed against upper Pliocene nearshore or inner-shelf sandstones.

Based on the distribution of the bedrock units, Pigeon Point formation to the southwest and Purisima formation to the northeast, between Whitehouse Creek and Pescadero Creek, the Frijoles fault appears to be the contact between the Pigeon Point formation in the Pigeon Point structural block and the Purisima formation in the Pomponio structural block. At only one point along the fault can the Purisima formation be found in fault contact with the Pigeon Point formation. In an upland area between Whitehouse and Gazos Creeks, the Frijoles fault is exposed in a series of shallow gullies. Below the soil horizons developed in colluvium are exposures of Purisima formation juxtaposed against Pigeon Point formation. Despite the lack of exposure, the areal distribution of the two formations suggests that the contact is a fault contact or that possibly the original depositional contact (unconformity) between the Pigeon Point and Purisima formations was controlled by the Frijoles fault and that subsequently the original depositional contact has been strongly deformed by Quaternary faulting.

Only near Point Año Nuevo does this pattern differ. There, the Frijoles fault juxtaposes two members of the Purisima formation against each other. There is insufficient outcrop information to determine the relationship of

FIGURE 18 (NEXT PAGE) Deformed Holocene sediments along the Frijoles fault, south shore of Point Año Nuevo. The dark bands are peats that probably formed in a sag pond along the fault.

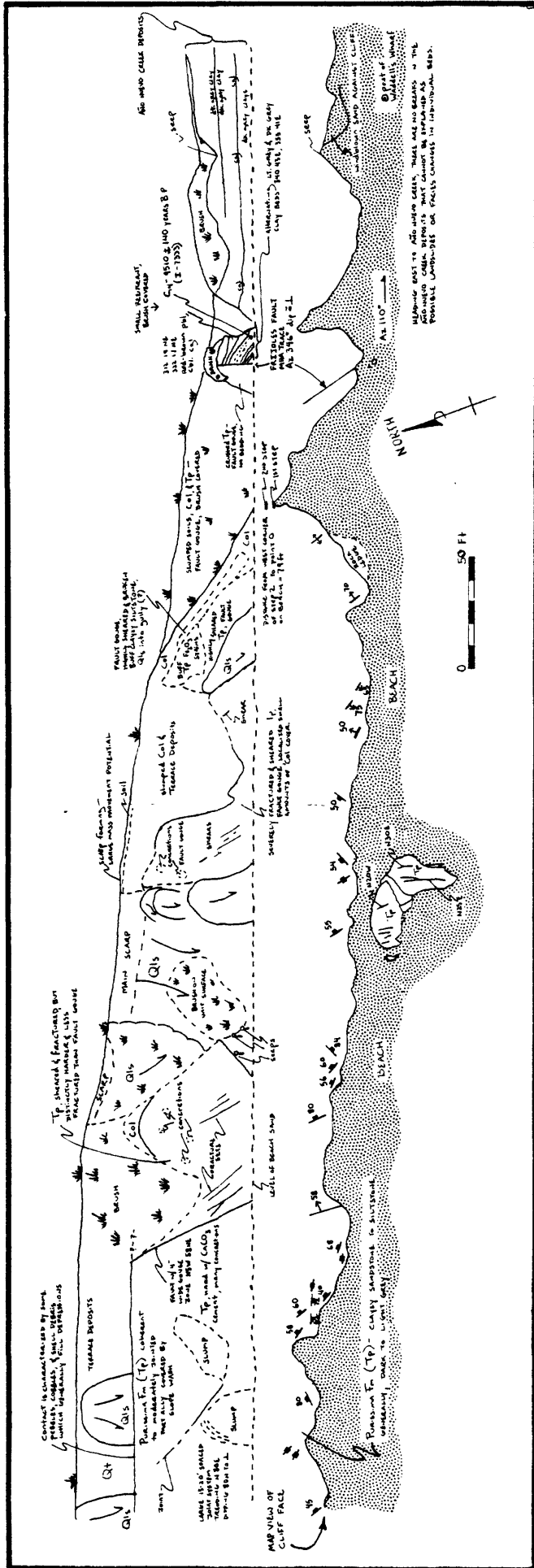
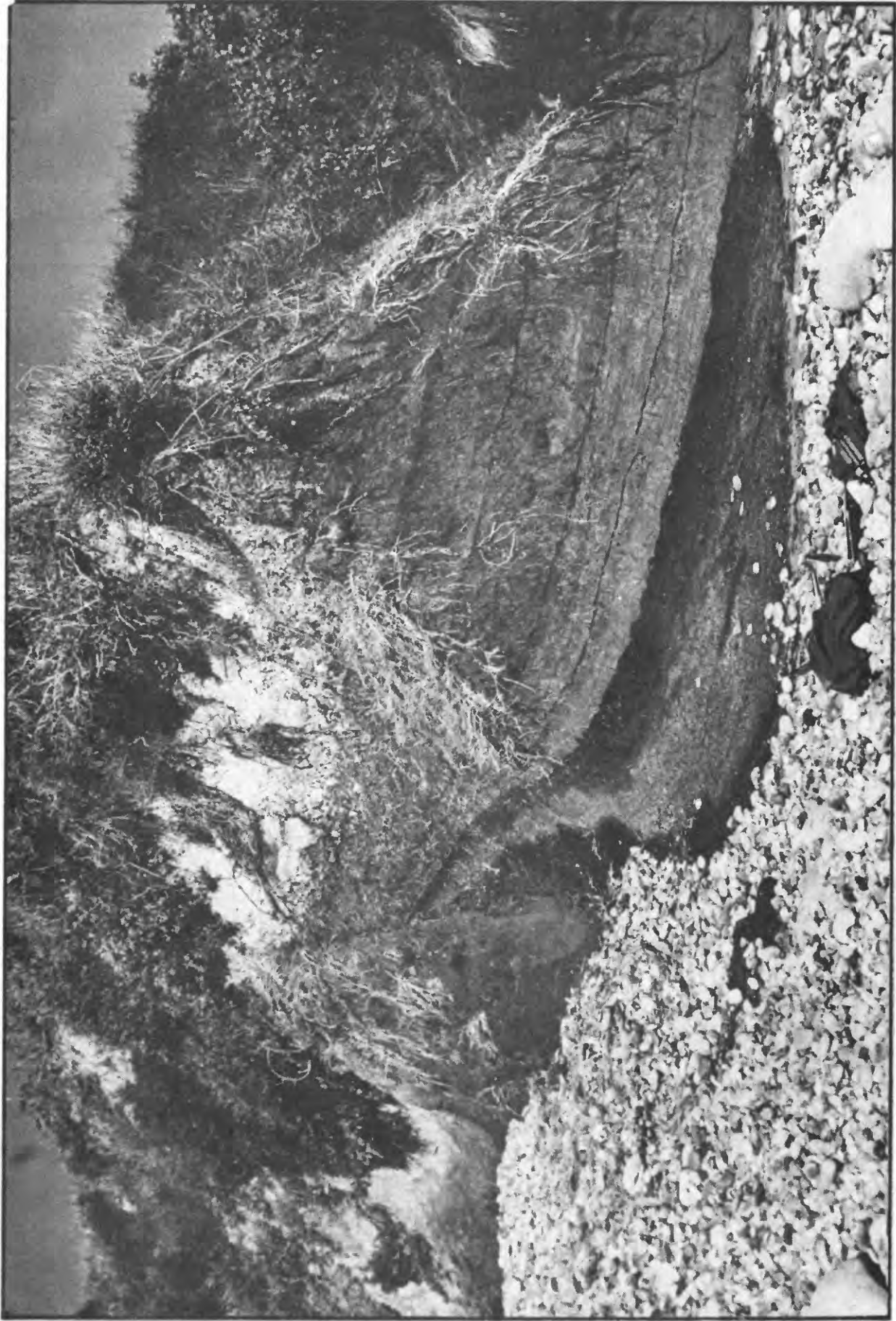


FIGURE 17 Generalized sea-cliff geology across the Frijoles fault on the south shore of Point Año Nuevo. Lower half of diagram is a map view of the sea cliff. Zone of intensely sheared rock in the sea cliff approximately 300 feet wide is characterized by landslides and slumps.



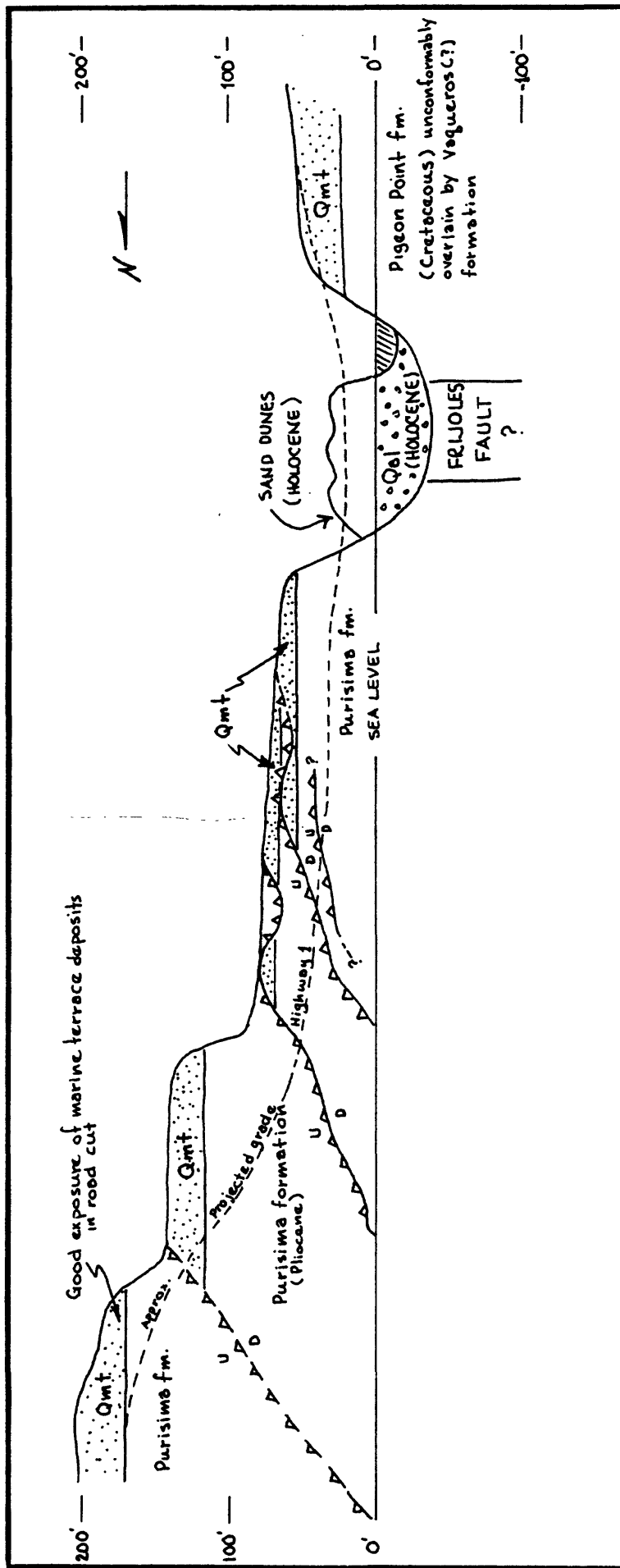


FIGURE 19 Generalized cross section showing the sea-cliff geology across the mouth of Pescadero Creek and the Frijoles fault.

8700 1000000

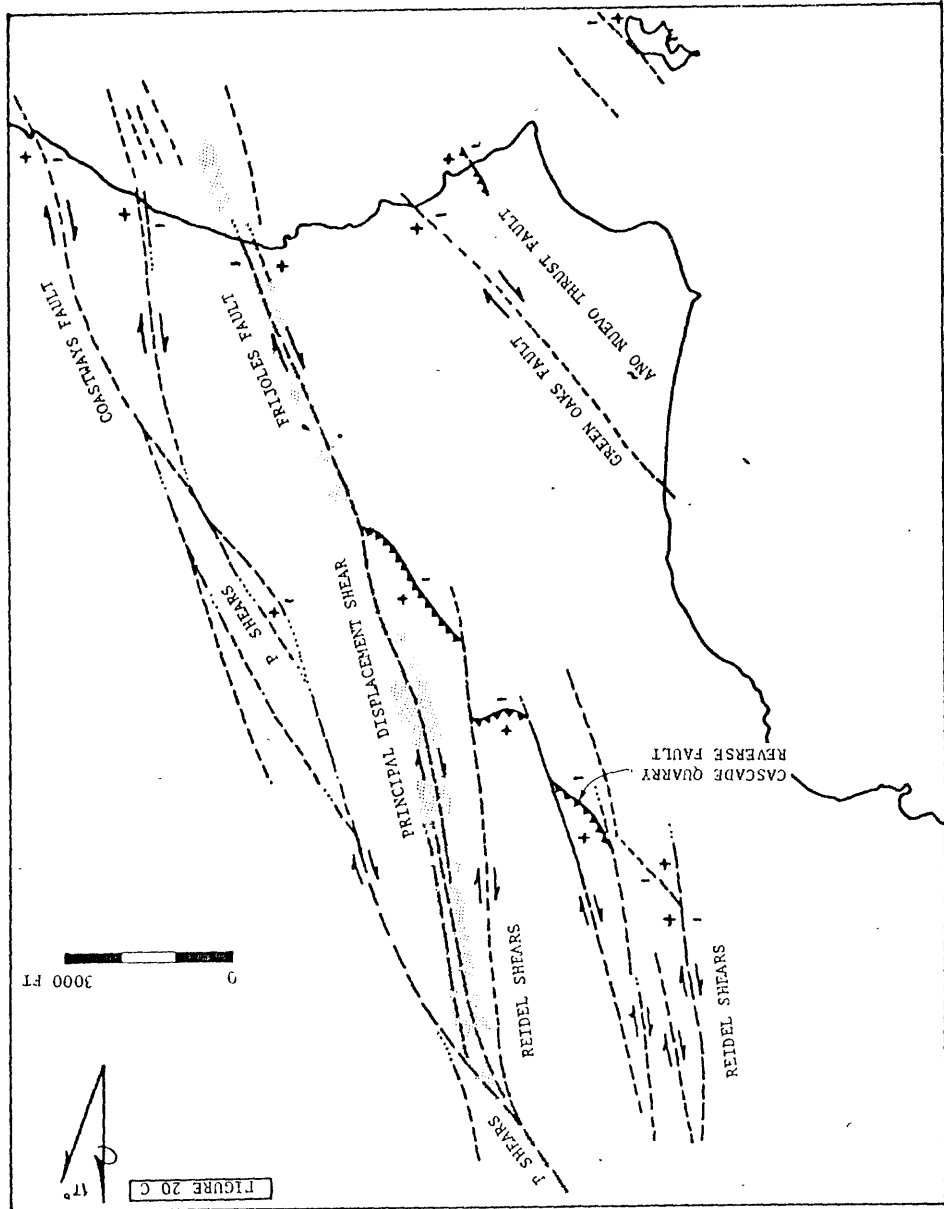
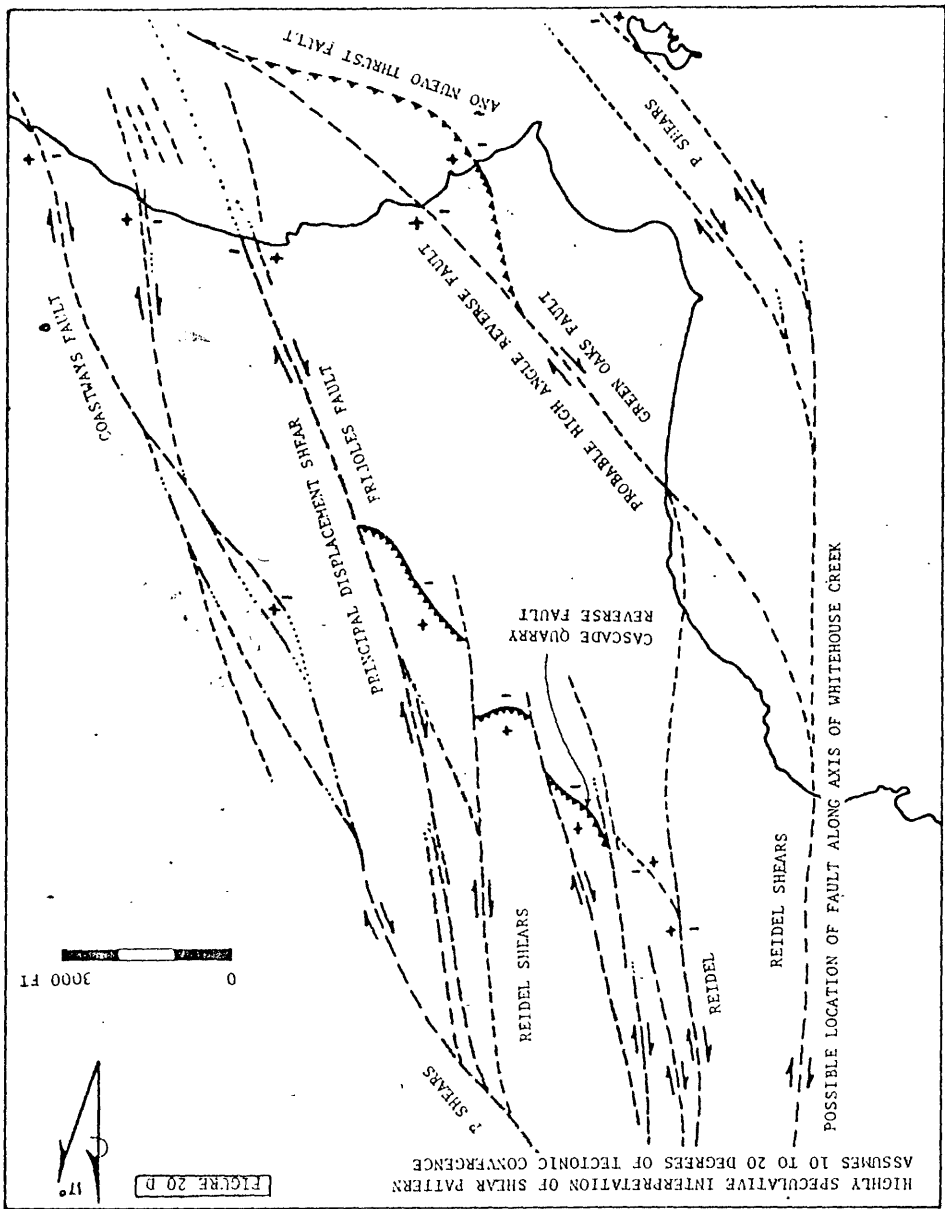
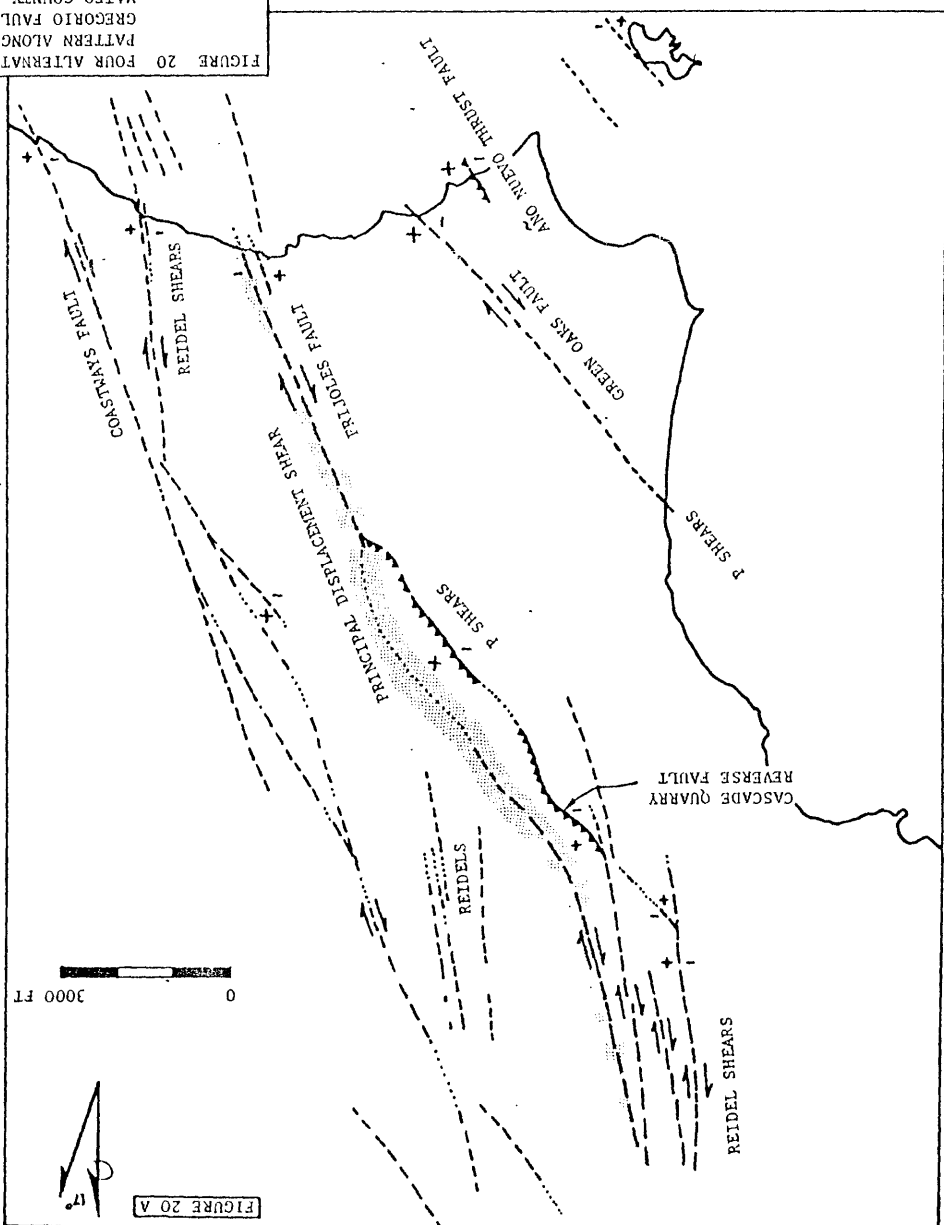
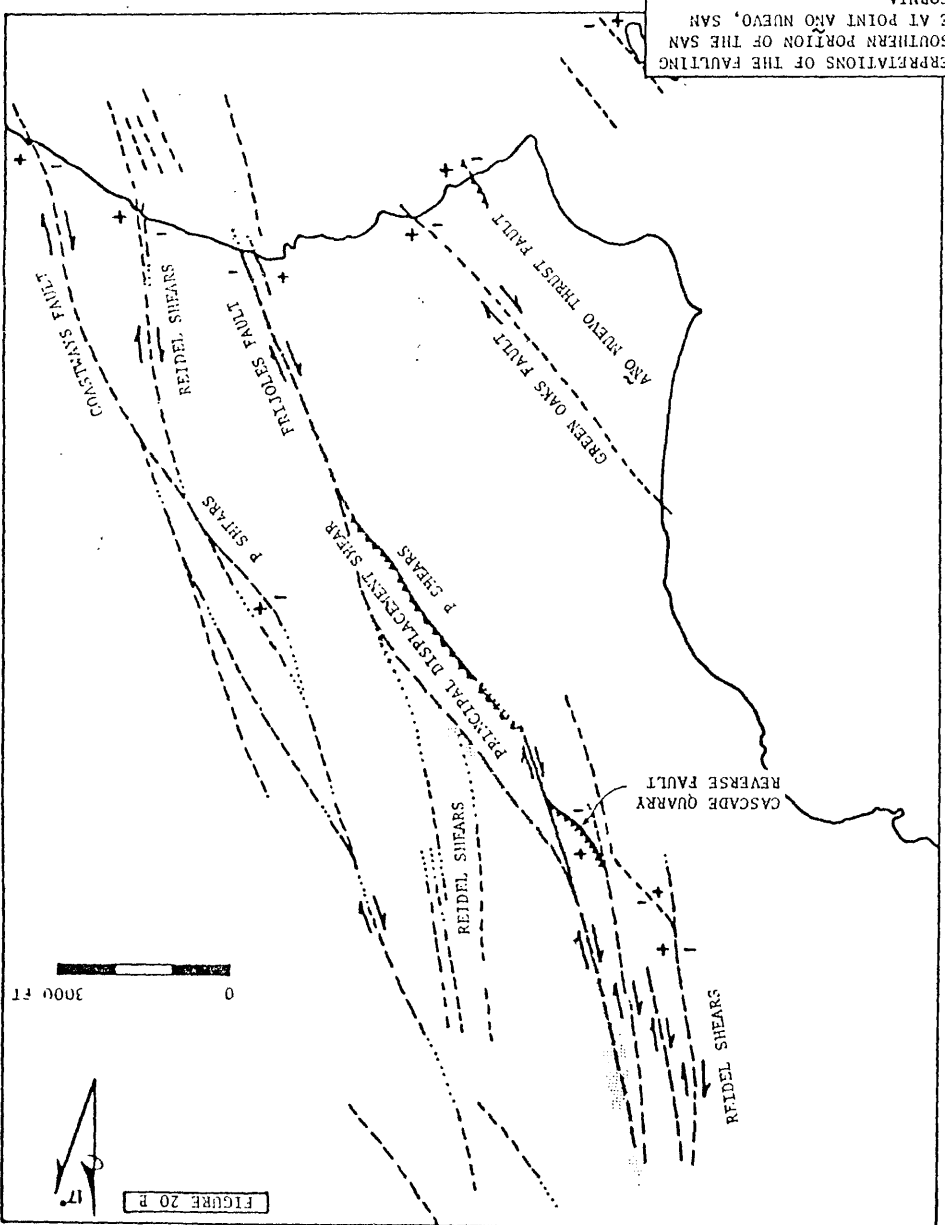


FIGURE 20  
 PATTERN ALONG THE SOUTHERN PORTION OF THE SAN  
 GREGORIO FAULT ZONE AT POINT AND NUEVO, SAN  
 MATEO COUNTY, CALIFORNIA  
 FAULT TERMINOLOGY AFTER IGALLENKO, 1970



the fault to the areal distribution of the members of the Purisima formation, and the complexity of the faulting at Año Nuevo (Figures 20, 21) makes it difficult to determine if the deposition of the Purisima formation near Año Nuevo was fault controlled.

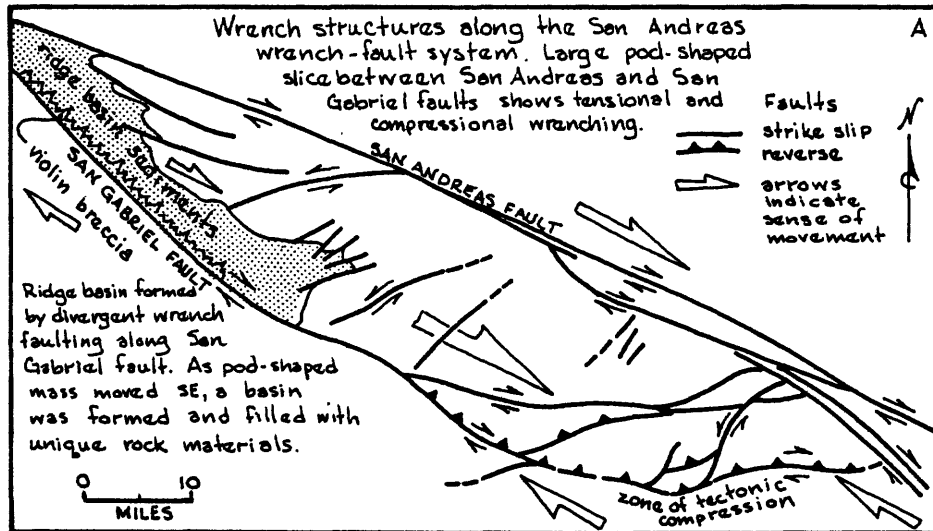
As indicated in Figure 19, the Quaternary marine terraces do not match across the mouth of Pescadero Creek. The lowest marine terrace south of the mouth of Pescadero Creek is equivalent to either the third or fourth emergent marine terrace near Point Año Nuevo and most likely is more than 500,000 years old. These terrace correlations are based on detailed field mapping in this area by Weber and Lajoie (1980) (Also refer to Weber and others, 1979). North of the mouth of Pescadero Creek, the lowest marine terrace apparently is equivalent to either the lowest (Santa Cruz - 105,000 years B.P.) or possibly the second emergent marine terrace (Cement - 200,000(?) years B.P.) at Point Año Nuevo. The terrace has been faulted complexly along a series of northeast-dipping reverse faults (Figure 19) that are interpreted as being part of the Frijoles fault.

PATTERN OF FAULTING AND FAULT OFFSETS - As indicated in Figures 1 and 5, the surface trace of the Frijoles fault does not consist of a single, well-defined fault break but along most of its onshore length apparently is composed of several strands that form a complex series of left-stepping en echelon faults with both strike-slip and reverse displacement. Along this portion of the fault, the primary through-going trace or principal displacement shear is composed of numerous small faults, and it seems reasonable to refer to the entire group of related faults and/or fractures as the Frijoles fault complex. Many of these faults have been mapped on aerial photographs primarily on the basis of geomorphic features. Because landforms are rapidly weathered and erosionally modified in the wet coastal climate, it is impossible to map all of the fault strands and fractures and to delineate with certainty the connections between individual fault strands within the Frijoles fault complex.

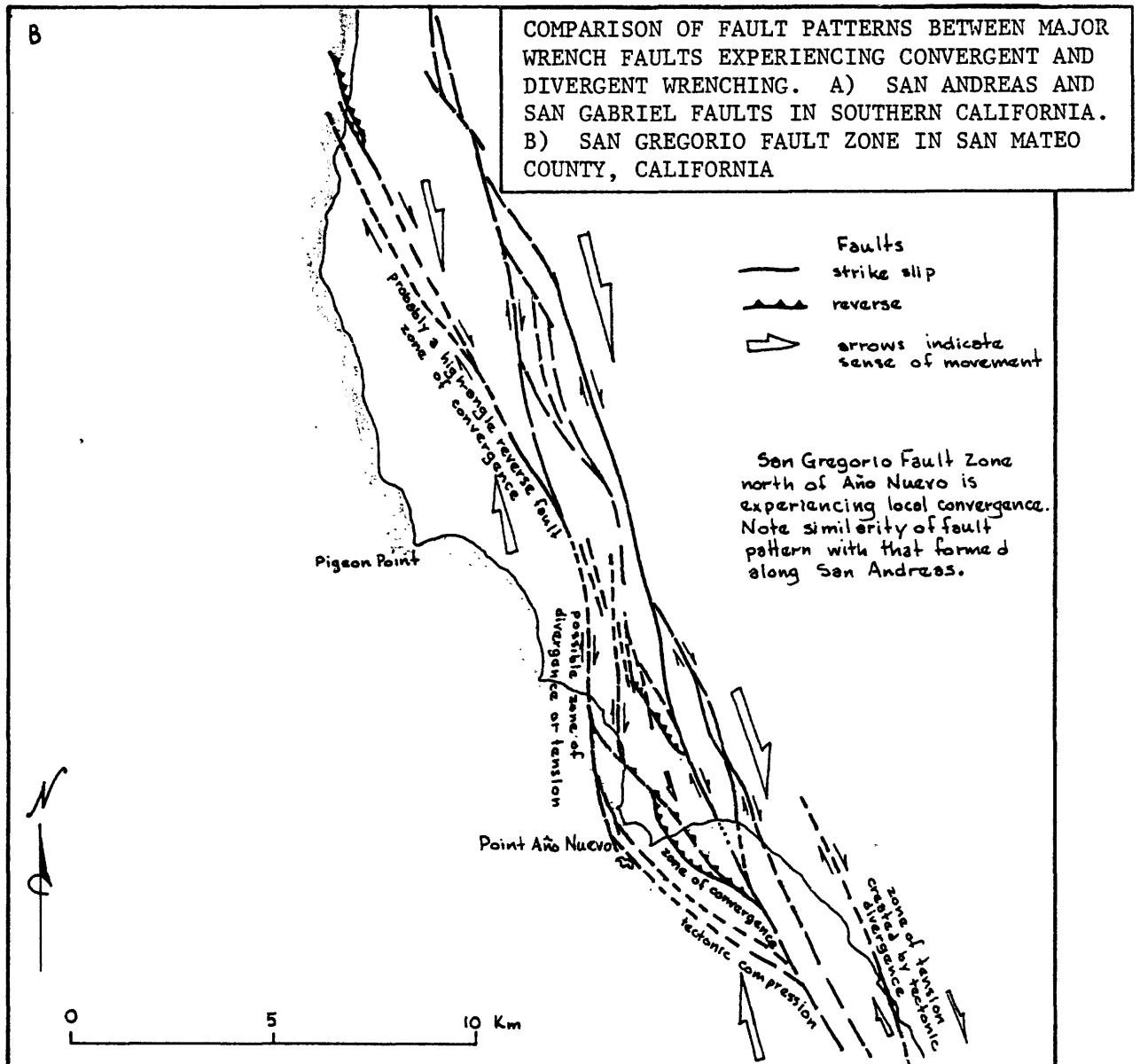
From the south shore of Point Año Nuevo northwest to the vicinity of the Green Oaks fan (Figure 5), the Frijoles fault apparently consists of a single, well-defined shear zone striking N 23 degrees W and dipping vertically. The fault is exposed in the sea cliff along the south shore (Figure 17) as a 300-ft.-wide zone of crushed and broken rock. Along the eastern edge of this sheared zone, Holocene fluvial deposits of Año Nuevo Creek are drag-folded into steeply-dipping orientations along the fault (Figures 17 and 18). There is an apparent 100-120-ft. vertical offset of the wave-cut platform of the 105,000-year-old marine terrace, with the southwest side upthrown with respect to the northeast side. Radiocarbon dating of peats and charcoal in the Año Nuevo Creek sediments indicates that the section of fluvial sediment varies in age from about 10,500 years B.P. at the base to 8,000 years B.P. at the top (K. R. Lajoie-unpublished dates).

Because there are no deposits of Año Nuevo Creek southwest of the fault, it is impossible to determine the total offset, either vertical or horizontal, of the 8,000-10,000-year-old deposits. The fault apparently acted as the southwest boundary of the depositional area for the fluvial deposits, and because the Pomponio block continued to drop, Año Nuevo Creek deposits never were deposited across the fault.

Northwest of the Green Oaks fan (Figure 5), near the abandoned drainages, the pattern of faulting and the relative fault offsets are more complex.



After Dibblaz 1968, Crowell 1954



Because exposures are poor and the flatlands are cultivated, it is difficult to map the fault traces with certainty. Figure 5 indicates the simplest interpretation of the faulting. Essentially, the Frijoles fault complex between the abandoned drainages and the northernmost portion of the Green Oaks fan (Figure 5) consists of a steeply-dipping reverse-oblique fault and a right-lateral strike-slip fault that probably merge at depth into a single fault. The reverse-oblique fault with a right-lateral component is well exposed only in a spillway and quarry wall on Cascade Ranch (Figures 2 and 5 and Plates XII to XVII). We will refer to it as the Cascade Quarry reverse fault. Its presence south of the Cascade Ranch Quarry area is inferred from geomorphic features, particularly two uplifted sections of marine terrace deposits. One is exposed in a road cut along Highway 1 and the other is inferred from seismic refraction data to exist at the top of the long linear hill that crops out in the middle of the terrace. The existence of the right-lateral strike-slip fault is inferred from observations of a wave-cut platform in the Cascade Ranch Quarry. There the wave-cut platform dips slightly to the northeast, but a second portion of the same platform is exposed at a higher elevation about 500 ft. to the east. Although the existence of a reverse fault between the two exposures of the wave-cut platform would explain the elevation difference, we infer the presence of a right-lateral strike-slip fault (Figure 20a) with a minor vertical component for two reasons: (1) The Cascade Quarry reverse fault is a small fault that has taken up only a small portion of the movement along the San Gregorio fault zone, and (2) the fault regime in the area is predominantly right-lateral strike-slip.

This obviously is not the only possible interpretation of the outcrop data. Figure 20 presents Weber's original interpretation (Weber and others, 1979; Weber and Lajoie, 1980) and three alternate interpretations of essentially the same outcrop data. The three alternate interpretations are based on direct comparisons and an attempt to match the fault pattern along the Frijoles fault with experimentally-derived fault and fracture patterns and with fracture patterns developed during earthquakes along large strike-slip faults elsewhere in the world.

Comparisons of the observed fault pattern along the southern portion of the San Gregorio fault zone with the fracture pattern of the August 1968 Dasht-e Bayaz (Iran) earthquake (Tchalenko & Ambraseys, 1970) and with numerous model studies (Tchalenko, 1970; Wilcox and others, 1973) indicate that left-stepping en echelon faults mapped north of the Cascade Creek fan (Figures 5 and 20) are Reidel shears (terminology of Tchalenko, 1970). The high-angle Cascade Quarry reverse fault (Figures 2, 5, and 20) apparently was formed along a P-shear direction with the vertical movement being only a minor component of the total movement along this fault. Similarly, the fault strand with predominantly strike-slip motion northeast of the reverse fault is formed along a P-shear direction.

A comparison of our analysis of the Frijoles fault with the work of Tchalenko (1970) indicates clearly that the principal displacement shear is formed along Reidel and P-shear directions as one would expect. The overall pattern is most comparable to the post-peak structure of a shear zone (Tchalenko, 1970, p. 1637 & 1638) and somewhat less comparable to the residual structure stage.

Because the southern portion of the San Gregorio fault zone appears to be more complex than the northern portion, and because reverse faulting appears to be quite common along the Frijoles fault and at Point Año Nuevo,

we compared the fault pattern with experimentally-derived fracture patterns and with fracture patterns along major faults where tectonic transpression or convergent wrenching has taken place (Wilcox and others, 1973; Lowell, 1972; Sylvester and Smith, 1976). During convergent wrenching or transpression, the movement is not confined to a well-defined shear couple with the structural blocks in the basement sliding past each other in parallel. Instead, the fault blocks converge toward each other. This is a common occurrence locally along wrench faults, and numerous studies (Wilcox and others, 1973, Sylvester and Smith, 1976) have indicated that strong convergence usually is accompanied by intense reverse faulting and/or thrusting.

Figures 20c and 20d illustrate two interpretations of the fault pattern of the Frijoles fault complex in which the principal displacement shear lies east of the reverse fault segment. In these interpretations we have assumed that the pattern has resulted from local convergence. Using this interpretation, it seems as if the Frijoles fault has been the principal displacement shear zone in the recent past. Nevertheless, it also appears as if the principal displacement zone transfers from the mapped trace of the Frijoles fault to the Coastways fault north of the Cascade Creek fan along a north-south trending Reidel shear. Hence, it is not necessary for the principal zone of movement in these interpretations to be confined to either the Coastways or the Frijoles fault, but it apparently may shift back and forth between the two different fault strands within the complexly-faulted Pomponio structural block. If convergent wrenching is occurring along the entire onshore trace of the Frijoles fault, then the segment of the fault from Cascade Quarry north to the mouth of Pescadero Creek may be a high-angle reverse fault with a large component of strike-slip movement. This configuration would help to explain some of the apparently anomalous air photo lineaments and geomorphic features along this section of the fault.

Figure 20d presents a highly speculative interpretation of the faulting near Point Año Nuevo; the numerous secondary traces in the sea cliff along the south shore are included in the localized zone of transpression. The fault pattern compares favorably with the pattern formed along the south side of the San Andreas fault in the pod-shaped slice between the San Andreas and the San Gabriel faults (See Figure 21, adapted from Wilcox and others, 1973, p. 90; after Dibblee 1968, and Crowell, 1954). The fault pattern near Año Nuevo, the presence of numerous active secondary traces, and the relative motions on all of the faults are explained reasonably well if the San Gregorio fault zone is experiencing right-lateral convergent wrenching.

Both of the interpretations based on right-lateral convergence are lent some support by the log of one of our exploratory trenches, Cascade Trench #3 (Plate XVIII, Figures 2 and 5). The trench was located on the Cascade Creek fan over what was thought to be the trace of the Cascade Quarry reverse fault. The site was selected on the basis of magnetometer surveys, seismic refraction studies, and hand auger core holes (Appendix B). The geophysical work and the core holes indicated a discrepancy in ground water levels and in the near-surface stratigraphy on opposite sides of the presumed fault trace. In addition, a minor change in slope across the proposed trench site was thought to be the remnant of a partially-degraded fault scarp.

Instead of a fault trace, the trench exposed two separate levels of stream terraces eroded into marine terrace sand and gravel (Plate XVIII). It is obvious that no fault trace passes through the trench site, and it is unlikely that the reverse fault trace lies either northeast or southwest

of the trench in the areas covered by the geophysical surveys. Based on these factors, the fault patterns presented in Figures 20c and 20d appear to be more reasonable than the original interpretation (Figure 20a) which requires that a rather large reverse fault traverse this area.

Although the exact configuration of the faults in this area is not known, there are enough field data that, combined with air photo interpretation, indicate that the late Tertiary and Quaternary pattern of faulting must be the result of continuing right-lateral strike-slip movement that probably has a strong component of convergence in the vicinity of Point Año Nuevo. Most of the faulting appears to be occurring along a principal displacement shear formed along Reidel shears and P-shears, and the location of this principal displacement shear appears to have changed through time.

LATE PLEISTOCENE SLIP RATES - Because of the uncertainties regarding the pattern of faulting along the Frijoles fault near Point Año Nuevo, it is difficult to determine the late Pleistocene rate of movement along the Frijoles fault. Nevertheless, some rough estimates can be made from the offset of stream channels crossing the Santa Cruz terrace and the offset of the shoreline angles of the Santa Cruz and Western terraces. Both Cascade Creek and Año Nuevo Creek with its former drainages have been offset right-laterally across the Coastways and Frijoles faults, the two primary strands of the San Gregorio fault zone. Because we know that the age of the shoreline angle of the Santa Cruz terrace is approximately 105,000 years B.P., we assume that sea level had dropped and the streams had established themselves in roughly linear drainages, perpendicular to the faults, across the former ocean floor by 100,000 years B.P. Nevertheless, it may well be that the roughly linear drainages were established much more recently.

Depending on how the offset of the channel is measured, Año Nuevo Creek may have been offset 487-914 m in 100,000 years, with an average offset rate of 0.5 to 0.9 cm/yr. Cascade Creek may have been offset 518-760 m in 100,000 years, with an offset rate of 0.5 to 0.76 cm/yr. These rates include movement across both of the primary faults.

A preliminary analysis of the offset of the shoreline angles of the two lowest marine terraces reported by Weber and Lajoie (1977, 1979) and by Weber, Lajoie, and Wehmiller (1977) indicates that the Frijoles fault probably had a late Pleistocene offset rate of 0.18 to 0.23 cm/yr. and that the Coastways trace probably had a rate of 0.48 to 1.5 cm/yr. Average rates across the two primary faults range from 0.72 to 1.73 cm/yr. with a best estimate of 0.8 to 1.0 cm/yr. Figure 22 shows the fault pattern and the shoreline angle configuration used in the original reconstruction; the fault pattern is identical to that of Figure 20a.

A reevaluation of the distribution of marine terrace remnants and shoreline angles with regard to the possible fault patterns in the Whitehouse Creek - Point Año Nuevo area is presented in Figures 23a-d. The fault patterns are far more complex than in the area where we measured offsets of stream channels. This complexity increases the difficulty of reconstructing the shoreline angles of the terraces across the fault zone. Realizing the limitations of the data, we have reconstructed the shoreline angles as best as possible and have used their offsets to estimate the rates of movement along the Frijoles fault complex, the Coastways faults, and the numerous Reidel shears lying between the two primary traces.

FIGURE 23 Four alternate interpretations of the pattern of faulting at Point Ano Nuevo showing the offset of shoreline angles of the Western(?) and Santa Cruz terraces. Fault terminology after Tchalenko, 1970.

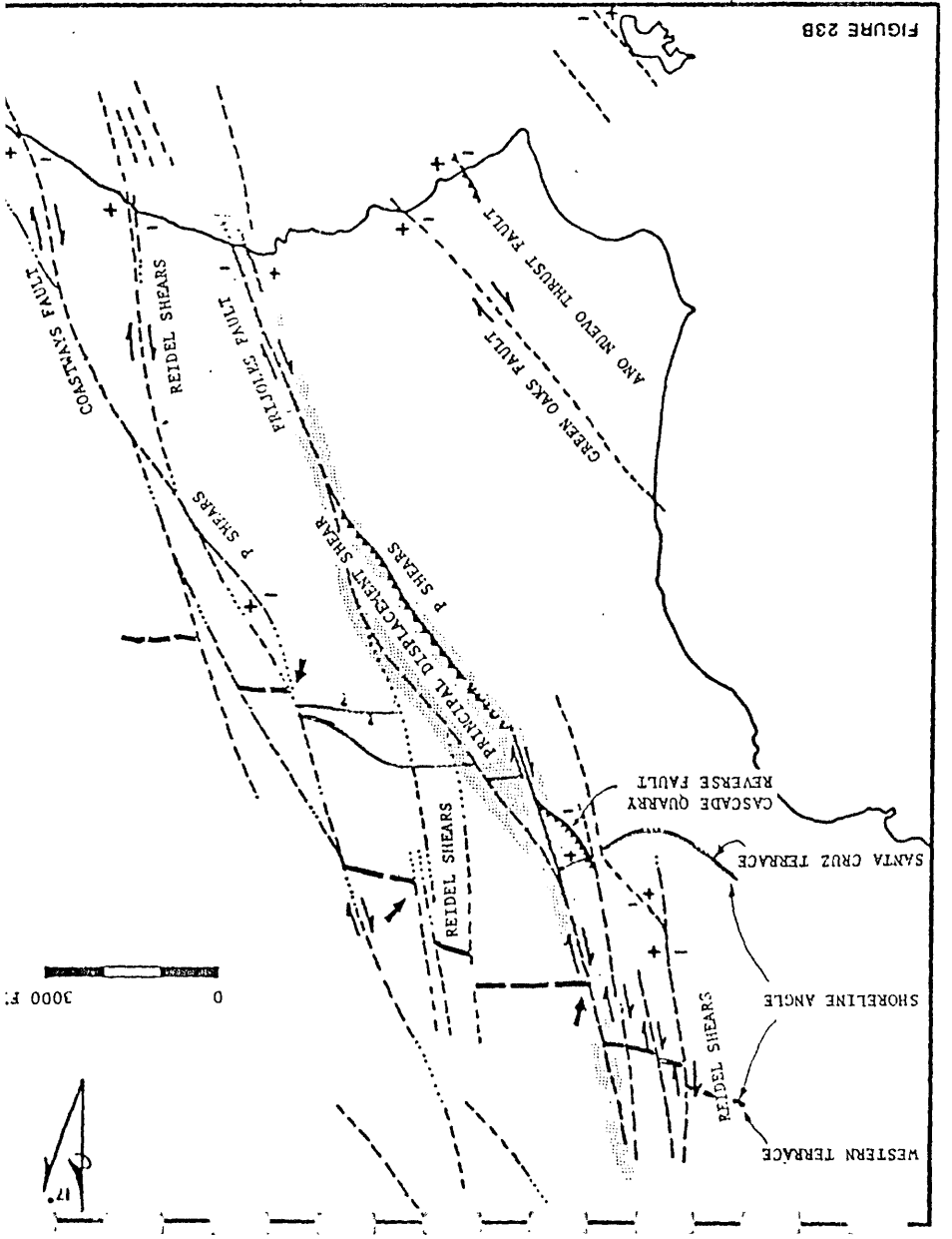
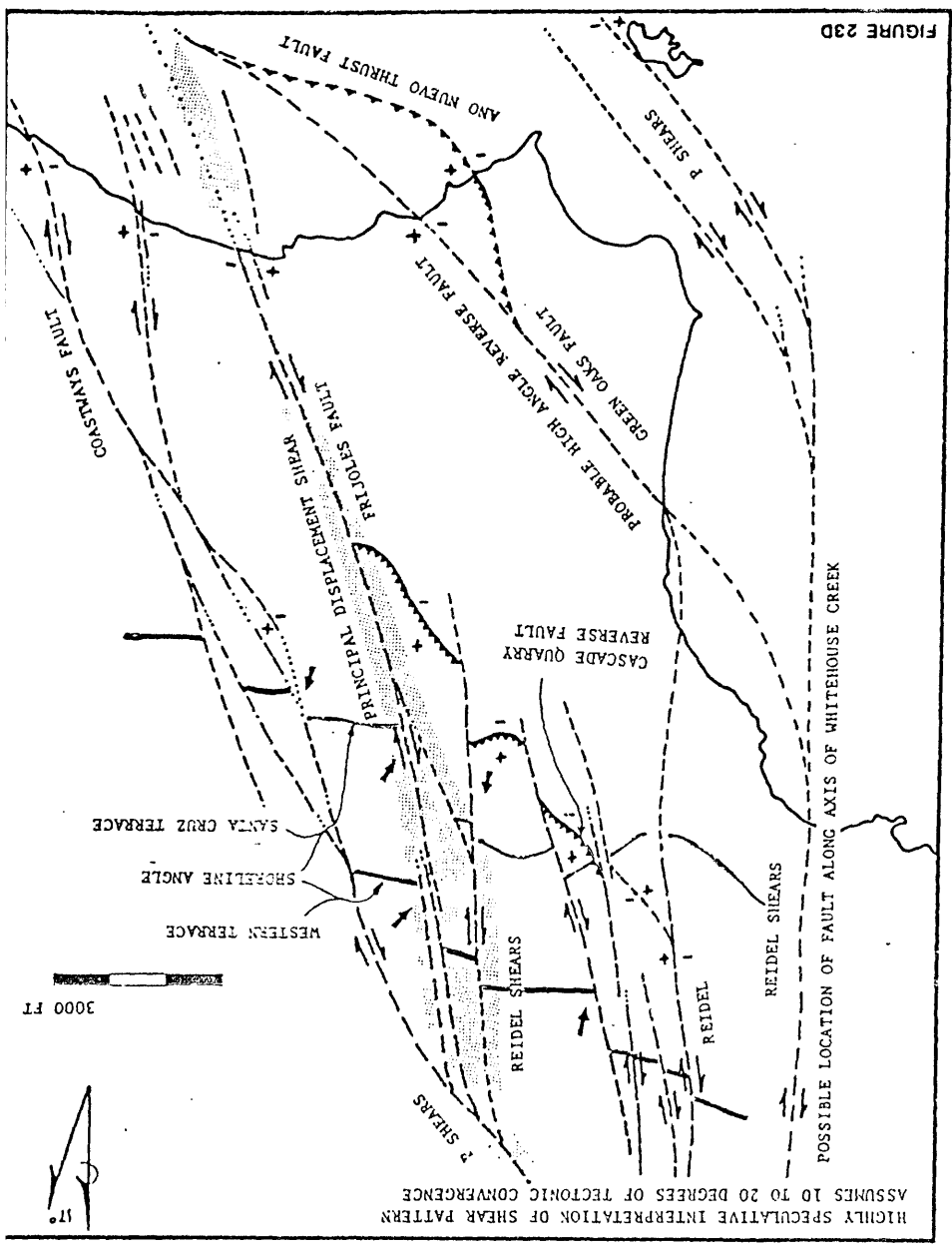
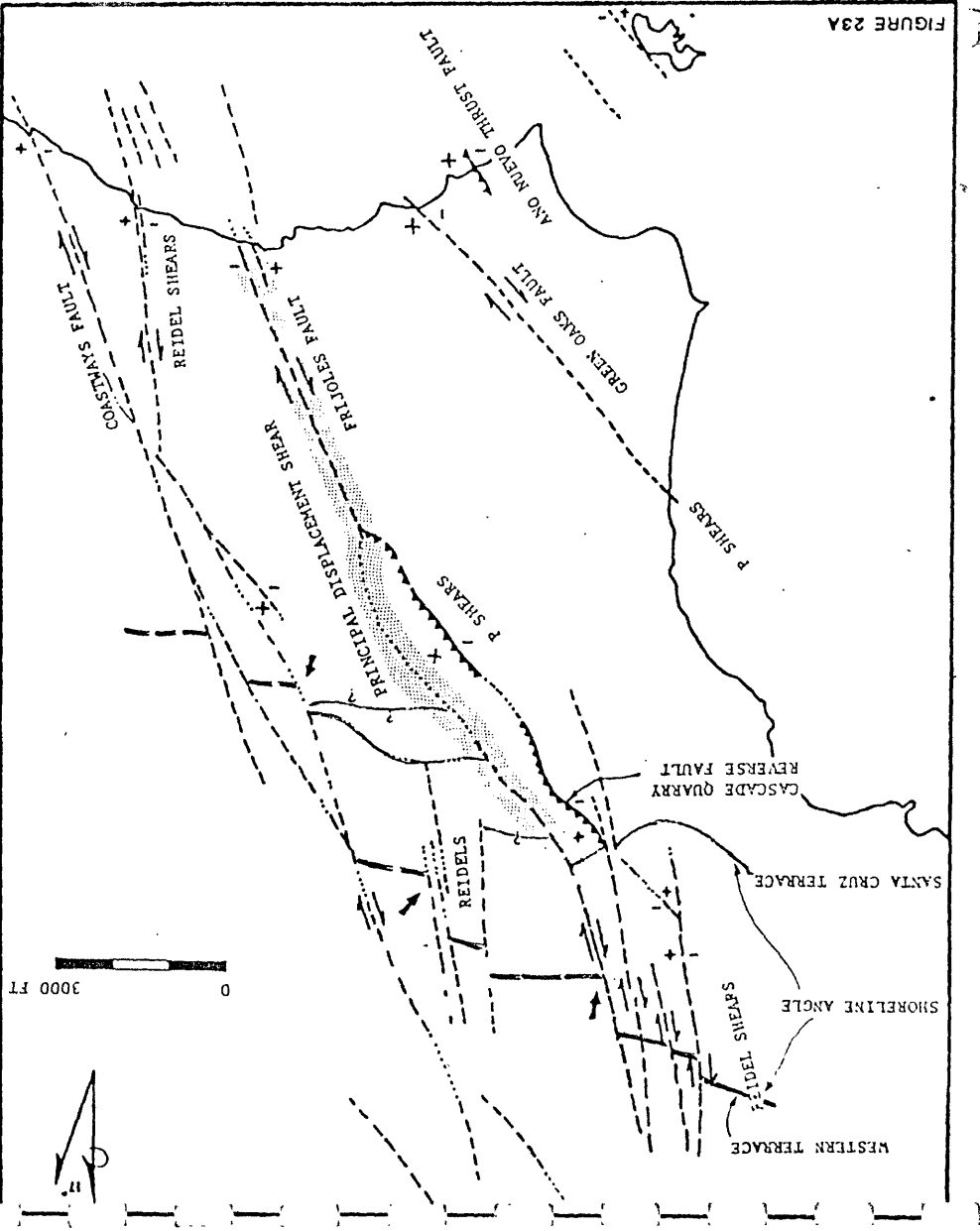
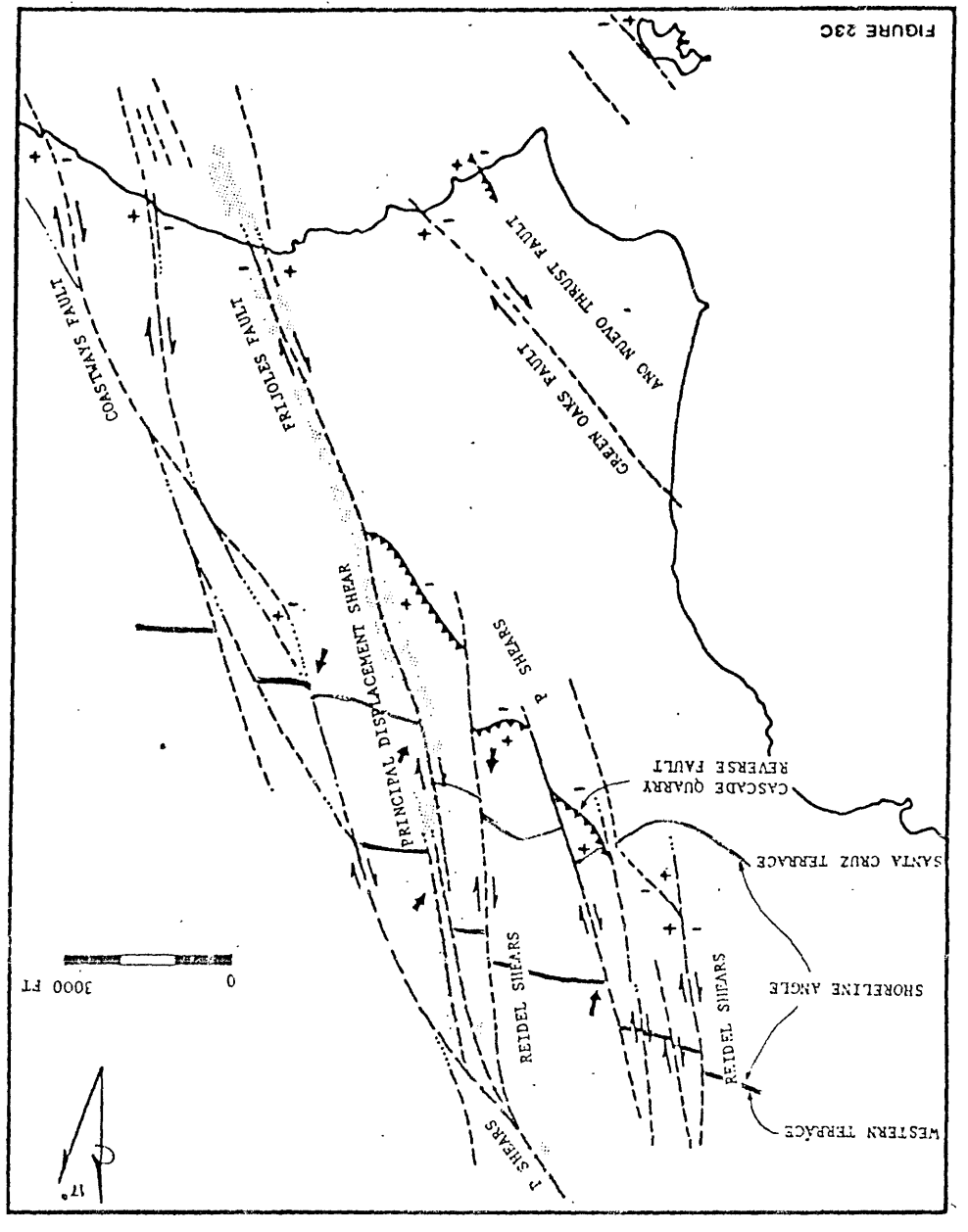


FIGURE 23D  
 HIGHLY SPECULATIVE INTERPRETATION OF SHEAR PATTERN  
 ASSUMES 10 TO 20 DEGREES OF TECTONIC CONVERGENCE  
 POSSIBLE LOCATION OF FAULT ALONG AXIS OF WHITEHOUSE CREEK  
 REIDEL SHEARS  
 REIDEL  
 WESTERN TERRACE  
 SHORELINE ANGLE  
 SANTA CRUZ TERRACE  
 CASCADE QUARRY  
 REVERSE FAULT  
 PRINCIPAL DISPLACEMENT SHEAR  
 P SHEARS  
 ANJO NUEVO THRUST FAULT  
 GREEN OAKS FAULT  
 PROBABLE HIGH ANGLE REVERSE FAULT  
 REIDEL SHEARS  
 P SHEARS  
 COASTWAY FAULT

FIGURE 23B  
 WESTERN TERRACE  
 SHORELINE ANGLE  
 SANTA CRUZ TERRACE  
 CASCADE QUARRY  
 REVERSE FAULT  
 PRINCIPAL DISPLACEMENT SHEAR  
 P SHEARS  
 ANJO NUEVO THRUST FAULT  
 GREEN OAKS FAULT  
 REIDEL SHEARS  
 P SHEARS  
 COASTWAY FAULT

FIGURE 23C  
 WESTERN TERRACE  
 SHORELINE ANGLE  
 SANTA CRUZ TERRACE  
 CASCADE QUARRY  
 REVERSE FAULT  
 PRINCIPAL DISPLACEMENT SHEAR  
 P SHEARS  
 ANJO NUEVO THRUST FAULT  
 GREEN OAKS FAULT  
 REIDEL SHEARS  
 P SHEARS  
 COASTWAY FAULT

FIGURE 23A  
 WESTERN TERRACE  
 SHORELINE ANGLE  
 SANTA CRUZ TERRACE  
 CASCADE QUARRY  
 REVERSE FAULT  
 PRINCIPAL DISPLACEMENT SHEAR  
 P SHEARS  
 ANJO NUEVO THRUST FAULT  
 GREEN OAKS FAULT  
 REIDEL SHEARS  
 P SHEARS  
 COASTWAY FAULT

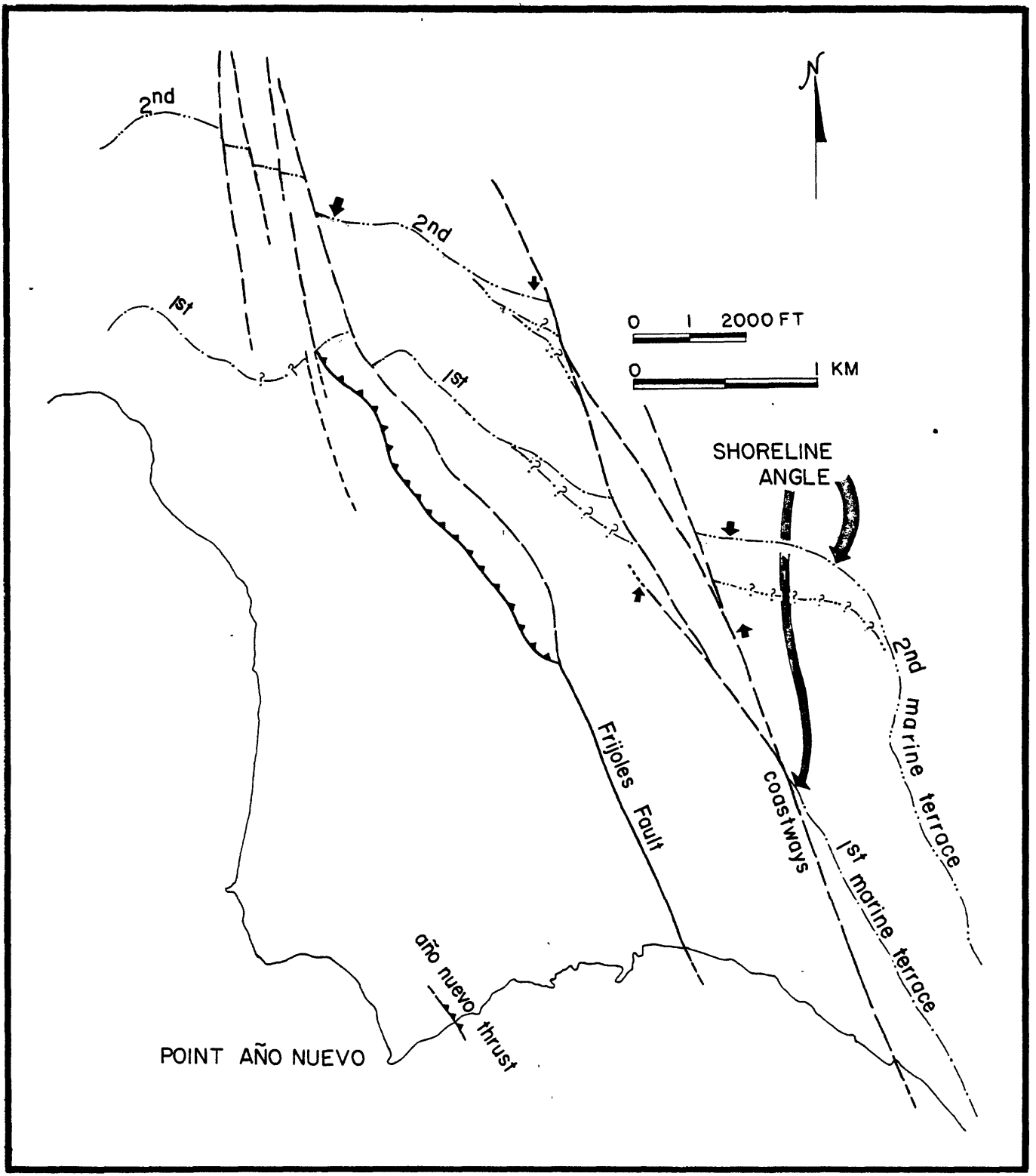


FIGURE 22 Deformation of the shoreline angles of the first (Santa Cruz) Marine terrace and second (Western) marine terrace along the Coastways and Frijoles faults at Point Año Nuevo. Arrows indicate the limits on the position of the shoreline angle.

We have determined potential ranges of rates of movement along the Frijoles fault, the Coastways fault, and the entire San Gregorio fault zone for offsets of both the Santa Cruz terrace and the Western terrace. These rates were determined for each of the four interpretations of fault patterns (Figure 20) and shoreline angle offsets (Figures 23) and are presented on Table 1.

In summary, our estimates of offsets of the marine terrace shoreline angles suggest an average late Pleistocene rate of movement ranging from 6.0 mm/yr (5.8 - 6.3 mm/yr) to 11 mm/yr (10.4 - 11.5 mm/yr). This range compares favorably with the displacement rate, 5-9 mm/yr, determined from stream channel offsets and with the long-term displacement rate, 7-9 mm/yr determined from Graham and Dickinson's (1978) data for post-middle Miocene slip.

One should note that the total offset of the Western terrace remains the same in all of the interpretations. This results from our greater certainty of the position of the terrace remnants and hence the probable position of the shoreline angle. In addition, although the total slip rate across the fault zone has been reasonably constant through time, the slip rate along any one primary trace or along any one set of shears probably varies. If the rates of movement that we have determined are approximately correct, most of the movement between 105,000 and 200,000 (or 400,000) years B.P. occurred on the Coastways fault and on the eastern and western sets of Reidel shears indicated in Figures 20a and 23b. Since 105,000 years B.P., the majority of the movement has occurred along the Frijoles fault and the east Reidel shears. This suggests that in areas of complex faulting, particularly those resulting from convergent wrenching along strike-slip fault zones, the principal zone of movement is not constrained to a single through-going trace through time; fault activity is transferred from one strand to another depending on the local buildup of stresses within the fault zone.

RELATION OF MOVEMENT ON THE CASCADE QUARRY REVERSE FAULT TO MOVEMENT ON THE FRIJOLES FAULT AND THE SAN GREGORIO FAULT ZONE - Because our detailed studies have been concentrated on the reverse fault exposed in the Cascade Ranch Quarry (Plates III, XIII, and XIV and Figures 2, 5, 20, and 23), it is important to understand the relationship of the nature and amount of movement on this secondary fault to the movement on both the Frijoles fault and, if possible, the entire fault zone. This relationship is not understood completely because we do not know the exact pattern of faulting in the area north of Point Año Nuevo, but reasonable inferences regarding movement on the Cascade Quarry reverse fault can be drawn from the following data.

Structural Attitude of Faults Exposed in Cascade Quarry Area - The Cascade Quarry reverse fault where exposed in the quarry, spillway and Cascade Trench #1 (Plates III and XII-XVII) contains a well-developed shear plane consisting of very clayey fault gouge. Well-preserved striations and slickensides present in numerous areas on the fault plane have trends that vary from N5 degrees W to N8 degrees E with plunges varying from 30 degrees to 45 degrees N. The strike and dip of the plane of the reverse fault vary considerably among the trench, quarry and spillway exposures, but they vary within limits.

More than 20 measurements were made in the quarry and trench on the most prominent fault plane, on shear surfaces in the fault gouge associated with the fault plane, and on some minor shears passing

Fault Pattern and Shoreline Angle Interpretations	Santa Cruz Terrace (105,000 yrs B.P.)	Western Terrace (If = 200,000 yrs B.P.) (If = 400,000 yrs B.P.)
FIGURE 23A	principal displacement shear 6.6 mm/yr to 9.6 mm/yr Cascade Quarry reverse fault .4-.7 mm/yr TOTAL 7.0-7.3 mm/yr low to 10.4 mm/yr	principal displacement shear and West Reidels 2.6 mm/yr. Coastways fault 6.4 mm/yr East Reidels 2.5 mm/yr TOTAL 11.5 mm/yr
FIGURE 23B	principal displacement shear 5.9 mm/yr Cascade Quarry reverse fault .4-.7 mm/yr TOTAL 6.3-6.6 mm/yr	principal displacement shear and West Reidels 2.6 mm/yr Coastways fault 6.4 mm/yr East Reidels 2.5 mm/yr TOTAL 11.5 mm/yr
FIGURE 23C	principal displacement shear West Reidels 3.2 mm/yr Cascade Quarry reverse fault 2.8 mm/yr TOTAL .4-.7 mm/yr 6.4-6.7 mm/yr	West Reidels 2.9 mm/yr principal displacement shear 2.2 mm/yr Coastways fault 6.4 mm/yr TOTAL 11.5 mm/yr
FIGURE 23D	principal displacement shear 5.5 mm/yr Cascade Quarry reverse fault .4-.7 mm/yr West Reidels 2.8 mm/yr TOTAL 8.7-9.0 mm/yr	West Reidels 2.6 mm/yr principal displacement shear 2.5 mm/yr Coastways fault 6.4 mm/yr TOTAL 11.5 mm/yr

Table 1. Rates of movement on the Frijoles and Coastways faults and the San Gregorio fault zone calculated from offsets of marine terrace shoreline angles.

through the liquefaction-injected sands. The strikes of the fault surfaces range from N22°W to N70°W, and the dips range from 23° to 62° NE. Most of the attitudes, however, lie within the range N32°-52°W, dipping 37°-46°NE. In general we would characterize the reverse fault in the quarry as striking N45°W and dipping 44°NE.

The fault dips much more steeply in the spillway exposure, varying from 55° to 65° NE. The strike of the main fault plane lies between N20°W and N35°W. An average attitude at the spillway exposure is N25°-27°W dipping 60°NE. The reason for the steeper dip in the spillway exposure is not known, but it may reflect the fact that the portion of the fault plane in the spillway probably was farther below the original ground surface than was the portion exposed in the quarry face and in the exploratory trench. Because most thrust faults flatten as they approach the surface, the fault would be expected to exhibit a more gentle dip in the quarry face and a steeper dip at depth. Unfortunately, we do not see a progressive steepening of dip from the upper quarry face to the trench floor, which is 30 ft. below the original ground surface.

The steeper dip in the spillway may be related to the more northerly strike of the fault plane. Because most of the movement in this area is thought to have occurred parallel to the Reidel shear direction (Figures 20, 21 and 23), the more northerly the dip the closer it is to the strike of the Reidel shears (N10°-15°E), which probably dip vertically. Because the reverse fault probably joins the Reidel shear at depth and to the southeast, the closer the strike of the plane of the reverse fault is to the trend of the Reidel shears (or the principal displacement shears that lie immediately to the east) the steeper the dip of the fault plane. The lower-angle dips are more common along the fault plane where it strikes at a greater angle to the trend of the Reidel shears (Refer to Figure 24).

Fault Striations and Slickensides - Direction of Movement - The slickensides and fault striations on the Cascade Quarry reverse fault were measured in the trench, the quarry wall, and the spillway. Any three to four readings taken in one area along the fault plane typically varied less than 5° in strike and in dip. Four average slickenside measurements from the main shear plane exposed in the trench, quarry, and spillway, and two measurements of well-developed slickensides along bedrock faults east of the main fault, are plotted in Figure 24. Selected strikes and dips of the fault plane at these points are also plotted. The trends of the striations vary from N5°W to N8°E with plunges of 17° - 37°N. Refer to Figure 20 for fault patterns, Figure 24 for plots of striation directions and fault plane attitudes, and Plates III, XII, XIII, XIV, and XVI for logs of the quarry, spillway and trench.

The close coincidence of the strike of the Reidel shears and the fault plane striations and slickensides suggests that movement along the Cascade Quarry reverse fault has occurred essentially parallel to the Reidel shears. If the fault plane striations (Figure 24) are truly indicative of the relative motions, it is possible that the hanging-wall block moved to the southeast parallel to the Reidel shears, S5°-10°E, while the footwall block was moving parallel to the striation direction, approximately 2° east of north. This results in approximately 12° of local convergence across the fault at this point.

FIGURE 24

Relative motions of hanging wall and footwall blocks along reverse fault. Blocks converging at angle between 10-15°.

0 2000 FT.

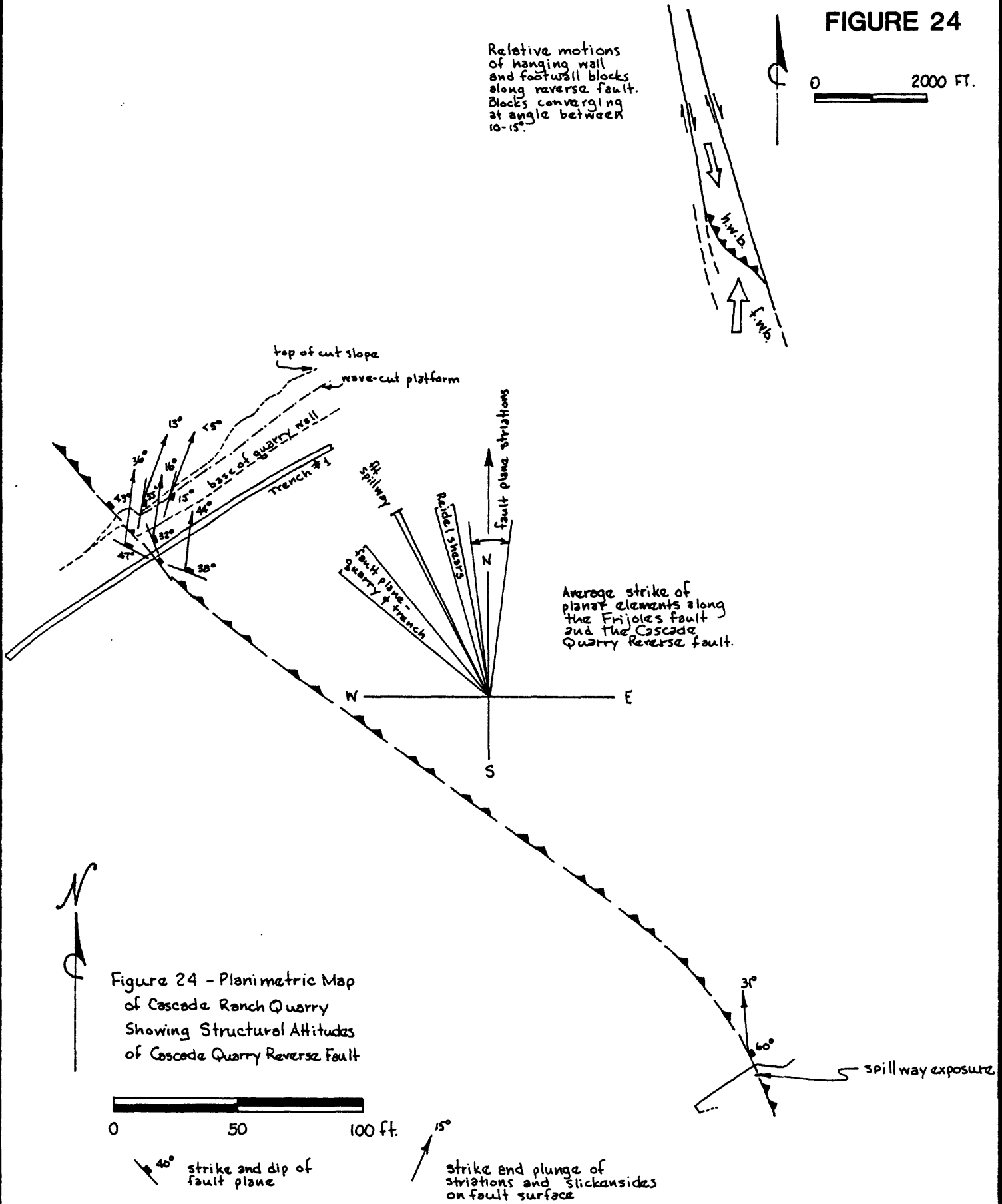


Figure 24 - Planimetric Map of Cascade Ranch Quarry Showing Structural Attitudes of Cascade Quarry Reverse Fault

0 50 100 ft.

40° strike and dip of fault plane

15° strike end plunge of striations and slickensides on fault surface

Using the geometry of movement indicated above, it appears as if the component of vertical movement across the Cascade Quarry reverse fault is much less than the component of horizontal movement. The ratio of the horizontal component of movement parallel to the Frijoles fault, the principal displacement shear, compared to the vertical component of movement along the Cascade Quarry reverse fault can be calculated in two different ways: 1) We can assume that the fault plane slickensides and striations indicate the actual direction of movement and thereby separate this oblique direction of movement into two components of movement or 2) We can assume that the hanging-wall block is moving essentially parallel to the Reidel shears, S5°-10°E, and that the plane of the reverse fault on the average strikes N42°W and dips 42° north-east within this fault block.

Analysis of the striation directions at the four areas of measurement along the fault plane indicates that the ratio of horizontal movement parallel to the principal displacement shear compared to the vertical displacement across the reverse fault ranges from 1.1 to 3.5:1. A reasonable average appears to be a ratio that lies between 1.7 and 1.9:1. An analysis of the relative components of movement based on the assumptions mentioned in 2) above indicates that the ratio of horizontal displacement to vertical displacement is between 1.8 and 1.85:1.

The fault patterns and the slickensides and striations on the principal fault plane in the quarry, Trench #1, and the spillway all indicate that the Cascade Quarry reverse fault is experiencing oblique movement and that the horizontal component of movement is greater than the vertical component of movement. All of our analyses indicate that the ratio of horizontal movement to vertical movement is approximately 1.8:1. For example, if a faulting episode results in 3 ft. of vertical displacement, the horizontal slip on the Cascade Quarry reverse fault would be 5.4 ft. (3 ft. x 1.8). The analyses also indicate that the hanging-wall block must have moved approximately parallel to the Reidel shears. The striations, therefore, indicate that the fault is under-going approximately 12° of local convergence at this point.

MAXIMUM PROBABLE VERTICAL AND HORIZONTAL SURFACE DISPLACEMENTS ALONG THE CASCADE QUARRY REVERSE FAULT. FAULT DIMENSIONS AND RELATIONSHIP TO EARTHQUAKE MAGNITUDE - Using the foregoing analysis of the movement along the Cascade Quarry reverse fault as a basis for relating the horizontal component of movement to the vertical, it is possible to estimate the maximum vertical and horizontal surface displacements that have occurred along this fault and thereby attempt to determine a reasonable range of values for the magnitudes of the earthquakes associated with the faulting events recorded in the quarry wall and trench exposures.

Based on our reconstruction of faulting events along the reverse fault, we believe that there are at least eight colluvial wedges, some with weakly developed soils, exposed on the footwall block in the quarry and trench. Refer to Figure 10 for a diagrammatic sketch of the formation of a wedge of colluvium by erosional modification of a fault scarp. We believe that each of these colluvial wedges records the erosional degradation of a scarp formed by a faulting event that occurred along the San Gregorio fault zone and that movement was concentrated along the reverse fault rather than along other faults in the zone.

Because of the width of the brecciated zone, the relatively large number of shears, and the zone of liquefaction-injected sands along the Cascade Quarry reverse fault, it has been impossible to reconstruct the history of movement as completely as for the Año Nuevo thrust fault. Consequently, it is difficult to determine accurately the amount of vertical surface displacement associated with each faulting episode.

We can, however, estimate the maximum vertical surface displacement associated with each faulting event by measuring the stratigraphic thickness of the colluvial wedge on the footwall block near the fault. The maximum surface displacement must have been at least as great as the thickness of the wedge because rock material was eroded off of the hanging-wall block to create the colluvial wedge. We have estimated from graphic reconstruction of the scarp that the original scarp height was about twice the thickness of the colluvial wedge and probably ranged from 1.5 to 2.2 times the thickness of the wedge. Using a scarp height of 2.0 to 2.2 times the wedge thickness, it is probable that the height of the original scarp associated with each colluvial wedge varied from 2.0 to 8.8 ft. A 2.0-to-2.2-ft.-high scarp would produce a colluvial wedge 1 ft. thick while an 8.0-to-8.8-ft.-high scarp would produce a 4-ft.-thick colluvial wedge.

Using the reconstructed scarp heights as the maximum vertical surface displacements, we approximated the magnitudes of the earthquakes that produced the vertical displacements by using the magnitude vs. maximum surface displacements plots of Bonilla and Buchanan (1970) for reverse faults and reverse-oblique faults. If the ratio of the horizontal component of movement to the vertical component of movement, as determined earlier, is 1.8:1, then a vertical displacement of 2.0 ft. would be accompanied by a horizontal displacement of 3.6 ft., and an 8.8-ft. vertical offset would be accompanied by 15.8 ft. of horizontal displacement. Reconstructed maximum vertical surface displacements accompanying horizontal offsets, and the estimated Richter magnitude earthquakes that would have produced these offsets, are listed in Table 2 for the seven distinct depositional units present on the footwall block in the quarry and trench exposures.

These values for expectable earthquake magnitude, 6.0 to 8.0, appear to be reasonable for a fault zone the size of the San Gregorio. It is of interest that for a fault exhibiting oblique movement, the magnitudes determined for the horizontal component are almost identical to the magnitudes determined for the vertical component. We did not attempt to calculate an expected magnitude for the actual oblique slip, the resultant of the vertical and horizontal slip components, because there are insufficient data for comparison. In addition, of all of the fault displacement - earthquake magnitude plots of Bonilla and Buchanan (1970) the data taken from reverse-oblique faults has the lowest correlation coefficient. This, however, may result from the small data base; there were only five examples from reverse-oblique faults.

The greatest inconsistency in comparing our data on maximum displacement to the standard regression curves is that the displacement data used by Bonilla and Buchanan (1970) and other researchers are all maximum observed displacements on primary faults or principal displacement shears. Our data are from a relatively small secondary or branch(?) fault, and it is impossible to be certain that the largest displacements produced during a particular

** Depositional Unit on footwall block	Stratigraphic Thickness of Qc Wedge (ft.)	Maximum Surface Displacement = Scarp Height = Thickness x (2.0-2.2)*** (ft.)	* Richter Magnitude (reverse fault curve)	Maximum Surface Displacement = Scarp Height = Thickness x 1.5*** (ft.)	* Richter Magnitude (reverse fault curve)	Maximum Calculated Horizontal Surface Displacement = Horizontal slip (ft.)	Richter Magnitude (from maximum horizontal displacement)	Average Richter Magnitude
A	1.8	3.6 - 4.0	7.0	2.7	6.8	6.5	7.3	7.1
B	2.7	5.4 - 6.0	7.5	4.0	7.1	9.7	7.6	7.5
C	1.3	2.6 - 2.9	6.7	7.0	6.3	4.7	7.1	6.9
D	1.0	2.0 - 2.2	6.3	1.5	6.0	3.6	6.9	6.6
E	3.0	6.0 - 6.6	7.7	4.5	7.3	10.8	7.7	7.7
F	4.0	8.0 - 8.8	8.0	6.0	7.6	14.4	7.9	8.0
G	4.0	8.0 - 8.8	8.0	6.0	7.6	14.4	7.9	8.0

\* Magnitude estimates from Bonilla & Buchanan (1970)

\*\* Refer to Plates XII, XIII and XIV for locations of depositional units.

\*\*\* Ratio of scarp height to thickness of colluvial wedge.

Table 2. Maximum surface displacements and estimated Richter magnitude associated with the seven depositional units on the footwall block of the Cascade Quarry reverse fault.

earthquake in the Frijoles fault complex occurred along the fault that we studied. The size of the displacements alone suggests that during the accompanying faulting events, the Cascade Quarry reverse fault must have been the primary site of fault movement.

Most estimates of maximum expectable earthquake magnitude have been made from fault dimensions, primarily fault length and surface rupture length (Bonilla and Buchanan, 1970; Mark, 1977; Mark and Bonilla, 1977; Slemmons, 1977; Bolt, 1978; Wyss, 1979; and Bonilla, 1980). The general correlation of earthquake magnitude with surface rupture length is poor (Bonilla and Buchanan, 1970, p. 14), and more recent work by Wyss (1979, 1980) suggests that the size of the expected earthquake source rupture area on the fault plane can be estimated as accurately as the probable surface rupture length and can be used to produce a better estimate of expected earthquake magnitude.

Despite numerous onshore and offshore studies of the large coastal fault systems, there is no agreement among researchers regarding the length of the San Gregorio fault zone or the possible length of surface rupture that might occur. If the San Gregorio fault zone extends only as far south as the vicinity of Point Sur, the total fault length is 115 miles (185 km). If, however, the coastal faults, Sur-Nacimiento, San Simeon, Hosgri, and San Gregorio, are connected in one large coastal boundary fault, the total length of the system could be 260 miles (420 km). Based on the study of Wentworth and others (1972), we will assume that the surface could be ruptured along 1/2 of the total fault length at one time. In that event, the surface rupture length could be either 93 km (58 miles) or 210 km (130 miles).

The estimated maximum expectable earthquake magnitude for different surface rupture lengths is presented in Table 3.

Fault length	Surface rupture length (1/2 of total)	Mag. after Bonilla & Buchanan 1970	Mag. after Mark and Bonilla 1977	Magnitude after Wyss (1979)	
				W = 15 km Area / mag	W = 20 km Area / mag
115 miles 185 km	58 miles 93 km	7.7 - 7.8	7.5 - 7.6	1380 km <sup>2</sup> / 7.3	1840 km <sup>2</sup> / 7.4
260 miles 420 km	130 miles 210 km	8.5 - 8.6	7.8	3105 km <sup>2</sup> / 7.6	4140 km <sup>2</sup> / 7.7

Table 3. Expected Richter magnitudes associated with specific surface rupture lengths.

The only apparent anomalous value among the maximum expected magnitudes based on rupture length is the 8.5 - 8.6 magnitude. That estimate is based on the original regression curves of Bonilla and Buchanan (1970) which probably are the least reliable. A reasonable estimate for the maximum expectable earthquake along the San Gregorio fault would be 7.5 - 7.8 Richter magnitude, based on the fault lengths.

The apparently are few estimates of maximum expectable earthquake magnitudes based on the maximum surface displacement - magnitude relationship. It is difficult to understand why so few attempts have been made; plots of magnitude versus displacement (Bonilla and Buchanan, 1970) show less scatter and generally have higher correlation coefficients than any of the other fault parameter plots. Other workers (Chinnery, 1969, Slemmons, 1977) also have found a high correlation between surface displacement and magnitude.

The fault displacement used by Bonilla and Buchanan (1970) was the maximum reported for each event and was restricted to the primary fault trace or main fault. The Cascade Quarry reverse fault obviously is not the primary fault in this area; it appears to be a relatively minor secondary or branch fault that experiences movement only intermittently. Nevertheless, the thicknesses of the depositional wedges on the footwall block and the cross-cutting relationships exposed in the quarry clearly indicate that the displacements along the fault were relatively large, large enough for the fault to have been the primary locus of movement during each of the associated earthquakes.

The surface displacements that must have occurred along the reverse fault are far larger than any of the observed displacements along secondary faults and branch faults during historic earthquakes (Bonilla, 1967). Bonilla's plots (1967, p. 24, 25) suggest that with rare exceptions maximum displacements on secondary and branch faults seldom exceed 30% of the displacement along the primary or main fault.

Based on these observations, our interpretation of the pattern of movement on the Cascade Quarry reverse fault is that the fault will experience movement intermittently and not during every major earthquake on the San Gregorio fault zone or the Frijoles fault. During each seismic event on a primary fault, however, there probably is a slight buildup of stress along the reverse fault. Eventually, after a sufficient number of earthquakes accompanied by displacement along the principal displacement shear, the local stresses build up to the point where movement along the reverse fault is triggered during the next earthquake. During this earthquake, the reverse fault experiences surface rupture and temporarily becomes a principal zone of displacement.

If this model is correct, the maximum earthquake magnitudes calculated for the Cascade Quarry reverse fault, although it was not the principal zone of displacement through late Pleistocene time, should be rough estimates of the magnitudes of earthquakes on the primary faults of the San Gregorio fault zone. In addition, the expected earthquake magnitudes based on maximum fault displacement are closely comparable to the expected magnitudes calculated from possible surface rupture lengths. In conclusion, we feel that several lines of evidence indicate that the magnitude of the maximum expectable earthquake that could occur on the San Gregorio fault zone is at least 7.7 to 7.9 and may exceed 8.0 Richter magnitude.

RATIO OF HORIZONTAL SLIP ON THE CASCADE QUARRY REVERSE FAULT TO HORIZONTAL SLIP ACROSS THE SAN GREGORIO FAULT ZONE AT POINT AÑO NUEVO - In devising our model for movement along the Cascade Quarry reverse fault we envision that the reverse fault moves only intermittently in response to the buildup of a local stress field within the Frijoles fault complex. Because we can determine a recurrence interval for faulting events of probable 6.0 - 7.9 magnitude along the reverse fault, we would be able to determine an approximate recurrence interval for earthquakes on the San Gregorio fault zone if we could determine what percent of the total horizontal slip across the San Gregorio fault zone is taking place along the Cascade Quarry reverse fault.

Field mapping of the Santa Cruz terrace and the position of the shoreline angle indicates that there probably has been only a small amount of horizontal slip along the Cascade Quarry reverse fault. The presence of a rather thick wedge of slopewash along the back edge of the terrace makes it impossible to locate the shoreline angle accurately enough in this area to map the offset across the reverse fault. Nevertheless, based on surface mapping, we can place a maximum limit of 200 ft. on the amount of horizontal movement along the reverse fault.

A second method of approximating the total amount of post-Santa Cruz terrace horizontal slip along the Cascade Quarry reverse fault is to use the estimated ratio of horizontal movement to vertical movement (1.8:1) because the total vertical offset of the Santa Cruz terrace can be determined within reasonable limits.

The exposures in the spillway indicate that the lowest stratigraphic unit on the footwall block exposed at the bottom of the spillway is part of a colluvial wedge that apparently formed during the erosion of a fault scarp along the reverse fault. The spillway cut is not deep enough to expose the shallow marine sands that must underlie the fluvial and colluvial sediments present on the footwall block. At least 10 ft. of shallow marine sands must be present because 10 ft. of marine sediment overlies the wave-cut platform on the hanging-wall block in the quarry. From the base of the spillway exposure of the colluvial deposits on the footwall block to the wave-cut platform on the hanging-wall block, the total vertical separation is 50 - 57 ft. Because the total vertical offset of the 105,000-year-old wave-cut platform (Santa Cruz terrace) must be at least 10 ft. greater than this amount, we can approximate the total vertical component of movement along the Cascade Quarry reverse fault in the past 105,000 years as 60 - 80 ft. If the ratio of the horizontal component of movement to the vertical component is 1.8:1, the total horizontal offset along this fault in the past 105,000 years is 110 - 150 ft.

As indicated previously in our analysis of the shoreline angle offset, the Santa Cruz terrace (105,000 years B.P.) has been offset cumulatively between 630 m (2067 ft) and 1155 m (3789 ft) right-laterally across the Frijoles and Coastways faults north of Point Año Nuevo. A reasonable average for the shoreline angle offset is 945 m (3100 ft). If the total horizontal offset along the Cascade Quarry reverse fault is 110 - 150 ft, the ratios for movement on that fault to movement across the San Gregorio fault zone are as follows:

Total horizontal offset on Cascade Quarry reverse fault (ft)	Ratio if horizontal offset across SGFZ is 2067 ft.	Ratio if horizontal offset across SGFZ is 3789 ft.	Ratio if horizontal offset across SGFZ is 3100 ft.
110	.053	.03	.035
150	.073	.04	.048

Table 4. Ratio of horizontal displacement on the Cascade Quarry reverse fault to horizontal displacement across the San Gregorio fault zone.

If our model for movement is valid and some type of consistent relationship or pattern exists between the Cascade Quarry fault and the Frijoles fault (or the San Gregorio fault zone), it appears that the Cascade Quarry reverse fault accounts for approximately 5% of the total horizontal displacement along the fault zone. In addition, we suggest that these ratios indicate that for every earthquake resulting in surface rupture along the Cascade Quarry reverse fault, there probably are nineteen additional earthquakes of similar magnitude along the San Gregorio fault zone near Point Año Nuevo.

RECURRENCE INTERVALS FOR FAULTING EVENTS ALONG THE FRIJOLES FAULT AND THE CASCADE QUARRY REVERSE FAULT -

Introduction - We have used and compared several different methods of approximating the recurrence intervals for major earthquakes along the San Gregorio fault zone in the vicinity of Point Año Nuevo. The methods used include a reconnaissance study of sag pond deposits exposed in the sea cliff, a detailed analysis of the Cascade Quarry reverse fault, and an approximation of recurrence intervals from the long-term slip rates using late Pleistocene marine terrace shoreline angle offsets.

Holocene Sag Pond Deposits at Point Año Nuevo - The sea-cliff exposures of the Frijoles fault along the south shore of Point Año Nuevo (Figures 5, 17 and 18) provide one method of approximating recurrence intervals along the Frijoles fault. The idea on which this approximation is based was originally suggested by Dr. K. R. Lajoie of the U. S. Geological Survey. We have interpreted the Holocene sediments that are in fault contact with crushed Purisima formation exposed in the sea cliff along the south shore of Año Nuevo (Figures 17 and 18) as being the products of deposition in a slowly-deepening sag pond. We visualize that each episode of sag-pond filling was initiated by an earthquake accompanied by surface rupture. The initial pond fill deposited after each deepening

characteristically consists of sandy silt with scattered pebbles. The grain size of the clastic sediments becomes finer with time, and the top of each of the sedimentary sequences consists of very fine-grained silts and dark gray to black organic-rich clay, essentially a peat.

There are six of these depositional sequences exposed in the sea cliff, indicating the recurrence of a similar depositional cycle at least six times. Although Dr. Lajoie and one of the authors (Weber) have not yet completed this work, we have obtained  $^{14}\text{C}$  dates on the peats and charcoal in the sediments. The lowest (oldest) of the peats (Figures 17 and 18) yields a  $^{14}\text{C}$  age of  $10,670 \pm 220$  years B.P., and the stratigraphically highest peat must be slightly older than 8500 years B.P. If each of the vertical transitions from peat to the overlying sandy silts represents a deepening or rejuvenation of the sag pond associated with an earthquake, there were six large earthquakes within 2200 years. This gives an approximate recurrence interval of 366 years. Although it is virtually impossible to determine earthquake magnitudes from the sag pond data alone, it is unlikely that earthquakes with magnitudes smaller than 6.5 would have been accompanied by the surface rupture or tectonic tilting that deepened the sag pond.

Late Pleistocene Slip Rates and Recurrence Intervals - Using the same technique used by Wallace (1970), we can estimate recurrence intervals if a long-term slip rate can be determined with sufficient accuracy. As indicated previously, the late Pleistocene slip rate determined from offset marine terrace shoreline angles and Graham and Dickenson's (1978) post-middle Miocene slip rate both lie between 0.6 - 1.1 cm/yr.

Using Wallace's equations (1970), Bonilla and Buchanan's (1970) fault parameters, and long-term slip rates of 0.6 cm/yr, 0.9 cm/yr and 1.1 cm/yr, we conclude that the probable recurrence intervals for large-magnitude earthquakes may be as follows:

Richter Magnitude	Recurrence Interval (years) if Long-Term Slip Rate = 0.6 cm/yr	Recurrence Interval (years) if Long-Term Slip Rate = 0.9 cm/yr	Recurrence Interval (years) if Long-Term Slip Rate = 1.1 cm/yr
8.0	850	566	463
7.5	450	266	218
7.0	200	133	109
6.5	150	66	55
6.0	50	33	27

Table 5. Recurrence intervals for given Richter magnitudes along the San Gregorio fault zone, determined from long-term slip rates.

The actual recurrence intervals may vary significantly from these rates. Because these long-term recurrence intervals are applicable to the fault zone as a whole, they may not be directly comparable with recurrence intervals determined for a single fault strand within the fault zone, such as those determined for the Frijoles fault from the sag pond deposits.

Analysis of Recurrent Movement Along the Cascade Quarry Reverse Fault - The techniques used in our analysis of the Cascade Quarry reverse fault were described earlier and consist of using cross-cutting relationships and the presence of colluvial wedges eroded off of the fault scarp as indicators of faulting events. Because the exposures of the Cascade Quarry reverse fault are more complex than those of the Año Nuevo thrust fault and because there is evidence of simultaneous movement on multiple fault strands, we have found it impossible to make a complete palinspastic reconstruction of the fault movement; consequently, we have tried to determine the number of faulting events by using:

- 1) Obvious truncation of stratigraphic units by faults.
- 2) Erosional and depositional truncation of faults.
- 3) Wedges of fault-scarp-derived colluvium on the footwall block.

The primary evidence for faulting events in this reconstruction are the wedges of colluvium. Consequently, we have given each distinguishable wedge of colluvium/soil a letter designation. For the quarry wall and Cascade Trench #1, we have distinguished seven colluvial wedges and have labeled the wedges consecutively A-G, with A the youngest. These units are indicated on the quarry and trench logs along with other evidence of the faulting events (Refer to Plates XII, XIII, XIV, XV and XVI). A fault truncating a depositional unit is obvious evidence of a faulting event, and where distinguishable these are indicated on the logs of the exploratory excavations. They are numbered consecutively with "Faulting Event" (FE) #1 being the fault along which the most recent movement has occurred.

Similarly, we were able to distinguish four wedges of colluvium in the spillway exposure, each of which was given a letter designation. The youngest of the four was arbitrarily labeled unit L and the three underlying units were labeled M, N, and O from youngest to oldest.

During our analysis of the sequence of faulting events along the Cascade Quarry reverse fault, we noted several aspects of the pattern of faulting and the geology on the footwall block that appear to be worthy of comment because they differ from the nature of the faulting found along the Año Nuevo thrust fault and because they contribute to making the interpretation of the number of faulting events more difficult. Specifically these geologic features are:

- 1) The fault planes for each succeeding faulting event do not show a uniform progression upward with each younger fault plane being stratigraphically higher within the sediments on the footwall block. One of the major fault planes for FE #3 (Plates XII, XIII, XIV) lies to the west of and below the principal zone of faulting. From the stratigraphic relationships, it is obvious that this fault must have moved after the deposition of Qc/soil D which truncates and buries the fault planes of FE #4 (Plate XIV). The other obvious fault plane of this sort lies again beneath and west of the main fault and is designated FE #4 on Plate XII. The shear plane, although poorly preserved, obviously truncates peds or pseudo-soil structures.

A third fault that lies below and west of the main fault is present in the exploratory trench (Cascade Trench #1) between the 75 and 105 ft. markers and is described in Note V (Plate XII). The presence of this fault is inferred from stratigraphic offsets within the colluvial deposits because there is no physical evidence of the fault plane. The absence of well-defined shear planes, clay gouge, and slickensides in a moderately to poorly-consolidated sandy colluvium is not unusual; similar situations have been encountered by other workers studying faults in recent sandy deposits (K. R. Lajoie, D. Herd, personal communication; Kahle, 1975; and Barrows, 1975).

- 2) The intensity of weathering appears to have been greater in the colluvial sediments exposed in Cascade Trench #1 and the spillway exposures than in those exposed in the quarry wall, particularly in the area beneath the main fault plane between the 47 and 70 ft. markers in the exploratory trench (Plate XII). In this area, there has been a general blurring and/or obliteration of bedding, sedimentary structures, and fault planes. With the exception of a few channels and pods of conglomerates, the area consists of clayey sand and sandy clay that is light gray with orange-brown mottling. The contacts of all of the Qc/soil units that are traceable to the west end of the trench fade and disappear as they are traced to the east into this area. This in itself drastically reduces the possibility of distinguishing features indicative of faulting, particularly for small events.

The presence of a high clay content and the obliteration of structures probably result from weathering processes. Much of the clay in these sediments appears to have been translocated by percolating ground water. This influx of clay into the interstices of an already clay-rich sediment, combined with the shrink-swell action of the clays, has destroyed any preexisting structures and has blurred or obliterated contacts.

The higher clay content of these sediments initially may have resulted preferential deposition of clay-rich sediments near the fault. According to our model, the clay-rich surface soils were the first materials eroded off of the scarp on the hanging-wall block and deposited on the footwall block nearest the scarp. Hence, the colluvial sediments near the fault may have had higher original clay contents. We do not know why weathering processes may have acted more intensely in this area below the fault, but it is possible that the area does not stay water-saturated for as long as areas not below the fault. Hence the area is subjected to more alternating wet-dry cycles and therefore more shrink-swell cycles.

- 3) The main fault plane where exposed in the Cascade Quarry spillway and Cascade Trench #1 has been the site of a relatively complex series of injections of fine to coarse-grained sand in a liquefied state. This layer of injected sand, lying within or just below the main fault plane, ranges in thickness from several inches to several feet and can be found along a 300-ft-long section of the fault plane.

The sands are interpreted as having been injected in a fluid state as a result of liquefaction during major earthquakes. The sand obviously is derived from the nearshore marine or beach sands in the terrace deposits overlying the old wave-cut platform on the footwall block. Therefore, the sand originated some 70-80 ft. below the present-day ground surface. The sands vary in grain size from fine to very coarse, and pebble- and granule-sized materials are common in these sands. Well-developed laminae, probably flow laminae, in the sands

are oriented parallel or subparallel to the trend of the fault. The field relationships suggest that there have been several episodes of intrusion or injection of liquefied sand, but it is essentially impossible to determine how many episodes of liquefaction have occurred.

Because the liquefied sands apparently did not always reach the surface, either as sandblows or as sand volcanoes, liquefaction events are of minimal use in determining recurrence intervals. Only the most recent of the liquefaction events, the one apparently related to FE #1, actually formed a sandblow at the surface (Plate XIV). Sandblows may have vented at the surface during other faulting events at other places along the trend of the fault, but there was no evidence of other sandblows in the trench, quarry, or spillway exposures.

As previously stated, the three factors described above have helped to make the interpretation of the number of faulting events more difficult and have made it almost impossible to recognize evidence of "small" faulting events in the sediments on the footwall block.

Consequently, we have tentatively concluded that there is evidence for a minimum of seven episodes of faulting in the quarry and trench exposures. The faulting events coincide with depositional Qc/soil units A-G. There also are four distinct Qc/soil units exposed in the spillway, indicating a minimum of four faulting events. It is extremely difficult to correlate these units in the spillway with units exposed in the exploratory trench, but two possible correlations exist:

- a) The most reasonable interpretation is that the four Qc/soil units L-0 in the spillway can be correlated directly with Qc/soil units D-G in the exploratory trench and spillway.
- b) Another possible interpretation is that the Qc/soil unit L in the spillway can be correlated with Qc/soil unit E in the trench. Using this interpretation we would conclude that there is evidence for a total of eight faulting events in the combined stratigraphy of the quarry wall, trench, and spillway.

Consequently, one interpretation is that there is evidence for seven faulting events, possibly eight, along the Cascade Quarry reverse fault.

A second interpretation includes a ninth episode of faulting that coincides with Qc/soil D on Plates XII and XIII. There is reasonably good evidence that Qc/soil units D and D', rather than being one depositional unit associated with one faulting event, actually are two depositional units associated with two faulting events. The reconstruction of the sequence of faulting is uncertain because the fault break for FE #3 lies below and west of the fault break for FE #4, but it does appear that the colluvial wedge associated with the ninth faulting event may have been removed by erosion.

In summary, our analysis suggests that there is evidence for seven to nine faulting events in the exposures along the Cascade Quarry reverse fault. Unfortunately, these events represent only part of the total number of faulting events on the fault because part of the colluvial sequence on the footwall block, in the lower portion of the spillway exposure, has not been mapped in detail. Between the base of the logged sequence in the spillway and the bottom of the spillway which is eroded into fault scarp colluvium, there is approximately 20 ft. of stratigraphic section. This 20-ft. section has not been logged because of problems in clearing the area of debris that came from the upper part of the spillway section when it was cleared. Nevertheless, if the size and thickness of the Qc/soil units in this section are the same as in the areas logged, there should be at least five additional Qc/soil units that coincide with faulting events.

Therefore, we conclude that the minimum number of faulting events that have occurred along the Cascade Quarry reverse fault during the past 105,000 years is 12, or possibly 14. This indicates that the maximum recurrence interval for earthquakes of 6.5 - 7.9 magnitude along this fault is 7500 - 8750 years.

It is possible to relate this record of faulting along the Cascade Quarry reverse fault to the history of fault movement across the entire San Gregorio fault zone at Point Año Nuevo. We indicated previously that the horizontal component of movement along the reverse fault is about 1/20 or 5% of the total late Pleistocene horizontal movement across the San Gregorio fault zone. If the reverse fault, as suggested earlier, moves intermittently in response to local buildups of stress produced by continuing movement across the entire fault zone, then the ratio of the total number of earthquakes along the San Gregorio fault zone at Point Año Nuevo to the number of earthquakes on the Cascade Quarry reverse fault is approximately 20:1. This suggests that the minimum number of earthquakes of magnitude 7.0 - 7.5 that have occurred on the fault zone in the past 105,000 years is 240 to 280. Therefore, the recurrence interval for major earthquakes on the San Gregorio fault zone, as determined from our study of faulting along the Cascade Quarry reverse fault, is 375 to 438 years.

Summary - The three different methods we have used for approximating recurrence intervals along the Frijoles fault and the San Gregorio fault zone at Point Año Nuevo have yielded remarkably similar values. The recurrence interval for faulting along the Frijoles fault at Point Año Nuevo is about 365 years as determined from the sag pond deposit. Long-term slip rates suggest a recurrence interval of 220 - 400 years for a 7.5 magnitude earthquake along the San Gregorio fault zone, and the analysis of the Cascade Quarry reverse fault suggests a recurrence interval of 375-440 years for a 7.0 - 7.5 magnitude earthquake.

Of the three techniques, it is difficult to determine whether one provides a better approximation than another because all three methods require the acceptance of assumptions regarding fault movement. We suggest, however, that these techniques provide a firm basis for concluding that the San Gregorio fault zone is active, having experienced Holocene movement on at least three fault strands. It is capable of producing an earthquake greater than 7.5 and possibly as great as or greater than 8.0 Richter magnitude, and the recurrence interval for major earthquakes (7.5 +) is between 225 and 400 years.

## CONCLUSIONS

The results of our work over the past two years can be divided into three distinct categories and summarized as follows:

I. EVIDENCE OF INDIVIDUAL FAULTING EVENTS AND DETERMINATION OF FAULT SCARP HEIGHT - Careful mapping of stratigraphic and structural relationships within zones of reverse faulting has enabled us to make reasonably complete reconstructions of the late Pleistocene history of faulting for two secondary faults within the San Gregorio fault zone. Our observations indicate that the basic model for recognition of faulting events, presented in Figure 10, is essentially correct. The formation and preservation of a fault scarp-driven colluvial wedge depends on many variables; a recognizable deposit may not form as a result of each faulting event. Nevertheless, a generalized minimum history of the faulting events is preserved in the sedimentary sequence on the footwall block. The formation of a recognizable colluvial wedge depends on the height of the fault scarp, the lithology, the rates of weathering and erosion, and the length of time between faulting events. Only rarely will evidence of faulting events accompanied by maximum surface displacements of less than 1½ ft. be preserved in the footwall block stratigraphy. Extremely large fault scarps (>8-9 ft. high) or scarps formed in well-consolidated rocks may not be degraded in the time interval between major earthquakes. Similarly, a short recurrence interval may preclude complete degradation of scarps between faulting events. Any sequence of events that results in incomplete degradation of the scarp may make recognition of individual faulting events difficult; two or more small faulting events may be indistinguishable from a single larger event in the stratigraphic record.

The record of faulting events also may be preserved in cross-cutting relationships between stratigraphic units and the faults. Within the fault zone there are other features characteristic of thrust faults that preserve the record of faulting events and can aid in historic reconstructions of faulting sequences. These include such features as "bulldozed" zones developed along the leading edge of overthrust plates, zones of "sub-fault conglomerate," and the characteristic upward splaying of small faults from the main fault.

Using the model for recognition of faulting events, it appears as if there is a general relationship between the thickness of the colluvial wedge and the height of the fault scarp that must have been eroded to form the wedge. Consequently, we feel it is possible to approximate the initial scarp height (in this study) as 1.6 to 2.2 times the measured thickness of the colluvial wedge. This scarp height:wedge thickness ratio can be used to approximate the maximum magnitudes of earthquakes associated with each faulting event.

II. PATTERNS OF FAULTING AND RELATIONSHIPS BETWEEN PRIMARY AND SECONDARY FAULTS WITHIN THE SAN GREGORIO FAULT ZONE - Analysis of the fault pattern near Point Año Nuevo indicates that the San Gregorio fault zone is a large right lateral strike-slip fault zone undergoing local convergence. The extreme complexity of the fault zone near Point Año Nuevo is probably related to about 12 degrees of convergence between the blocks on opposite sides of the Frijoles fault.

The geologic data and the pattern of faulting indicate the presence of two major through-going faults (primary faults) or principal displacement shear zones - the Frijoles fault and the Coastways fault. These two faults have been the loci of essentially all of the middle to late Pleistocene movement.

There is strong evidence that both of these faults have been zones of continuing activity since the mid-late Tertiary. The Coastways fault was the primary zone of displacement between 220,000 and 105,000 years B.P. with only minor offset along the Frijoles fault. In contrast, most of the movement along the fault zone in the past 105,000 years appears to have occurred along the Frijoles fault.

In addition to the principal displacement shears there are numerous small(?) secondary faults that have experienced late Pleistocene movement. It is possible to relate the amount of movement on one secondary fault, the Cascade Quarry reverse fault, to movement on the Frijoles and Coastways faults. If our analysis of marine terrace deformation is correct, the Cascade Quarry reverse fault experiences only 5% of the total movement across the fault zone. It appears that movements on the reverse fault are relatively large, with vertical surface displacements of 3 - 8 ft. and horizontal displacements of up to 12-13 ft. It appears therefore as if the sizes of the individual surface displacements along the secondary traces studied, the Cascade Quarry reverse fault and the Año Nuevo thrust fault, are similar to the size of the surface displacements along the primary faults, the Coastways fault and the Frijoles fault.

Because of these observations, we question the concept that secondary faults experience only small surface displacements, a fraction of the size of the accompanying displacements along the primary fault. We suggest that faulting events along both the Cascade Quarry reverse fault and the Año Nuevo thrust fault occur infrequently. When an earthquake accompanied by surface rupture on a secondary trace does occur, the secondary trace temporarily acts as the primary locus of faulting, and surface displacements are greater on the "secondary" fault than on the principal displacement shear. We see no evidence to suggest that the secondary faults in the San Gregorio fault zone regularly experience small displacements during major faulting events on the primary faults.

We suggest that the Cascade Quarry reverse fault experiences significant displacement during only one out of 20 major earthquakes along the San Gregorio fault zone, but during this one event the displacements are large and fault movement is centered on the Cascade Quarry reverse fault. The pattern of fault movement probably is similar along the Año Nuevo thrust fault except that that fault experiences displacement in probably only one out of 30-35 major earthquakes along the fault zone.

III. MAXIMUM CREDIBLE EARTHQUAKE AND RECURRENCE INTERVALS FOR EARTHQUAKES ALONG THE SAN GREGORIO FAULT ZONE - The magnitude of the maximum credible earthquake that could occur along the San Gregorio fault zone was estimated in three ways. First, we determined the maximum surface displacements that have occurred along the Cascade Quarry reverse fault from our studies of structural geology of the fault and the thickness of the colluvial wedges deposited on the footwall block. Using the regression analysis of Bonilla and Buchanan (1970) we determined that earthquakes must have varied from 6.0 to 8.0 Richter magnitude to produce the calculated surface displacements.

Because of uncertainties in our analysis of maximum displacements we conclude that the maximum credible earthquake that could occur along the San Gregorio fault zone is between Richter magnitude 7.7 and 7.9, and we suggest that the maximum credible earthquake might exceed magnitude 8.0.

Two additional methods that we used to estimate the maximum credible earthquake magnitude were: (1) to estimate the surface rupture length and (2) to estimate the size of the area of rupture on the fault plane (Wyss, 1979). The estimates for the maximum credible earthquake vary from 7.3 to 7.6 for a fault 115 miles long and from 7.6 to 7.8 for a fault 260 miles long. We conclude that the maximum credible earthquake for the San Gregorio fault zone is at least 7.6 - 7.7 and may be greater than 8.0 Richter magnitude. We have attempted to determine the recurrence interval for major earthquakes along the San Gregorio fault zone at Point Año Nuevo using three methods. (1) Long-term slip rates determined from offset marine terrace shoreline angles suggest that the recurrence interval for 7.5 magnitude earthquakes is 220-400 years. (2) Our study of the Cascade Quarry reverse fault indicates that the maximum recurrence interval ranges from 375 to 440 years for a 7.0-7.5 magnitude earthquake. (3) The analysis of cyclical sag pond deposits exposed along the south shore of Point Año Nuevo indicates a recurrence interval of about 365 years for an earthquake of magnitude 6.5 or greater. Consequently, we conclude that a realistic estimate of the recurrence interval for major earthquakes (M=7.5) along the San Gregorio fault zone is between 225 and 400 years, with a best estimate of 300-325 years.

## GEOLOGIC REFERENCES

- Alpine Geophysical Associates Inc., 1971, Geophysical survey offshore Davenport, California: prepared for Pacific Gas and Electric Company.
- Barrows, A. G., 1975, Surface effects and related geology of the San Fernando earthquake in the foothill region between Little Tujunga and Wilson Canyons: in Oakeshott, G. B., editor, San Fernando, California, earthquake of 9 February 1971: California Div. Mines and Geology Bull. 196, p. 97-117.
- Bloom, A. L., Broecker, W. S., Chappell, J.M.A., Matthews, R. K., and Mesolella, K. J., 1974, Quaternary Sea Level Fluctuations on a Tectonic Coast: New  $^{230}\text{Th}/^{230}\text{U}$  dates from the Huon Peninsula, New Guinea: Quaternary Research, v. 4, p. 185-205.
- Bolt, B. A., 1978, Incomplete formulations of the regression of earthquake magnitude with surface fault rupture length: Geology, v. 6, p. 233-235.
- Bonilla, M. G., 1967, Historic surface faulting in continental United States and adjacent parts of Mexico (A factor in nuclear facility siting and design): U. S. Geol. Survey, T.I.D. - 24124 (U. S. Dept. of Commerce, Springfield, Virginia 22151), 36 p.
- , 1980, Comment on estimating maximum expectable magnitudes of earthquakes from fault dimensions: Geology, v. 8, no. 4, p. 162-163.
- and Buchanan, J. M., 1970, Interim report on worldwide historic surface faulting: U. S. Geol. Survey Open-File Report, 32 p.
- Brabb, E. E., 1970, Preliminary geologic map of the central Santa Cruz Mountains, California: U. S. Geol. Survey, San Francisco Bay Region Environment and Resources Planning Study, Basic Data Contribution 6.
- , Clark, J. C., and Throckmorton, C. B., 1977, Measured sections of Paleogene rocks from the California Coast Ranges: U. S. Geol. Survey Open-File Report 77-714, 114 p.
- Bradley, W. C., and Addicott, W. O., 1968, Age of first marine terrace near Santa Cruz, California: Geol. Soc. America Bull., v. 79, p. 1203-1210.
- Bradley, W. C., and Griggs, G. B., 1976, Form, genesis, and deformation of central California wave-cut platforms: Geol. Soc. America Bull., v. 87, p. 433-449.
- Branner, J. C., Newsom, J. F., and Arnold, R., 1909, Description of the Santa Cruz Quadrangle: U. S. Geol. Survey Geol. Atlas, Folio 163, 11 p.
- Bucknam, R. C. and Anderson, R. E., 1979, Estimation of fault-scarp ages from a scarp-height-slope-angle relationship: Geology, v. 7, no. 1, p. 11-14.

- Burke, D. B., 1979, Log of a trench in the Garlock fault zone, Fremont Valley, California: U. S. Geol. Survey Misc. Field Studies Map MF-1028.
- Chinnery, M. A., 1969, Earthquake magnitude and source parameters: Seismological Soc. America Bull., v. 59, no. 5, p. 1969-1982.
- Clark, J. C., 1966, Tertiary stratigraphy of the Felton-Santa Cruz area, Santa Cruz Mountains, California: Ph.D. thesis, Stanford University, Stanford, California.
- , 1970, Geologic map of the southwestern Santa Cruz Mountains between Año Nuevo Point and Davenport, California: U. S. Geol. Survey Open-File Report - 1:24,000.
- , and Brabb, E. E., 1978, Stratigraphic contrasts across the San Gregorio fault, Santa Cruz Mountains, west central California: in E. A. Silver and W. R. Normark, eds., San Gregorio-Hosgri fault zone, California: California Div. Mines and Geology Special Report 137, p. 3-12.
- Coppersmith, K. J., and Griggs, G. B., 1978, Morphology, recent activity and seismicity of the San Gregorio fault zone: in E. A. Silver and W. R. Normark, eds., San Gregorio-Hosgri fault zone, California: California Div. Mines and Geology Special Report 137, p. 33-41.
- Crowell, J. C., 1954, Geology of the Ridge basin area, Los Angeles and Ventura Counties: in R. H. Jahns, ed., Geology of Southern California: California Div. Mines and Geology Bull. 170, Map Sheet 7.
- Dibblee, T. W., Jr., 1968, Displacements on the San Andreas fault system in the San Gabriel, San Bernardino, and Jacinto Mountains, southern California: in W. R. Dickinson and A. Grantz, eds., Proceedings of conference on geologic problems, San Andreas fault system: Stanford Univ. Pubs. Geol. Sci., v. II, p. 260-278.
- Earth Sciences Associates, 1972, Davenport power plant site geology investigation: prepared for Pacific Gas and Electric Co.
- Gawthrop, W. H., 1978, Seismicity and tectonics of the central California coastal region: in E. A. Silver and W. R. Normark, eds., San Gregorio-Hosgri fault zone, California: California Div. Mines and Geology Special Report 137.
- Graham, S. A., and Dickinson, W. R., 1978, Apparent offsets of on-land geologic features across the San Gregorio-Hosgri fault trend: in E. A. Silver and W. R. Normark, eds., San Gregorio-Hosgri fault zone, California: California Div. Mines and Geology Special Report 137, p. 13-23.
- Greene, H. G., Lee, W. H. K., McCulloch, D. S., and Brabb, E. E., 1973, Faults and earthquakes in the Monterey Bay region, California: U. S. Geol. Survey Misc. Field Studies Map MF-518, 14 p.
- Griggs, G. B., 1973, Earthquake activity between Monterey and Half Moon Bay, California: California Div. Mines and Geology, California Geology, v. 26, no. 5, p. 103-110.

- Hall, N. T., Sarna-Wojcicki, A., and Dupre, W. R., 1974, Faults and their potential hazard in Santa Cruz County, California: U. S. Geol. Survey Misc. Field Studies Map MF-626, 1:62,500.
- Hill, M. L., and Dibblee, T. W., Jr., 1953, San Andreas, Garlock and Big Pine faults, California - a study of the character, history and tectonic significance of their displacements: Geol. Soc. America Bull. v. 64, p. 443-458.
- Kahle, J. E., 1975, Surface effects and related geology of the Lakeview fault segment of the San Fernando fault zone: in Oakeshott, G. B. editor, San Fernando, California, earthquake of 9 February 1971: California Div. Mines and Geology Bull. 196, p. 119-135.
- Kennedy, G. L., 1978, Pleistocene paleoecology, zoogeography, and geochronology of marine invertebrate faunas of the Pacific northwest coast (San Francisco Bay to Puget Sound): unpublished Ph.D. dissertation, Univ. of California Davis, 824 p.
- Lowell, J. D., 1972, Spitzbergen Tertiary orogenic belt and the Spitzbergen fracture zone: Geol. Soc. America Bull., v. 83, no. 10.
- Mark, R. K., 1977, Application of linear statistical models of earthquake magnitude versus fault length in estimating maximum expectable earthquakes: Geology, v. 5, p. 464-466.
- \_\_\_\_\_, and Bonilla, M. G., 1977, Regression analysis of earthquake magnitude and surface fault length using the 1970 data of Bonilla and Buchanan: U. S. Geol. Survey Open-File Report 77-614.
- Mitchell, G. D., 1928, The Santa Cruz earthquake of October 1926: Seismological Soc. America Bull., v. 18, no. 3, p. 153-312.
- Oakeshott, G. B., ed.; 1975, San Fernando, California, earthquake of 9 February 1971: California Div. Mines and Geology Bull. 196, 463 p.
- Shackleton, N. J., and Opdyke, N. D., 1973, Oxygen isotope and paleomagnetic stratigraphy of equatorial Pacific core, V 28-238: Oxygen isotope temperatures and ice volumes on a  $10^5$  and  $10^6$  year scale: Quaternary Research, 3(1); p. 39-55, figs. 1-9, tables 1-4.
- Sieberg, A., 1923, Erdbebenkunde: Jena, p. 99-104.
- Sieh, K. E., 1978, Prehistoric large earthquakes produced by slip on the San Andreas fault at Pallett Creek, California: Jour. Geophysical Research, v. 83, no. B8, p. 3907-3939.
- Sims, J. D., 1975, Determining earthquake recurrence intervals from deformational structures in young lacustrine sediments: Tectonophysics, v. 29, p. 141-152.
- Slemmons, D. B., 1977, Faults and earthquake magnitude: U. S. Army Corps of Engineers, Waterways Experiment Station, Misc. Papers S-73-1, Rept. 6, p. 1-129.

- Sylvester, A. G. and Smith, R. R., 1976, Tectonic transpression and basement-controlled deformation in San Andreas fault zone, Salton Trough, California: *Am. Assoc. Petroleum Geologists Bull.*, v. 60, no. 12, p. 2081-2102.
- Tchalenko, J. S., 1970, Similarities between shear zones of different magnitudes: *Geol. Soc. America Bull.*, v. 81, no. 6, p. 1625-1640.
- , and Ambraseys, N. N., 1970, Structural analysis of the Dasht-e Bayaz (Iran) earthquake fractures: *Geol. Soc. America Bull.*, v. 81, no. 1, p. 41-60.
- Touring, R. M., 1959, Structure and stratigraphy of the La Honda and San Gregorio quadrangles, San Mateo County, California: Ph.D. thesis, Stanford University, Stanford, California, 228 p.
- U. S. Geological Survey and National Oceanic and Atmospheric Administration, 1971, The San Fernando, California, earthquake of February 9, 1971: *U. S. Geol. Survey Prof. Paper 733*, 254 p.
- Wallace, R. E., 1970, Earthquake recurrence intervals on the San Andreas fault: *Geol. Soc. America Bull.*, v. 81, p. 2875-2890.
- 1977, Profiles and ages of young fault scarps, north-central Nevada: *Geol. Soc. America Bull.*, v. 88, no. 9, p. 1267-1281.
- 1978, Patterns of faulting and seismic gaps in the Great Basin province: in *Methodology for identifying seismic gaps and soon-to-break gaps: Proceedings of Conference VI, May 25-27, 1978: U. S. Geol. Survey Open-File Report 78-943*, p. 858-868.
- 1980, Active faults, paleoseismology, and earthquake hazards: *U. S. Geol. Survey Preprint for: Seventh World Conference on Earthquake Engineering, Istanbul, Turkey, September 1980.*
- Weber, G. E., and Lajoie, K. R., 1977, Late Pleistocene and Holocene tectonics of the San Gregorio fault zone between Moss Beach and Point Año Nuevo, San Mateo County, California: *Geol. Soc. America Abstracts with Programs*, v. 9, no. 4, p. 524.
- 1979, Late Pleistocene rates of movement along the San Gregorio fault zone, determined from offset of marine terrace shoreline angles: Weber, G. E., Lajoie, K. R. and Griggs, G. B., *Field trip guide - coastal tectonics and coastal geologic hazards in Santa Cruz and San Mateo Counties, California: Cordilleran Section of Geol. Soc. America, 75th Annual Meeting*, p. 101-111.
- 1980, Map of Quaternary faulting along the San Gregorio fault zone, San Mateo and Santa Cruz Counties, California: *U. S. Geol. Survey Open-File Report.*
- and Griggs, G. B., eds., 1979, *Field trip guide - coastal tectonics and coastal geologic hazards in Santa Cruz and San Mateo Counties, California: Cordilleran Section of Geol. Soc. America, 75th Annual Meeting*, 191 p.

- \_\_\_\_\_, and Wehmiller, J. F., 1977, Quaternary deformation along a major branch of the San Andreas fault in central California: Abst. International Symposium on Recent Crustal Movements, Stanford Univ., July 1977.
- Wehmiller, J. F., Lajoie, K. R., Kvenvolden, K. A., Peterson, E., Belknap, D. F., Kennedy, G. L., Addicott, W. O., Vedder, J. G. and Wright, R. W., 1977, Correlation and chronology of Pacific Coast marine terrace deposits of the continental United States by fossil amino-acid stereochemistry-technique evaluation, relative ages, kinetic model ages, and geologic implications: U. S. Geol. Survey Open-File Report 77-680, 106 p.
- Wentworth, C. M., Bonilla, N. G., and Buchanan, J. M., 1972, Seismic environment of the sodium pump test facility at Burro Flats, Ventura County, California: U. S. Geol. Survey, Open-File Report, 42 p.
- Wilcox, R. E., Harding, T. P., and Seely, D. R., 1973, Basic wrench tectonics: Am. Assoc. Petroleum Geologists Bull., v. 57, no. 1, p. 74-96.
- Wright, R. H., 1971, Map showing locations of samples dated by radiocarbon methods in the San Francisco Bay Region: U. S. Geol. Survey Misc. Field Studies Map MF-317.
- Wyss, M., 1979, Estimating maximum expectable magnitude of earthquakes from fault dimensions: Geology, v. 7, p. 336-340.
- \_\_\_\_\_, 1980, Reply: Estimating maximum expectable magnitudes of earthquakes from fault dimensions: Geology, v. 8, no. 4, p. 163-164.

APPENDIX A  
Año Nuevo Thrust Fault  
Point Año Nuevo

- Seismic Refraction Surveys
- Magnetometer Surveys
- Logs of Hand Auger Core Holes
- Logs of Test Pits

Refer to Plates I and II and Figure 2  
for location of survey lines, test pits,  
and core holes.

MAGNETOMETER AND SEISMIC REFRACTION STUDIES OF THE FRIJOLES FAULT  
AND THE CASCADE QUARRY REVERSE FAULT

Geophysical studies were conducted over a relatively wide area along the Frijoles fault in an attempt to locate the fault accurately and to help in the siting of exploratory trenches. The magnetic and seismic surveys were of limited use because at best they allowed the delineation of broad structural features only, and most of those already had been recognized geomorphically. The presence of numerous fences, buried pipes, and underground cables limited or prevented the use of the magnetometer in many areas, particularly in the vicinity of the quarry and near the reservoir.

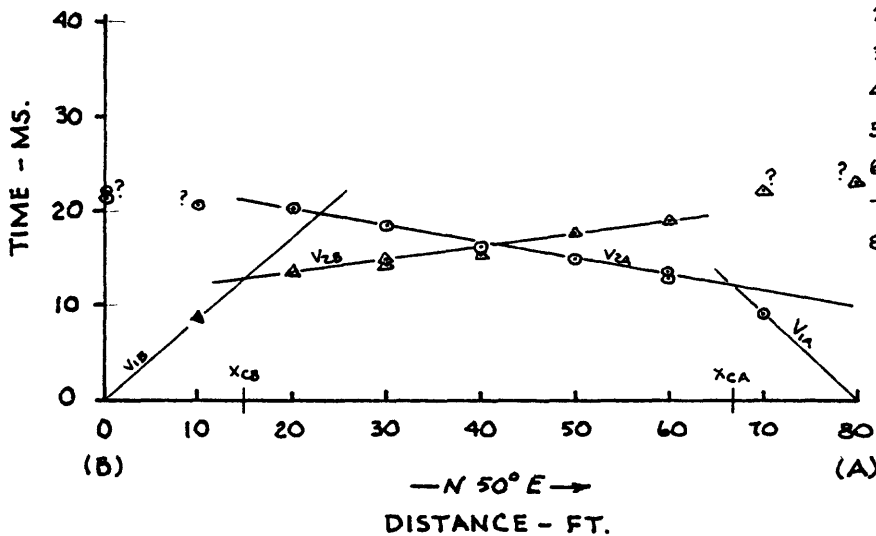
In general, seismic surveys provided little information that could be used to aid fault location and the siting of exploratory trenches. Several surveys in the upland areas of the second and third marine terraces were discontinued because of the highly variable and anomalous data. The seismic refraction technique could, however, be used in some instances to determine stratigraphic variations and variations in depth to ground water on opposite sides of a fault.

Because the seismic refraction data were ambiguous, the location for Cascade Trench No. 2 was selected on the basis of geomorphic expression and the certainty that we could locate the reverse fault. The location of Cascade Trench No. 3, on the Cascade Creek alluvial fan, was chosen primarily on the basis of magnetometer and seismic refraction surveys and on the stratigraphy in three hand auger holes (Refer to Appendix B). Our initial interpretation of the data suggested the presence of a fault offsetting the deposits of Cascade Creek and creating a ground water barrier. As indicated in the log for Cascade Trench No. 3 (Plate XVIII), there is no evidence of faulting; the differences in lithology and in the depth to the water table are created by stream terraces eroded into the underlying marine terrace sediments.

Overall, we found the magnetometer to be essentially useless for our work. The magnetic susceptibilities of the upper Tertiary and Quarternary sediments apparently vary only slightly. There appears to be no mineralization associated with the fault shear zones, and the water content of the rocks is variable. Consequently, there are no sharp or clear anomalies that can be used to locate the surface trace of the fault to within 25-50 ft. The only magnetometer survey with a sharp break in the profile that lay within 25-50 ft. of the fault is Survey No. 1.

The break in the profile is at the point where the fault is exposed at the surface. But where the fault is buried under colluvium and/or alluvium, its location cannot be accurately determined.

SEISMIC SURVEY SS-AN-1  
6-28-78 Weber & Lettirez



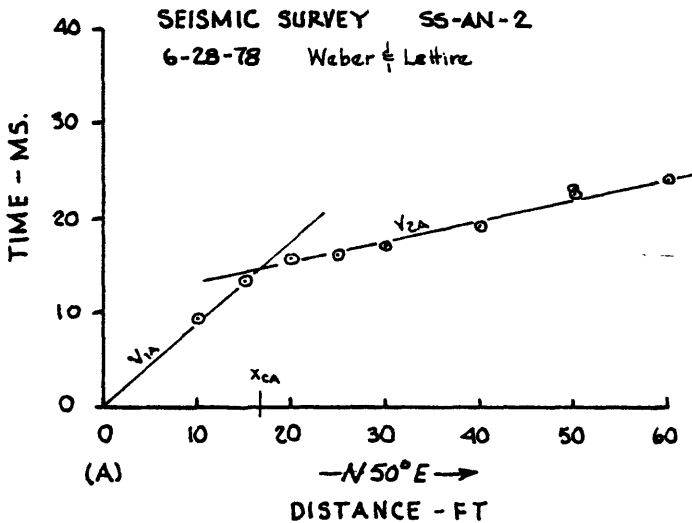
Geophone Pos. A	
Dist. (ft.)	Time (ms.)
10	9.2
20	13.6 (12.9)
30	15.0
40	16.2
50	18.5
60	20.0
70	20.6
80	21.4 (22.0)

$V_{1A} = 1050 \text{ ft/sec}$   
 $V_{2A} = 6000 \text{ ft/sec}$   
 $x_{CA} = 13 \text{ ft}$   
 $D_A = 5.4 \text{ ft.}$

Geophone Pos. B	
Dist. (ft.)	Time (ms.)
10	8.6
20	13.5
30	14.3 (15.0)
40	15.6
50	17.9
60	19.1
70	22.3
80	23.3 ?

$V_{1B} = 1180 \text{ ft/sec}$   
 $V_{2B} = 7200 \text{ ft/sec}$   
 $x_{CB} = 15 \text{ ft}$   
 $D_B = 6.4 \text{ ft}$

SEISMIC SURVEY SS-AN-2  
6-28-78 Weber & Lettirez

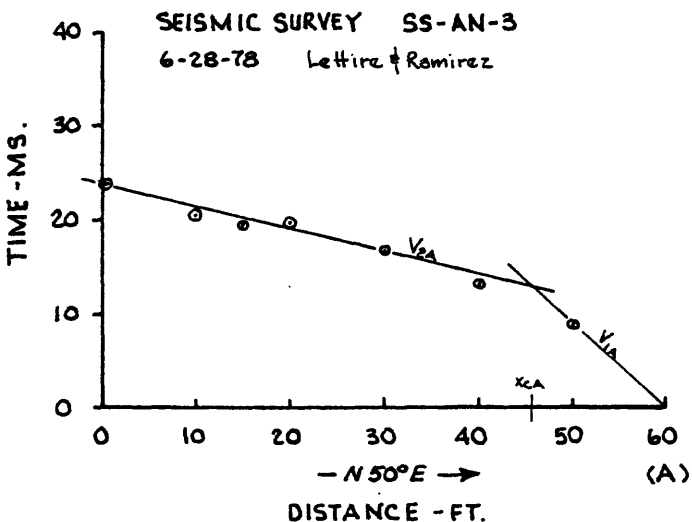


Geophone Pos. A	
Dist. (ft)	Time (ms)
10	9.3
20	15.9 (15.5-16.5)
30	17.2
40	19.2
50	23.1 (22.5±)
60	24.0

$V_{1A} = 1100 \text{ ft/sec}$   
 $V_{2A} = 4700 \text{ ft/sec}$   
 $x_{CA} = 17 \text{ ft}$   
 $D = 6.7 \text{ ft}$

15 ft	13.3
25 ft	16.0-16.3

SEISMIC SURVEY SS-AN-3  
6-28-78 Lettirez & Ramirez

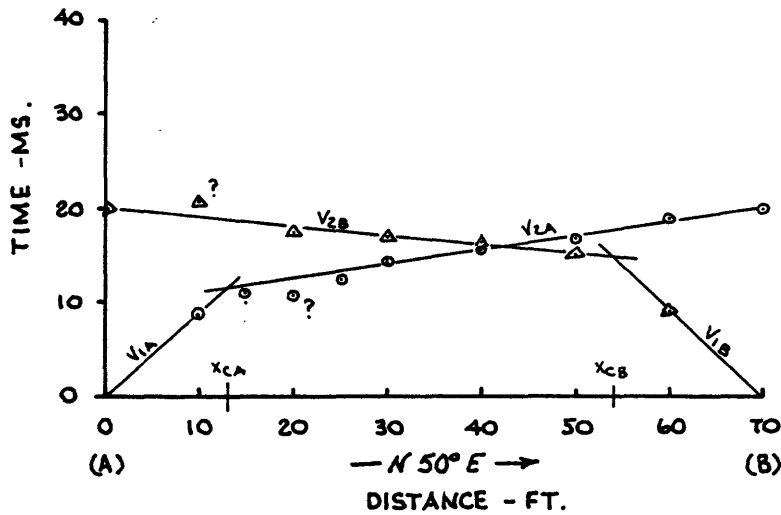


Geophone Pos. A	
Dist. (ft)	Time (ms.)
10	8.8
20	13.1
30	16.7
40	19.7
50	20.5
60	23.9

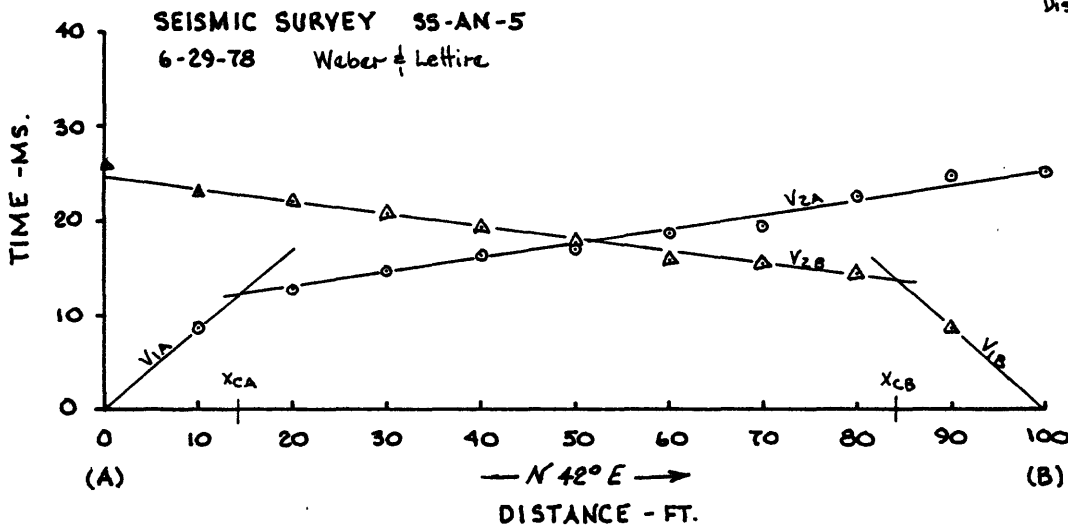
$V_{1A} = 1125 \text{ ft/sec}$   
 $V_{2A} = 4200 \text{ ft/sec}$   
 $x_{CA} = 14 \text{ ft}$   
 $D = 5.3 \text{ ft.}$

45 ft - 19.4

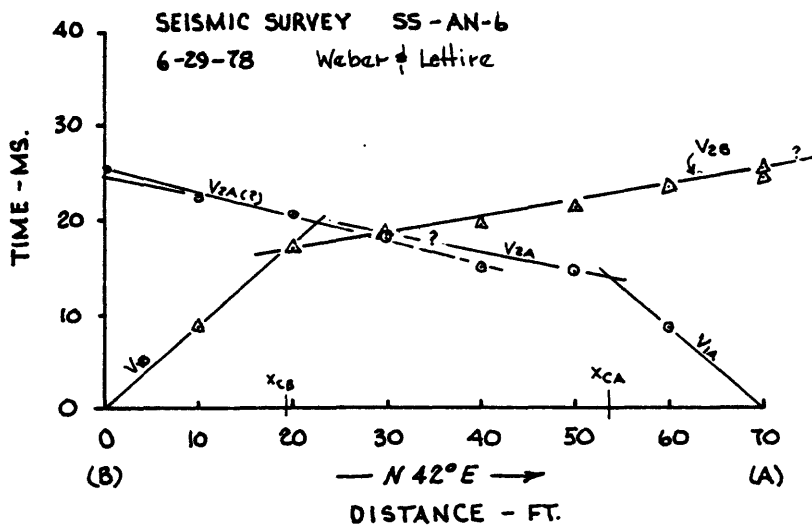
SEISMIC SURVEY SS-AN-4  
6-29-78 Weber & Lettice



Geophone Pos. A		Geophone Pos. B	
Dist. (ft.)	Time (ms.)	Dist. (ft.)	Time (ms.)
10	8.6	10	9.0
20	10.7 (10-10.5)	20	15.2
30	14.3	30	16.3
40	15.6	40	17.0
50	16.7	50	17.3
60	18.9	60	20.6 ?
70	20.0	70	20.0
V <sub>1A</sub> = 1150 ft/sec		V <sub>1B</sub> = 1100 ft/sec	
V <sub>2A</sub> = 6800 ft/sec		V <sub>2B</sub> = 10200 ft/sec	
X <sub>CA</sub> = 13 ft		X <sub>CB</sub> = 16 ft	
D <sub>A</sub> = 5.5 ft		D <sub>B</sub> = 7.2 ft.	

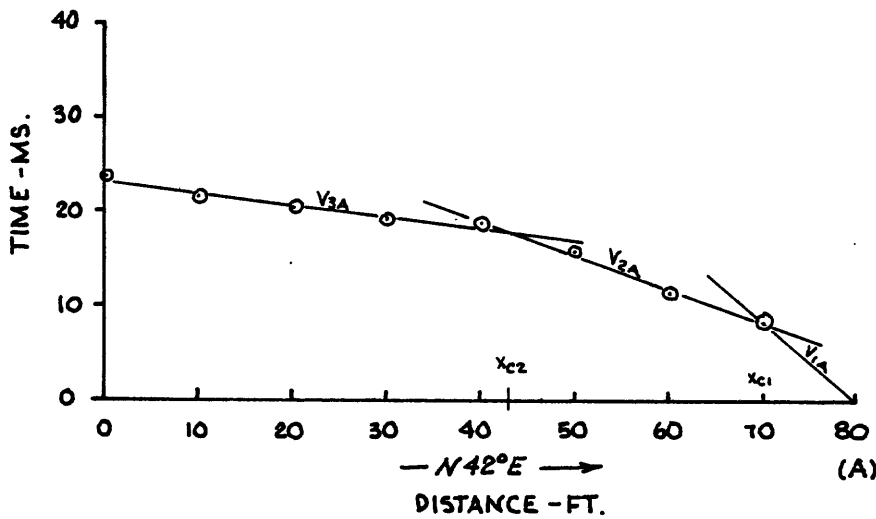


Geophone Pos. A		Geophone Pos. B	
Dist. (ft.)	Time (ms)	Dist. (ft.)	Time (ms)
10	8.6	10	8.7
20	12.7	20	14.4
30	14.6	30	15.5
40	16.4	40	15.9
50	17.1	50	17.6
60	18.8	60	19.3
70	19.5	70	20.7
80	22.5	80	22.0
90	24.8	90	23.2
100	25.2	100	26.0
V <sub>1A</sub> = 1200 ft/sec		V <sub>1B</sub> = 1150 ft/sec	
V <sub>2A</sub> = 6700 ft/sec		V <sub>2B</sub> = 7800 ft/sec	
X <sub>CA</sub> = 14 ft		X <sub>CB</sub> = 16 ft	
D <sub>A</sub> = 5.8 ft		D <sub>B</sub> = 6.9 ft	

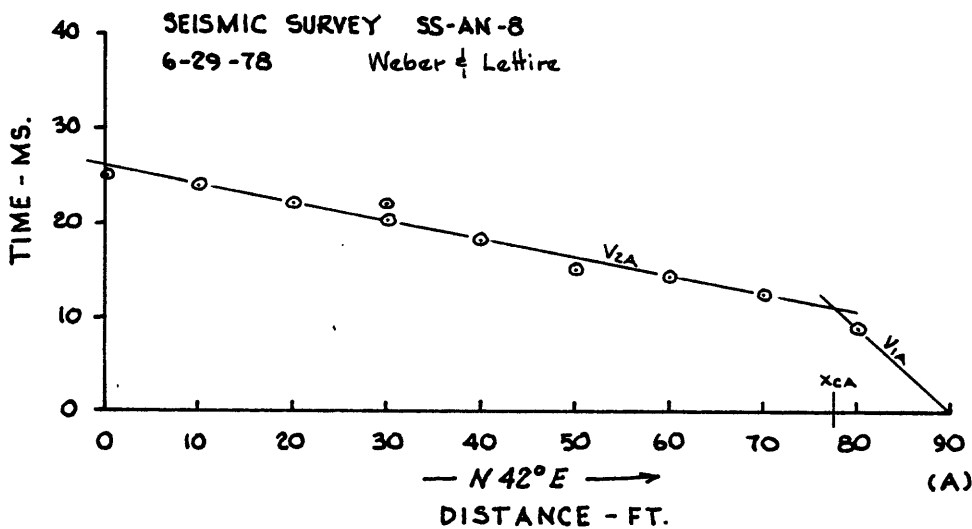


Geophone Pos. A		Geophone Pos. B	
Dist. (ft.)	Time (ms)	Dist. (ft.)	Time (ms)
10	8.7	10	8.7
20	14.6	20	17.0
30	15.0	30	18.3
40	18.0	40	19.5
50	20.6 (21.0)	50	21.4
60	22.4	60	23.5
70	25.5	70	24.5 (25.5)
V <sub>1A</sub> = 1100 ft/sec		V <sub>1B</sub> = 1100 ft/sec	
V <sub>2A</sub> = 5100 ft/sec		V <sub>2B</sub> = 6100 ft/sec	
V <sub>2A(2)</sub> = 3900 ft/sec			
X <sub>CA</sub> = 16 ft		X <sub>CB</sub> = 19 ft	
D <sub>A</sub> = 6.4 ft		D <sub>B</sub> = 7.9 ft	

SEISMIC SURVEY SS-AN-T  
6-29-78 Weber & Lettice

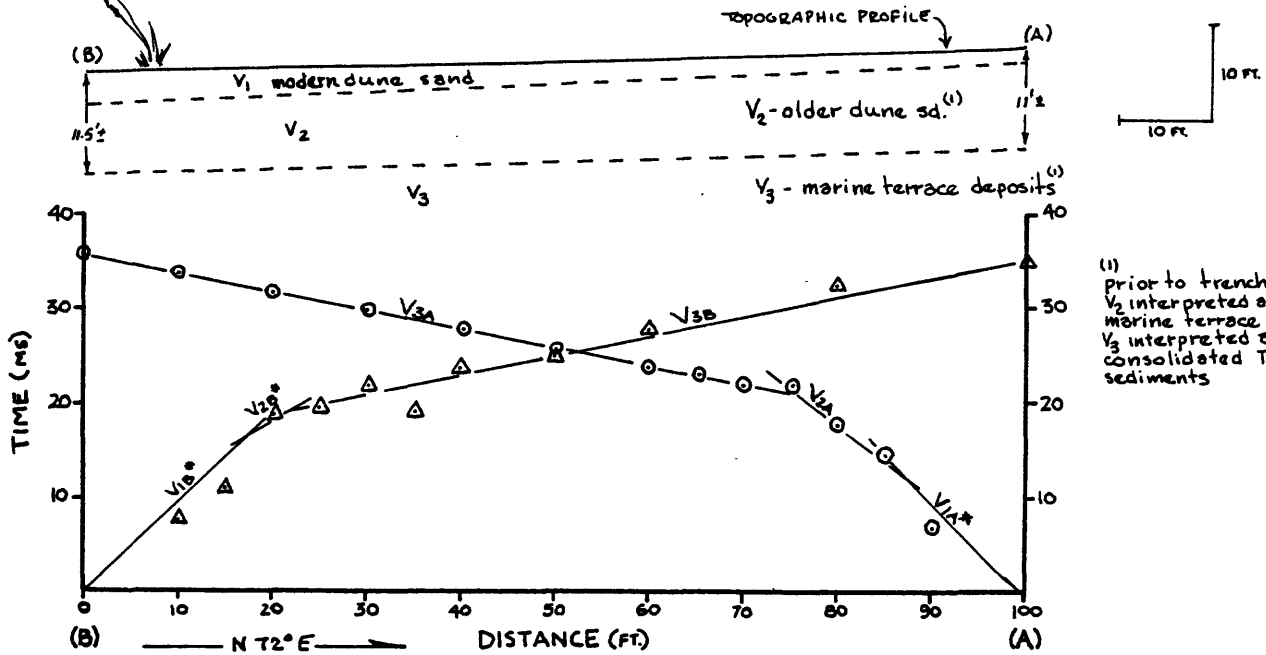


Geophone Pos. A	
Dist. (ft.)	Time (ms.)
10	8.3
20	11.4
30	15.8
40	18.7
50	19.1 (18.3-18.5)
60	20.3
70	21.5
80	23.7
V <sub>1A</sub> = 1150 ft/sec    x <sub>c1</sub> = 10 ft	
V <sub>2A</sub> = 2800 ft/sec    x <sub>c2</sub> = 37 ft	
V <sub>3A</sub> = 8000 ft/sec	
D <sub>1</sub> = 3.2 ft	
D <sub>2</sub> = 15.5 ft	



Geophone Pos. A	
Dist. (ft.)	Time (ms.)
10	9.1
20	12.6
30	14.2
40	15.0
50	18.1
60	22.1 (20.1)
70	22.0
80	24.0
90	25.0
V <sub>1A</sub> = 1050 ft/sec	
V <sub>2A</sub> = 5200 ft/sec	
x <sub>cA</sub> = 12 ft	
D = 4.9 ft	

SEISMIC SURVEY SS-AN-9



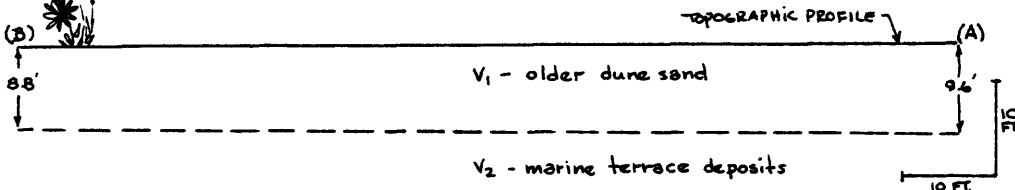
(1) prior to trenching - V<sub>2</sub> interpreted as marine terrace deposits V<sub>3</sub> interpreted as consolidated Tertiary sediments

DISTANCE	TIME		VELOCITIES (FT. PER SECOND)		CRITICAL DISTANCES (FT.)		
	A	B	A	B	A	B	
10	6.4	7.3			X <sub>C1</sub>	15	16.5
15	14.4	10.9	V <sub>1</sub>	1050*	X <sub>C2</sub>	25	22.5
20	17.3	18.3	V <sub>2</sub>	1450			
25	21.3	19.2	V <sub>3</sub>	5350			
30	21.7	21.7					
35	22.6	18.9					
40	23.4	23.7					
50	25.5	25.2					
60	27.7	27.4					
70	29.4						
80	31.6	32.1			D <sub>1</sub>	2.0	3.5-4.0
90	33.7				D <sub>2</sub>	11.0	11.5
100	35.0	35.2					

\* THESE VELOCITIES ARE ASSUMED, SINCE COMPACTED ROAD MATERIAL PRODUCES HIGHER THAN NORMAL VELOCITIES.

IF A SOIL VELOCITY IS ASSUMED, THEN THE CALCULATED DEPTH IS A MINIMUM DEPTH

SEISMIC SURVEY SS-AN-10

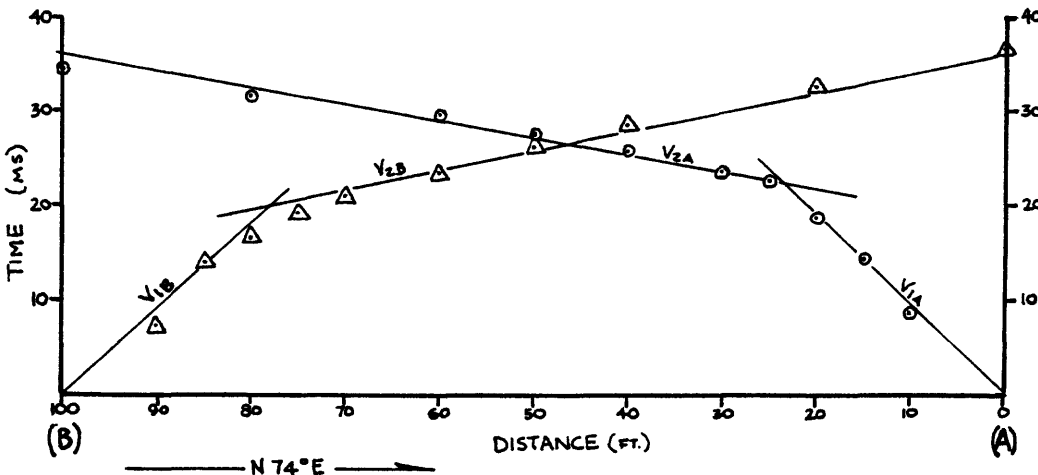


DISTANCE	TIME	
	A	B
10	8.7	7.1
15	14.2	14.0
20	18.4	16.5
25	22.6	19.2
30	23.4	21.0
40	25.8	23.5
50	27.2	26.1
60	29.3	28.5
80	31.4	32.7
100	34.6	36.4

VELOCITIES (FT. PER SECOND)		
	A	B
V <sub>1</sub>	1060	1100
V <sub>2</sub>	5750	4900

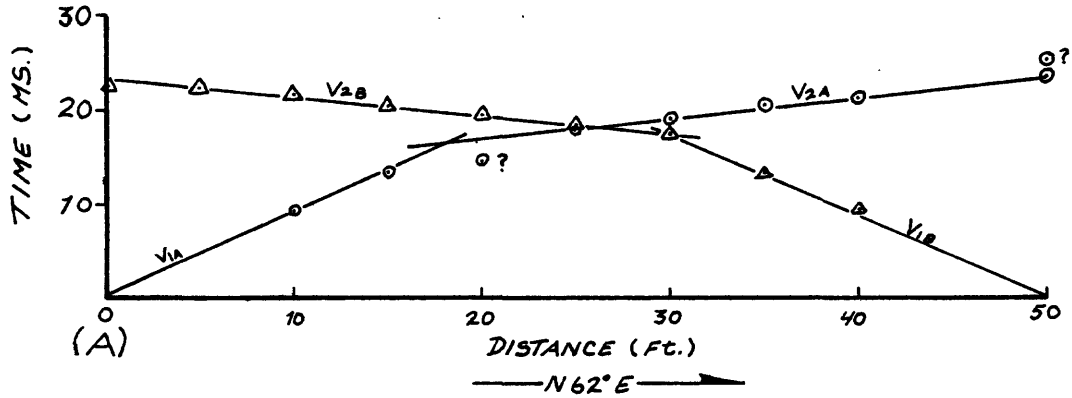
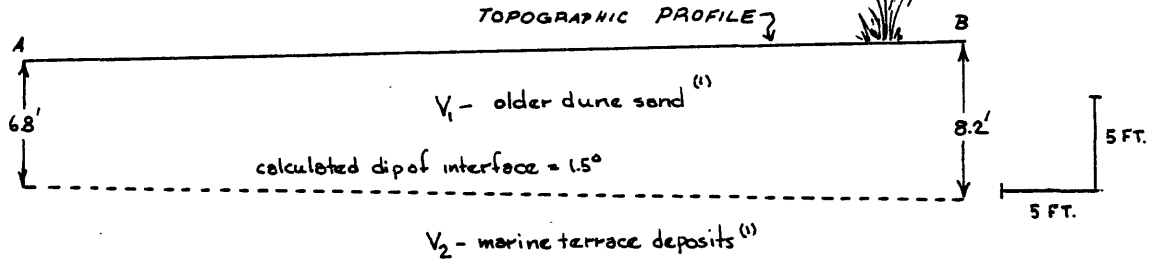
CRITICAL DISTANCES (FT.)		
	A	B
X <sub>C1</sub>	24	22

DEPTH TO INTERFACE (FT.)		
	A	B
D <sub>1</sub>	9.6	8.8



SEISMIC SURVEY SS-AN-11

Brown  
Oshiro  
Miller



DISTANCE	TIME	
	A	B
10	9.3	9.5
15	13.8	13.8
20	14.2	17.8
25	18.2	18.4
30	19.1	19.9
35	20.5	20.4
40	21.2	21.9
45		22.2
50	23.9 (25.1)	22.4

VELOCITIES (Ft./Sec.)

$V_1$  A B

$V_2$  4470 5600

CRITICAL DISTANCES (Ft.)

$X_c$  A B

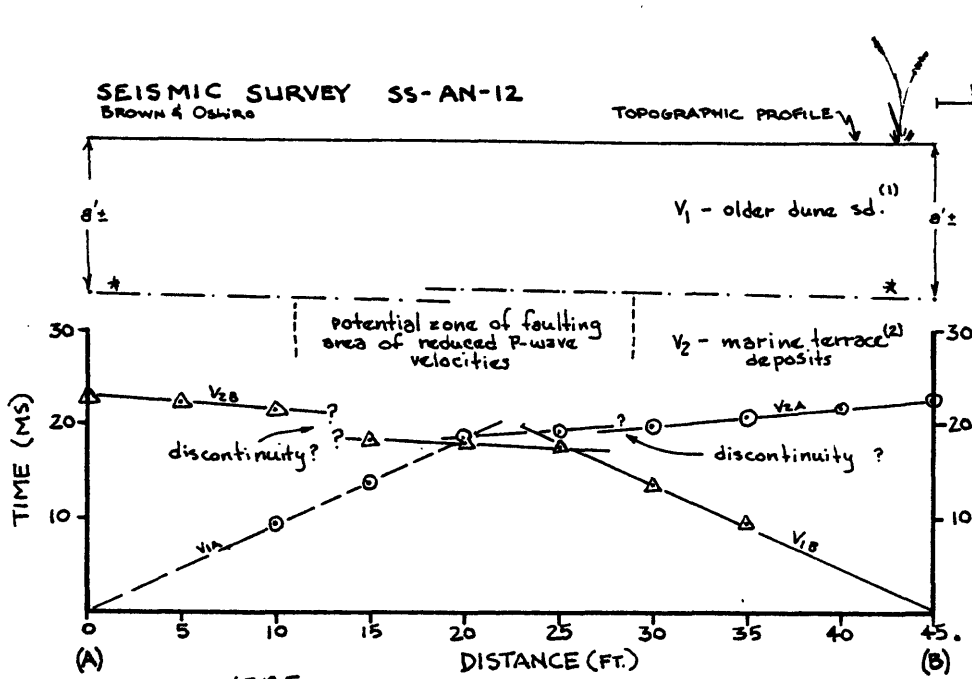
DEPTH TO INTERFACE (Ft.)

A B

6.8 8.2

(1) prior to trenching -  
 $V_1$  interpreted as marine terrace deposits  
 $V_2$  interpreted as Tertiary sediments

SEISMIC SURVEY SS-AN-12  
BROWN & Oshiro



DISTANCE (FT.)	TIME (MS)	
	A	B
10	9.5	9.4
15	13.9	13.7
20	18.6	17.4
25	19.1-19.3	18.3
30	19.8	18.2
35	20.8	21.7
40	21.9	22.2
45	22.7	22.8

VELOCITIES (FT. PER SECOND)

	A	B
V <sub>1</sub>	1070	1080
V <sub>2</sub>	5150	7400

CRITICAL DISTANCE (FT.)

	A	B
X <sub>c</sub>	20.5	19.0

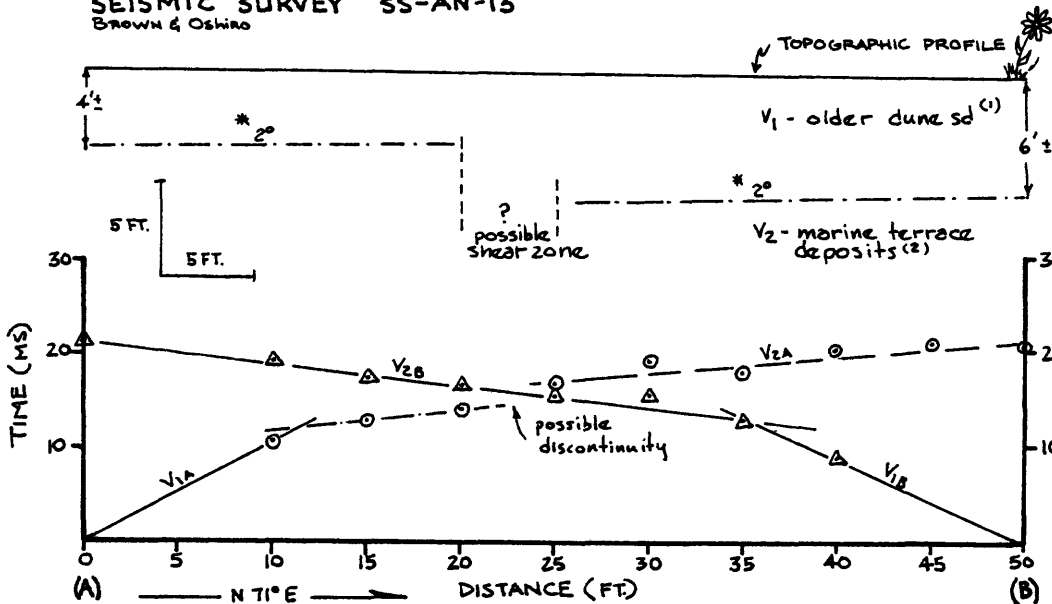
DEPTH TO BEDROCK (FT.)

	A	B
D	8.3	8.2

\* Dip of interface between V<sub>1</sub> - V<sub>2</sub> should be 1.5° - 2.0° using Bison tables 10-5 & 10-8 (Handbook of Engineering Geophysics)

- (1) prior to trenching V<sub>1</sub> interpreted as marine terrace deposits
- (2) prior to trenching V<sub>2</sub> interpreted as Tertiary sediments

SEISMIC SURVEY SS-AN-13  
BROWN & Oshiro



DISTANCE (FT.)	TIME (MS)	
	A	B
10	10.4	8.7
15	12.8	12.7
20	14.0	15.4
25	16.8	15.4-14.6
30	19.0	16.4
35	17.8	17.3
40	20.1	19.1
45	20.9	—
50	20.4	21.2

VELOCITIES (FT. PER SECOND)

	A	B
V <sub>1</sub>	960	1170
V <sub>2</sub>	5750	4450

CRITICAL DISTANCE (FT.)

	A	B
X <sub>c</sub>	10	15

DEPTH TO INTERFACE (FT.)

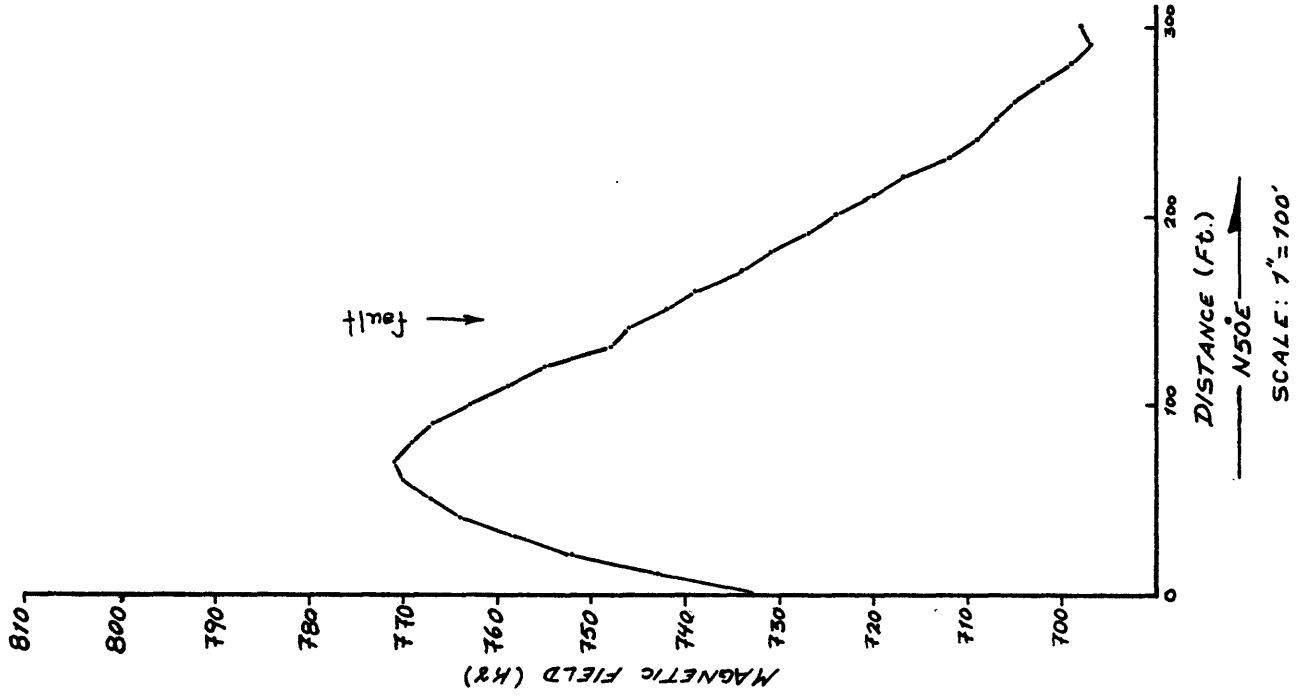
	A	B
D	4.3	6.1

Scatter on points precludes one clear-cut interpretation possibly a fault is present in V<sub>2</sub> materials with possibly a step in the interface between V<sub>1</sub> and V<sub>2</sub>.

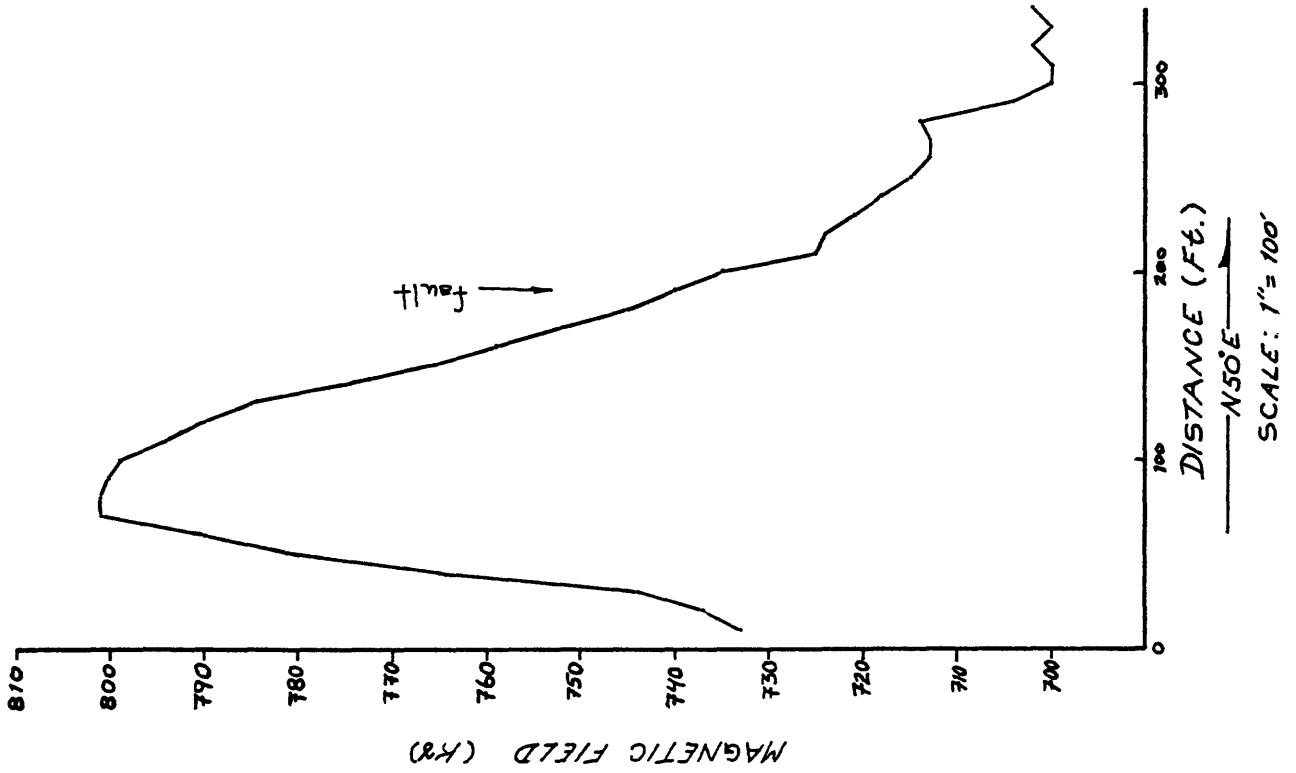
\* 2° dip of interface between V<sub>1</sub> - V<sub>2</sub> assumed on the information from surveys SS-AN-9, 10, 11, & 12

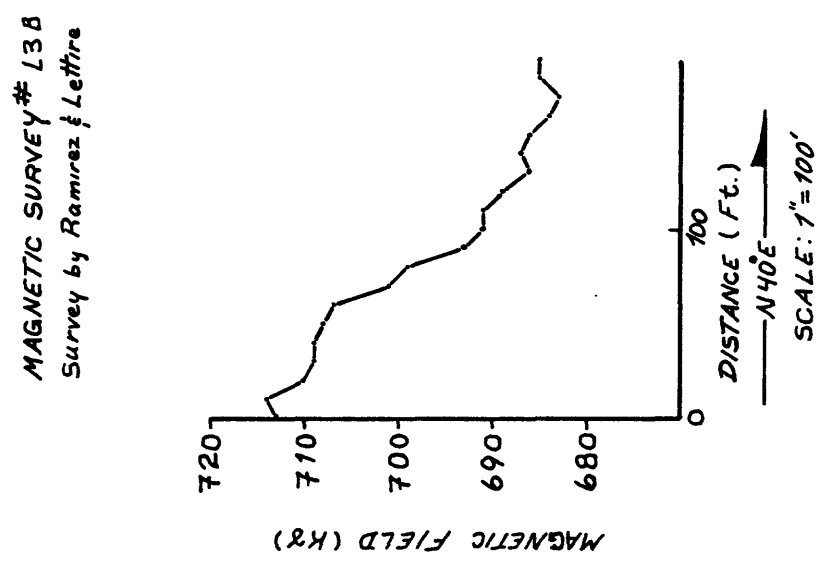
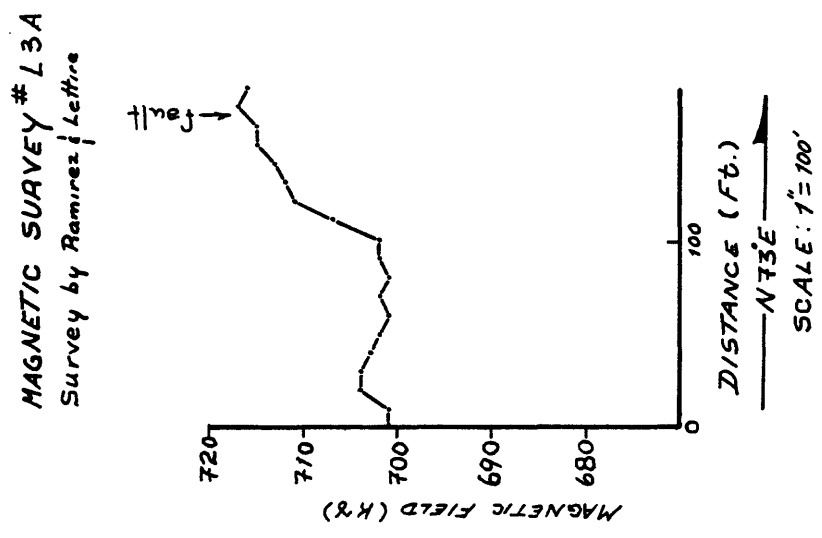
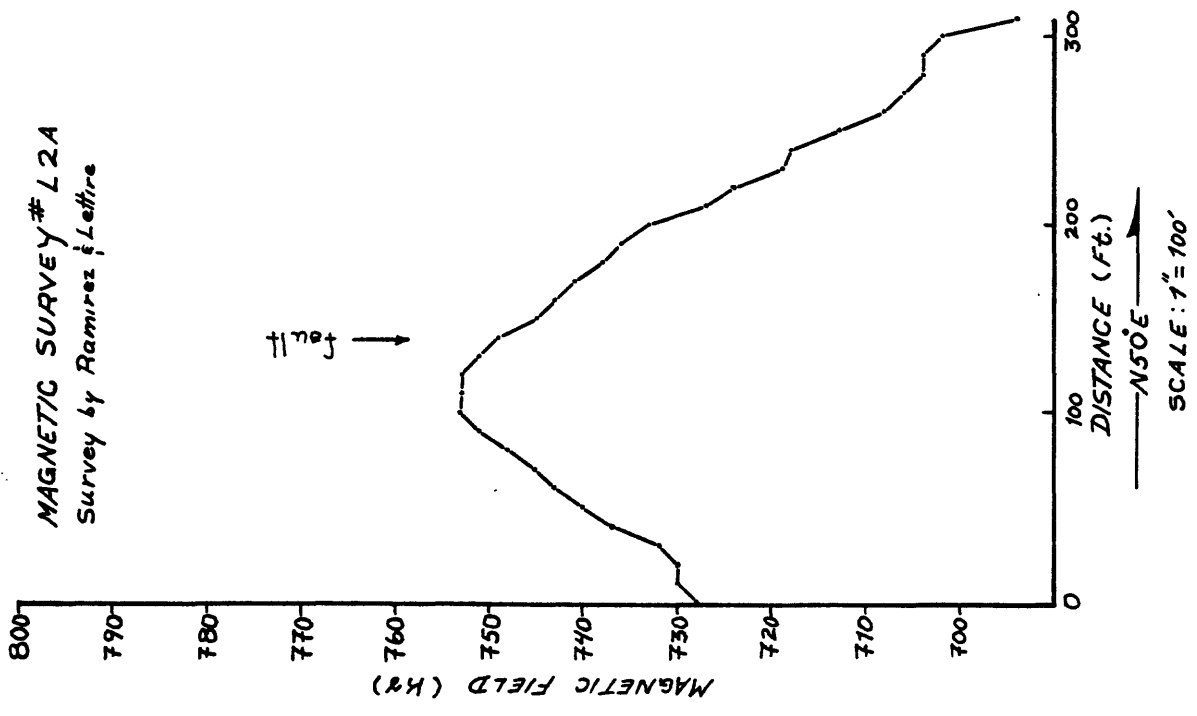
- (1) prior to trenching V<sub>1</sub> interpreted as marine terrace deposits
- (2) prior to trenching V<sub>2</sub> interpreted as Tertiary sediments

MAGNETIC SURVEY # L1A  
Survey by Ramirez & Lettine

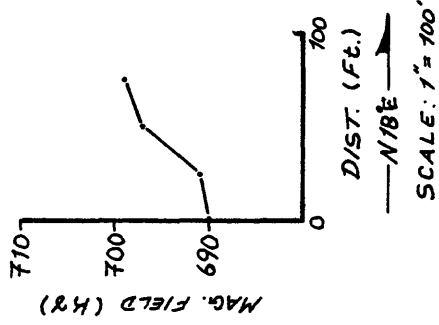


MAGNETIC SURVEY # Lo  
survey by Ramirez & Lettine

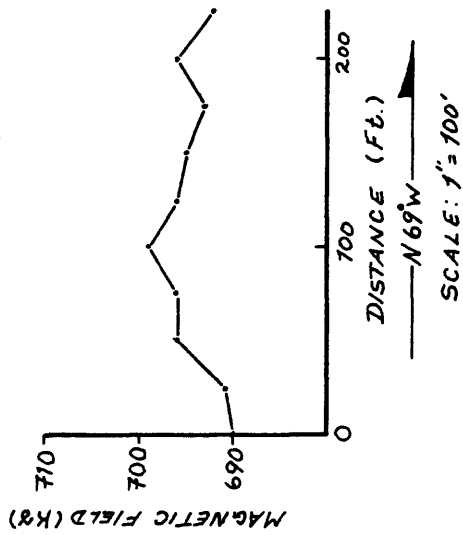




MAGNETIC SURVEY # L4A  
 Survey by Ramirez & Lettice



MAGNETIC SURVEY # L4  
 Survey by Ramirez & Lettice



#### Magnetic Survey L5

Readings are almost uniform along entire survey line. Total variation of 16 gammas (16 $\gamma$ ) from highest to lowest reading. Profile not plotted.

#### Magnetic Survey L6

Readings vary only 11 $\gamma$  from highest to lowest. Profile not plotted.

#### Magnetic Survey L7

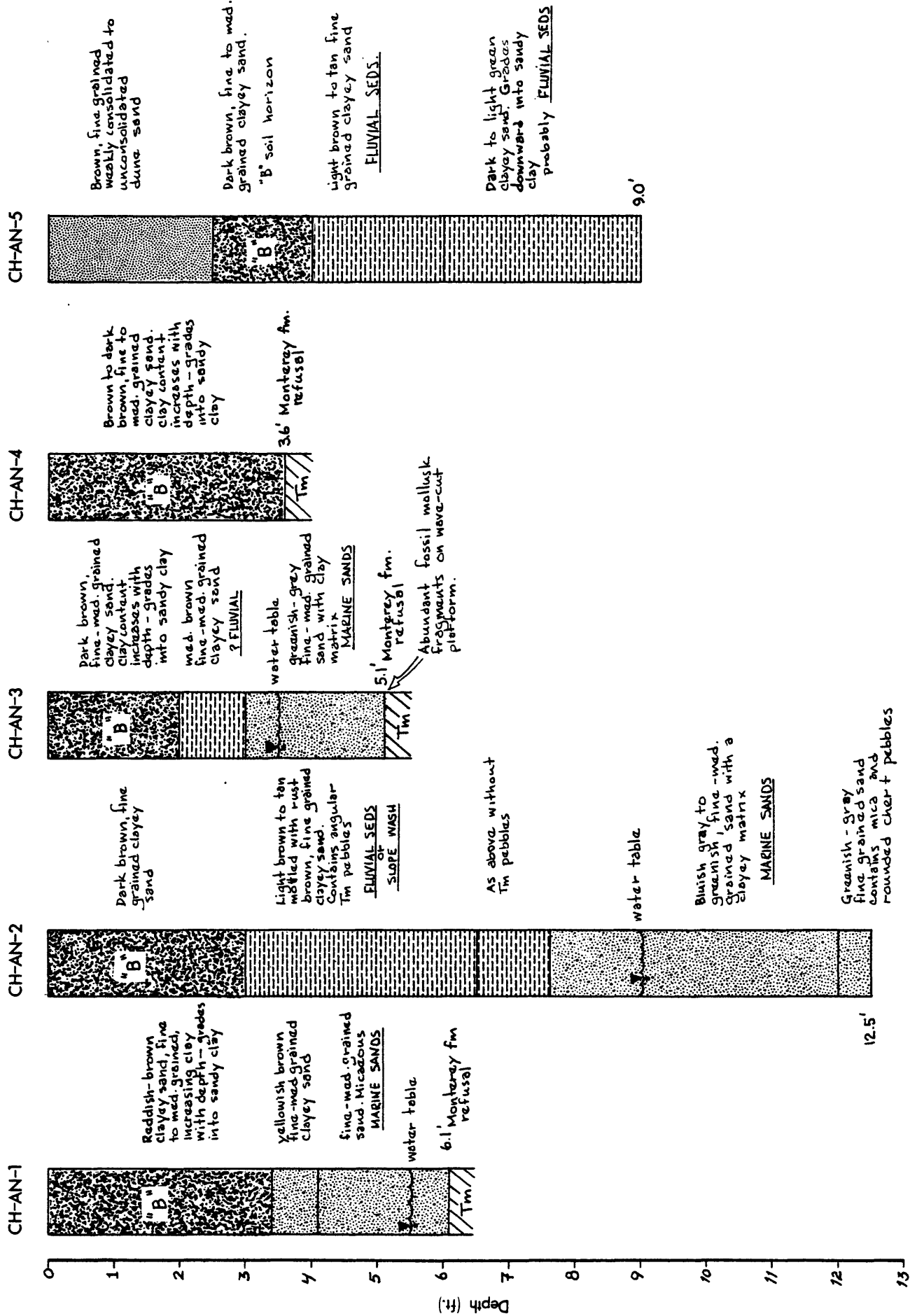
Total variation of only 8 $\gamma$  from highest to lowest reading. Profile not plotted.

#### Magnetic Survey L8

Readings vary only 10 $\gamma$  from highest to lowest reading. Profile not plotted.

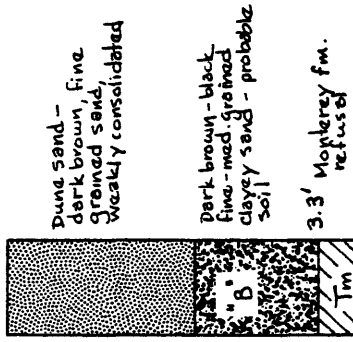
Over the entire area in the dune field covered by Magnetic Surveys L5 - L8, the total variation between the highest and lowest readings was 37 $\gamma$  with no systematic variation. There is no indication of faulting on these surveys, and all of the variations are believed to be related to variations in water content in the overlying dune sands and minor variations in the amount of magnetite present within the dune sands.

CORE HOLES FROM POINT AÑO NUEVO

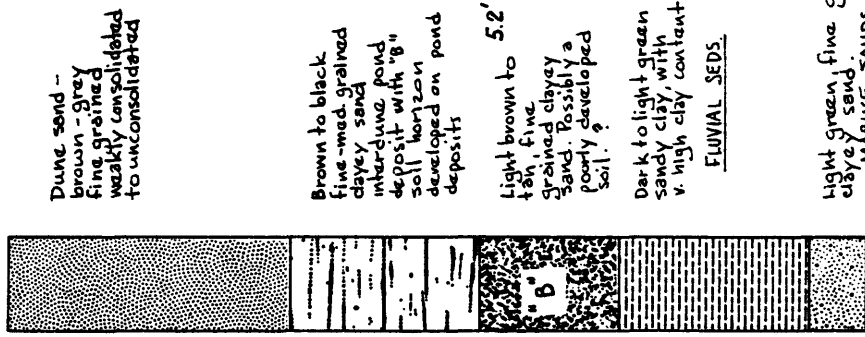


CORE HOLES FROM POINT AÑO NUEVO cont'd.

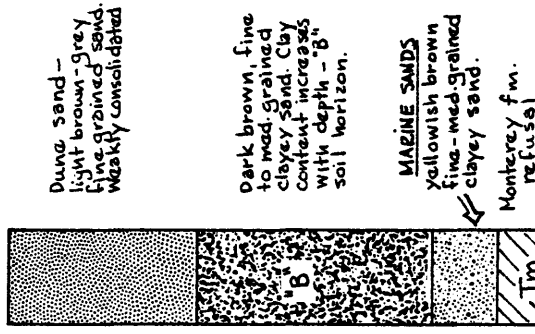
CH-AN-6



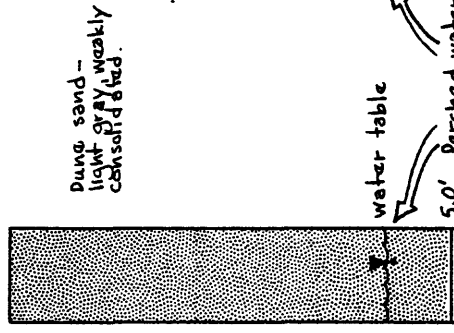
CH-AN-7



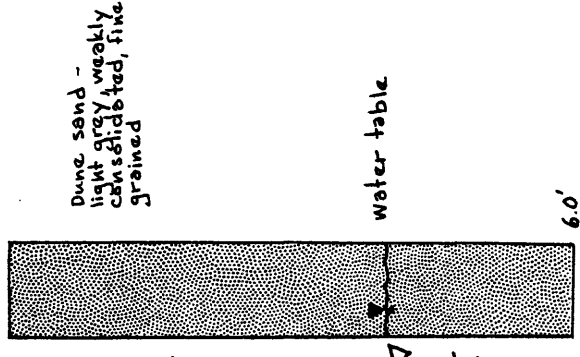
CH-AN-8



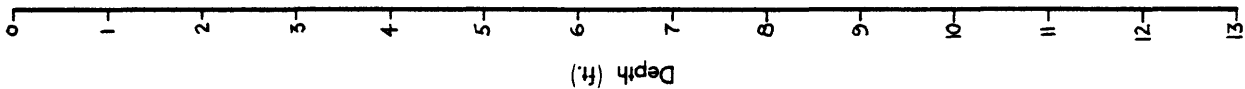
CH-AN-9



CH-AN-10



Borings could not be advanced due to continuing collapse of hole below water table.



CORE HOLES FROM POINT AÑO NUEVO cont'd.

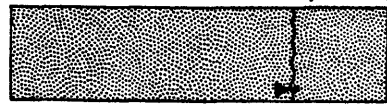
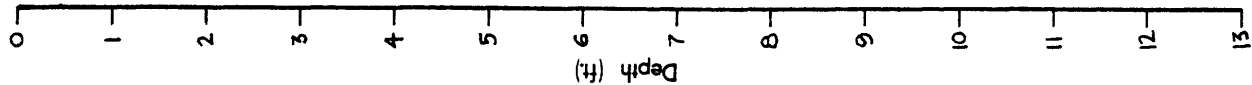
CH-AN-11 unsuccessful

CH-AN-12

CH-AN-13

CH-AN-14

CH-AN-15



unconsolidated light gray dune sand

water table

4.0'

Perched water in dune sands. Aquiclude is the "B" horizon developed on the clay rich fluvial deposits

Boring could not be advanced due to continuing collapse of hole below the water table.



unconsolidated to weakly consolidated dune sand

water table

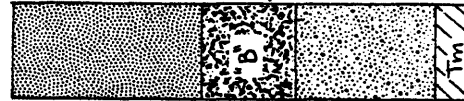
4.5'

Black, fine to med. grained clayey sand - interdune pond deposits

light brown to tan fine grained clayey sand - possibly B soil horizon.

Dark to light green sandy clay

FLUVIAL SEDS



unconsolidated to weakly consolidated, fine grained, light gray dune sand

water table

4.5'

Fine to med. grained clayey sand. Light brown color. ? older, weakly consolidated dune sand? ? "B" horizon. Greenish gray, fine to med. grained sand, clayey matrix. MARINE SANDS

Monterey fm. refusal



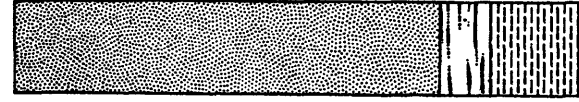
unconsolidated to weakly consolidated, light gray dune sand

Black fine to med. grained clayey sand. interdune pond deposits.

6.0'

Dark to light green sandy clay

FLUVIAL SEDS



unconsolidated to weakly consolidated, fine grained, light gray, dune sand.

Dark gray-black, fine to med. grained, clayey sand - interdune pond deposits

Dark to light green clayey sand

FLUVIAL SEDS

CORE HOLES FROM POINT AÑO NUEVO cont'd.

CH-AN-16



Dune sand -  
fine grained,  
light gray sand  
unconsolidated

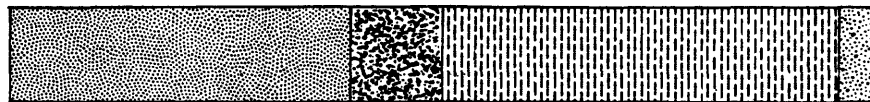
Fine - med. grained  
clayey sand  
? FLUVIAL?

Greenish gray, fine  
to med. grained  
sand with minor  
amount of clay

MARINE SANDS

4.2' Monterey Fm.  
refusal

CH-AN-17



Dune sand -  
fine grained, light  
gray weakly  
consolidated

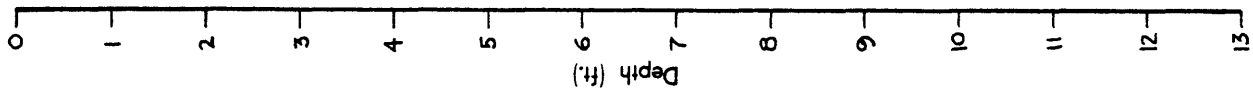
Dark to med. brown  
sandy clay - clayey sand  
? 8' soil horizon

Light to dark green  
sandy clay

FLUVIAL SEDS.

Green sandy clay with  
subrounded Tm pebbles  
? MARINE SANDS?

9.2'



AÑO NUEVO THRUST FAULT -

EXPLORATORY TRENCHING - JULY 30, 1979

AN-TP1 - AN-TP3

Test pits were excavated along the road in the dune field in an attempt to locate the thrust fault in the vicinity of the road. None of the pits was logged because of the unstable condition of the pits. The upper 6-7 ft. of each pit was either loose or very poorly-consolidated dune sand that caved into the pits almost as fast as they were excavated. All of the pits were similar in their stratigraphy within the limits of accuracy imposed by the conditions.

<u>Depth</u>	<u>Materials</u>
0-2 1/2 ft	Loose, unconsolidated dune sand with essentially no soil. Fine-grained, light gray sand.
2 1/2-3 ft	Layer of black organic-rich dune sand.
3-5 ft	Dune sand, light gray grading to dark gray with depth. Very weakly consolidated, caves readily. Top of perched water table at about 5 ft. Water is perched on the soil horizons developed in the marine terrace deposits.
5-7 ft	Dark gray dune sand and/or portions of the "A" soil horizon developed on the terrace deposits. Water saturated, with water seeping into pit.
7-9 ft	Bright green sandy clay. Appears to be soil developed on the clay-rich fluvial deposits of the marine terrace sequence.
9-13 ft	Marine terrace deposits. Varying shades of green and gray. Sandy clays in the upper portion, but getting sandier with depth. Pebble conglomerates near bottom of pit.

The bedrock wave-cut platform was not reached in any of these pits. The terrace deposits are thick enough to suggest that if the thrust fault is present in this area, it must lie to the northeast of Pit AN-TP1, and any further exploration for the fault should be in this area.

AN-TP4

Test pit AN-TP4, excavated at the end of the road across the bedrock (Monterey formation) ridge in the dune field, was not logged. The pit revealed that there was no faulting associated with either side of the ridge. The Monterey formation was difficult to excavate; the pit consequently was 2-3 ft. deep and about 50 ft. long. The pit exposed very thin, unconsolidated dune sand lying on top of Monterey formation siliceous shale and mudstone. The beds dip about 25 degrees to the southwest. We interpret this outcrop to be a stack on the original wave-cut platform rather than the result of faulting or other deformation.

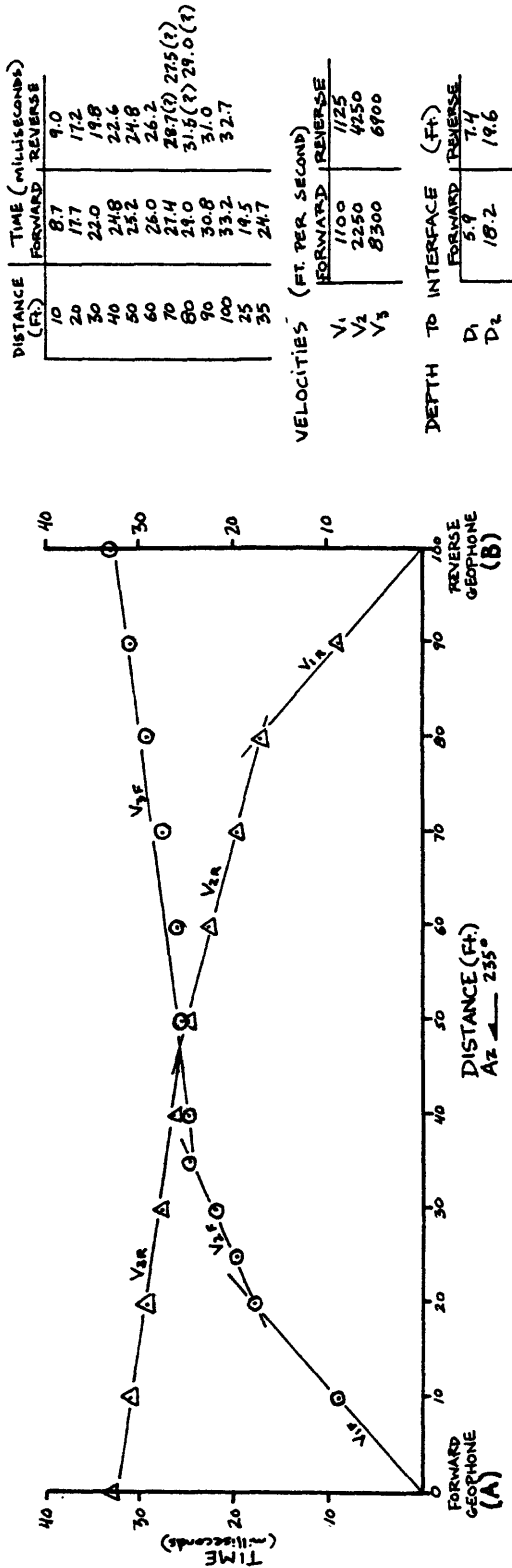
APPENDIX B  
Frijoles Fault  
Cascade Ranch

- Seismic Refraction Surveys
- Magnetometer Surveys
- Logs of Hand Auger Core Holes

Refer to Plate III and Figure 2 for  
location of survey lines and core holes.

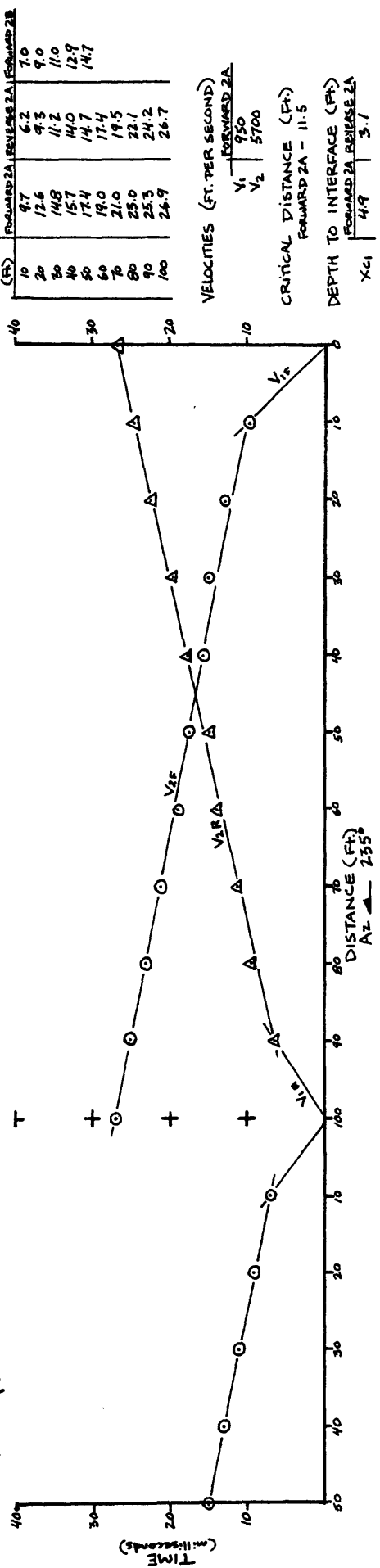
# SEISMIC SURVEY SS-CR-1

Weber & Lettner

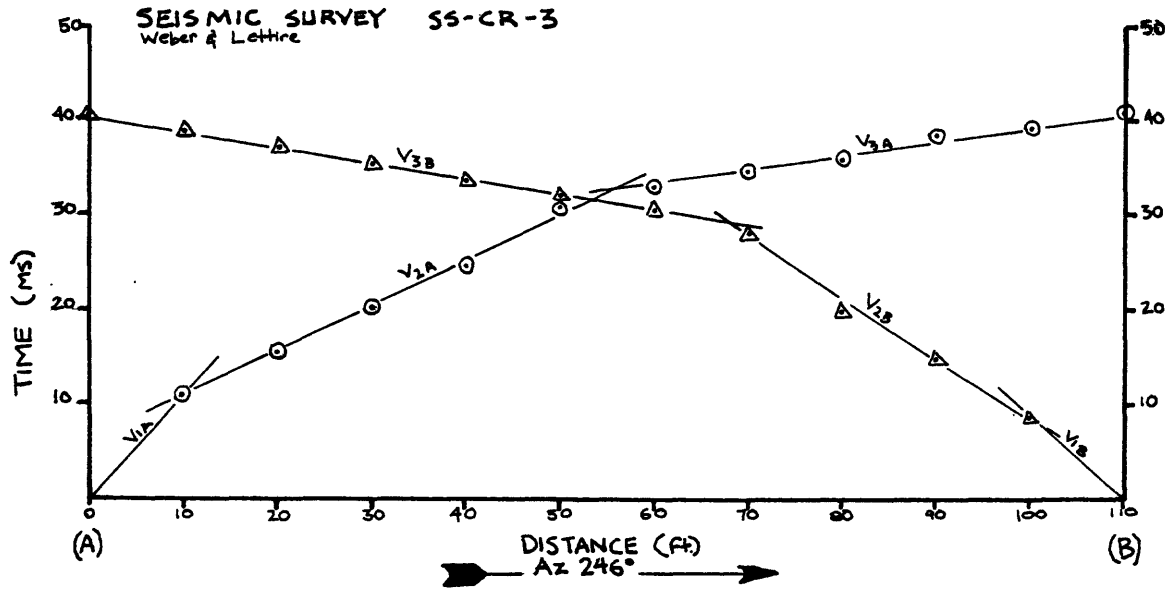


# SEISMIC SURVEY SS-CR-2

Weber & Lettner



SEISMIC SURVEY SS-CR-3  
Weber & Lettine



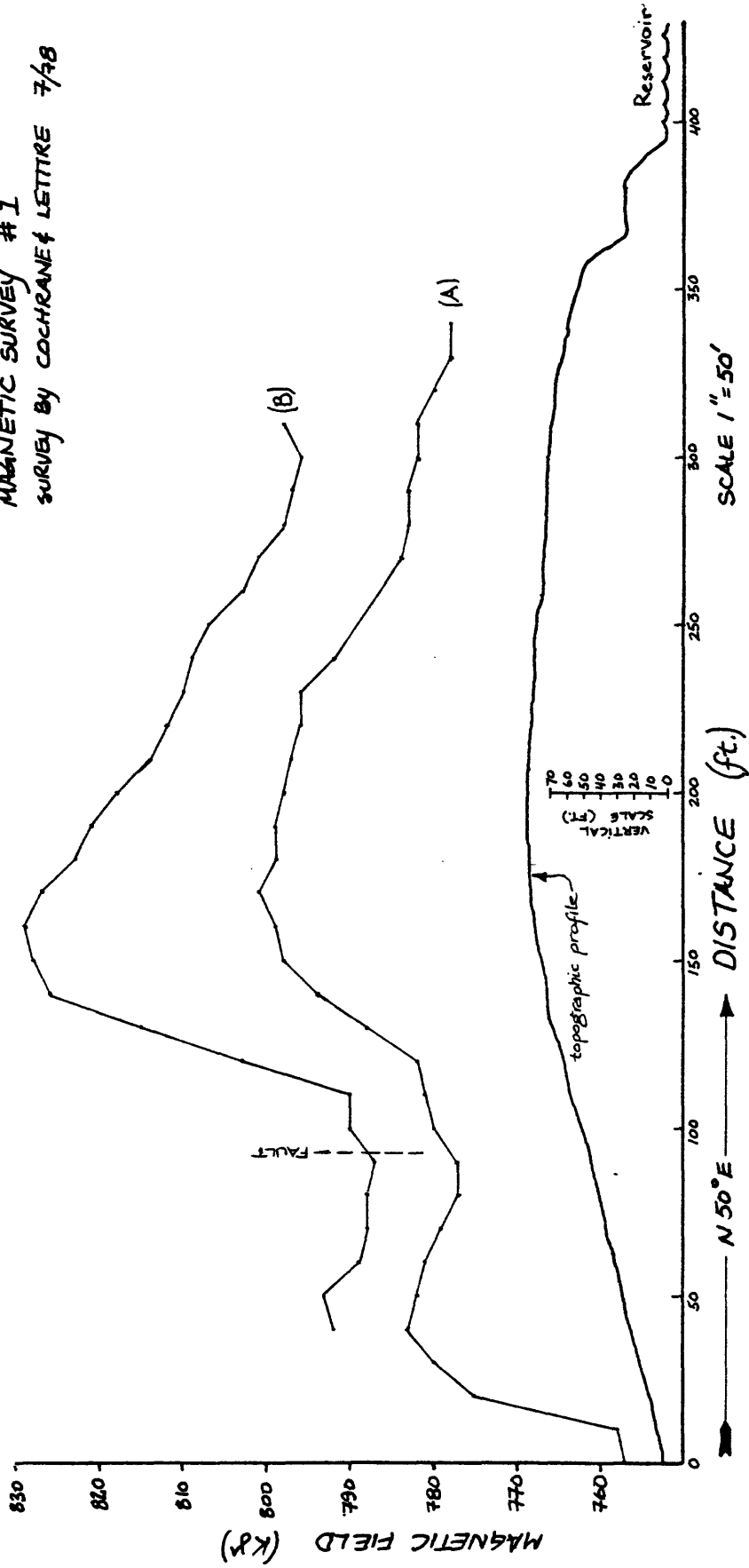
DISTANCE (ft.)	TIME (ms)	
	A	B
10	11.0	8.5
20	15.7	15.1
30	20.1	20.0
40	24.4	28.0
50	31.0	30.3
60	33.0	31.8-32.0
70	34.5	33.5
80	36.0	35.3
90	38.6	37.0
100	39.0	38.7-39.0
110	40.5	40.3

	VELOCITIES (feet per second)	
	A	B
V <sub>1</sub>	900	1100
V <sub>2</sub>	2100	1600
V <sub>3</sub>	7000	6200

	CRITICAL DISTANCES (ft.)	
	A	B
X <sub>C1</sub>	9.0	10.0
X <sub>C2</sub>	56.0	42.0

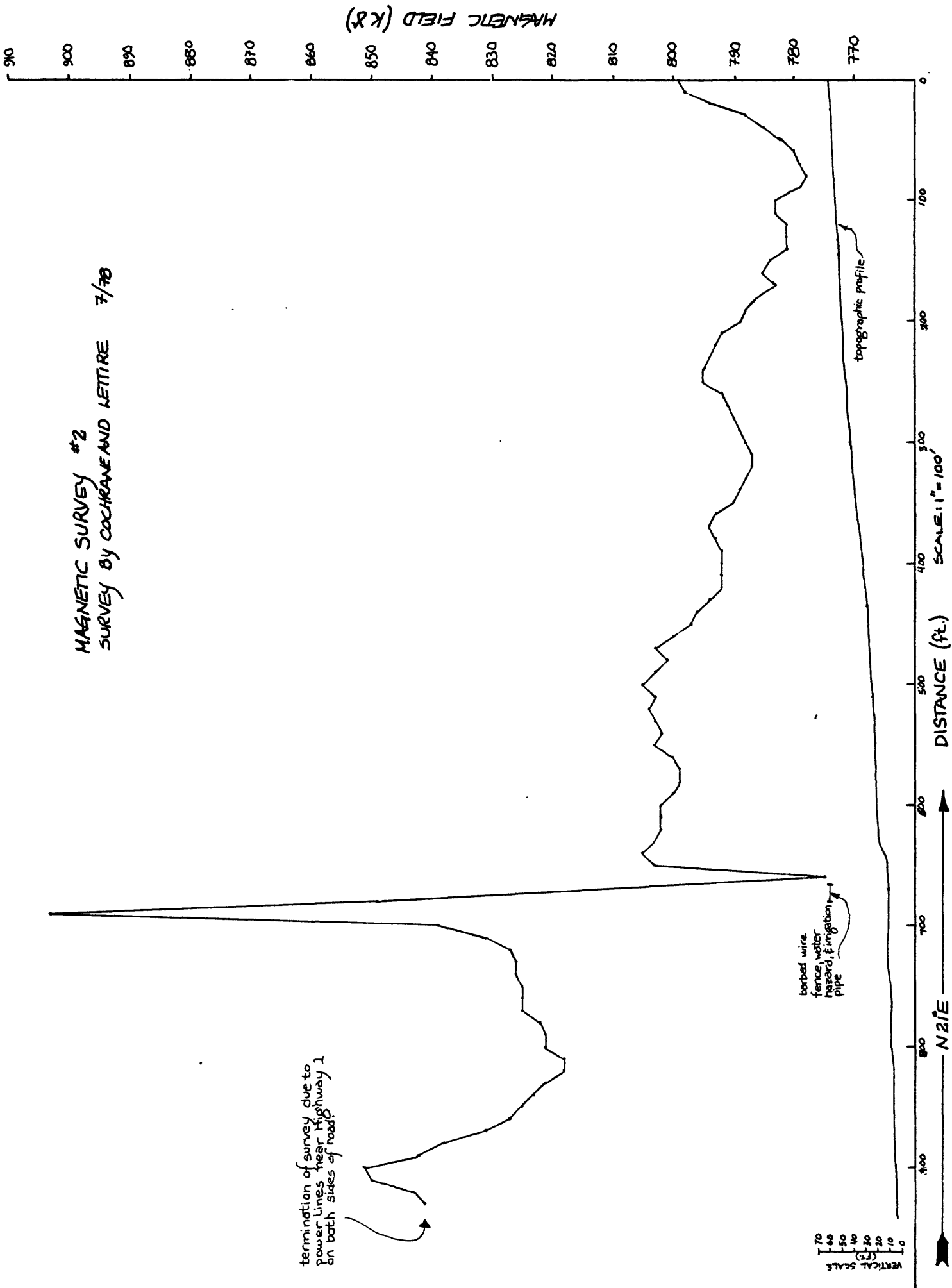
	DEPTH TO INTERFACE (ft.)	
	A	B
D <sub>1</sub>	2.8	2.6
D <sub>2</sub>	22.8	18.3

MAGNETIC SURVEY #1  
 SURVEY BY COCHRANE & LETTRE 7/98



"B" is a signature profile over an area where fault location is known. Represents similar profile to "A", running parallel to "A", 36 feet to the SE.

MAGNETIC SURVEY #2  
 SURVEY BY COCHRANE AND LETTICE 7/78



termination of survey due to  
 power lines near Highway 1  
 on both sides of road.

barbed wire  
 fence, water  
 hazard, & irrigation  
 pipe

topographic profile

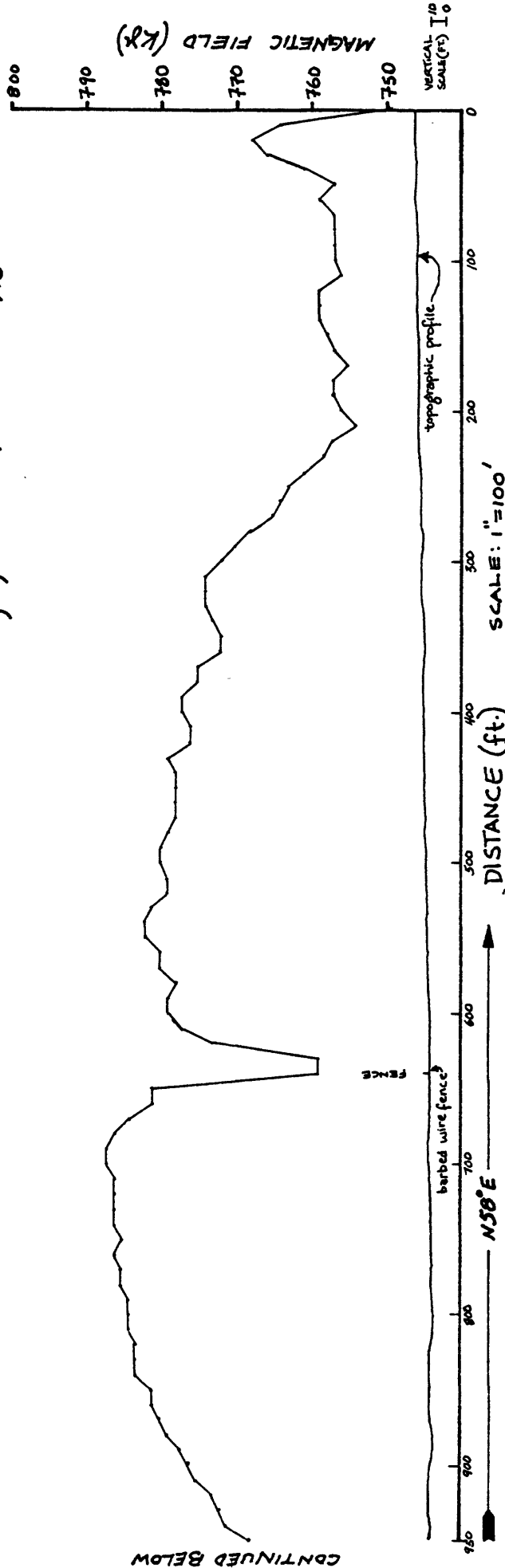
SCALE: 1" = 100'

DISTANCE (ft.)

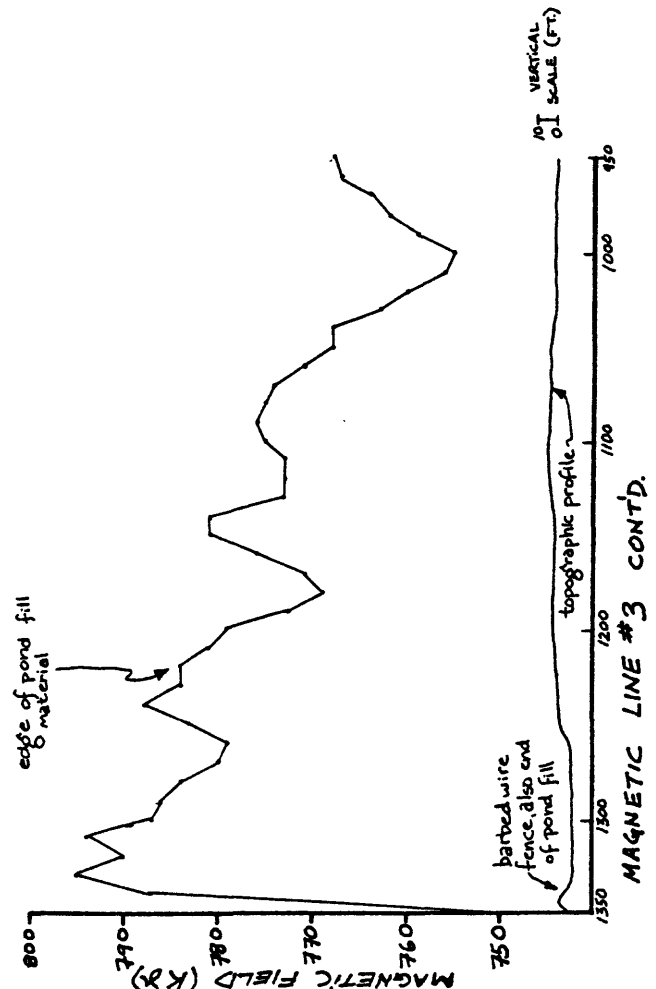
N 21° E

VERTICAL SCALE  
 70  
 60  
 50  
 40  
 30  
 20  
 10  
 0

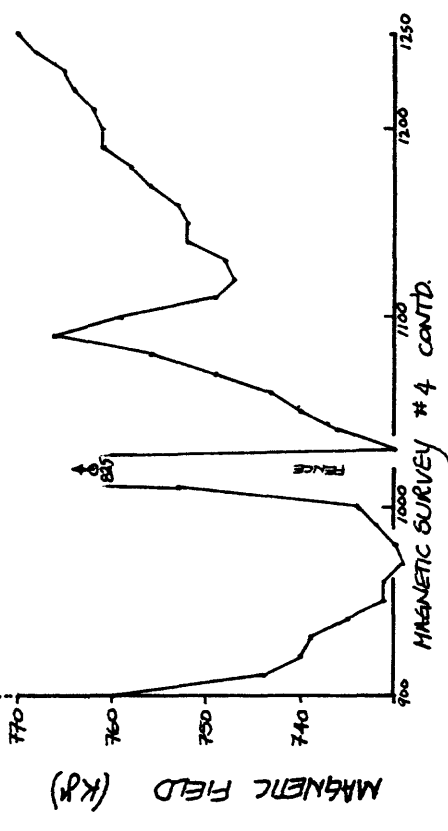
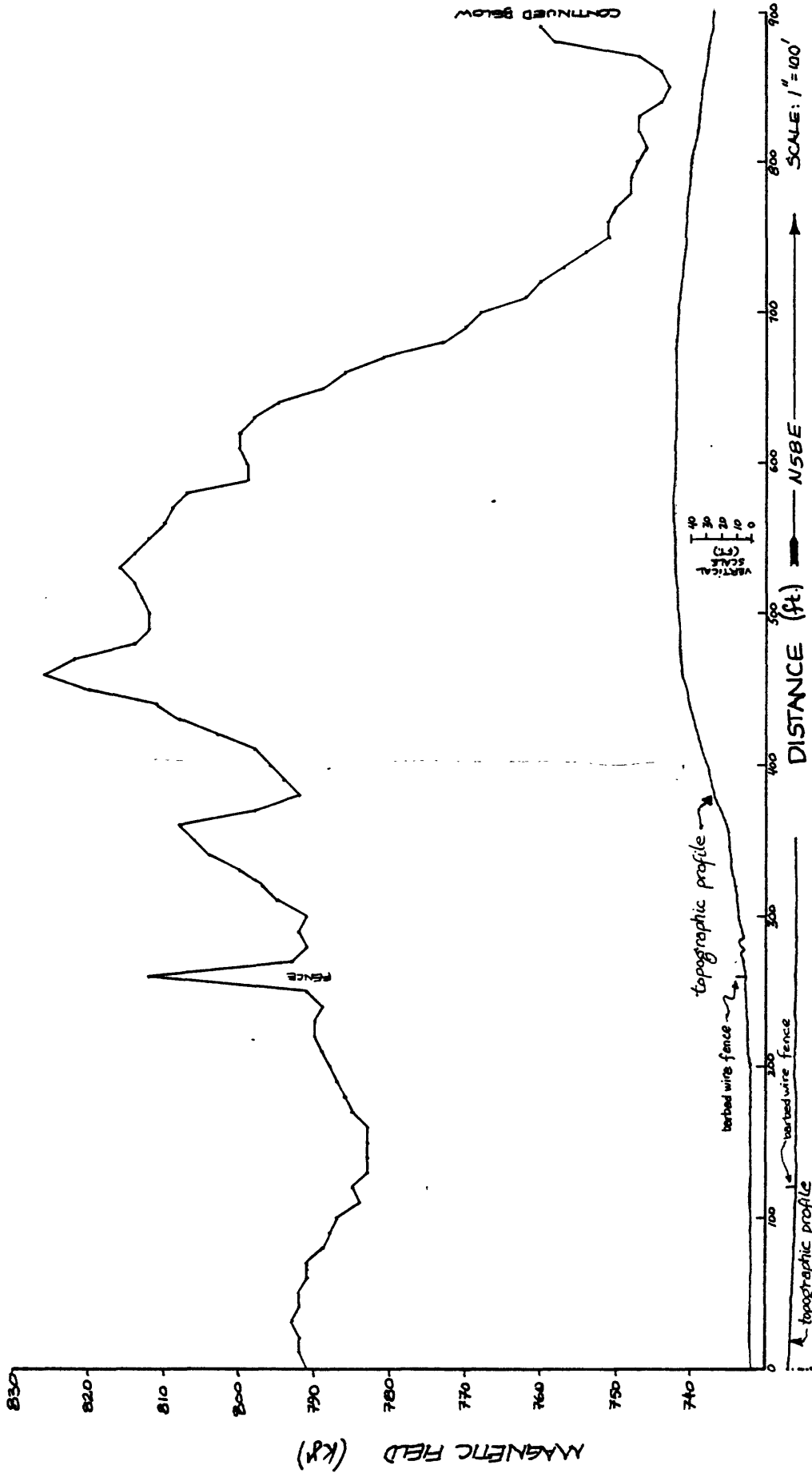
MAGNETIC SURVEY #3  
 SURVEY BY COCHRANE & LETTRE 7/78



CONTINUED BELOW



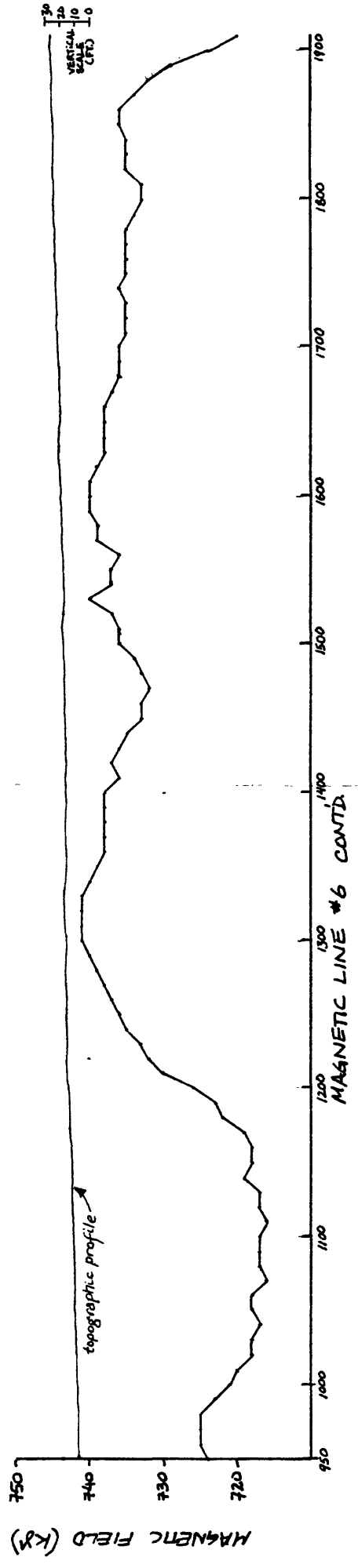
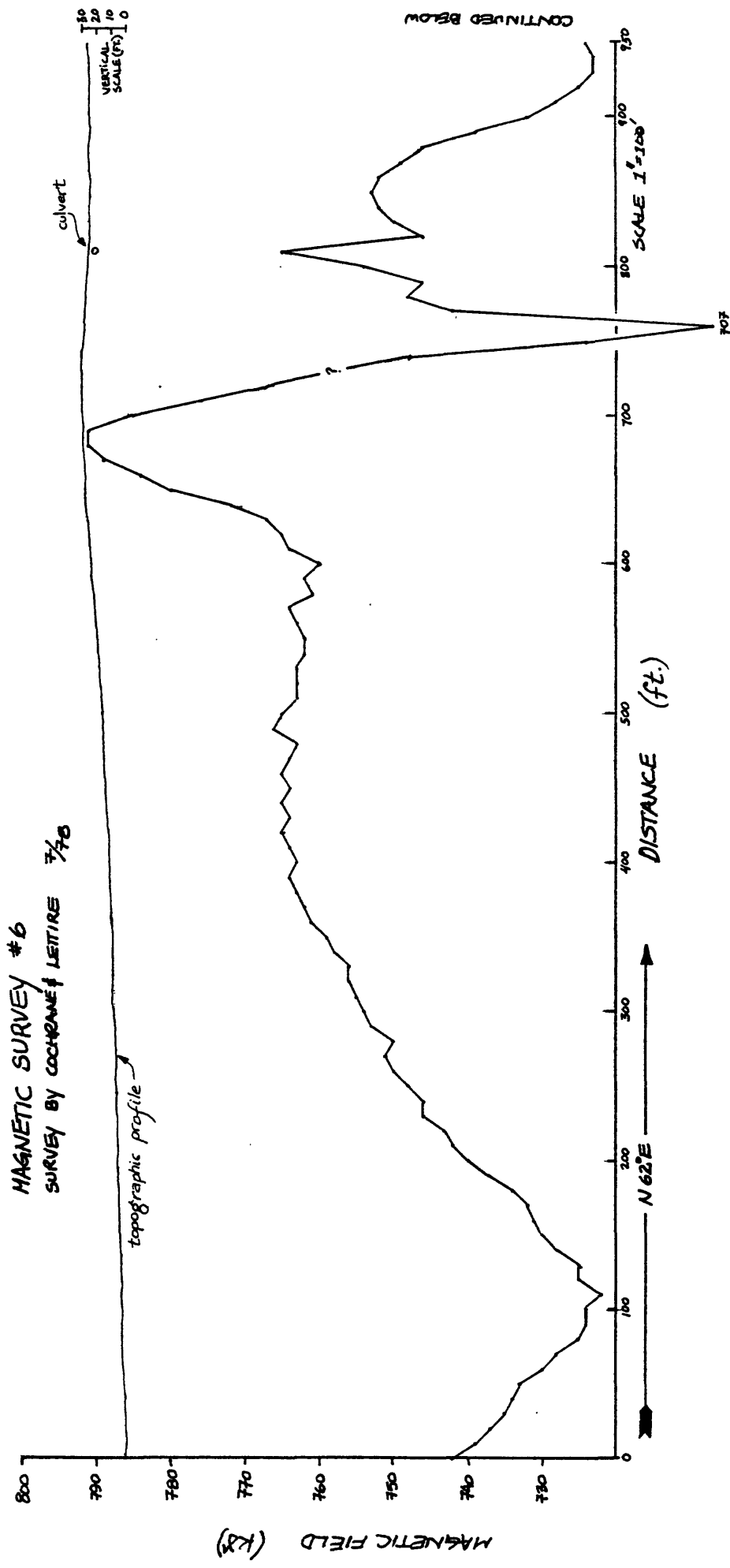
MAGNETIC LINE #3 CONTD.



MAGNETIC SURVEY # 4  
 SURVEY BY COCHRANE LETTER 7/78

MAGNETIC SURVEY # 5  
SURVEY BY COCHRANE & LETTRE 7/78





MAGNETIC SURVEY #7  
 SURVEY BY COCHRANE & LETTICE 7/78

SPECIAL NOTE: The readings obtained during this survey were adversely affected by buried cables (telephone). In view of anomalous data the survey was abandoned and no topographic profile was constructed.

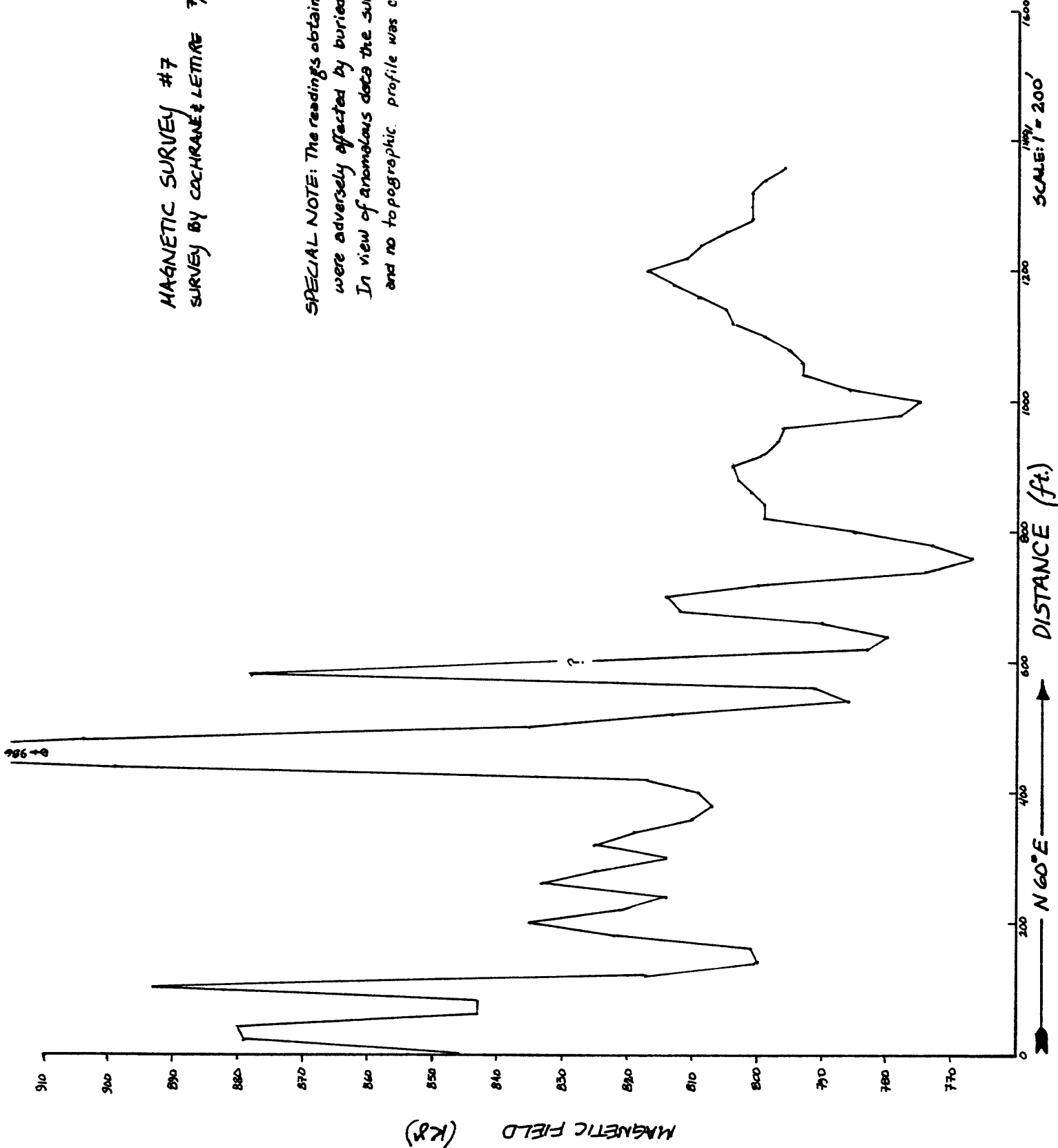
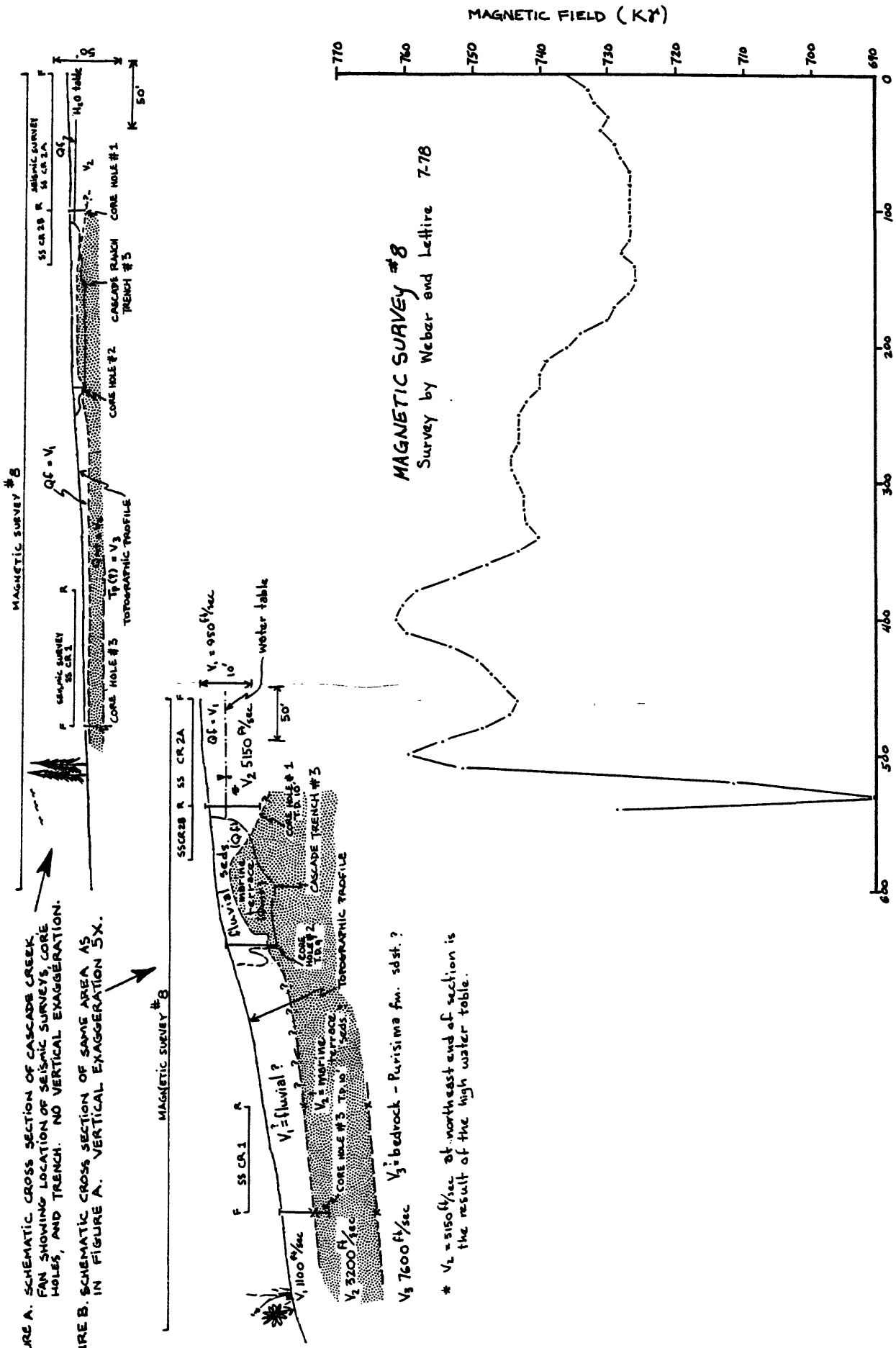


FIGURE A. SCHEMATIC CROSS SECTION OF CASCADE CREEK FAN SHOWING LOCATION OF SEISMIC SURVEY'S CORE HOLES, AND TRENCH. NO VERTICAL EXAGGERATION.

FIGURE B. SCHEMATIC CROSS SECTION OF SAME AREA AS IN FIGURE A. VERTICAL EXAGGERATION 5X.



MAGNETIC SURVEY #8  
Survey by Weber and Lettner 7-78

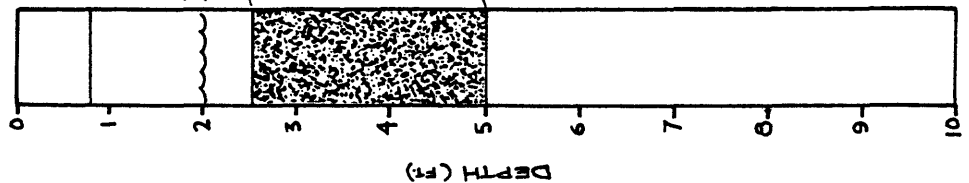
DISTANCE (FT)  
Az 235°

\*  $V_2 = 5150 \text{ ft/sec}$  at northeast end of section is the result of the high water table.

$V_3$  bedrock - Purisima fm. sd st.?

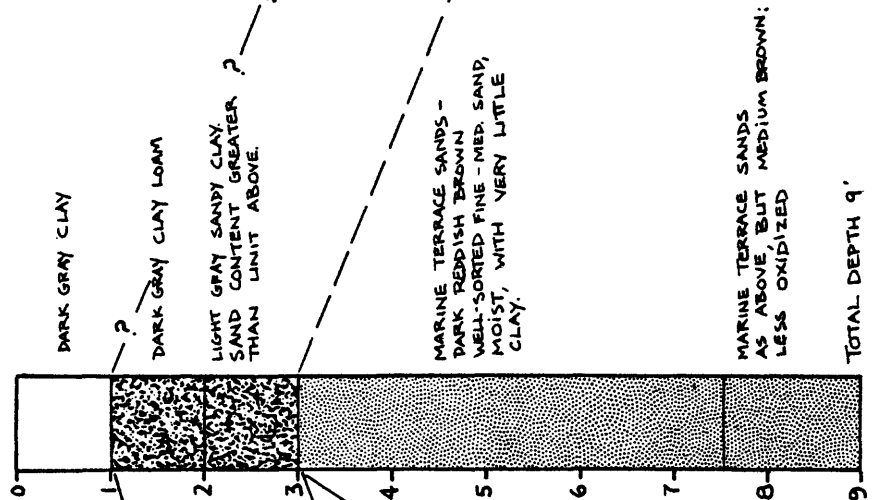
CORE HOLES FROM CASCADE CREEK FAN

CORE HOLE # 1



TOTAL DEPTH: 10'

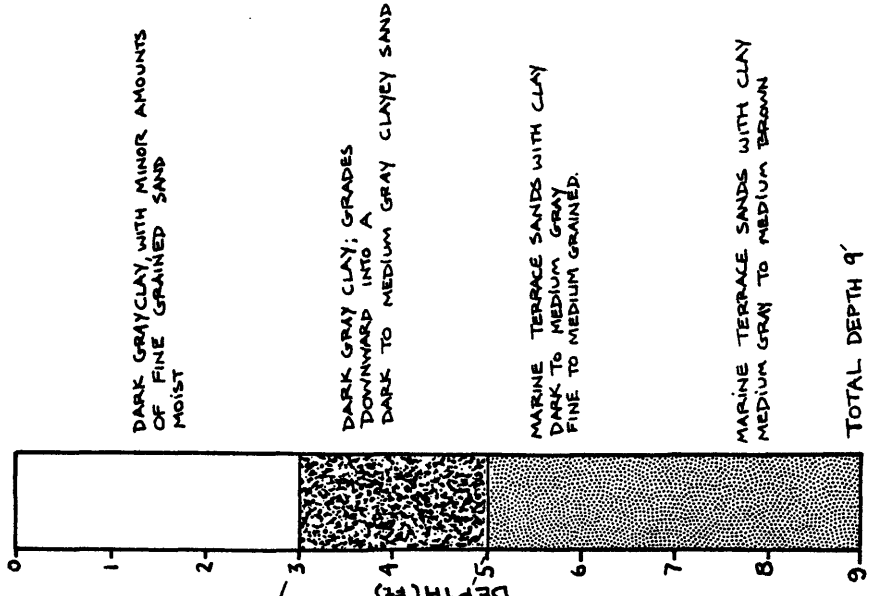
CORE HOLE # 2



TOTAL DEPTH 9'

NO WATER TABLE

CORE HOLE # 3



TOTAL DEPTH 9'

NO WATER TABLE

EXPLANATION OF SYMBOLS USED ON  
TRENCH, SEA-CLIFF, AND QUARRY WALL LOGS  
(Plates IV-VIII, XII-XIV, and XVI-XVIII)

-  Depositional contact - dashed where obscured, dotted where inferred.
-  Gradational contact - no clear, sharp boundary between units.
-  Thin prominent bed - symbol indicates the principal constituent: s - sand, pbl - pebbles, cbl - cobbles, c - clay or silt.
-  Gradual lithologic change within stratum.
-  Large clasts of locally-derived sediment - symbol indicates composition (i.e. Tm - Monterey formation).
-  Fault or fracture - dashed where lost as a distinct trace.
-  Fault gouge and/or fault breccia - predominantly clay mixed with sheared and brecciated rock.
-  Knocker - hard, resistant block of rock surrounded by intensely sheared and fractured rock or fault gouge. Rock often tightly cemented by CaCO<sub>3</sub>, Fe<sub>2</sub>O<sub>3</sub>, or SiO<sub>2</sub>. Symbol indicates rock type (i.e. ss. - sandstone).

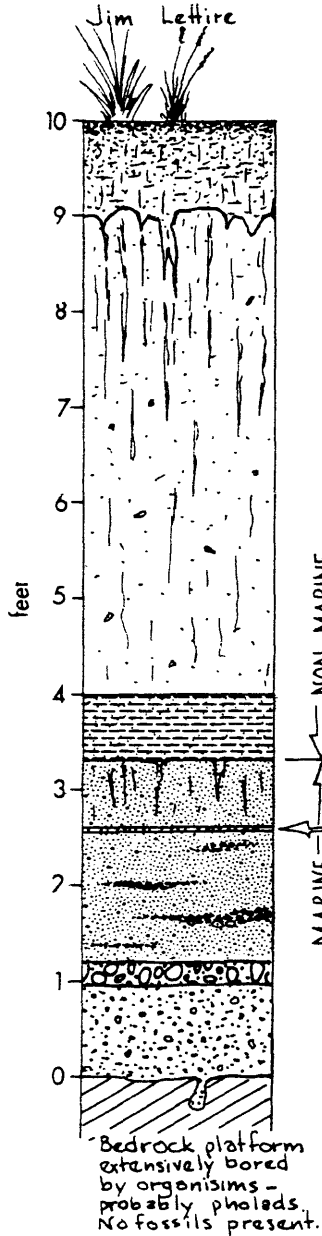
PLATE X.

AÑO NUEVO STRATIGRAPHIC SECTION 5 — Marine Terrace Deposits

Logged by: 7-78 SW of thrust fault — [downdropped block]

Gerald E. Weber

Jim Lettice



Dark grey to light grey sandy-silty clay. Minor amounts of organic material and humus in upper foot. The "A" soil horizon developed on the clay-rich fluvial sediments.

Light brown-tan sandy clay with scattered Santa Cruz mudstone pebbles and chips of Monterey formation. Extremely high clay content obscures bedding and structures. Blocky and prismatic peds developed throughout, but more prominent in upper half. Clay skins present along peds.

The soil structure may be an "apparent" soil structure related to shrink-swell of non-pedogenic clays in these clay-rich fluvial sediments.

Lt. grey to tan sandy clay. No apparent soil structure

Lt. grey very clayey fine-grained sand. Scattered pebbles. Apparent development of peds with clay skins (?). Peds possibly from paleosols as they are filled with clay, apparently derived in part from overlying unit. Very micaceous fine-grained sand

? Paleo Soil ?

Micaceous, well-laminated, fine-grained sand. Minor amount of clay. Mottled grey-red brown. Contains Santa Cruz mudstone (T<sub>sc</sub>) and Monterey formation (T<sub>m</sub>) clasts. Thin discontinuous pebble and cobble conglomerates within sand.

Pebble-cobble conglomerate - matrix, fine sand

Light grey-dark grey micaceous fine-grained sand. Well-developed laminations in the mica-rich portions. Contains numerous cobbles and pebbles of T<sub>v</sub> and T<sub>m</sub>. (Basal unit)

Vaqueros formation - T<sub>v</sub> - Dusky-yellowish-brown phosphatic mudstone and thick-bedded sandstones

PLATE XV.

PLATE XV

CASCADE RANCH STRATIGRAPHIC COLUMN - Marine Terrace Stratigraphy on Uplifted Block

Logged by: John Pinkston 5-79

Dark grey clayey loam to loamy sand. Texture variable. Minor organic material near surface. "A" soil horizon

Light grey sandy clay mottled with orange-brown. Weakly-developed soil structure.

"B" soil horizon developed in marine sands.

Fine-to medium-grained sand. Massive, no discernable bedding. Sorting fair. A few scattered pebbles. Sand contains 10-15% dark particles.

Medium-grained sand with abundant scattered pebbles of mudstone and sandstone

Medium-grained sand. Contains lenses of fine-grained sand and also coarse sand. No bedding - massive except for the few lenses.

Coarse-grained sand. Weakly consolidated. Upper portion a channel of pebble conglomerate with interbedded lenses of medium sand.

Medium-grained sandstone. Weakly to moderately consolidated and cemented. Low hardness. Lenses of pebble conglomerate. Grades into a coarse sand near top of unit. Bedding indistinct. A few fine laminae.

← Lens of very micaceous fine-grained sand.  
Well-bedded coarse-grained sand with a few scattered pebbles.

← Pebble conglomerate lens.

Pebble-cobble conglomerate

Bedrock - Fine-grained silty sandstone - Purisima fm.

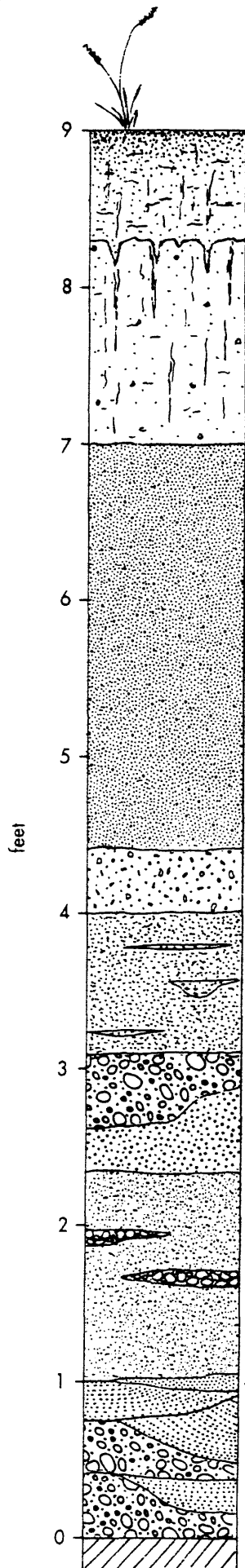


PLATE IX.

AÑO NUEVO STRATIGRAPHIC SECTION 4 — Marine Terrace Deposits

Logged by: 7-78

Gerald E. Weber

Jim Lettice

